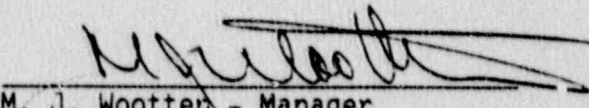


INDIAN POINT UNIT 2 - FINAL REPORT  
ON THE STEAM GENERATOR INSPECTION,  
REPAIR, AND RESTORATION EFFORTS  
DURING THE 1990 MID-CYCLE INSPECTION

ISSUE DATE: JULY 1990

PREPARED FOR CONSOLIDATED EDISON COMPANY

APPROVED:

  
M. J. Wooten - Manager  
Steam Generator Technology and Engineering

WESTINGHOUSE ELECTRIC CORPORATION  
NUCLEAR SERVICES DIVISION  
P. O. BOX 355  
PITTSBURGH, PENNSYLVANIA 15230

Copyright by Westinghouse Electric 1990, © All Rights Reserved

DOC 110196 000801  
PDR ADCK 05000247  
PLC

## FOREWORD

This nonproprietary report bears a Westinghouse copyright notice. The NRC is permitted to make the number of copies of this report necessary for its internal use and such additional copies which are necessary in order to have one copy available for public viewing in the appropriate docket files in the public document room in Washington, D.C. and in local public document rooms as may be required by NRC regulations if the number of copies submitted is insufficient for this purpose. The NRC is not authorized to make copies for the personal use of members of the public who make use of the NRC public document rooms. Copies of this report or portions thereof made by the NRC must include the copyright notice.



## TABLE OF CONTENTS

- 1.0 INTRODUCTION
  - 1.1 OVERVIEW
  - 1.2 CONCLUSIONS
- 2.0 1990 INSPECTION RESULTS AND STEAM GENERATOR FABRICATION HISTORY
  - 2.1 GIRTH WELD INSPECTIONS
  - 2.2 FEEDWATER NOZZLE INSPECTION
  - 2.3 FEEDWATER PIPE INSPECTION
  - 2.4 FEEDRING (HEADER) BRACKET INSPECTION
  - 2.5 OTHER INSPECTIONS
  - 2.6 COMPARISON WITH PREVIOUS INSPECTIONS (1987 AND 1989)
  - 2.7 S/G FABRICATION HISTORY
- 3.0 METALLURGICAL EVALUATIONS
  - 3.1 BOAT SAMPLE EVALUATIONS
  - 3.2 EVALUATIONS AND TESTS
  - 3.3 RESULTS OF GIRTH WELD/TRANSITION CONE SAMPLES EXAMINATIONS
  - 3.4 RESULTS OF 1989 WELD REPAIR AREA SAMPLE EXAMINATIONS
  - 3.5 RESULTS OF NOZZLE BORE SAMPLE EXAMINATIONS
  - 3.6 RESULTS OF FEEDRING SUPPORT EXAMINATIONS
  - 3.7 CONCLUSIONS
- 4.0 EVALUATION OF STEAM GENERATOR OPERATIONS AND CHEMISTRY
  - 4.1 CHEMISTRY BACKGROUND
  - 4.2 EFFECT OF PLANT OPERATIONS ON STEAM GENERATOR MATERIAL CONDITION
  - 4.3 SUMMARY
- 5.0 EVALUATION FOR GIRTH WELD, TRANSITION CONE, FEEDRING BRACKETS AND STRAPS
  - 5.1 THERMAL HYDRAULICS
  - 5.2 STRESS ANALYSIS
  - 5.3 FRACTURE MECHANICS EVALUATION
  - 5.4 CONCLUSIONS
  - 5.5 REFERENCES
- 6.0 EVALUATION FOR FEEDWATER NOZZLE REGION
  - 6.1 THERMAL HYDRAULICS
  - 6.2 STRESS ANALYSIS
  - 6.3 FRACTURE MECHANICS EVALUATION
  - 6.4 DISCUSSION AND CONCLUSIONS
  - 6.5 REFERENCES

## TABLE OF CONTENTS (cont.)

### 7.0 REPAIR AND MITIGATING ACTIONS

- 7.1 GIRTH WELD
- 7.2 FEEDRING SUPPORTS
- 7.3 FEEDWATER NOZZLE REGION
- 7.4 NEAR TERM MITIGATING ACTIONS

### 8.0 FUTURE PLANS

- 8.1 GENERAL
- 8.2 INSPECTION PROGRAM FOR 1991 REFUELING OUTAGE
- 8.3 ACTIONS
- 8.4 CONDENSER AND FEEDWATER HEATER CHANGEOUT
- 8.5 LONG RANGE PLANNING

### 9.0 SUMMARY AND CONCLUSIONS

APPENDIX A: EMBEDDED FLAW EVALUATION

APPENDIX B: GIRTH WELD INSPECTION DATA

APPENDIX C: GIRTH WELD INDICATION MAPS

APPENDIX D: FEEDRING SUPPORT INSPECTION DATA

APPENDIX E: FEEDRING SUPPORT GRINDING AND REPAIR MAPS

APPENDIX F: FEEDWATER NOZZLE INSPECTION DATA

APPENDIX G: FEEDWATER NOZZLE GRINDING AND REPAIR MAPS



## 1.0 INTRODUCTION

### 1.1 OVERVIEW

On February 24, 1990 Indian Point 2 shutdown to perform a mid-cycle inspection of the steam generator upper cylinder to transition zone (girth) welds and feedwater nozzles. The inspections were extended to include internal weld surfaces and the generator internals above the girth weld, transition zone shell areas below the girth weld, feedwater ring brackets, the nozzle bore and connecting feedwater piping and a lower cone to shell weld and the stub barrel to shell weld. All indications identified as cracks were removed by grinding. Weld repairs meeting the requirements of ASME Code Case N-432 or Section XI 1983 edition through Winter 1985 addenda were accomplished, as necessary, on the feedwater piping, feedwater nozzle, feedring brackets and upper shell to transition cone girth weld.

Metallurgical investigations were conducted on material samples from girth welds, transition cone, nozzle bore and feedring brackets.

Stress analyses and fracture mechanics evaluations were performed to determine the necessary repairs and to support plant operation until the next refueling outage. The fracture analysis approach used was based on a modification of the fracture mechanics criteria of ASME Section XI. The Section XI fracture criteria found in paragraph IWB-3600 are normally used to justify continued operation without removal of cracks. In this case all cracks have been removed and/or repaired.

### 1.2 CONCLUSIONS

The repairs made to the feedwater piping, feedwater nozzle, and feedring brackets involved restoration of these items to their original design condition or a modified equivalent. The weld repair made to the girth weld restored this item to a condition to meet ASME Code requirements to support the remainder of current cycle of plant operation.



Metallurgical analysis determined that the cracking was caused by corrosion fatigue or stress corrosion mechanisms depending upon location, loads and environmental conditions. As a result of changes made in 1989 (modification of feedwater flow control valve and removal of downcomer resistance plates) the impact of fatigue mechanism has been minimized.

Stress analyses and fracture mechanics evaluations determined that the post repair condition of the steam generators satisfy necessary criteria to support continued plant operation until at least the next refueling outage without any detriment to the structural integrity of the steam generators.

The wet layup process has been modified to introduce nitrogen as a sparging gas to displace air from the steam generator for future outages.

It is believed that this modification and the mitigating actions to reduce the dissolved oxygen in auxiliary feedwater now being implemented will significantly retard the process of pitting, crack initiation and growth.

Appropriate inspections of the repaired areas will be made at the next refueling outage.

## 2.0 1990 INSPECTION RESULTS

During the 1990 outage, inspections of steam generators and steam generator fabrication history were accomplished in five areas; girth welds, feedwater nozzles, feedwater piping, feedring supports and other areas of the steam generator shells. Details of the inspections are described below.

### 2.1 GIRTH WELD INSPECTIONS

The girth weld inspection plan previously established for the 1990 outage was to initially examine by magnetic particle (MT) techniques one third of the inner circumference of two steam generators. If indications were found, the MT inspection would be expanded to 100% of the girth weld on the steam generators selected, and the remaining two steam generators would have one of their girth weld circumference examined. Finally, if indications were again found, the inspections would be expanded to 100% of the girth welds in all four steam generators.

In each examination phase, MT indications were found and, therefore, 100% of all girth welds were examined by MT for each steam generator. This represents a band of approximately 7 inches wide and 44 feet in circumferential length on the inside surface.

A summary of the locations and depth of grinding for removal of the indications is provided in Appendices B and C. During the girth weld MT examination, some indications were noted at a distance of 6 to 7 inches above the girth weld in Steam Generator 21. The indications appeared to be in remnants of welds from a fabrication attachment that were incompletely removed. These indications were removed and the areas were verified to be indication free.

The depth of girth weld grinding to remove some of the indications in Steam Generator 22 was below the minimum wall permitted. Weld repairs were required to restore the girth weld. Nine areas were weld repaired using the temper bead repair technique, as covered by ASME Boiler and Pressure Vessel Code, Section IX Case N-432.



While this technique precluded the need for a stress relieving post weld heat treatment, it required an expanded nondestructive examination. Specifically, an area 10 inches below the toe of any repair weld had to be examined by ultrasonics (UT), radiography (RT), and MT. This amounted to examining approximately 25 linear feet of the circumference of Steam Generator 22 by the techniques cited.

The results of these inspections were that a number of indications were found within the 10 inch band below the girth weld, and none were found in the band above the girth weld. A boat sample of one indication located below the girth weld was analyzed and was found to contain weld metal.

Since these inspection results implied cracking in the base metal below the girth weld, an expanded volumetric examination program was conducted using UT. This expanded program ultimately included the following: a 10 inch band below the toe of the girth weld, 360 degrees around all steam generators; one third of the transition cone for two steam generators which included the total length of a longitudinal weld, one half of each of the adjacent plates, and the lower transition zone to shell girth weld, and any interior welded attachments, if detected.

The results of these inspections were that no indications were found in any region other than the 10 inch band below the toe of the girth weld (approximately 14 inches below the centerline of the girth weld).

To further assure that the cracking was limited to the girth weld region, a UT examination was performed at the stub barrel to shell weld. Also, visual examinations were conducted at intersections of longitudinal and circumferential welds in the steam drum region. Again, in all instances, there were no relevant indications.

Subsequent examination of construction/assembly records by Consolidated Edison at Westinghouse and Lukens Steel revealed that welds were made at a distance of approximately 4 to 6 inches below the top of the transition cone to facilitate field alignment. To confirm the presence of welds in this



location, all indications below the girth weld in Steam Generators 21 and 24 were macro-etched to confirm the presence of a weld. All of these indications, 7 in Steam Generator 21 and 7 in Steam Generator 24, respectively, were found to have evidence of a weld. Based upon this sample, one indication from Steam Generator 23 was also randomly selected and macro-etched to confirm that a weld was at the indication; evidence of weld metal was found.

All indications were ground out and confirmed to be indication free by MT. Therefore, it was concluded that all of these indications were due to welds made during fabrication of the steam generators to facilitate assembly. Although the welds were ground, portions of the welds were not removed; the weld remnants eventually cracked and were found by the NDE following the weld repairs.

## 2.2 FEEDWATER NOZZLE INSPECTION

The previously established inspection plan for the nozzles was to examine by liquid penetrant (PT), and/or MT 2 of the 4 feedwater nozzle faces. If indications were found all nozzle faces would be examined. In addition, the nozzle bores would be remotely examined by fiberscope.

In each examination phase, indications were found and the inspection was expanded. To facilitate examinations of the nozzle bore, the thermal sleeves were removed from all four steam generators.

The methods of examining the bore with the thermal sleeve removed included PT, MT and to the extent possible UT and RT. The surface examinations were 360 degrees around, but in some cases were somewhat limited by the geometry of the nozzle.

The results of these additional inspections was that indications were found in the lower section of the nozzle bore primarily in the longitudinal orientation, and in the nozzle to pipe weld, circumferentially.

To better determine the mechanism of cracks within the bore region, a boat sample was removed. The results of this metallographic examination is discussed in a later section of this report.

The method of repair was to grind out all indications detected, weld back all ground areas, and to return the nozzle bore and knuckle regions to their original configuration. For the nozzle to pipe welds, the entire weld was removed and replaced.

The welding technique employed for the repairs to the nozzle face and bore was the temper bead technique.

After all repair welds were made and the nozzle machined to its original configuration, the acceptance NDE was by MT of all welded areas plus 5 inches on all sides. Also, UT and RT was performed 360 around the nozzle, to the extent practical, for acceptance and to establish a new Section XI baseline.

To further assure that no cracking was present, the thermal sleeves were examined by MT. No indications were found.

The greatest depth of cracking in the bore occurred in Steam Generator 24 and the greatest depth of cracking at the nozzle face occurred in Steam Generators 23 and 24. A summary of the maximum grindouts associated with each of nozzles appears in Table 2.2-1.

TABLE 2.2-1  
INSPECTION RESULTS  
NOZZLE AREA  
GRINDING DEPTH, IN. MAX.

SG	FACE AT BRACKET	KNUCKLE	BORE	PIPE WELD
21	0.44	0.40	0.198	0.318
22	0.40	0.00	0.295	0.388
23	0.70	0.13	0.217	0.200
24	0.70	*	0.347	0.270

\*Grinding began before baseline measurements.

## 2.3 FEEDWATER PIPE INSPECTION

The feedwater pipe was examined as a consequence of finding indications in the nozzle to pipe weld region which extended upstream of the weld. The method of detection was by visual (VT) and/or MT.

The inspection plan was to continue examining the feedwater pipe welds from the interior at each successive weld joint until the pipe and weld was visual and/or MT clear.

The examinations revealed indications in the feedwater piping. The feedwater piping upstream of the nozzles in all four steam generators were then examined.

The upstream examinations showed indications along the bottom bore area. Consolidated Edison made a decision to replace feedwater piping sections that were cracked. Replacement feedwater pipe sweeps leading to the nozzles were installed on Steam Generators 21 and 24; replacement sections of piping were installed on Steam Generators 22 and 23.

## 2.4 FEEDRING (HEADER) BRACKET INSPECTIONS

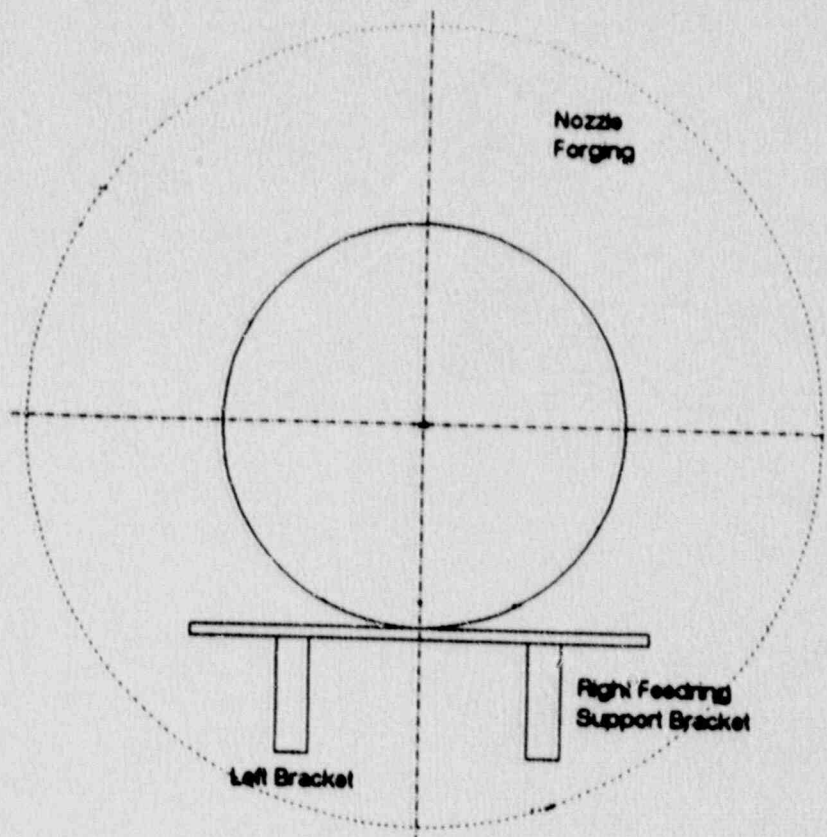
As a result of finding cracks surrounding the nozzle shelf brackets, inspections were expanded to all feedwater ring supports in all four steam generators. A depiction of these supports, their orientation relative to the feedwater nozzle and their designations is shown in Figure 2.4-1 and a detail of an A, B or C bracket is shown in Figure 2.4-2. The method of detection was either PT or, where access was available, by MT.

The method of the repair was to grind out all indications until PT or MT clear and to weld back to the original configuration unless specifically modified.

The welding technique was the temper bead process per ASME Sec. III, 1983 Winter 85 and the acceptance requirements were MT and UT.

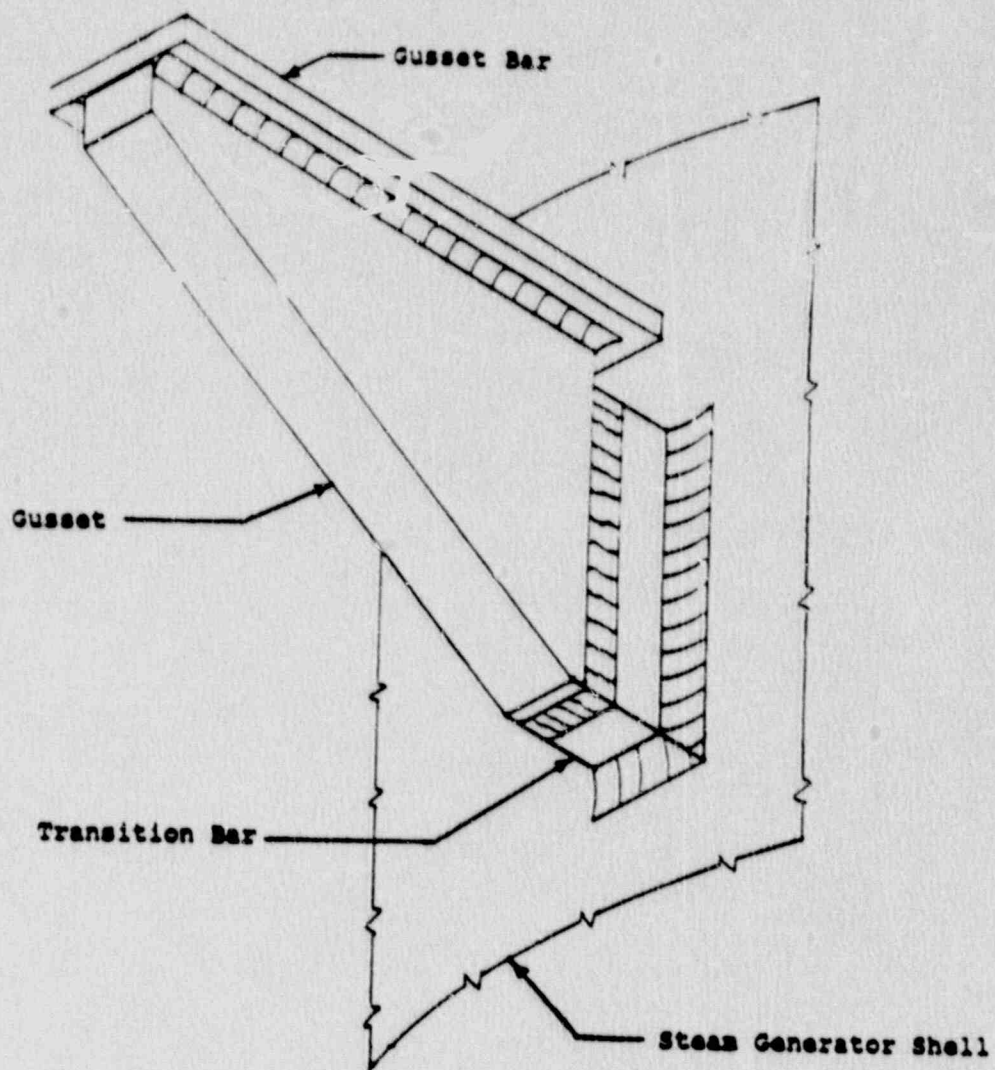


In the case of the shelf brackets for Steam Generators 21, 22, 23, and 24 the brackets were removed and placed outside of the nozzle forging onto the steam generator wall. In all cases, welding techniques employed and acceptance NDE used was consistent.



Feeding Support Geometry at Nozzle

Figure 2.4-1



Feeding A-B-C Support - Isometric View

Figure 2.4-2



## 2.5 OTHER INSPECTIONS

In addition to the above inspections, other specific steam generator areas were examined. The examinations, extent and specific NDE techniques are summarized in Table 2.5-1. These examinations included the following:

(a) 4 Inch Inspection Port - Steam Generator 22

Visual and PT examination of the bore no linear indications found, pitting was present. Macroetching of the bore of the hole revealed almost 100% weld metal.

(b) Weld Seams - Steam Generator 23

Visual examination of two (2) longitudinal, vertical, welds in the upper barrel shell was performed. Pitting was observed in weld, HAZ and base metal. No evidence of cracking was found.

(c) Weld Seam Intersections - Steam Generator 22

Weld intersections between longitudinal and circumferential welds were examined visually. The areas examined were above and below the upper deck plate. These welds, located in the steam area, showed very little evidence of pitting.

(d) Auxiliary Feedwater Injection Point - Steam Generator 22 Feedwater Line

Borescope examination of a region 6 inches into and around the 4 inch diameter feedwater auxiliary injection penetration revealed no cracks or linear indications.

(e) Underwater Inspection of Plate Material

A top/down video inspection was conducted to demonstrate that pitting, which has been determined to be a necessary precursor of cracking, was limited to the girth weld region. The video inspection showed that the number and severity (size and depth) of the pits decreased substantially as the distance from the girth weld increased.

Additional inspections of other welds along the steam generator barrel were considered unnecessary since the areas containing the stresses, geometry, and other necessary precursors to the cracking phenomenon were bounded by the examinations performed.

TABLE 2.5-1  
EXPANDED INSPECTIONS

Steam Space		
Demister to Head weld		SG 24 VT
Manway		SG 21 MT
3/4" Penetration		SG 21 VT
Plate Welds		SG 23 VT
T Sections		SG 22 VT
Water Space		
3/4" Instrument Penetration	-	SG 22,23 VT
Lower Girth Weld (Trans. Cone)	-	SG 21,22 1/3 UT
Cone Longit. Weld	-	SG 21,22 VT
Cone Plate	-	SG 21,22 1/3 UT
8" Handhole	-	SG 23 PT
6" Handhole	-	SG 23 PT
2" Penetration	-	SG 22 PT
Stub Barrel to Shell Weld	-	SG 21 UT
Attachment Weld	-	SG 21 UT
T Sections	-	SG 21,24 VT
Top/Down Video	-	SG 24 VT
Feedwater Line/Nozzles		
Thermal Sleeve	-	ALL, MT
At SG	-	ALL, MT
At AFW Injection	-	SG 22 VT



## 2.6 COMPARISON WITH PREVIOUS INSPECTIONS (1987 & 1989)

In November of 1987, ultrasonic (UT) examination performed over one-third of the length of the Steam Generator 22 girth weld revealed several indications on the inside circumference. The evidence of these indications prompted Con Edison to perform visual (VT) and magnetic particle (MT) examinations of the inside circumference of this weld seam. A localized inspection, and subsequently a 360 degree inspection, disclosed corrosion pitting and closely spaced intermittent linear indications over a large extent of the circumference. These indications were basically observed in the toe area of the weld in the contoured region between the weld and shell/cone regions.

After finding the indications in Steam Generator 22, the inspection was expanded to 100% UT and MT examination of the same welds in Steam Generators 21, 23 and 24. Examination results revealed similar, though less numerous, indications in these steam generators.

The repair process for the removal of all linear surface flaws involved controlled grinding, followed by a complete 360 degree MT examination. All ground surfaces were contoured to a maximum slope of 2:1. All final contoured surfaces were given a complete 360° MT examination and found free of linear indications. Subsurface flaws, recorded from the initial UT examination, were evaluated in accordance with Code allowables. A baseline UT examination was performed following the repair. No unacceptable indications per the ASME Code Section XI were noted. Additional Information regarding these inspections and repairs is provided WCAP-11730.

During the 1989 refueling outage, visual (VT) and magnetic particle (MT) examinations were conducted initially on 1/3 of the inside circumference of the Steam Generator 22 girth weld. These examinations were conducted as part of the ongoing steam generator girth weld examination program as identified previously in a Con Edison letter to the NRC dated December 11, 1987. Linear indications were detected during this examination. Subsequently 100% of the inside circumferences of the girth welds in all four steam generators were inspected. Linear indications were also detected in these additional examinations.

As was performed in the 1987 repair, the removal of all 1989 linear indications involved controlled grinding, followed by a complete 360° MT examination. All adjacent surfaces were contoured to a 2:1 slope. All final surfaces were found to be acceptable by a MT examination. In order to satisfy fracture mechanics criteria, some areas in Steam Generator 22 were weld repaired.

Also during the 1989 outage, a visual examination was conducted on the Steam Generator 22 feedwater nozzle inside radius section. The visual examinations detected several linear indications within the nozzle inner radius section in the bottom 120° segment of the nozzle. Visual and liquid penetrant tests were subsequently performed on the nozzles of all four steam generators. Steam Generator 22 and 23 nozzles contained similar indications whereas none were detected in Steam Generators 21 and 24. During the course of performing liquid penetrant tests on the nozzles, linear indications were also detected in support bracket welds directly below the nozzle inside radius section on Steam Generators 22 and 23. No such indications were detected in Steam Generators 21 and 24.

As a result of detecting the linear indications in the nozzle inner radius section an expanded inspection program was initiated to determine the overall condition of the feedwater nozzles. This program included radiography of all four nozzle to feedwater inlet piping welds, ultrasonic examinations of all four nozzle bores, and a borescopic examination of segments of the Steam Generator 22 and 23 thermal sleeve inside diameter surfaces and outside diameter surfaces and the nozzle bore inside diameter surfaces. The indications on the Steam Generator 22 and 23 nozzle inner radii were removed by grinding and the indications on the Steam Generator 22 and 23 support bracket welds were removed and repair welded.

Additional information regarding these inspections and repairs is provided in WCAP-12292.

Following the 1989 refueling outage, a mid-cycle inspection program (February 1990) for the steam generator transition cone upper girth weld and feedwater

nozzle was planned. Results of these inspections have been summarized in Sections 2.1 thru 2.5 of this report.

Comparisons of 1990 and previous inspections are summarized in Appendices B and C.

## 2.7 STEAM GENERATOR FABRICATION HISTORY

Reviews of Indian Point Unit 2 steam generator materials properties, welding data, and fabrication histories have been previously reported by Westinghouse reports WCAP-11730 and WCAP-12292. These reports basically concentrated on the area of the girth weld that joined the upper and lower steam generator assemblies during their original field installation. No specific deviations from industry standards related to the four steam generators (#21, 22, 23, 24) fabrication, materials, welding, post weld heat treatment or nondestructive testing were noted. These steam generators were manufactured by the Westinghouse Heat Transfer Division, Lester, PA and their subcontractors and recorded as serial numbers 16A5780-1, -2, -3, -4 respectively. All pressure boundary plate material for the barrels and cone sections including the upper hemispherical head was produced by Lukens Steel Company. Forgings in the secondary side pressure boundary were produced by other material manufacturers.

Figure 2.7-1 identifies the components and sub-assemblies of the steam generators.

### 2.7.1 Lower Shell Assembly - Fabrication at Lukens Steel Inc., Coatesville, PA

The lower shell assembly consists of three sections, one cone and two half shell cylinders. The cone is fabricated using three separate plates, longitudinally welded and post weld heat treated for 1 hour at 1125°F. The two half shell cylinders were separately welded longitudinally and each post weld heat treated in a furnace for 1 hour at 1125°F. The cylinders were joined circumferentially and were furnace heat treated for an additional hour. The cone was circumferentially welded to the half shells and the



entire subassembly post weld heat treated for 8 hours at 1125°F in a stress relieving furnace.

As described by Westinghouse drawings 799D023 - Shell Fabrication (Lower), 679J446 - Tube Bundle Assembly and Details, and Lukens Steel Drawing D-12877 - Cone and Shell Assembly the inside surface of the transition cone had welded to it, prior to PWHT, the following pieces that remain as part of the final assembly. Four alignment pads (0.25" x 2" x 2") located three inches down from the top weld end preparation and a wrapper alignment block (1.5" x 1.5" x 9") located approximately four feet down from the weld end preparation.

During fabrication of the lower transition cone (stiffener ring) weld a 2" thick cone brace was fillet welded in six segments to the cone I.D. This plate was positioned approximately four inches from the final field closure weld preparation, with each fillet weld approximately 3 inches long, for a total of 36 inches on the plate top and 36 inches on the plate underside. This brace was located in a region of the cone where discontinuities were found during the 1990 steam generator girth weld examination.

In addition to the cone brace the lower end of the lower shell barrel ("A") had a similar barrel brace (stiffener ring) installed approximately three inches from the weld end preparation. Post weld heat treatment was performed after installation of the braces.

#### 2.7.2 Tube Plate and Stub Barrel Assembly - Fabricated at Westinghouse Lester, PA

The tube plate forging whose primary face is Inconel clad and accessories welded to the secondary side surface is welded circumferentially to a stub barrel. The stub barrel was formed and fabricated at Lukens Steel and was post weld heat treated (PWHT) for four hours at 1125°F prior to shipment. After welding the tube plate and stub together circumferentially they were then furnace PWHT at 1125°F for four hours. After PWHT the tube plates were drilled for subsequent fabrication and tubing.

### 2.7.3 Tube Bundle Assembly (Tube Plate and Stub Barrel to Lower Shell Assembly) - Fabricated at Westinghouse Lester, PA

The tube plate and stub barrel assembly was circumferentially welded to the lower shell assembly using standard W weld process specification 600924. The weld was then induction PWHT at the following approximate times at temperature:

#21	#22	#23	#24
1125°F - 12 hrs.	1125°F - 12 hrs.	1125°F - 8 hrs.	1125°F - 16 hrs.
			1050°F - 4 hrs.

Steam Generator 24 was PWHT longer because of a minor repair and for correcting a roundness fit up dimension at the lower shell end. The width of the effective PWHT area during induction heating is approximately 12 to 16 inches.

After PWHT a wrapper (non-pressure boundary) was installed into the lower shell and secured to the lower assembly by a series of blocks, wedges, and keys. Any welded attachments to the shell barrels had been installed prior to PWHT. No welding was performed between the wrapper and lower shell at that time. After insertion of support plates and locking devices, U-bend tubes were installed and the ends rolled and welded to the primary side Inconel clad. After all tubing and secondary side operations were completed, the clad channel head castings were welded to the primary side of the tube plate. This weld was then induction PWHT at  $1125^{\circ}\text{F} \pm 25^{\circ}\text{F}$  one 16.5 hr period for Steam Generators 22 and 24 and for two 16.5 hr periods for Steam Generators 21 and 23 (because of intermediate weld repairs).

### 2.7.4 Upper Shell Assembly

This major pressure boundary components of the upper shell assembly consists of a lower shell barrel ("H"), upper shell barrel ("J"), elliptical head, feedwater nozzle, steam outlet nozzle, manway pad, and various bosses and support components. All welding of these pressure boundary components and

attached support components was accomplished prior to PWHT and final nondestructive testing. The minimum PWHT time and temperature any component received was approximately four hours at  $1125^{\circ} \pm 25^{\circ}\text{F}$ . Material chemical and mechanical properties of the lower shell barrel ("H") was previously transmitted by WCAP-11730. All plate material for the barrels and elliptical head was produced by Lukens Steel Company. The other forgings and components were produced by other material manufacturers.

#### 2.7.5 Upper Head

The upper head was fabricated by welding two pieces of formed plate, joining the steam outlet nozzle, and attaching lifting lugs per the criteria of Westinghouse drawing 629C230. This assembly then required a PWHT of approximately 4 1/2 hours at  $1125^{\circ} \pm 25^{\circ}\text{F}$ .

#### 2.7.6 Upper Barrels (H & J)

The upper ("J") and lower barrel ("H") sections of the upper shell assembly were longitudinally welded as two half cylinders. Shell bracing was welded in the end of each barrel approximately 3 inches from the weld preparation during this fabrication step. Feedwater ring support hardware pads and brackets were welded to the shells prior to PWHT which was then performed at  $1125^{\circ} \pm 25^{\circ}\text{F}$  for approximately 4 1/2 hours as required by drawing . The shell braces were removed during subsequent fabrication operations. The longitudinal weld seams of Steam Generator 21 and 22 were welded by Lukens Steel and Steam Generator 23 and 24 were welded by Foster Wheeler Corporation. Circumferential joining of the barrel sections and upper head occurred at a subsequent step at a different location.

Subsequent fabrication steps for each steam generator are listed below.

#### 2.7.7 Steam Generator #21 (16A5780-1) Upper

The upper half of the upper shell assembly that included the "J" Barrel and elliptical head with steam outlet nozzle installed was circumferentially



joined by Lukens Steel. The lower barrel ("H") was joined to the ("J") barrel by Westinghouse.

#### 2.7.8 Steam Generator #22, #23, #24 (16A5780-2, -3, -4) Upper

Two shell barrels ("H" and "J") and the upper elliptical head with the steam outlet nozzle weld in place were shipped to Sun Shipbuilding and Dry Dock Company for final fabrication of the upper assembly. Sun Ship joined barrels ("J" and "H") with a circumferential weld, joined the upper head to the shell barrels at the circumferential joint, and installed the feedwater nozzle, manway and bosses in the shell barrels. After completion of welding and preliminary radiography the units were PWHT at  $1125^{\circ} \pm 25^{\circ}\text{F}$  for four hours minimum. No abnormal repairs or discontinuities were seen in review of the fabrication history available. Non-pressure boundary components of the upper assemblies were installed after PWHT.

#### 2.7.9 Final Closure Weld - Upper to Lower Assemblies

Final circumferential closure welds joining and PWHT of the upper and lower halves of each steam generator was accomplished on site at Indian Point 2 by Westinghouse. Clips welded to the outside surface of the upper and lower halves provided alignment and support until the inside surface of the girth weld was completed. Upon completion of welding and in-process radiography to ensure removal of any unacceptable discontinuities the steam generator were PWHT by induction heating. WCAP-11730 previously provided PWHT time and temperatures and other associated weld information. The PWHT information is repeated below for reference.

<u>Steam Generator</u>	Post Weld Heat Treat (PWHT) <u>Time at Temperature</u>	PWHT Equivalent
		<u>1125°F ± 25°F</u> (Expressed in Hrs)
Steam Generator 21 (16A5780-1)	7 hrs @ 1050°F - 1150°F (3 hrs 35 minutes @ 1125° ± 25°F)	3.6

<u>Steam Generator</u>	<u>Post Weld Heat Treat (PWHT)</u> <u>Time at Temperature</u>	<u>PWHT Equivalent</u> <u>1125°F ± 25°F</u> <u>(Expressed in Hrs)</u>
Steam Generator 22 (16A5780-2)	12 hrs @ 1025°F - 1150°F (4 hrs 15 minutes @ 1125°F ± 25°F)	4.25
Steam Generator 23 (16A5780-3)	7 hrs 30 min @ 1050°F - 1150°F (3 hrs 45 minutes @ 1125°F ± 25°F)	3.75
Steam Generator 24 (16A5780-4)	12 hrs @ 1000°F - 1150°F (4 hrs 10 minutes @ 1125°F ± 25°F)	4.15

The effective band of PWHT during this final cycle is approximately 16 inches.

#### 2.7.10 General and Conclusion

Westinghouse Lester in addition to normal in house inspection performed follow-up inspections and review at all the subtier fabricators. The welding procedures and fabrication methods used were at some point witnessed during the fabrication cycles. Upon completion of this and previous reviews Westinghouse concluded that the fabrication methods and cycles were consistent with other similar steam generators. The fabricators used for these steam generators were the same as used for previous and subsequent units. There are no known discontinuities or fabrication abnormalities discovered by review of the histories.

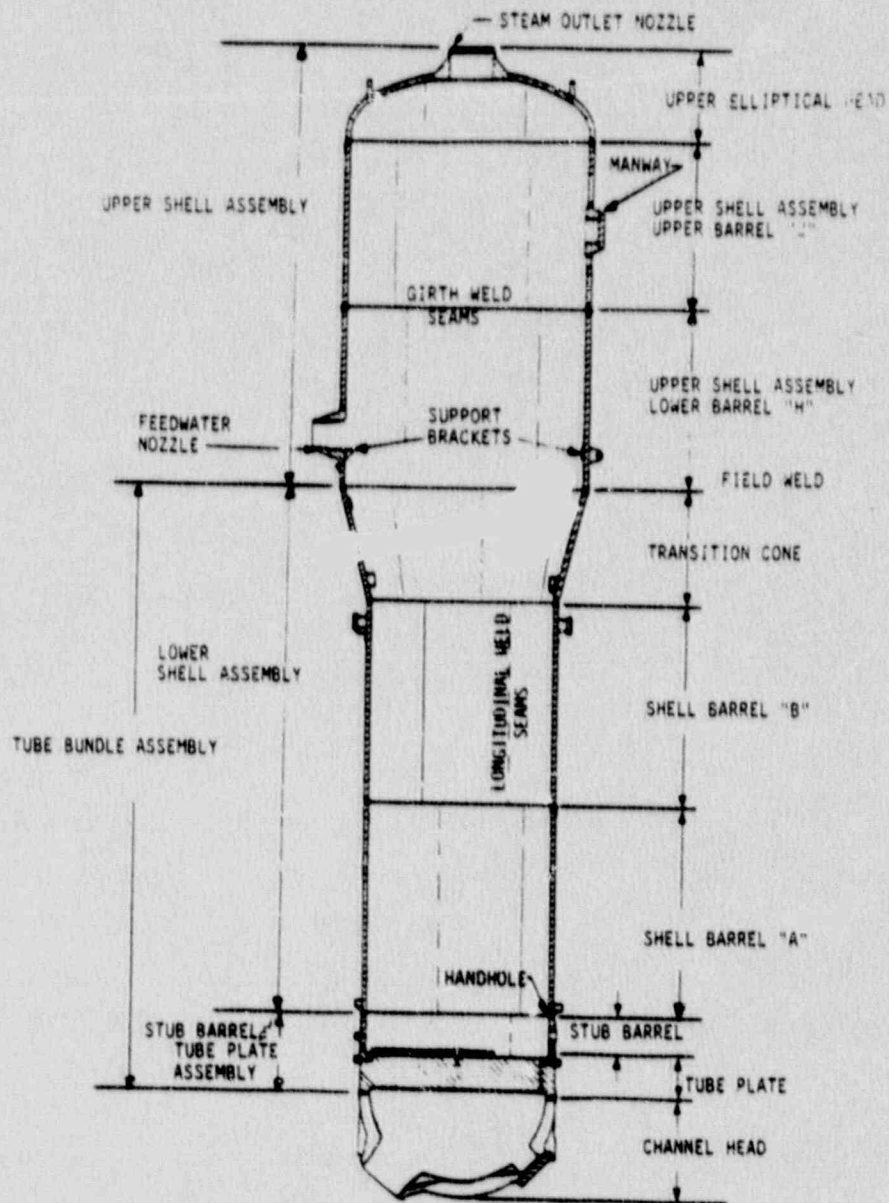


Figure 2.7-1



### 3.0 METALLURGICAL EVALUATIONS

The metallurgical evaluations presented in this section include:

- o Metallurgical investigation of the boat samples taken from the internal surface of several steam generators to establish the mechanism and cause(s) of cracking.
- o Mechanical property tests on the material from service to examine if it meets the original material property requirements.

The evaluations and results are summarized below.

#### 3.1 BOAT SAMPLE EVALUATIONS

This section summarizes the results of the metallurgical investigation of boat samples containing indications from the steam generator girth weld, cone, feedring support and nozzle regions removed during the 1989 and 1990 outages. The investigation included the following boat samples taken during the 1990 outage:

- o One boat from the girth weld of Steam Generator 24
- o One boat from the girth weld of Steam Generator 22 (from 1989 weld repair area)
- o One boat from the transition cone just below the girth weld of Steam Generator 22
- o One boat from the nozzle bore of Steam Generator 24
- o Three feedring supports from Steam Generator 21 and 24

The evaluation included the following major tasks:

- o Surface examination of the as-received boat samples by light optical and scanning electron microscopy techniques
- o Metallographic examination of the boat sections containing the major cracked regions by light optical microscopy

- o Fractographic examinations of the freshly opened and endoxed cracks by light optical and scanning electron microscopy techniques
- o High resolution transmission electron microscopy examination of replicas from the fracture face
- o Hardness traverse measurements of the material microstructure containing the cracked regions
- o Chemistry evaluation of the crack deposits, ID surface deposit scrapings and weld and base materials.

## 3.2 EVALUATIONS AND TESTS

### 3.2.1 Surface Examinations

The as-received surface condition of the boat samples was examined for surface corrosion, cracks, pitting and deposits visually and by low power light optical microscopy. The surface condition was documented by photographic recordings. The results of the surface examinations are illustrated in Figures 3.2-1 and 3.2-2. Figure 3.2-1 illustrates the typical surface condition of the girth weld samples.

Figure 3.2-2 illustrates the surface condition of the nozzle bore sample.

### 3.2.2 Metallographic Examinations

Light optical metallographic examinations were performed on transverse sections containing the major cracked regions of the boat samples. The examinations were conducted to establish the depth and distribution of cracking and to identify initiation sites and propagation directions, the cracking morphology and its relationship to the local microstructure. The results of the metallographic examinations are illustrated in Figures 3.2-3 and 3.2-4. Figure 3.2-3 illustrates the typical transgranular morphology of cracks seen at the girth weld.

Figure 3.2-4 illustrates the crack transgranular morphology at the feeding thermal liner support bracket plate to weld interface.

### 3.2.3 Fractographic Examinations

Fractographic examinations were conducted on freshly opened and endoxed fracture faces by light optical, scanning electron and replica transmission electron microscopy techniques. Light optical fractographic examinations primarily established the crack initiation sites, propagation directions and the presence of beach marks or crack arrest lines while the scanning electron fractography established the morphology of the fracture and of the crack deposits. The high resolution transmission electron microscopy conducted on endoxed fracture faces established the presence of fine fracture features such as fatigue striations. The results of the fractographic examinations from both the 1989 and 1990 outages are illustrated in Figures 3.2-5 through 3.2-10. Figures 3.2-5, 3.2-6 and 3.2-9 show the 1989 outage examinations on the girth weld boat samples from Steam Generator 22 and Steam Generator 24. Figure 3.2-5 illustrates a light optical fractograph from the Steam Generator 24 boat sample indicating beach marks. Figure 3.2-6 illustrates a light optical fractograph from the Steam Generator 22 boat sample showing a smooth and continuous crack with multiple origins. Figure 3.2-9 shows a scanning electron fractograph of the endoxed fracture surface from the Steam Generator 24 boat sample. Fine fatigue striations are observed.

Figure 3.2-8 shows a representative light optical fractograph from the 1990 Steam Generator 22 boat sample taken in the core region below the girth weld. A smooth river pattern fracture is observed.

Figures 3.2-7 and 3.2-10 illustrate light optical and scanning electron fractographs, respectively, of the 1990 Steam Generator 24 nozzle bore boat sample. Numerous beach marks are seen on Figure 3.2-7. Figure 3.2-10 indicates that fine fatigue striations are present.

### 3.2.4 Chemistry Evaluations

Chemistry evaluations were conducted to examine the role of any contaminants in the cracking process and to confirm the material chemistry. The chemistry analysis of the crack deposits in the boat samples was conducted by energy dispersive x-ray (Edax) analysis. Wet chemistry analysis was conducted on



the ID surface deposit scrapings of the steam generator. The results of the energy dispersive x-ray chemistry analysis are typically presented in Figure 3.2-11.

The results show that all the crack deposits consistently comprise copper species.

### 3.2.5 Hardness Measurements

Microhardness measurements were conducted on polished and etched sections near the cracked regions to establish the strength of the local microstructure and the associated residual stresses.

For the girth weld/transition cone samples (original surfaces), the results of the hardness measurements of the heat affected zone and base metal regions in the near vicinity of the pitting and cracks typically showed hardness values ranging from 20 to 37 Rockwell 'C' in the heat affected zone region and an average value of 91 Rockwell 'B' in the base metal.

Hardness values of the 1989 weld repair area sample having no cracks were measured as 25-28 Rockwell 'C' in the weldment, 23-31 Rockwell 'C' in the heat affected zone, and 89-91 Rockwell 'B' in the base metal.

### 3.2.6 Mechanical Property Tests

Tensile, Charpy V-notch and fatigue endurance test were conducted on axially-oriented samples machined from the plate material from steam generator feed ring supports. The results are summarized in Table 3.2-1. The results shown here demonstrate that the material meets the tensile, Charpy toughness and fatigue property requirements expected of the original material.

## 3.3 RESULTS OF GIRTH WELD/TRANSITION CONE SAMPLES EXAMINATIONS

The results of the surface examinations on the boat samples from the girth welds of Steam Generators 22 and 24 and the cone below the girth weld on Steam Generator 22 (see Section 3.1 above) showed evidence of surface pitting

and corrosion products. The ID surface indications seen were primarily associated with linked-up surface pits and were oriented circumferentially at the cone and girth weld region. The results of the metallographic examinations by light optical and scanning electron microscopy techniques on transverse sections of the boat samples showed that the indications were cracks that initiated from surface pits and both were filled with oxide. Multiple crack initiation was often seen originating from the pitting in the vicinity of the major cracks. The cracking exhibited minor branching although the crack growth was generally straight and followed a radially outward direction towards the external surfaces of the vessel. The cracks were extensively filled with iron oxide deposits including the crack tip regions. The metallographic examinations showed that the pitting and crack initiation in the cone and girth weld samples occurred at either the weld metal, weld-to-base metal interface or in the heat affected zone regions. The presence of copper, and occasionally zinc and sulphur was seen in the crack deposits. Chemistry evaluation of the crack deposits by Edax analysis and wet chemistry analysis of the surface scrapings confirmed the presence of copper. The results of the hardness measurements of the heat affected zone and base metal regions in the near vicinity of the pitting and cracks typically showed hardness values ranging from 20 to 37 Rockwell 'C' in the heat affected zone region, and an average value of 91 Rockwell 'B' in the base metal.

The results of the fractographic examinations of samples taken during the 1987, 1989 and 1990 inspections revealed evidence of two distinctly different modes of environmentally assisted fracture morphology depending on the crack examined and the location of boat sample taken. The fracture morphology showed evidence of extensive beach marks in some cracks with evidence of fine fatigue striations (1989 outage only), suggesting crack extension with minor branching under intermittent loading conditions (corrosion fatigue) while other cracks (1989 and 1990 outages) showed smooth continuous crack extension (and no fatigue striations) characteristic of environmentally assisted crack growth under static load conditions (stress corrosion).

### 3.4 RESULTS OF 1989 WELD REPAIR AREA SAMPLE EXAMINATIONS

Some minor pitting was seen on the welded surface. These were shallow and widely scattered. Hardness survey showed values of 25-28 Rc in the weldment, 23-31 Rc in the heat-affected-zone, and 89-91 Rb in the base metal. There were no cracks in the 1989 weld repair sample.

### 3.5 RESULTS OF NOZZLE BORE SAMPLE EXAMINATIONS

Surface examination of the nozzle bore sample from Steam Generator 24 showed axial cracking associated with linked up surface pits. Metallographic examinations showed multiple crack initiation from oxide covered pits. The examinations further showed that the nozzle bore crack measured approximately 0.07 inch at its deepest location. Scanning Electron Microscope (SEM) fractographic examination of the endoxed fracture faces confirmed evidence of fine fatigue striations in the cracks containing beach marks suggesting the role of fatigue loads in the cracking process. The evidence of oxide covered pits, multiple crack initiation from the pits and the presence of copper contaminants suggest that the cracking was initiated at the surface pits and caused by corrosion. Replica transmission electron fractography examinations confirmed the presence of fine fatigue striations. The presence of fatigue striations confirm the mechanism of propagation to be corrosion fatigue.

### 3.6 RESULTS OF FEEDRING SUPPORT EXAMINATIONS

The feedring thermal sleeve support consists of two triangular support brackets spanned by a shelf plate. These brackets were welded to the shell with a full penetration and a fillet weld all around. The shelf was welded to the brackets with fillet welds. A general arrangement of this configuration is shown in Figure 2.4-1.

Cracking was seen in the support brackets plates and at welds. Samples of brackets from all four generators were examined by Westinghouse, Massachusetts Institute of Technology (M.I.T.), Lehigh University and Lucius Pitkin, Inc.



Examination of the Steam Generator 21 bracket showed straight, heavily corroded cracks with blunt, rounded tips, indicating that the cracks had been present for a long time and were non-propagating. This is typical of the other support bracket cracks examined. Mechanical properties, including fatigue endurance limit and impact strength, were within the acceptable range and did not show any noticeable degradation.

### 3.7 CONCLUSIONS

One boat sample (Steam Generator 24) taken during the 1989 inspections showed that surface pitting contributed to the crack initiation and showed evidence of extensive beach marks in the crack, suggesting crack extension under intermittent loading (corrosion fatigue). The fracture morphology of the rest of the 1989 samples and the 1990 samples, however, indicated that surface pitting contributed to the crack initiation and showed primarily a smooth continuous crack extension with slight branching (and no fatigue striations) characteristic of environmentally assisted crack growth under static load conditions (stress corrosion). Based on the overall results of the evaluation, it is concluded that the cracking in the Indian Point Unit 2 steam generator girth weld and transition cone is caused by corrosion fatigue and/or stress corrosion mechanisms. As a result of changes made in 1989 (modification of feedwater flow control valve and removal of downcomer resistance plate), the impact of fatigue mechanism has been minimized.

The cracking in the nozzle bore region is clearly caused by a corrosion fatigue mechanism. The presence of a multitude of fine fatigue striations suggests that the cracking in the bore may have been induced by cyclic fatigue loads and may have occurred over a long period of time. Surface pitting contributed to the crack initiation.

The results of the tensile, Charpy toughness and fatigue property tests on the bracket plate material confirmed that the material did not suffer any degradation from its original condition as a result of service conditions.

TABLE 3.2-1

MECHANICAL PROPERTY TEST RESULTS  
FEEDRING SUPPORT SHELF MATERIAL STEAM GENERATOR 21

1. Tensile Tests

	<u>0.2% Yield Strength</u>	<u>Tensile Strength</u>	<u>Total Elongation</u>	<u>Reduction In Area</u>
	(ksi)	(ksi)	(%)	(%)
Shelf Material	47.35	70.39	28.6	63.6
ASTM A 516 GR 70 MAT'L	38	70-90	21	-

2. Charpy Toughness Tests

Upper Shelf: 98.5 ft lbs. at 50°F

Lower Shelf: 1 ft lbs. at -100°F

FATT: 25°F

3. Fatigue Tests

Endurance Limit: ~33 ksi

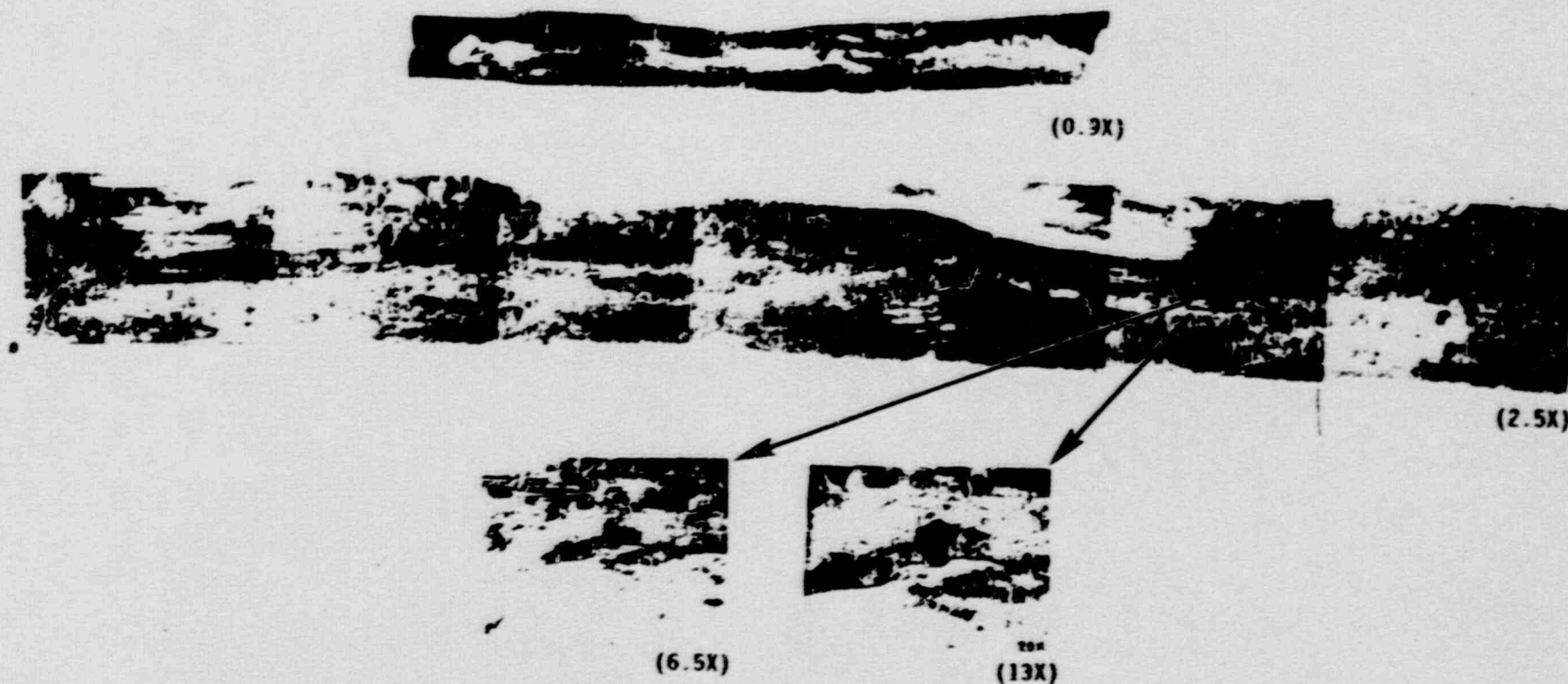


Figure 3.2-1 As-received surface appearance of the boat sample from Steam Generator 24 girth weld, illustrating the surface pitting and cracking seen on the ID surface. (1989 outage examinations)





(1.35x)

Figure 3.2-2 Surface appearance of the as-received boat sample from the nozzle bore. (SG #24 1990 outage examinations)

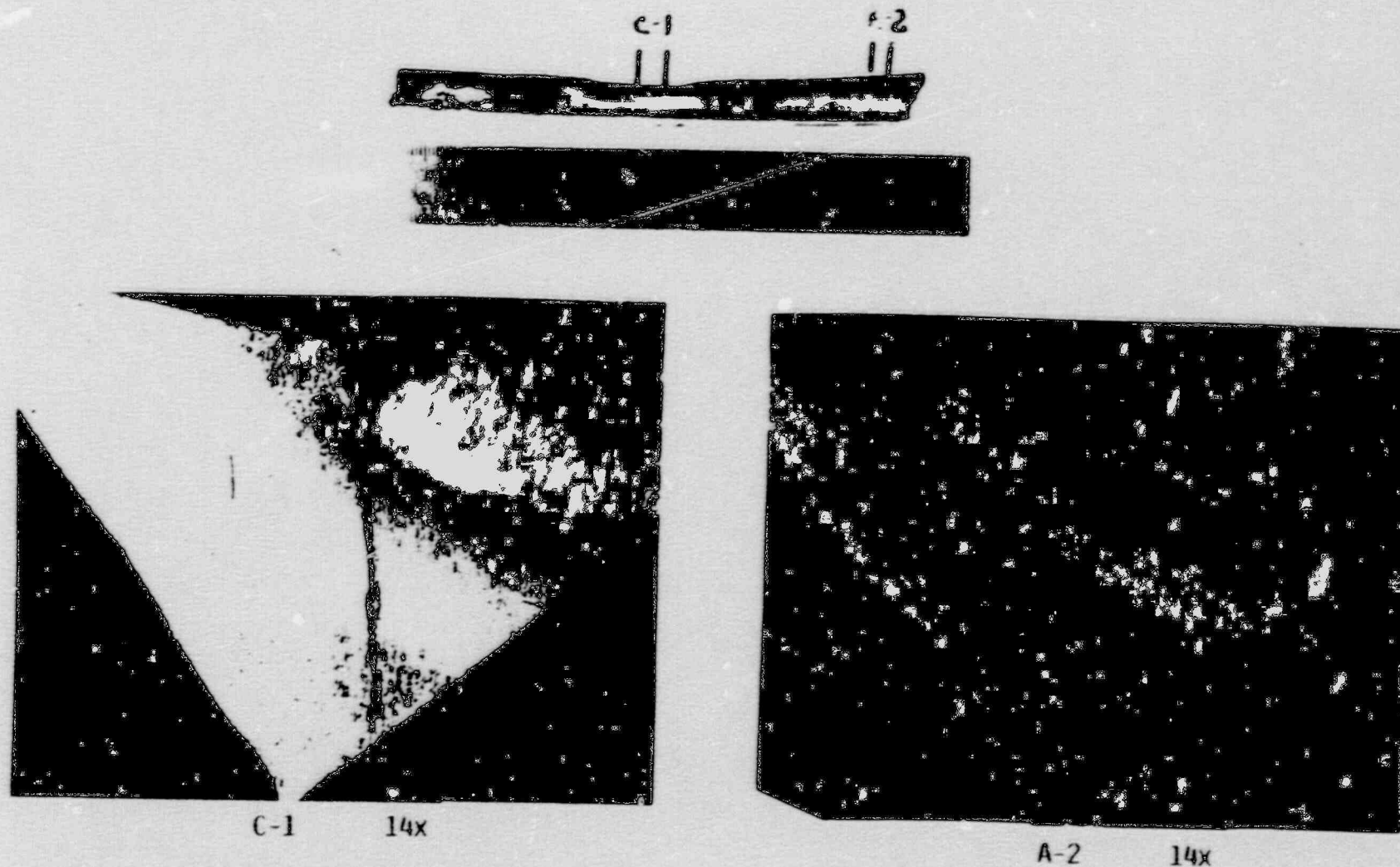


Figure 3.2-3 Metallographic examination results illustrating the cracking morphology and microstructure.  
(SG #24 1989 outage examinations)

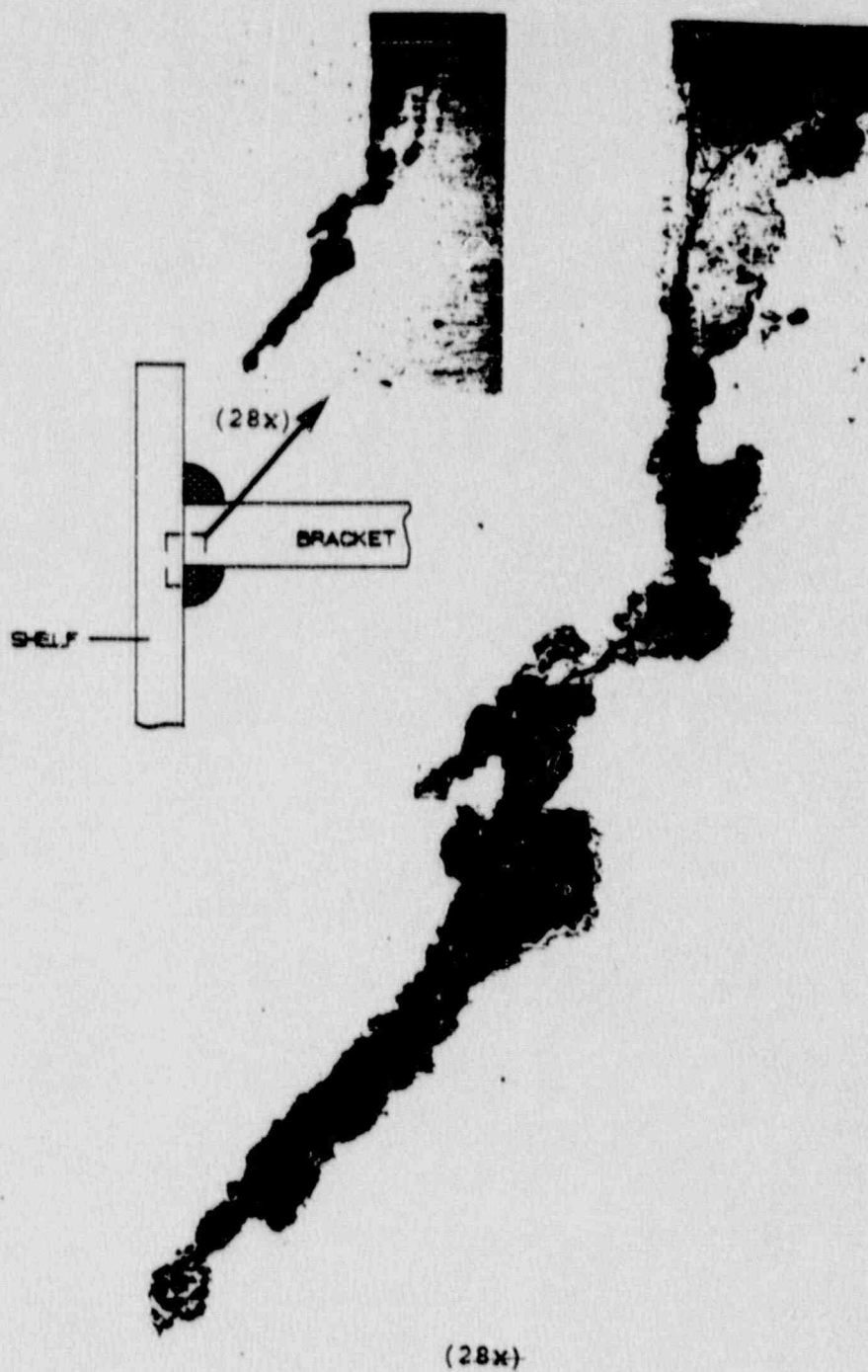


Figure 3.2-4 Metallography results illustrating the morphology of cracking at the feedring thermal liner plate to weld interface. (SG 21 1990 outage examinations)



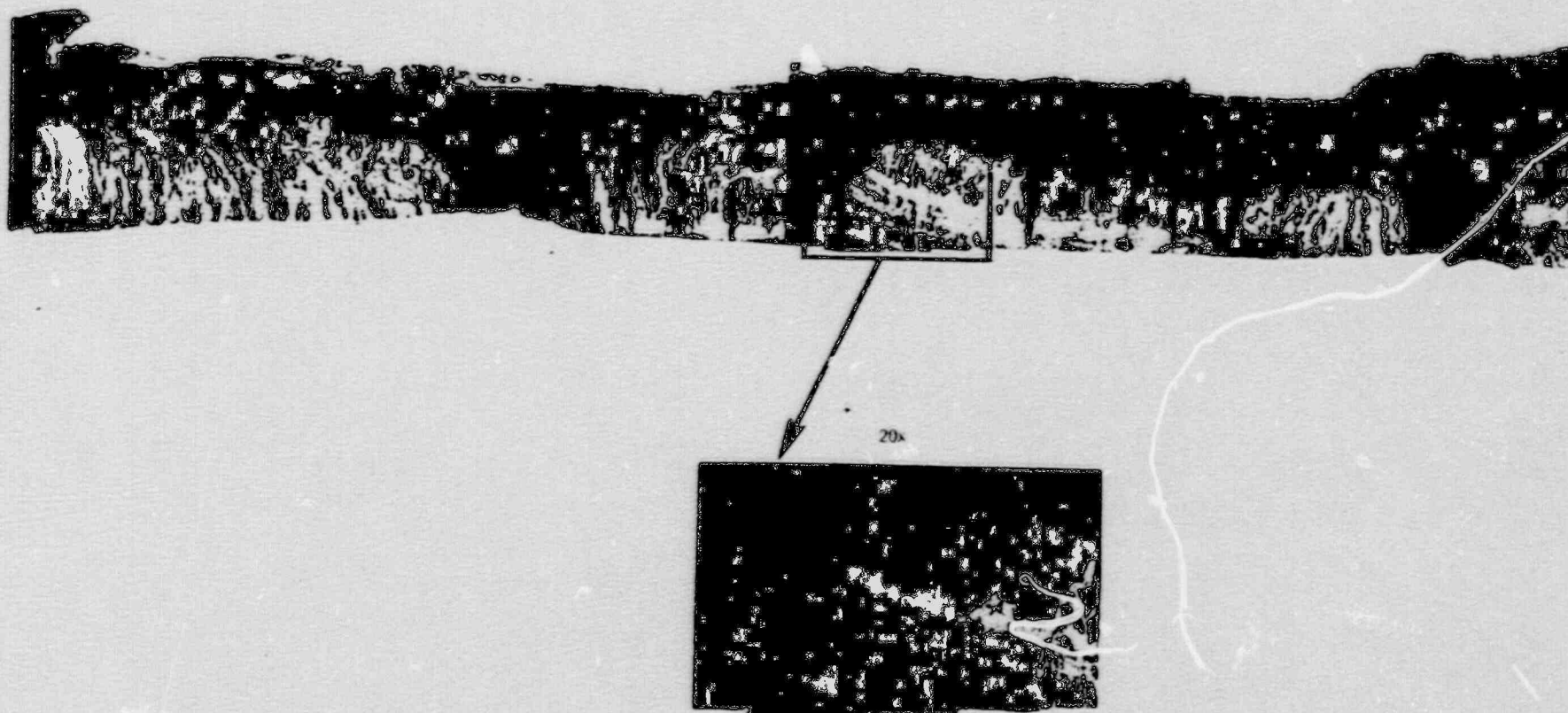


Figure 3.2-5 Light optical fractography results illustrating the beach marks seen in the endoxed fracture face in the girth weld sample from the 1989 outage.  
(SG #24 1989 outage examinations)

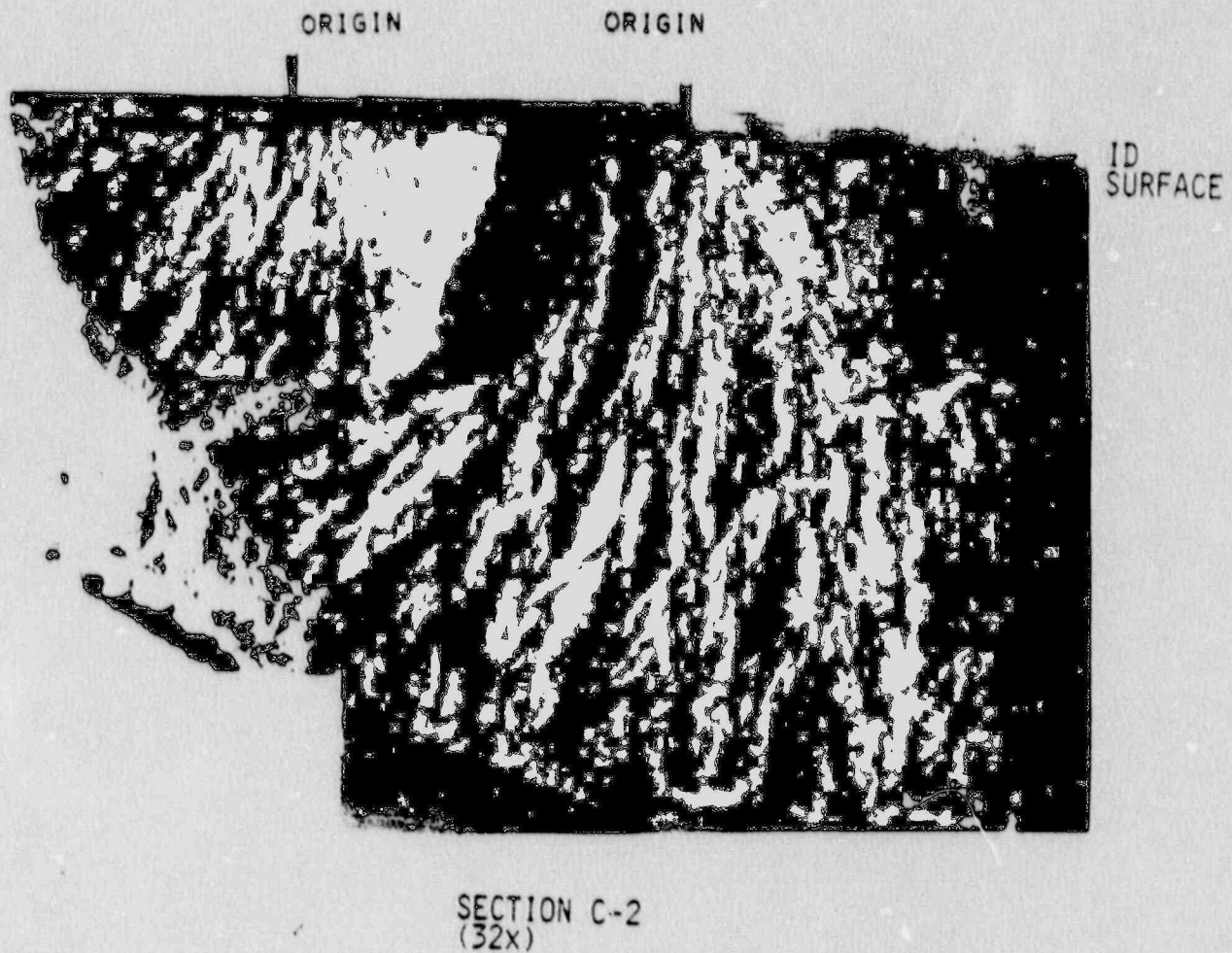
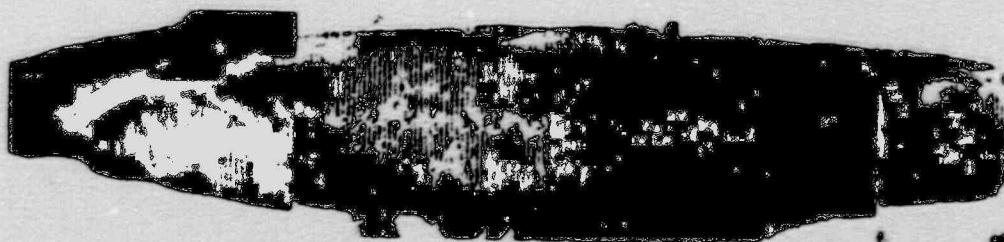


Figure 3.2-6 Light optical fractograph illustrating the fracture morphology seen in the SG #22 boat sample from the 1989 outage.



(1.2x)

Figure 3.2-7 Light optical fractograph of the crack in the boat from the nozzle bore. (SG #24 1990 outage examinations)





Figure 3.2-8 Light optical fractograph showing smooth river pattern in the boat from the cone region below the girth weld. (SG #22, 1990 outage examinations)

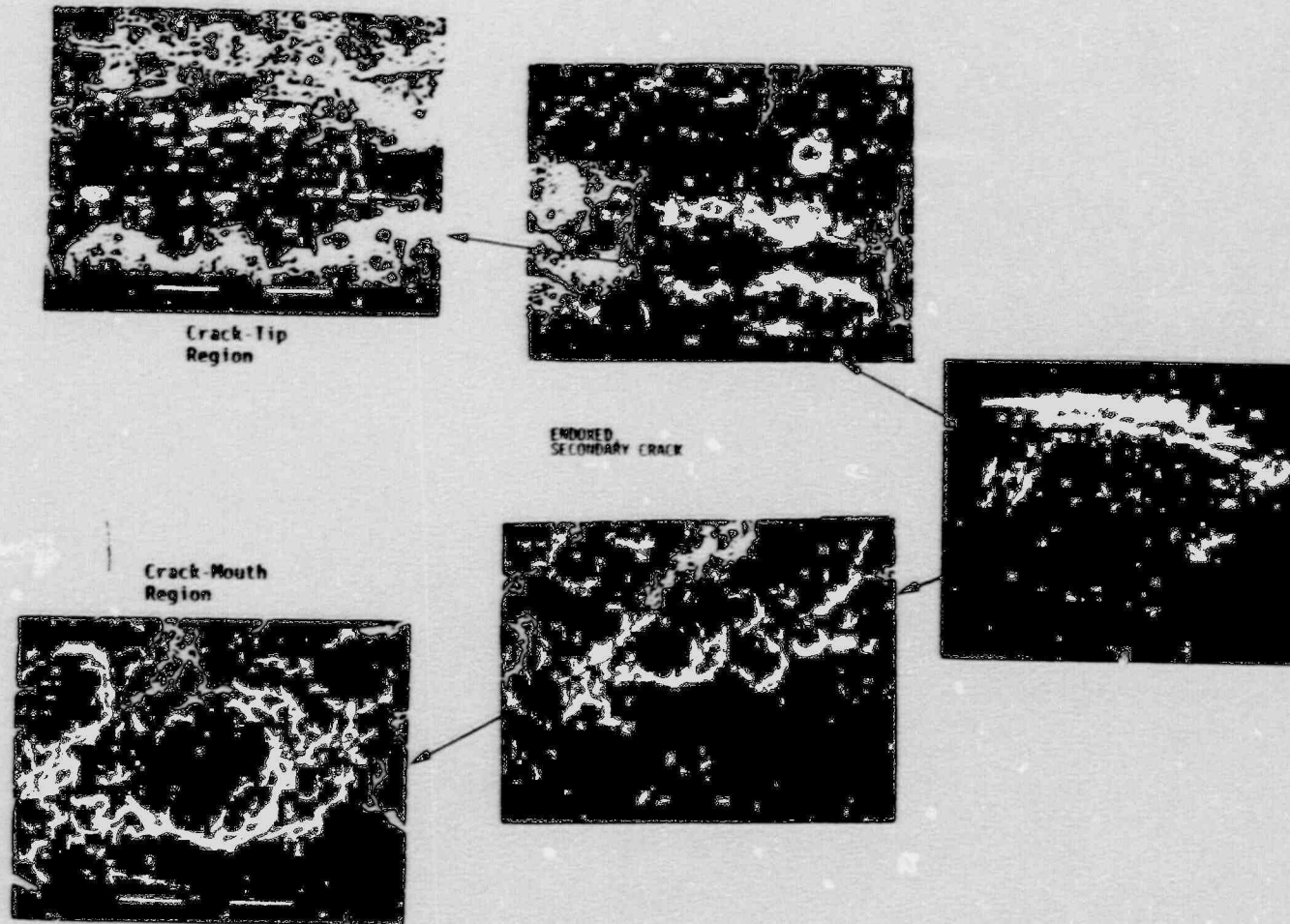


Figure 3.2-9 Scanning electron fractograph of the endoxed fracture face illustrating the presence of fatigue striations in the girth weld sample from the 1989 outage. (SG #24, 1989 outage examinations)

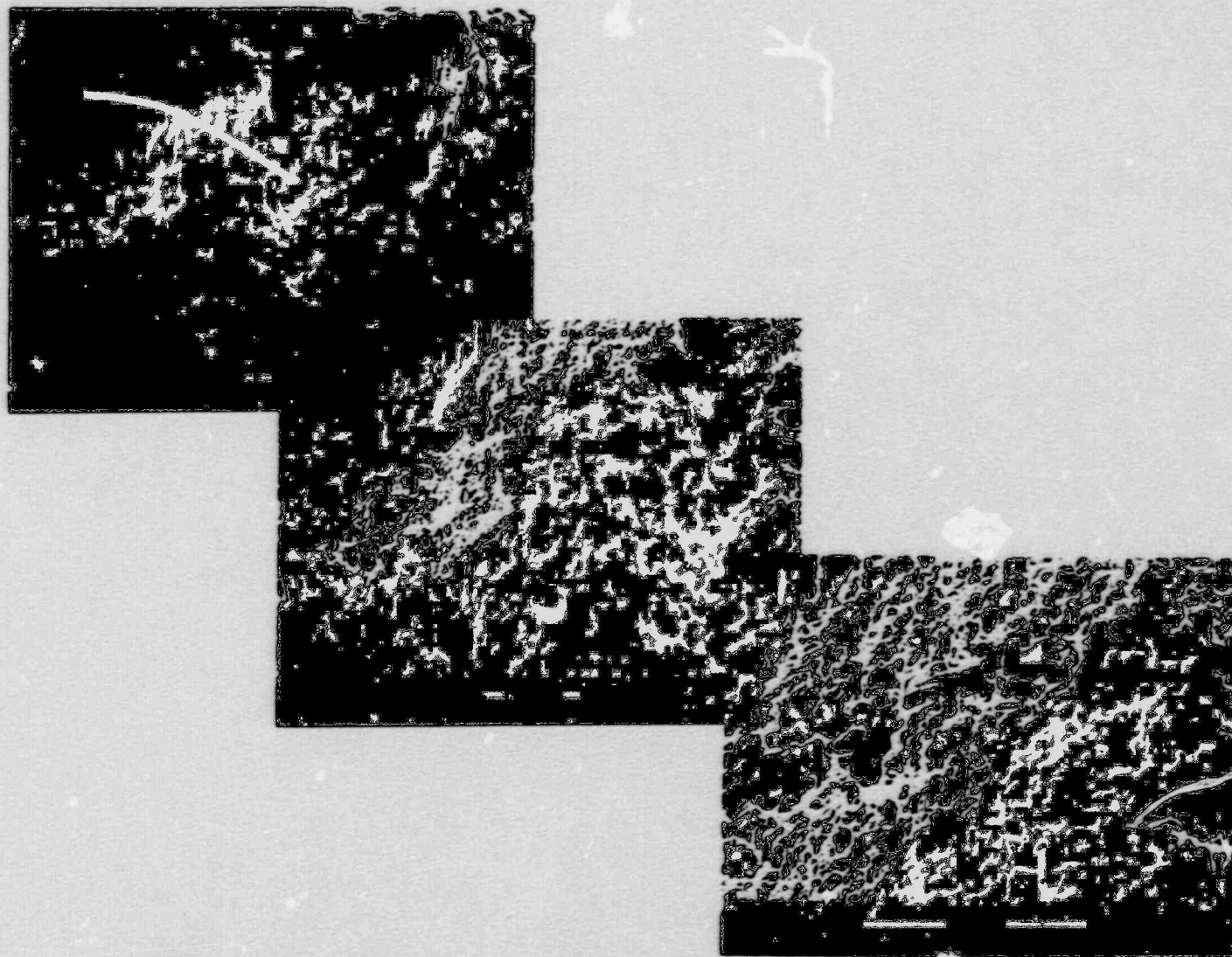


Figure 3.2-10 Scanning electron fractographs illustrating fine fatigue striations in the nozzle bore samples. (SG #24, 1990 outage examinations)



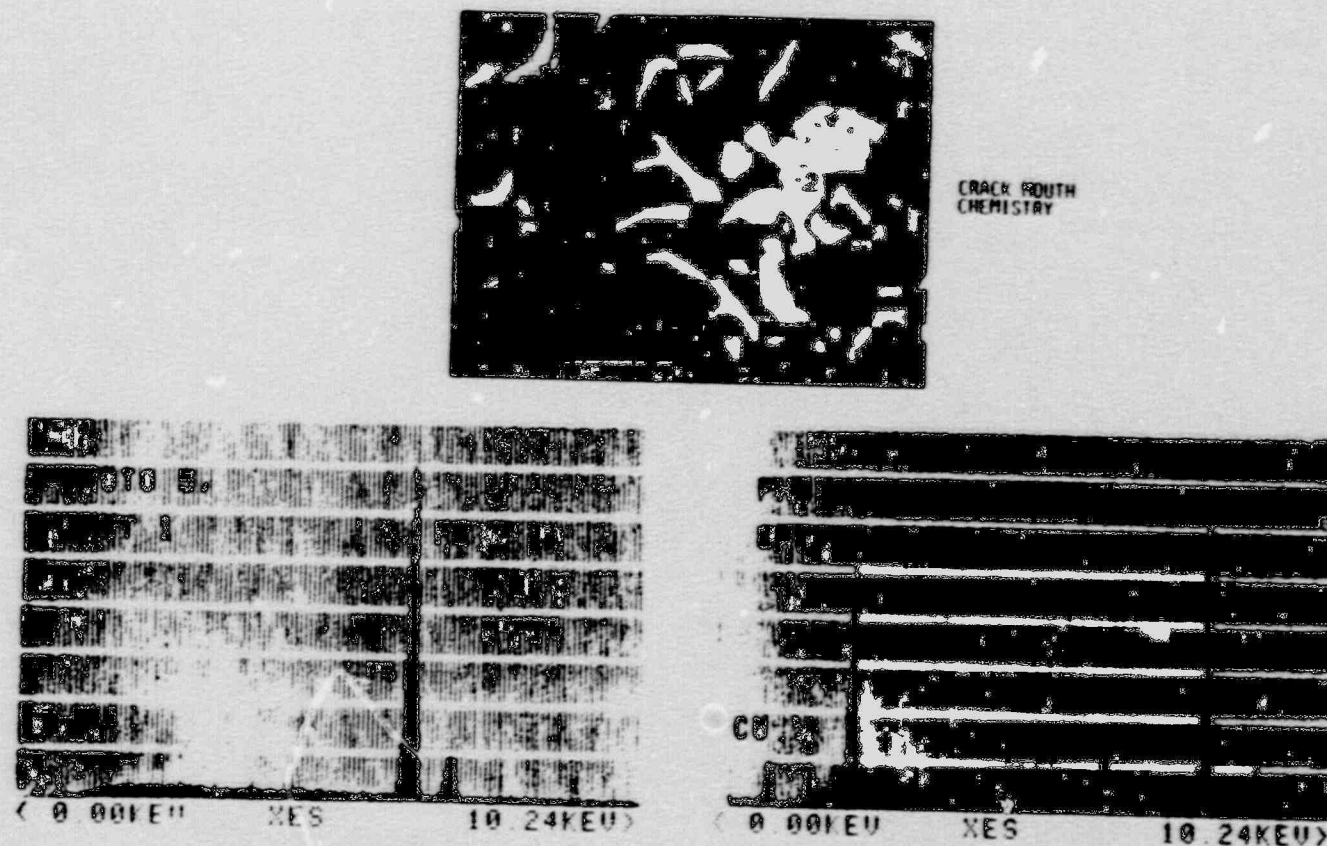


Figure 3.2-11 Energy dispersive X-ray analysis results from the SG #24 girth weld boat sample crack, 1989 outage.

#### 4.0 EVALUATION OF STEAM GENERATOR CHEMISTRY AND OPERATIONS

##### 4.1 CHEMISTRY BACKGROUND

Indian Point 2 contains four 44 Series steam generators manufactured by Westinghouse. The plant began functional testing in 1971 and began commercial operation in 1974. Phosphate was used for corrosion control until 1975 when the chemistry was changed to AVT (ammonia/hydrozine). In 1979, the chemistry was changed to AVT/Boric Acid to further eliminate steam generator tube thinning and minimize tube denting. This chemistry treatment has continued until the present and has been typical of industry practices.

##### 4.1.1 Operational Chemistry

Chemistry parameters for Indian Point 2 have historically been typical of comparable plants using Ammonia/Boric Acid treatment.

Feedwater dissolved oxygen concentrations have been measured to be less than 5ppb over the operating life of the plant. Significant reductions in steam generator blowdown chlorides have been achieved over the past operating cycles. Presented below are the average Chloride and Dissolved Oxygen concentrations over the past operating cycles.

<u>Operating Cycle</u>	<u>1978-79</u>	<u>1979-80</u>	<u>1981-82</u>	<u>1983-84</u>	<u>1984-86</u>	<u>1986-87</u>	<u>1988-89</u>
Dissolved Oxygen in Condensate ppb (avg)	10	3	2	13	9	4	6
Chloride in Steam Generator Blowdown, ppb (avg)	68	63	41	54	34	18	10

##### 4.1.2 Plant Materials and Water Sources

During original plant construction Indian Point 2 low pressure feedwater heaters and MSR's were tubed with 90-10 copper-nickel alloy while the high pressure heaters contained 80-20 copper-nickel alloys. The condenser tubes

were fabricated from admiralty brass. The metals and alloys used in the fabrication of secondary components at Indian Point 2 are typical of other nuclear power plants. Many nuclear plants, including Indian Point 2, are in the process of changing out the copper alloys in the secondary system to copper free alloys to eliminate the build up of copper in the sludge and the plate-out of this element in the steam generators and other secondary system components. In addition, replacement of the copper alloys permits the operation of the condensate/feedwater systems at a higher pH, thereby, minimizing corrosion of the iron alloys in these systems.

The MSR's and the high pressure feedwater heaters were replaced with ferrous alloy tubes (439 and 304L stainless steels, respectively) at Indian Point 2 in 1982. These units were determined to be the major contributors to the introduction of feedwater copper. In 1987, the copper in the remaining feedwater heaters was replaced with type 304L stainless steel, with the exception of the low pressure feedwater heaters in the neck of the condenser. The remaining copper tubing in the system, including the condenser tubes will be replaced in the next two refueling outages.

Cooling water delivery to the condenser comes from the Hudson River, which has seasonally and tidally contained chloride concentration of 5000ppm to 0.1ppm. Condenser leakage results in the river water impurities entering the secondary cycle and ultimately the steam generators. These impurities will concentrate in the steam generators due to the large mass of steam being generated. In the low flow and stagnant areas, called crevices, the impurity concentrating effects could contribute to corrosion of steam generator materials. The scheduled replacement of the condenser tubes with titanium will essentially eliminate condenser leakage.

Original plant design provided for make-up water to the plant from a conventional demineralizer water treatment facility with city water being the water source. Numerous upgrades to the original facility have improved make-up water quality and reduced steam generator contaminants. The quality of the make-up water at Indian Point 2 has historically been within the recommended guidelines of Westinghouse and EPRI.



#### 4.1.3 Sludge Composition

Sludge analyses from the Indian Point 2 steam generators have consistently shown iron and copper as the predominant components. Zinc and nickel are also present and, to a lesser degree, calcium, magnesium and silica. Corrosion of various secondary system components and condenser leakage account for the elements found in the sludge.

The sludge analysis from Indian Point 2 and steam generators of other sites suggest that it is unlikely that the sludge, which concentrates on the tubesheet and lower support plates, has any significant effect on the corrosion in the steam generator girth weld areas.

#### 4.2 EFFECT OF PLANT OPERATIONS ON STEAM GENERATOR MATERIAL CONDITION

There are periods in which the steam generator internals may be subject to higher corrosion rates than those which occur during normal full power operation. Shutdowns, draindowns and startups can cause the steam generator internals to be exposed to oxygen concentrations in excess of 7 ppm. During startups and shutdowns, various auxiliary systems are utilized to cool the plant. One of these is the auxiliary feedwater system which supplies feedwater to the steam generators to control the temperature in the reactor coolant system. The major source of this water is the condensate storage tank. This water is injected directly into the secondary side of the steam generator without heating. For many plants, this water is oxygen saturated without chemicals to control oxygen (hydrazine) and pH (ammonia). Both these chemicals act to reduce the likelihood of corrosion of the internal surfaces of the steam generators and other internal surfaces. Indian Point 2 has completed modifications to reduce the thermal transient during auxiliary feed and reduce the dissolved oxygen concentrations of the condensate storage tank.

##### 4.2.1 Comparison of Plant Auxiliary Feedwater Practices

The introduction of oxygen into the steam generator, through auxiliary feedwater or air, may be a factor in the girth weld cracking that has been

identified in a number of steam generators. This condition has not been limited to any one particular model of the Westinghouse steam generators.

Table 4.2-1 lists four plants along with Indian Point 2 that have experienced this condition. Two plants, Surry and Trojan, minimize the introduction of oxygenated water into the steam generators during startup. Zion and Turkey Point introduce oxygen saturated water into the steam generators from the auxiliary feed system.

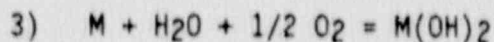
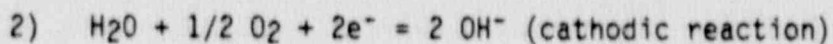
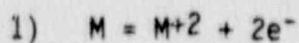
In the past, the Indian Point 2 condensate storage tank (CST) had been open to the atmosphere, resulting in oxygen saturated water. The addition of oxygen through the auxiliary feedwater system to the steam generators may have been a major contributing factor to girth weld cracking at elevated temperatures. Oxygen alone or in combination with other chemicals can promote general and enhanced localized corrosion of the materials in the steam generator, depending on local temperatures and the quantity of dissolved oxygen.

A recent (June 1990) installation of a nitrogen sparging system in the CST at Indian Point 2 has demonstrated to be effective in maintaining the oxygen concentration in the CST below 100 ppb. The CST contains a floating rubber diaphragm which was designed to inhibit oxygen from the atmosphere dissolving in the water. However, the space below the diaphragm is vented to the atmosphere. An installed sparging system provides a nitrogen cover gas between the water and the diaphragm. In addition, the nitrogen is maintained at a slightly positive pressure to purge a vent line blocking the entrance of oxygen into the condensate tank.

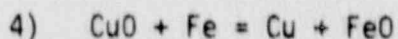
#### 4.2.2 Corrosion Mechanisms of Nuclear Steam Generators During Wet Layup

The transport of secondary system corrosion products into the steam side of a steam generator can result in the accumulation of iron and copper sludges on the tubesheet and deposits on other internal surfaces. Sludge piles containing these materials have been associated with the development of conditions which may influence steam generator tube cracking and thinning. In addition, the presence of copper and copper compounds in these deposits

may contribute to the corrosion of steam generator construction materials (i.e., girth weld pitting), if they are disassociated from the sludge piles. To minimize the formation of corrosion products in the steam generators, revised layup procedures have been instituted for both short and long term shutdowns. One important consideration during layup is to exclude oxygen from the steam generator internals. Oxygen can promote corrosion of carbon steel surfaces (i.e., girth weld) particularly at the air/water interface where the metallic surfaces are constantly exposed to water and atmospheric oxygen. Localized differential aeration cells can be formed leading to pitting. The general chemical reactions that occur in these cells may be described basically as follows:



where M is the base metal. Copper oxide can also play an important role in the formation of pits on metal surfaces according to the following reaction:



The exclusion of oxygen would stop the cathodic reaction in equation 2, thereby eliminating the potential for pitting which could potentially lead to metal cracking.

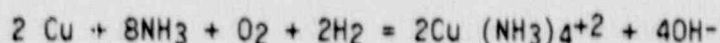
There are times during maintenance and inspections that the steam generator secondary-side must be drained, thereby exposing the steam generator materials to air. During these maintenance and inspection activities, the steam generators are maintained at ambient temperatures. The steam generators are maintained in this condition for the shortest time possible to complete the work. Partial refill of the steam generator secondary side for upper internal servicing and inspection generally follows the lower internal services work. Water levels are generally raised to the upper part of the steam generator transition cone in the vicinity of the girth weld. Fill



water for this may be from the condensate storage tank. In the past, the CST water has had up to 10ppm atmospheric oxygen. The duration for the services performed in this area can vary widely from a few days to weeks. Table 4.2.2 lists some of the various secondary side services that have been performed on a steam generator with the approximate time required for each task. However, the exposure of the steam generator internals solely to atmospheric oxygen during maintenance activities, when the steam generators are at low temperatures, does not appear to be a major contributing factor in the cause of girth weld cracking. In addition, the steam generators are at ambient containment temperatures during this time. Higher temperature is believed to increase metal corrosion in the presence of oxygen.

#### 4.2.3 Steam Generator Wet Layup Practices at Indian Point 2

Indian Point 2 has placed steam generators in wet layup during cold shutdown whenever maintenance activities did not interfere. In the past, the layup consisted of filling each steam generator to above the J-tubes with water and chemically adjusted to a pH of greater than 9.8 up to 10.5 with ammonia to minimize the dissolved oxygen concentration with hydrazine. Industry guidelines on layup chemistry are presented in Table 4.2.3. The recent modification to the CST will provide for the introduction of oxygen free water (less than 100ppb) into the steam generators from the CST. In addition, the wet layup procedures have been enhanced to include nitrogen sparging the steam generators during future wet layups. This layup condition, while attempting to protect internal surfaces, will also result in the dissolution of copper from the sludge pile. The presence of the oxygenated layup water will react with copper in aqueous solutions of ammonia according to the following reaction:



Indian Point 2 had also performed a modified layup by adding additional ammonia to remove the copper that has accumulated in the steam generator during power operations. This modified layup includes a pH greater than or equal to 9.8, consistent with industry guidelines, with a maximum of 10.8. The additional ammonia in the presence of the oxygen saturated layup water,

is intended to solubilize more copper. This process "soaks" each generator for 4 to 6 hours then it is drained to waste. This process may be repeated 1 to 2 times more if time is available.

Copper remaining on the inside surfaces of the steam generator shell after draining may cause the formation of local galvanic corrosion cells which could contribute to pitting in the girth weld area. The present practice of adding ammonia and hydrazine to within industry guidelines will continue at Indian Point 2 with the enhancement of minimizing the addition of oxygen from the water source (i.e., CST).

#### 4.3 SUMMARY

- 1) The dissolution of copper during layup conditions with oxygenated water, the activation of the carbon steel surfaces and the subsequent long term exposure of the steam generator upper internals to atmospheric oxygen during servicing has the possibility of promoting girth weld pitting/cracking in the Indian Point 2 steam generators. However, the threshold levels associated with dissolved oxygen, chemical and material related factors are not precisely known.
- 2) The periodic use of oxygen saturated auxiliary feedwater during startup and hot standby is likely to cause some general corrosion of steam generator materials and aid in the formation of localized pits. This factor alone, however, does not seem to be the primary contributor to girth weld cracking at IP2.
- 3) The time for the implementation of steam generator wet-layup will vary from plant to plant depending on the maintenance activities performed. It is likely that general corrosion of steam generator internal components may occur at the air-water interface during the time it is open to the atmosphere, particularly when the interface is at the highly stressed welds in the transition cone area. However, due to ambient temperatures during maintenance activities, the corrosion during layup is not a major contributing factor in the cause of girth weld cracking.

- 4) To alleviate the potential for the possible effects described above, the CST has been modified to reduce the dissolved oxygen concentration during auxiliary feedwater injections. In addition, a nitrogen sparging gas will be utilized to minimize the presence of air in the steam generators during wet layup where possible given required maintenance and inspection activities.



Table 4.2-1  
Comparison of Plant Secondary Side Materials and Chemistry

	S/G Mode and Chemistry	On-Line	Condenser Tubing	Feedwater Tubing	Circulating Cooling Water	Girth Weld Repair	Aux. Feed Source	O <sub>2</sub> Sat ?	Full-Flow Condensate Polishing
Indian Point 2	44 (4-loop) AVT/Boric acid	1974	Admiralty Metal	SS/CU Replacement-ongoing	Brackish	Last Several Outages (Repeats)	CST - Directly into S/G	Yes <sup>1</sup>	None
Surry	51F (3-loop) AVT	1-1981 2-1980 Replacement	Titanium	SS/Cu Replacement-ongoing	Sea	U-1 - 86 U-2 - 85 (No repeat cracking)	CST-Into condenser for deaeration before S/G	No	Deep Bed
Zion	51 4-loop AVT	U-1 06/73 U-2 12/73	S.S.	S.S.	Fresh-Lake Michigan	U-1 - 1989 U-2 - 1990 No repeat cracking	CST-Directly into S/G	Yes	None
Turkey Pt.	44F 3-loop AVT	U-3 '72 U-4 '73	Titanium	S.S.	Sea	No - Replacement S/G	CST-Not directly into S/G	Yes	Powdex
Trojan	51A 4-loop AVT/Boric acid	12-75	CuNi 70/30	CuNi 90/10	Natural tower fresh (Columbia River)	No	CST-Directly into S/G	No (10 ppb)	Powdex

<sup>1</sup> Prior to 1990. Nitrogen blanket installed June 1990.

Table 4.2-2

Secondary Side Services and Approximate Time Required for Their Completion in  
a Steam Generator

Items	Task	Time Estimates Days
(1)	Steam Generator Draindown/Refill	2
(2)	Removal/Reinstallation Hand Hole Cover	3
(3)	Removal of Tubeline Blocking Device	1
(4)	Sludge Lancing	5
(5)	Tubesheet Drying	1
(6)	Foreign Object Search and Retrieval	Variable 2 day typical
(7)	Flowslot Photography	2
(8)	Secondary Side Inspections	
	(a) J-Nozzle	1
	(b) Feedring/brackets	1
	(c) Girth weld	2
	(d) Steam drum/moisture separators	1
(9)	Additional effort - not required in all steam generators	
	(a) J Tube replacement	13
	(b) Antivibration bar	9-30
	(c) Steam drum replacement	16
	(d) Girth weld repair	Variable
	Totals 1 to 8	21 days/SG

Table 4.2-3  
EPRI Guidelines for Steam Generator Water  
During Cold Shutdown/Wet Layup

Control Parameters	Normal Value	Initiate Action	Value Prior to Heat-up >200°F
pH (Ferrous System)	≥9.8	<9.8	≥9.0
pH (Ferrous/Copper System)	≥9.8	<9.8	8.5 - 9.2
Hydrazine, ppm	≥75	<75	-
Sodium, ppb	≤1000	>1000	≤100
Chloride, ppb	≤1000	>1000	≤100
Sulfate, ppb	≤1000	>1000	≤100
Boron, ppm	<1	>1	-
Dissolved O <sub>2</sub> , ppb	≤100	>100	-

- (a) Conformance with pH guideline may be waived prior to achieving no load temperature and passing steam forward to turbine.



### 5.3 EVALUATION FOR GIRTH WELD, TRANSITION CONE, FEEDRING BRACKETS AND STRAPS

This section of the report summarizes analysis efforts for the girth weld, transition cone, and the feedring brackets and straps at Indian Point 2. Separate discussions are provided for the thermal hydraulic evaluation, the calculation of stresses for the affected components, and a fracture mechanics evaluation to determine critical flaw sizes and crack growth rates.

The various analyses are performed using a combination of finite element and conventional analysis techniques. Stresses used in evaluating the feedring brackets and straps, and in performing the fracture mechanics analysis are taken from prior analyses (see WCAP's 11730 and 12292, Revision 2). The units for stress, force and moments used in this section and other sections of this report are KSI, KIPS and INCH-KIPS respectively, unless otherwise noted.

#### 5.1 THERMAL HYDRAULIC ANALYSIS

The design and normal operating, steady state and transient conditions considered in the girth weld analysis are summarized in Table 5.1-1. Secondary side operating conditions for temperature and pressure used in the analysis are based on uprating conditions. Other loads imposed on the steam generator and internals, such as nozzle end loads and loads resulting from flow induced vibration, do not affect the girth weld region of the shell and have not been considered in the analysis. Seismic loads have also been shown to not have a significant effect on the girth weld region.

In the prior girth weld evaluations, two of the transients, reactor trip and feedwater cycling, have been shown to result in significant thermal effects on the girth weld. Subsequent to these evaluations, however, an operational change was instituted which substantially mitigates the thermal influence of the reactor trip transient. In brief, the isolation of feedwater flow to the steam generator following a reactor trip was delayed, thus maintaining hot feedwater and steam generator water level at a higher level before initiating auxiliary feedwater flow. This, in effect, causes the reactor trip transient

to be very similar to the feedwater cycling transient. For the present analysis, reactor trip is considered to be the same as feedwater cycling.

During hot standby when auxiliary feedwater is injected (feedwater cycling), the water level in the steam generator is at least seven inches above the feedring. Cold water from the feedring mixes with the pool on its way to the downcomer region and contacts the shell with a minimum temperature of 427°F about 13 inches above the girth weld. A plot showing the fluid temperature on the inside surface as a function of time is shown in Figure 5.1-1. Note the oscillatory nature of the water entering the downcomer region which results from the introduction of the higher density cold water. Over time, a static head difference develops between the downcomer region and the body of water on the tube-side of the wrapper. Eventually, the bundle-side water level rises above the top of the primary separator and saturated water spills into the downcomer region. This causes the water in the sub-cooled downcomer region to quickly increase in temperature with a decrease in density, thus reducing the static head difference with the bundle-side water. The bundle-side water level drops and the flow of saturated water into the downcomer region stops. The auxiliary feed flow, however, continues, and the process repeats itself, resulting in the cyclic temperature response. The boundary conditions for the feedwater cycling heat transfer analysis are summarized in Table 5.1-2 by region. The elements contained in each of the regions, for one of the grind conditions considered previously, are shown in Figure 5.1-2.

For the remaining transients, temperatures either 1) do not involve a change in feedwater temperature, 2) have thermal effects which are mitigated by the resident water pool and which are therefore not considered to be significant, or 3) are enveloped by auxiliary feedwater injection.

The thermal response of the girth weld as a function of time is provided in Figure 5.1-3 for the feedwater cycling transient. These plots are for the 1.0 inch grind, but are representative of each of the cases considered. This plot shows the oscillatory response of the feedwater cycling transient. Using this plot as a guide, stresses are calculated at the times corresponding to the maximum and minimum thru-wall gradients shown in Figure 5.1-3.

TABLE 5.1-1

INDIAN POINT 2 (IPP)  
SUMMARY OF TRANSIENT CONDITIONS  
(From Design Specification E-676219, Rev. 2)

TRANSIENT

- |    |                               |
|----|-------------------------------|
| 1  | Plant Heatup                  |
| 2  | Plant Cooldown                |
| 3  | Plant Loading / Unloading     |
| 4  | Small Step Load Increase      |
| 5  | Small Step Load Decrease      |
| 6  | Steady-State Fluctuations (+) |
| 7  | Steady-State Fluctuations (-) |
| 8  | Large Step Load Decrease      |
| 9  | Loss of Load                  |
| 10 | Loss of Power                 |
| 11 | Loss of Flow                  |
| 12 | Reactor Trip                  |
| 13 | Feedwater Cycling             |
| 14 | Secondary Hydrotest (Init.)   |
| 15 | Secondary Hydrotest (Subs.)   |
| 16 | Secondary Side Leak Tests     |
| 17 | Seismic (OBE)                 |



TABLE 5.1-2

SUMMARY OF TRANSIENT BOUNDARY CONDITIONS  
FEEDWATER CYCLING TRANSIENT

<u>TIME</u>	<u>SATURATED TEMPERATURE</u>	<u>FLUID TEMPERATURE</u>	<u>FILM COEFFICIENT REGION 1</u>	<u>FILM COEFFICIENT REGION 2</u>
0	547.0	547.0	24.0	76.0
10	546.5	538.0	270.9	322.9
20	546.0	530.0	323.9	375.9
50	545.0	502.0	422.4	472.4
75	543.6	534.0	806.2	2002.2
90	543.0	522.0	360.6	412.6
110	542.0	504.0	434.2	486.2
150	540.2	468.0	532.0	584.0
175	539.1	531.0	792.0	1988.0
190	538.4	518.0	357.4	409.4
220	537.1	490.0	464.6	516.6
275	534.6	453.0	553.2	605.2
300	533.5	524.0	805.3	2001.3
330	532.1	497.0	423.5	475.5
375	530.1	459.0	525.4	581.4
450	526.8	520.0	778.2	1974.2
480	525.4	492.0	416.9	468.9
530	523.2	450.0	534.3	596.3
560	522.0	427.0	580.7	632.7
600	520.0	512.0	791.0	1987.0

Time has units of seconds

Temperatures have units of degrees Fahrenheit

Film Coefficients have units of BTU/hr-ft<sup>2</sup>-°F

Notes:

1. See Figure 5.1-2 for region definition
2. Film coefficient in Region 0= $\infty$ , and does not change with time.

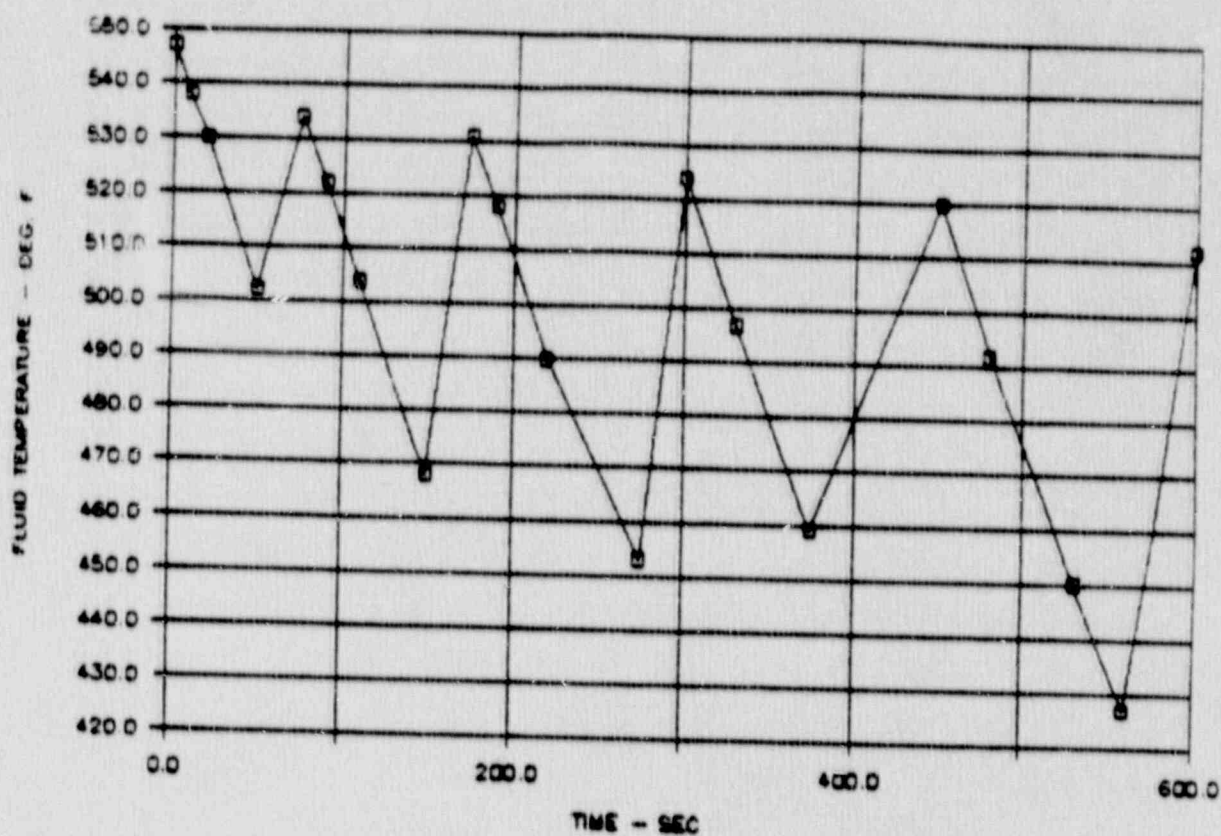


FIGURE 5.1-1  
FEEDWATER CYCLING TRANSIENT  
FLUID TEMPERATURE VERSUS TIME

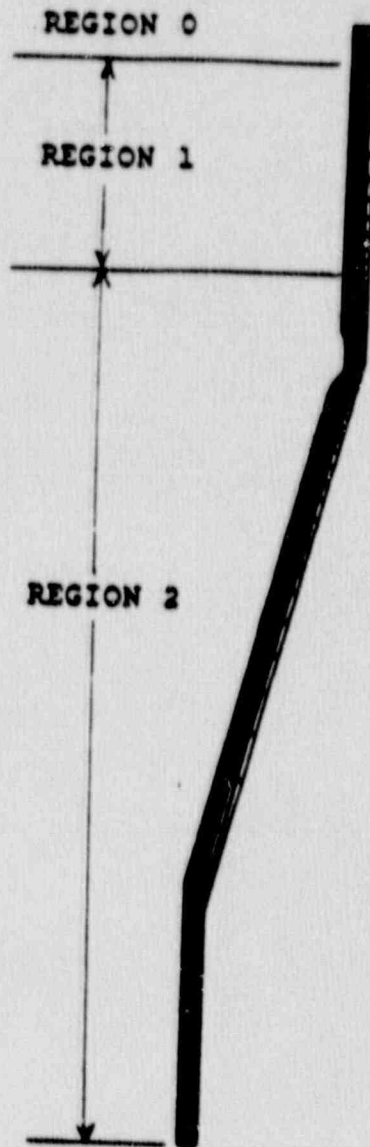


FIGURE 5.1-2  
FEEDWATER CYCLING BOUNDARY CONDITIONS  
0.75" GRIND REGION DESIGNATION



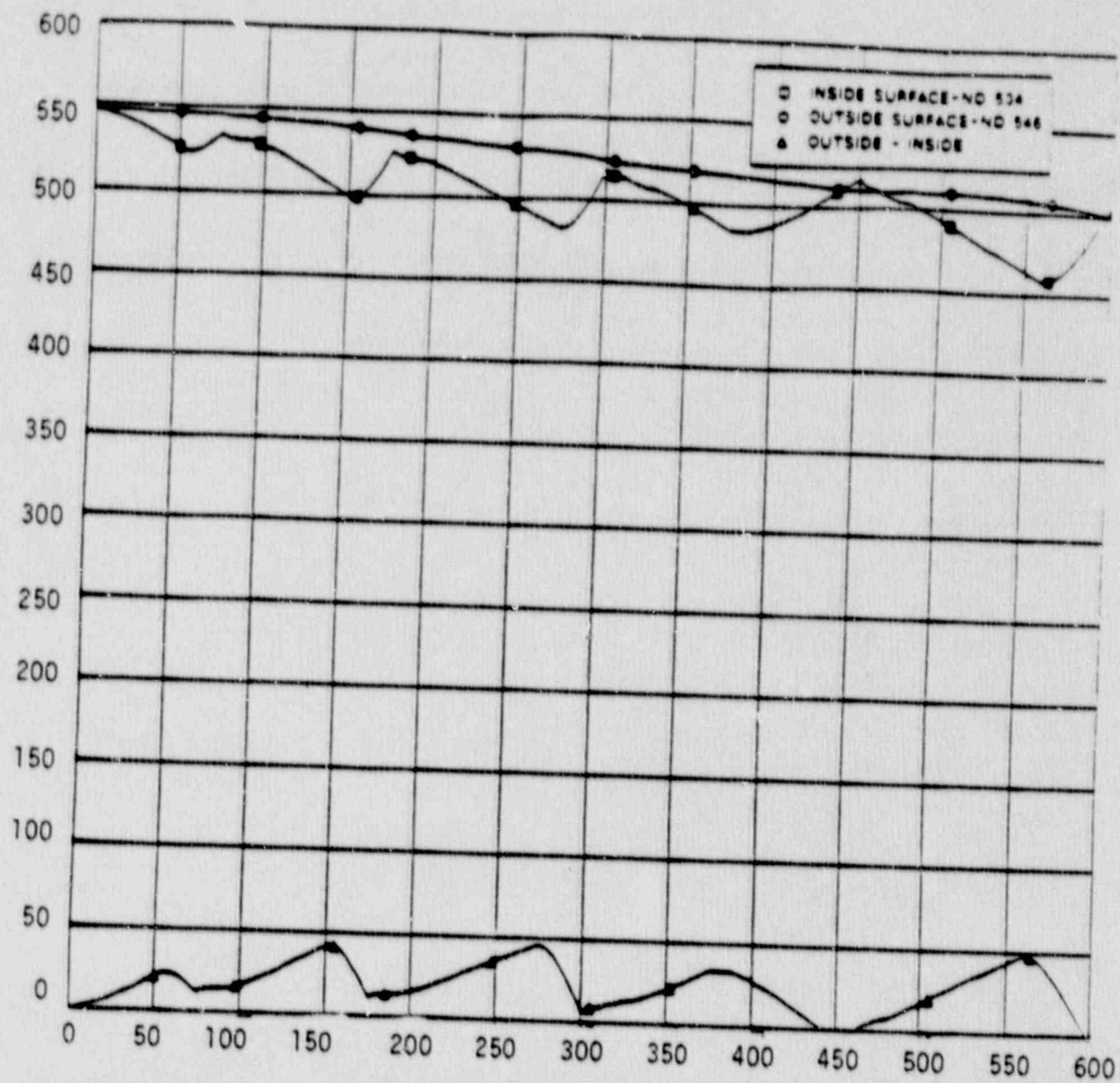


FIGURE 5.1-3  
METAL TEMPERATURE VERSUS TIME  
FEEDWATER CYCLING TRANSIENT

## 5.2 STRESS ANALYSIS

### 5.2.1 Uniform Grind Analysis Description

In the prior girth weld analyses, four different grind depths have been analyzed, 0.5 inch, 0.75 inch, 1.0 inch, and 1.25 inches. The analyses are referred to as uniform grinds, because the analysis assumes the grind to have a constant shape and to extend 360° around the circumference of the steam generator. The blend-out to the shell inner surface is with a 2:1 taper at each end of the land. A 0.5 inch radius is assumed at the blend of the taper to the land.

The steady state and transient pressure and temperature stress solutions are obtained using finite element models. The models are quite similar in geometry. The finite element model for 0.75 inch grind is shown in Figure 5.2-1. Each of the models is composed of eight-noded axisymmetric isoparametric elements. There are six elements through the thickness, each having a mid-side node for a total of thirteen integration points. Both above the girth weld region and below the bottom of the shell cone, sufficient lengths of the shell cylinder are modeled to eliminate any end effects from the stress solution. To account for pressure end-cap loads, axial loads are applied to the model in the form of pressures along the top face of the model, with the bottom face of the model being constrained axially. The finite element solutions are obtained using the WECAN computer program, a Westinghouse proprietary general purpose finite element program.

Through-thickness stress distributions in the grind region, as well as the cone below the grind and in the shell above the grind, are determined using the computer program WECEVAL. Evaluations are performed for cuts thru the shell wall identified as "analysis sections" (ASN's). The analysis sections used for each of the four grind geometries are shown in Figures 5.2-2 through 5.2-5 for the 0.50 inch, 0.75 inch, 1.0 inch, and 1.25 inch grinds, respectively.

Through-thickness stress distributions are generated in tabular form for each ASN, with the limiting stress condition being used. For the critical flaw

size analysis, with the system modification essentially eliminating the reactor trip transient, the limiting condition now becomes the feedwater cycling transient. In general, the limiting time occurs at 275 seconds into the transient. Some variation in the critical transient time is found to occur for analysis sections away from the grind region.



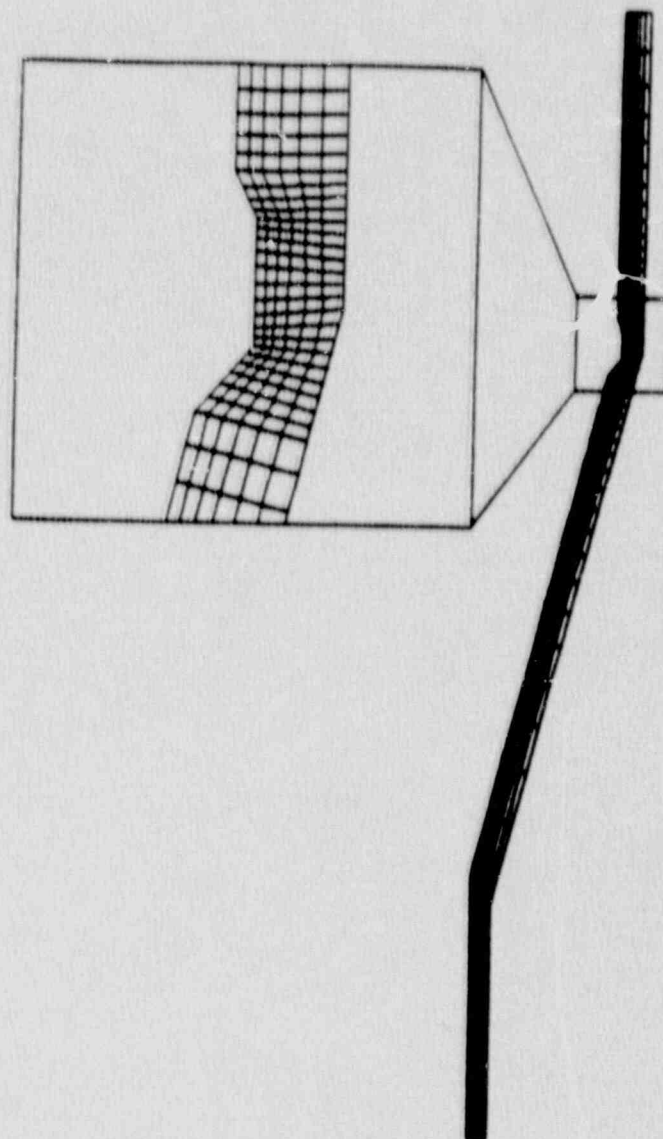


FIGURE 5.2-1  
FINITE ELEMENT MODEL FOR 0.75" GRIND

ASN 27 @ Y=119.

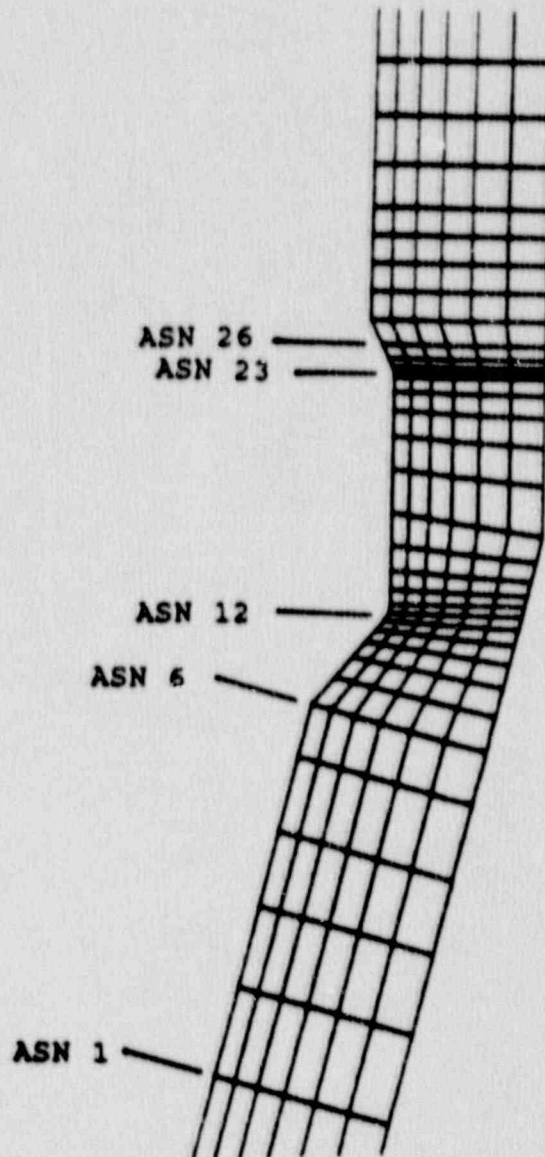


FIGURE 5.2-2  
ANALYSIS SECTION LOCATIONS  
0.50" GRIND MODEL

ASN 28 @ Y = 119.

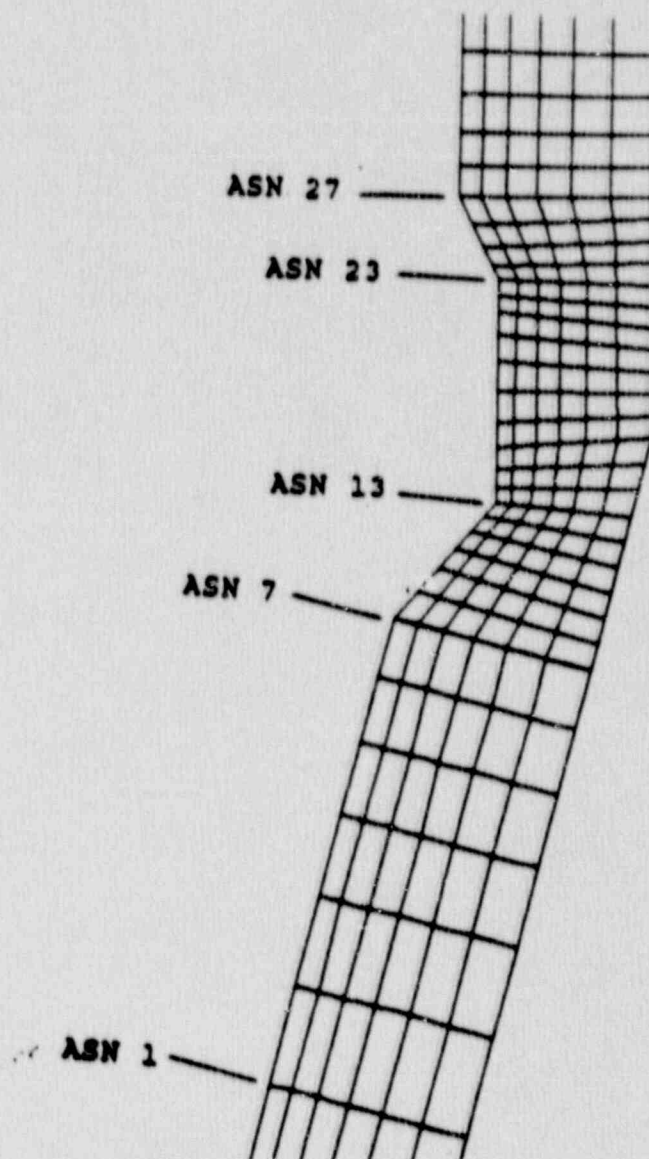


FIGURE 5.2-3  
ANALYSIS SECTION LOCATIONS  
0.75" GRIND MODEL



ASN 28 @ Y = 119.

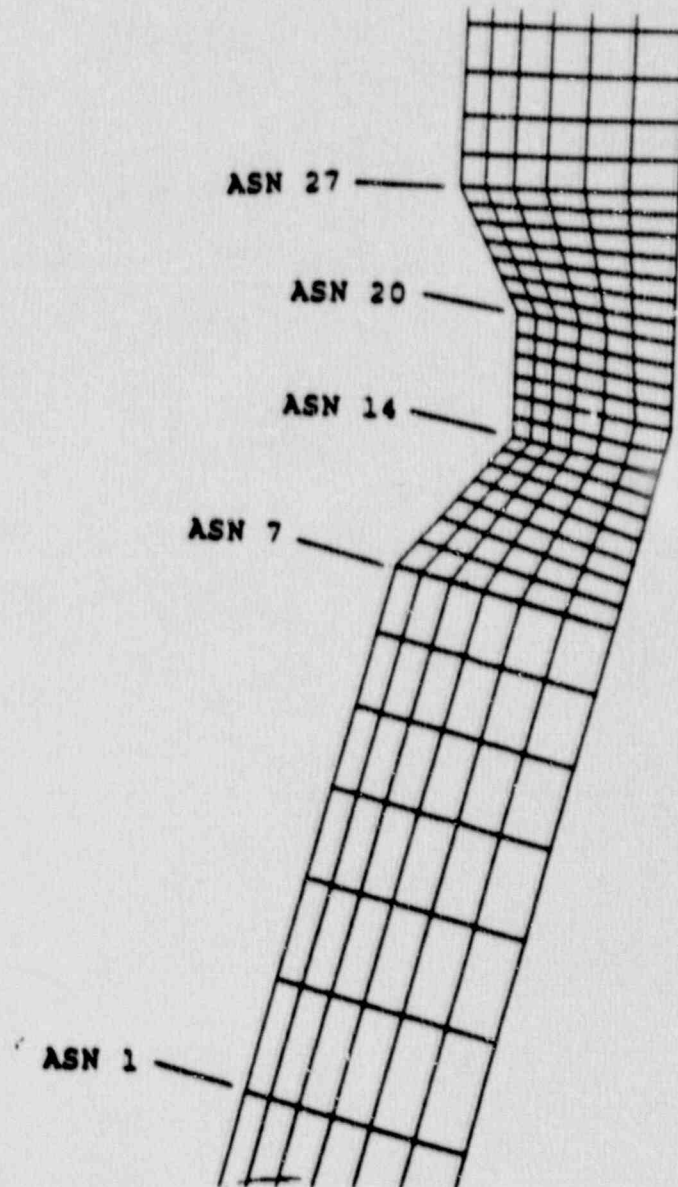


FIGURE 5.2-4  
ANALYSIS SECTION LOCATIONS  
1.0 " GRIND MODEL

ASN 27 @ Y=119.

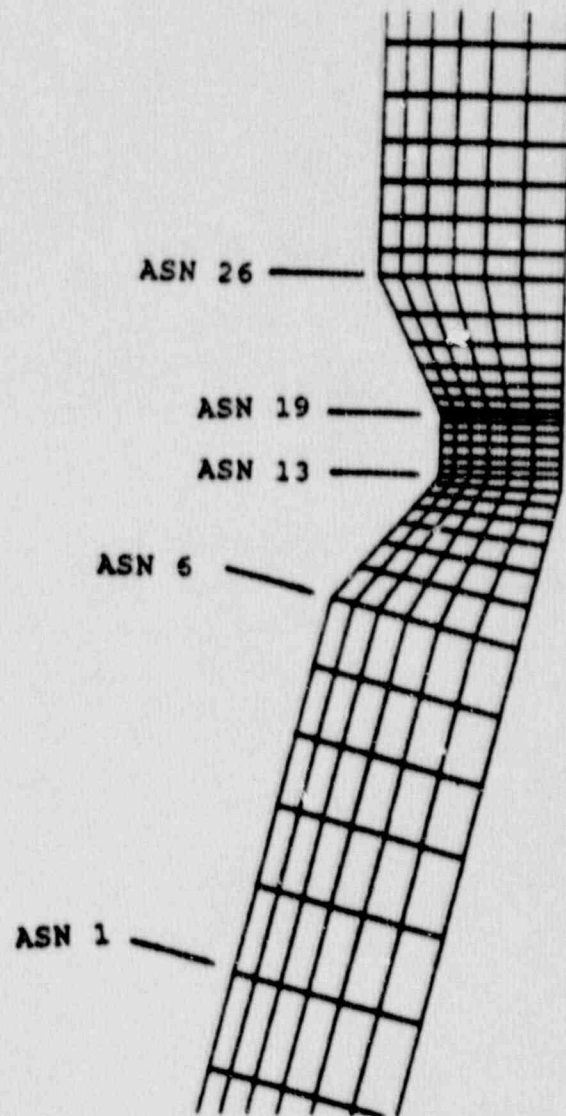


FIGURE 5.2-5  
ANALYSIS SECTION LOCATIONS  
1.25 " GRIND MODEL

## 5.2.2 Bracket Analysis

### 5.2.2.1 Feeding Bracket Relocation and Modification

Feedwater nozzle thermal sleeve junction to feeding is supported by a bracket welded to the main shell. Because of degradations observed in the weld area of the bracket, the brackets were moved to newer locations and the design was modified. The modified brackets were moved away from the nozzle flow area to minimize the bracket stresses due to the effects of bypass flow. A schematic plan view of the modified bracket support area is shown in Figure 5.2.2-1. Figure 5.2.2-2 shows the locations of the existing and the relocated modified brackets. The geometry of the existing bracket is shown in Figure 5.2.2-3 and that of the modified bracket in Figure 5.2.2-4. The analysis is based on bracket material ASME SA-516 Grade 70 and shelf/shelf-support material ASTM A-576 Grade 1018.

Since the support points to the feeding remain unchanged, the mechanical and seismic loads acting at the support locations will be assumed to remain unchanged. The stresses at the shelf, shelf-supports, and brackets are calculated on the basis of loads obtained previously in the original stress report (Reference 1). According to this report, the seismic loads govern and even those do not constitute significant loading. These loads are given below:

- a) Horizontal load on either of the two horizontal U-straps is 1150 lbs.
- b) Vertical load on either of the two vertical U-straps is 1230 lbs.
- c) Vertical load on any of the feedwater ring bracket supports is 820 lbs.

The stresses in the existing bracket and shelf/shelf-support, calculated for the vertical load of 820 lbs, are small. The stresses in the replacement bracket and shelf/shelf-support are even less than those for the existing



ones, and well within the allowable stresses for the materials used. Stresses and allowables are given in table 5.2.2-1.

The original shelf of the bracket is 1.5 inches away from the shell at the centerline of the feedwater nozzle. This distance has been increased to 3.1 inches for the modified bracket. This modification will prove beneficial to the bracket and shelf by reducing the probability of cold bypass water, leaking through the gap between the thermal liner and the feedwater nozzle, to impinge the bracket and shelf.

The replacement bracket has higher stiffness than the original bracket. Therefore, the deflection at the bracket support of the feedwater ring junction due to the same hydraulically induced load will be smaller at the replacement bracket compared of that at the original bracket.

Since the stresses in the bracket adjacent to the shell are small, they will have little effect on shell stresses. The shell stresses may be considered to be decoupled from the effects of the bracket stresses. The stress field in the shell at the existing bracket location near the feedwater nozzle has been compared with that at the new location in the shell for the modified bracket based on stresses obtained in the analyses performed for feedwater nozzle and girth weld. The existing location near the feedwater nozzle is found to be more critical than that at the new location in the shell away from the feedwater nozzle. Since the stress conditions at the new location of the bracket are more favorable than those at the existing bracket location, the new location is more desirable.

#### 5.2.2.2 Feeding Support Brackets A, B, C

During the mid-cycle inspection of the secondary side of the steam generators at Indian Point 2, visual and magnetic particle inspection of the feedwater nozzle inner radius and welds of the support brackets beneath the feeding/nozzle area revealed a number of linear indications. With the finding of linear indications in the nozzle area near the feeding support brackets, the inspection was extended to include all other feeding support brackets and straps in all four steam generators. The indications associated with the feeding brackets were predominantly in the shell heat-affected zone adjacent to the weld. All indications were removed by grinding.

This section describes the work performed in determining the grinding contours at each of the brackets which would permit operation for an assumed cycle of 300 days before further repair is necessary and identification of locations where weld repair is required.

To provide an option of welding or repair by grinding, the following procedure was followed:

- 1) Obtain the stress distribution through the thickness of the wall for the load condition which produces the maximum stresses normal to the observed cracks from the girth weld finite element analysis performed previously (Reference 2).
- 2) Adjust the stress distribution through the thickness to account for the reduced thickness after grinding and for a range of stress concentration factors that could be introduced by the grind contour. The adjusted stress distributions have the same net force and moment acting on the reduced section as did the original stress distribution in step (1).
- 3) Perform critical flaw size calculations for a range of aspect ratios for each of the stress distributions determined in step (2). Determine the maximum crack depths that satisfy the

$K_I = 200/\sqrt{10}$  ksi/ $\sqrt{\text{in}}$  criterion for each stress concentration factor and aspect ratio considered. (This work is described in Section 5.3).

- 4) Conservatively assuming that the existing cracks developed during the last operating cycle (212 days), the postulated cracks for an assumed cycle of 300 days are obtained by multiplying the depth of the observed cracks by 300/212.
- 5) The grind geometry after contouring is assumed to be a U-shaped notch with a one-half inch minimum radius. The stress concentration produced by this geometry is obtained from Peterson (Reference 3), Figure 39a, and multiplied by  $(D/d)^2$  to relate it to the unnotched thickness.
- 6) The crack depth from step (4) along with the appropriate aspect ratio are used to determine the allowable stress concentration factor from the results obtained in step (3). If that stress concentration factor is greater than the one determined in step (5), then the U-shaped notch assumed for the grind geometry is acceptable. Otherwise, a slope must be specified for the sides of the notch to reduce the stress concentration factor. That slope is determined using Figure 38 from Peterson.
- 7) The inspection reports of the grind locations and depths are then checked to determine whether the required grind contour can be performed without undercutting any adjacent structures such as feeding support brackets. If so, the contouring is acceptable. Otherwise, weld repair is required.

#### Adjusted Stress Distributions:

To account for the reduced thickness of the shell after grinding and for a range of stress concentration factors that could be introduced by the grind contour, the stress distribution through the thickness is adjusted as follows:



- 1) The thickness is reduced by the amount of the material ground away during the removal of indications.
- 2) The inside surface stress is multiplied by stress concentration factors ranging from 1.5 to 2.5 in steps of 0.5.
- 3) For each assumed stress concentration factor, the resulting stress distribution is required to have the same net force and moment acting on the reduced section as did the original stress distribution on the initial thickness.

The stress through the thickness is assumed to have the form:

$$\sigma = a + by + cy^2 + dy^3$$

The conditions to be satisfied are:

- 1) At  $y = 0$ ,  $\sigma = SCF * S(0)$  (1)
- 2) The integral of the stress through the reduced thickness is equal to the net force on the section produced by the original stress distribution through the initial thickness.
- 3) The integral of the stress times the distance from the mid-surface through the reduced thickness is equal to the net moment about the mid-surface produced by the original stress distribution.

An additional condition must be specified to permit solution of the fourth unknown. Since the outside surface stress is not likely to be affected significantly by local grinding effects on the inside surface, a reasonable assumption is that the outside surface stress is the same for both the original stress distribution and the adjusted stress distribution. This provides the fourth condition needed to solve for the unknowns in the cubic equation.

In equation (1) above, SCF is the applied stress concentration factor and  $S(0)$  is the value of the original stress at the inside surface. If  $F$  is the net force on the section produced by the original stress distribution, and  $M$  the net moment about the midsurface produced by the original stress distribution, the four conditions to be satisfied by a result in:

$$SCF * S(0) = a$$

$$F = \int_0^t (a + by + cy^2 + dy^3)dy$$

$$M = \int_0^t (a + by + cy^2 + dy^3)(y - t/2)dy$$

$$S_0 = a + bt + ct^2 + dt^3$$

where  $t$  is the thickness of the reduced section, and  $S_0$  the outside surface stress in the original stress distribution. Letting  $S = SCF * S(0)$ , these four equations give:

$$a = S$$

$$F = at + bt^2/2 + ct^3/3 + dt^4/4$$

$$M = (bt^3 + ct^4)/12 + 3dt^5/40$$

$$S_0 = S + bt + ct^2 + dt^3$$

From these,

$$a = S$$

$$b = (S_0 - S)/t - ct - dt^2$$

$$c = 3(S_0 + S)/t^2 - 6F/t^3 - 3dt/2$$

$$d = -120 M/t^5 - 10(S_0 - S)/t^3$$

#### Equivalent Force and Moment:

The equivalent force and moment of the original stress distribution can be determined using numerical integration. The stress is known at discrete points through the thickness. Assuming a piece-wise linear variation from point to point, the stress is given by:

$$S = S_i + (Y - Y_i)(S_{i+1} - S_i)/(Y_{i+1} - Y_i)$$

The equivalent force and moment for one segment are given by:

$$F_i = \int_{Y_i}^{Y_{i+1}} (S_i + b(Y - Y_i)) dY$$

$$M_i = \int_{Y_i}^{Y_{i+1}} (S_i + b(Y - Y_i))(Y - t/2) dY$$

$$\text{where } b = (S_{i+1} - S_i)/(Y_{i+1} - Y_i)$$

Integrating and substituting for b,

$$F_i = (S_{i+1} + S_i)(Y_{i+1} - Y_i)/2$$

$$M_i = \{S_{i+1}(2Y_{i+1} + Y_i)/6 + S_i(Y_{i+1} + 2Y_i)/6 - t(S_{i+1} + S_i)/4\}(Y_{i+1} - Y_i)$$

The total force and moment acting on the section are then the sums of  $F_i$  and  $M_i$  from  $i = 1$  to  $N$ , where  $N$  is the number of segments.

Adjusted Stresses for Brackets A, B, C:

The maximum depth grinds for the steam generators were:

21      0.45 inches



22	0.60 inches
23	0.48 inches
24	0.426 inches

The adjusted stress distributions for each of these grind depths for a range of stress concentration factors that could result from the grind contours were generated as described above. Tables 5.2.2-2 to 5.2.2-4 contain the adjusted stress distributions for Steam Generators 21, 23, and 24. These stress distributions were used to generate a series of curves for each steam generator (see Section 5.3) of critical crack depth versus crack aspect ratio for each of the potential stress concentration factors.

#### Required Grind Contours:

At each grind location around the feedring brackets, the existing cracks are conservatively assumed to have developed during the last operating cycle (212 days). The postulated cracks for the assumed operating cycle of 300 days are obtained by multiplying the depth of the observed cracks by 300/212.

The grind geometry after contouring is assumed to be a U-shaped notch with a one-half inch minimum radius. The stress concentration produced by this geometry is obtained from Peterson (Reference 3), Figure 39a, and multiplied by  $(D/d)^2$  to relate it to the unnotched thickness.

The postulated crack depth from above along with the appropriate aspect ratio (the length of the crack divided by its depth) are used to determine the allowable stress concentration factor. If that stress concentration factor is greater than the one determined using Peterson, then the U-shaped notch assumed for the grind geometry is acceptable. Otherwise, a slope must be specified for the sides of the notch to reduce the stress concentration factor. That slope is determined using Figure 38 from Peterson.

The above process was followed for each of the areas in which indications were removed by grinding adjacent to the feedring support brackets A, B, C of Steam Generators 21, 23, and 24 as well as for the weld pads D, E, F, G of Steam Generators 23 and 24. The above process was not followed for Steam

Generator 22 because it was decided that welding was the most expeditious method of repair. The results of this procedure are given in Tables 5.2.2-5 through 5.2.2-9.

#### Areas Requiring Weld Repair:

The inspection reports of the grind locations and depths are then checked to determine whether the required grind contour can be performed without undercutting any adjacent structures such as feedring support brackets. If so, the contouring is acceptable. Otherwise, weld repair is required.

A graphical technique was used to determine the acceptability of the grind contours. Figure 5.2.2-5 illustrates the procedure. The support bracket and the locations and depths of the grindouts are drawn to scale. The depth and location of a grindout relative to the bracket are taken from the field inspection report for that bracket. These dimensions are shown on Figure 5.2.2-5 for the grindout on the left side of Steam Generator 21, Bracket C. Referring to Table 5.2.2-5 for this location, a slope of 4.7 is required to reduce the stress concentration factor to an acceptable value. If a slope is required, as it is in this case, that is also drawn to scale tangent to the one-inch diameter circles at the bottom of the grindout. As can be seen, this slope undercuts the bracket. Thus weld repair is required for the left side of the bracket. The right side does not require a weld repair since the required contour intersects the shell surface outside the bracket.

Table 5.2.2-10 summarizes the results of this investigation. A total of thirteen areas were determined by analysis to require weld repair in Steam Generators 21, 23, and 24. The process of evaluating weld repair versus repair by grinding was not undertaken for Steam Generator 22 because it was determined that all brackets in Steam Generator 22 will be weld repaired. Table 5.2.2-10 therefore does not contain data for Steam Generator 22. During the repair of the feedring support brackets, it was decided to weld repair and restore to the original contours all ground out areas adjacent to the feedring support brackets.

TABLE 5.2.2-1  
STRESS SUMMARY FOR MODIFIED BRACKET AND SHELF/SHELF-SUPPORT

Description of Component/Material	Maximum stress in psi	Maximum allowable stress in psi
Shelf/Shelf-support ASTM A-576 Gr 1018	1,440	20,000
Bracket ASME SA-516 Gr 70	134	28,100



TABLE 5.2.2-2  
ADJUSTED STRESSES FOR S/G 21, BRACKETS A, B, C

**Original Stress Distribution**

Node	Distance	Stress
1285	0.0000	33.508
1535	0.4011	26.717
1537	0.8619	21.403
1539	1.3913	17.527
1541	1.9993	14.936
1543	2.6977	13.447
1545	3.5000	12.995

**Numerical Integration**

Force	Moment
12.0782	-18.8056
11.0868	-12.4946
10.3046	-6.5144
9.8687	-0.6196
9.9114	5.8714
10.6071	14.2831

Totals    63.8567    -18.2796

**IPP Steam Generator 21 - Brackets A, B, C**

Maximum Grind Depth        0.45  
Remaining Thickness        3.05

Cubic Distribution        Stress = SCF\*S1 + by + cy<sup>2</sup> + dy<sup>3</sup>  
Hoop Stresses Through Remaining Thickness (ksi)

Distance	Stress Concentration Factor		
	1.5	2.0	2.5
0.0000	50.262	67.017	83.771
0.5083	28.804	28.029	27.253
1.0167	18.515	12.309	6.104
2.0333	16.231	16.851	17.472
3.0500	12.995	12.995	12.995

TABLE 5.2.2-3  
ADJUSTED STRESSES FOR S/G 23, BRACKETS A, B, C

**Original Stress Distribution**

**Numerical Integration**

Node	Distance	Stress
1285	0.0000	33.508
1535	0.4011	26.717
1537	0.8619	21.403
1539	1.3913	17.527
1541	1.9993	14.936
1543	2.6977	13.447
1545	3.5000	12.995

Force	Moment
12.0782	-18.8056
11.0868	-12.4946
10.3046	-6.5144
9.8687	-0.6196
9.9114	5.8714
10.6071	14.2831

Totals    63.8567    -18.2796

**IPP Steam Generator 23 - Brackets A, B, C**

Maximum Grind Depth            0.48  
Remaining Thickness            3.02

Cubic Distribution             $\text{Stress} = \text{SCF} \cdot S1 + by + cy^2 + dy^3$   
Hoop Stresses Through Remaining Thickness (ksi)

Distance	Stress Concentration Factor		
	1.5	2.0	2.5
0.0000	50.262	67.017	83.771
0.5033	29.196	28.420	27.644
1.0067	18.966	12.761	6.556
2.0133	16.334	16.954	17.575
3.0200	12.995	12.995	12.995

TABLE 5.2.2-4  
ADJUSTED STRESSES FOR C/G 24, BRACKETS A, B, C

**Original Stress Distribution**

Node	Distance	Stress
1285	0.0000	33.508
1535	0.4011	26.717
1537	0.8619	21.403
1539	1.3913	17.527
1541	1.9993	14.936
1543	2.6977	13.447
1545	3.5000	12.995

**Numerical Integration**

Force	Moment
12.0782	-18.8056
11.0868	-12.4946
10.3046	-6.5144
9.8687	-0.6196
9.9114	5.8714
10.6071	14.2831

**Totals    63.8567    -18.2796**

**IPP Steam Generator 24 - Brackets A, B, C**

**Maximum Grind Depth        0.426**  
**Remaining Thickness        3.074**

Cubic Distribution         $\text{Stress} = \text{SCF} \cdot S_1 + by + cy^2 + dy^3$   
**Hoop Stresses Through Remaining Thickness (ksi)**

Distance	Stress Concentration Factor		
	1.5	2.0	2.5
0.0000	50.262	67.017	83.771
0.5123	28.498	27.723	26.947
1.0247	18.161	11.955	5.750
2.0493	16.149	16.769	17.390
3.0740	12.995	12.995	12.995



TABLE 5.2.2-5  
GRIND CONTOURS FOR S/G 21, BRACKETS A, B, C

Right

S/G 21, A Bracket		S/G 21, B Bracket		S/G 21, C Bracket	
D/d	1.1401	D/d	1.1364	D/d	1.0736
r/d	0.1629	r/d	0.1623	r/d	0.1534
Aspect Ratio	22.0000	Aspect Ratio	22.0652	Aspect Ratio	38.9167
Crack Size	0.6085	Crack Size	0.5943	Crack Size	0.3396
$K_t (D/d)^2$	2.4825	$K_t (D/d)^2$	2.4019	$K_t (D/d)^2$	2.2016
Allowable SCF	2.0200	Allowable SCF	2.0350	Allowable SCF	2.2300
SCF Ratio	0.8137	SCF Ratio	0.8473	SCF Ratio	1.0129
Fig. 38, $K_{ts}$	1.5541	Fig. 38, $K_{ts}$	1.5759	Fig. 38, $K_{ts}$	NA
Fig. 38, Alpha	153.0000	Fig. 38, Alpha	149.0000	Fig. 38, Alpha	0.0000
Min. Slope	4.1653	Min. Slope	3.6059	Min. Slope	0.0000

Left

S/G 21, A Bracket		S/G 21, B Bracket		S/G 21, C Bracket	
D/d	1.1182	D/d	1.0636	D/d	1.1475
r/d	0.1597	r/d	0.1548	r/d	0.1639
Aspect Ratio	25.5676	Aspect Ratio	34.3704	Aspect Ratio	20.7556
Crack Size	0.5236	Crack Size	0.3821	Crack Size	0.6368
$K_t (D/d)^2$	2.3507	$K_t (D/d)^2$	2.2861	$K_t (D/d)^2$	2.5415
Allowable SCF	2.2000	Allowable SCF	2.2000	Allowable SCF	2.0100
SCF Ratio	0.9359	SCF Ratio	0.9708	SCF Ratio	0.7909
Fig. 38, $K_{ts}$	1.7594	Fig. 38, $K_{ts}$	1.8737	Fig. 38, $K_{ts}$	1.5264
Fig. 38, Alpha	131.0000	Fig. 38, Alpha	120.0000	Fig. 38, Alpha	156.0000
Min. Slope	2.1943	Min. Slope	1.7321	Min. Slope	4.7046

Top

S/G 21, A Bracket		S/G 21, B Bracket		S/G 21, C Bracket	
D/d	1.0671	D/d	NA	D/d	NA
r/d	0.1524	r/d	NA	r/d	NA
Aspect Ratio	16.5455	Aspect Ratio	NA	Aspect Ratio	NA
Crack Size	0.3113	Crack Size	NA	Crack Size	NA
$K_t (D/d)^2$	1.9926	$K_t (D/d)^2$	NA	$K_t (D/d)^2$	NA
Allowable SCF	2.4100	Allowable SCF	NA	Allowable SCF	NA
SCF Ratio	1.2095	SCF Ratio	NA	SCF Ratio	NA
Fig. 38, $K_{ts}$	NA	Fig. 38, $K_{ts}$	NA	Fig. 38, $K_{ts}$	NA
Fig. 38, Alpha	0.0000	Fig. 38, Alpha	NA	Fig. 38, Alpha	NA
Min. Slope	0.0000	Min. Slope	NA	Min. Slope	NA

Bottom

S/G 21, A Bracket		S/G 21, B Bracket		S/G 21, C Bracket	
D/d	1.1076	D/d	1.0870	D/d	1.1006
r/d	0.1582	r/d	0.1553	r/d	0.1572
Aspect Ratio	11.0294	Aspect Ratio	11.6071	Aspect Ratio	8.4375
Crack Size	0.4811	Crack Size	0.3962	Crack Size	0.4528
$K_t (D/d)^2$	2.3922	$K_t (D/d)^2$	2.2802	$K_t (D/d)^2$	2.2532
Allowable SCF	2.3800	Allowable SCF	2.3800	Allowable SCF	2.5000
SCF Ratio	0.9949	SCF Ratio	1.0437	SCF Ratio	1.1086
Fig. 38, $K_{ts}$	1.9401	Fig. 38, $K_{ts}$	NA	Fig. 38, $K_{ts}$	NA
Fig. 38, Alpha	90.0000	Fig. 38, Alpha	0.0000	Fig. 38, Alpha	0.0000
Min. Slope	1.0000	Min. Slope	0.0000	Min. Slope	0.0000

TABLE 5.2.2-6  
GRIND CONTOURS FOR S/G 23, BRACKETS A, B, C

Right

S/G 23, A Bracket		S/G 23, B Bracket		S/G 23, C Bracket	
D/d	1.1041	D/d	1.1146	D/d	1.1475
r/d	0.1577	r/d	0.1592	r/d	0.1639
Aspect Ratio	24.2424	Aspect Ratio	29.1111	Aspect Ratio	20.2222
Crack Size	0.4670	Crack Size	0.5094	Crack Size	0.6368
$K_t (D/d)^2$	2.2552	$K_t (D/d)^2$	2.3109	$K_t (D/d)^2$	2.5415
Allowable SCF	2.1700	Allowable SCF	2.0700	Allowable SCF	2.0000
SCF Ratio	0.9622	SCF Ratio	0.8957	SCF Ratio	0.7869
Fig. 38, $K_{ts}$	1.7801	Fig. 38, $K_{ts}$	1.6661	Fig. 38, $K_{ts}$	1.5188
Fig. 38, Alpha	122.0000	Fig. 38, Alpha	140.0000	Fig. 38, Alpha	157.0000
Min. Slope	1.8040	Min. Slope	2.7475	Min. Slope	4.9152

Left

S/G 23, A Bracket		S/G 23, B Bracket		S/G 23, C Bracket	
D/d	1.0838	D/d	1.1589	D/d	1.0972
r/d	0.1563	r/d	0.1656	r/d	0.1567
Aspect Ratio	26.6667	Aspect Ratio	21.8333	Aspect Ratio	29.3548
Crack Size	0.4245	Crack Size	0.6792	Crack Size	0.4387
$K_t (D/d)^2$	2.2131	$K_t (D/d)^2$	2.6057	$K_t (D/d)^2$	2.2391
Allowable SCF	2.2000	Allowable SCF	1.8500	Allowable SCF	2.2900
SCF Ratio	0.9941	SCF Ratio	0.7100	SCF Ratio	1.0227
Fig. 38, $K_{ts}$	1.8390	Fig. 38, $K_{ts}$	1.3774	Fig. 38, $K_{ts}$	NA
Fig. 38, Alpha	100.0000	Fig. 38, Alpha	166.0000	Fig. 38, Alpha	0.0000
Min. Slope	1.1918	Min. Slope	8.1443	Min. Slope	0.0000

Top

S/G 23, A Bracket		S/G 23, B Bracket		S/G 23, C Bracket	
D/d	NA	D/d	NA	D/d	1.1111
r/d	NA	r/d	NA	r/d	0.1587
Aspect Ratio	NA	Aspect Ratio	NA	Aspect Ratio	9.0857
Crack Size	NA	Crack Size	NA	Crack Size	0.4953
$K_t (D/d)^2$	NA	$K_t (D/d)^2$	NA	$K_t (D/d)^2$	2.2963
Allowable SCF	NA	Allowable SCF	NA	Allowable SCF	2.4000
SCF Ratio	NA	SCF Ratio	NA	SCF Ratio	1.0452
Fig. 38, $K_{ts}$	NA	Fig. 38, $K_{ts}$	NA	Fig. 38, $K_{ts}$	NA
Fig. 38, Alpha	NA	Fig. 38, Alpha	NA	Fig. 38, Alpha	0.0000
Min. Slope	NA	Min. Slope	NA	Min. Slope	0.0000

Bottom

S/G 23, A Bracket		S/G 23, B Bracket		S/G 23, C Bracket	
D/d	NA	D/d	1.1589	D/d	1.1182
r/d	NA	r/d	0.1656	r/d	0.1597
Aspect Ratio	NA	Aspect Ratio	9.8333	Aspect Ratio	10.6216
Crack Size	NA	Crack Size	0.6792	Crack Size	0.5236
$K_t (D/d)^2$	NA	$K_t (D/d)^2$	2.6057	$K_t (D/d)^2$	2.3382
Allowable SCF	NA	Allowable SCF	2.2300	Allowable SCF	2.3400
SCF Ratio	NA	SCF Ratio	0.8558	SCF Ratio	1.0008
Fig. 38, $K_{ts}$	NA	Fig. 38, $K_{ts}$	1.6603	Fig. 38, $K_{ts}$	NA
Fig. 38, Alpha	NA	Fig. 38, Alpha	145.0000	Fig. 38, Alpha	0.0000
Min. Slope	NA	Min. Slope	3.1716	Min. Slope	0.0000



TABLE 5.2.2-7  
GRIND CONTOURS FOR S/G 24, BRACKETS A, B, C

Right

S/G 24, A Bracket		S/G 24, B Bracket		S/G 24, C Bracket	
D/d	1.1290	D/d	1.0703	D/d	1.1327
r/d	0.1613	r/d	0.1529	r/d	0.1618
Aspect Ratio	24.6500	Aspect Ratio	34.2609	Aspect Ratio	22.1220
Crack Size	0.5660	Crack Size	0.3255	Crack Size	0.5802
$K_t (D/d)^2$	2.4347	$K_t (D/d)^2$	2.0048	$K_t (D/d)^2$	2.4505
Allowable SCF	2.0500	Allowable SCF	2.3000	Allowable SCF	2.0700
SCF Ratio	0.8420	SCF Ratio	1.1472	SCF Ratio	0.8447
Fig. 38, $K_{ts}$	1.6082	Fig. 38, $K_{ts}$	NA	Fig. 38, $K_{ts}$	1.6134
Fig. 38, Alpha	149.0000	Fig. 38, Alpha	0.0000	Fig. 38, Alpha	150.0000
Min. Slope	3.6059	Min. Slope	0.0000	Min. Slope	3.7321

Left

S/G 24, A Bracket		S/G 24, B Bracket		S/G 24, C Bracket	
D/d	1.1006	D/d	1.0606	D/d	1.1218
r/d	0.1572	r/d	0.1515	r/d	0.1603
Aspect Ratio	30.3438	Aspect Ratio	39.4000	Aspect Ratio	25.9474
Crack Size	0.4528	Crack Size	0.2830	Crack Size	0.5377
$K_t (D/d)^2$	2.2411	$K_t (D/d)^2$	1.9348	$K_t (D/d)^2$	2.3784
Allowable SCF	2.1000	Allowable SCF	2.3300	Allowable SCF	2.0500
SCF Ratio	0.9371	SCF Ratio	1.2043	SCF Ratio	0.8619
Fig. 38, $K_{ts}$	1.7336	Fig. 38, $K_{ts}$	NA	Fig. 38, $K_{ts}$	1.6290
Fig. 38, Alpha	132.0000	Fig. 38, Alpha	0.0000	Fig. 38, Alpha	146.0000
Min. Slope	2.2460	Min. Slope	0.0000	Min. Slope	3.2709

Top

S/G 24, A Bracket		S/G 24, B Bracket		S/G 24, C Bracket	
D/d	NA	D/d	NA	D/d	1.1218
r/d	NA	r/d	NA	r/d	0.1603
Aspect Ratio	NA	Aspect Ratio	NA	Aspect Ratio	6.7105
Crack Size	NA	Crack Size	NA	Crack Size	0.5377
$K_t (D/d)^2$	NA	$K_t (D/d)^2$	NA	$K_t (D/d)^2$	2.3784
Allowable SCF	NA	Allowable SCF	NA	Allowable SCF	2.4500
SCF Ratio	NA	SCF Ratio	NA	SCF Ratio	1.0301
Fig. 38, $K_{ts}$	NA	Fig. 38, $K_{ts}$	NA	Fig. 38, $K_{ts}$	NA
Fig. 38, Alpha	NA	Fig. 38, Alpha	NA	Fig. 38, Alpha	0.0000
Min. Slope	NA	Min. Slope	NA	Min. Slope	0.0000

Bottom

S/G 24, A Bracket		S/G 24, B Bracket		S/G 24, C Bracket	
D/d	1.0936	D/d	1.0574	D/d	1.1386
r/d	0.1563	r/d	0.1511	r/d	0.1627
Aspect Ratio	11.4333	Aspect Ratio	15.7895	Aspect Ratio	9.3427
Crack Size	0.4245	Crack Size	0.2689	Crack Size	0.6028
$K_t (D/d)^2$	2.2131	$K_t (D/d)^2$	1.9119	$K_t (D/d)^2$	2.4761
Allowable SCF	2.4200	Allowable SCF	2.4500	Allowable SCF	2.3000
SCF Ratio	1.0935	SCF Ratio	1.2814	SCF Ratio	0.9289
Fig. 38, $K_{ts}$	NA	Fig. 38, $K_{ts}$	NA	Fig. 38, $K_{ts}$	1.7742
Fig. 38, Alpha	0.0000	Fig. 38, Alpha	0.0000	Fig. 38, Alpha	132.0000
Min. Slope	0.0000	Min. Slope	0.0000	Min. Slope	2.2460



TABLE 5.2.2-8  
GRIND CONTOURS FOR S/G 23, WELD PADS D, E, F, G

S/G 23, Pad D		S/G 23, Pad E		S/G 23, Pad F		S/G 23, Pad G	
D/d	1.0294	D/d	1.0294	D/d	1.0806	D/d	1.0294
r/d	0.1471	r/d	0.1471	r/d	0.1515	r/d	0.1429
Aspect Ratio	39.0000	Aspect Ratio	42.0000	Aspect Ratio	21.0000	Aspect Ratio	42.0000
Crack Size	0.1415	Crack Size	0.1415	Crack Size	0.2830	Crack Size	0.1415
$K_t (D/d)^2$	1.7485	$K_t (D/d)^2$	1.7485	$K_t (D/d)^2$	1.9123	$K_t (D/d)^2$	1.8121
Allowable SCF	2.7800	Allowable SCF	2.7800	Allowable SCF	2.4400	Allowable SCF	2.7800
SCF Ratio	1.5889	SCF Ratio	1.5889	SCF Ratio	1.2759	SCF Ratio	1.5342
Fig. 38, $K_{ts}$	NA	Fig. 38, $K_{ts}$	NA	Fig. 38, $K_{ts}$	NA	Fig. 38, $K_{ts}$	NA
Fig. 38, Alpha	0.0000	Fig. 38, Alpha	0.0000	Fig. 38, Alpha	0.0000	Fig. 38, Alpha	0.0000
Min. Slope	0.0000	Min. Slope	0.0000	Min. Slope	0.0000	Min. Slope	0.0000

Right

S/G 23, Pad D		S/G 23, Pad E		S/G 23, Pad F		S/G 23, Pad G	
D/d	1.1290	D/d	1.0294	D/d	1.0838	D/d	1.0294
r/d	0.1613	r/d	0.1471	r/d	0.1563	r/d	0.1429
Aspect Ratio	9.7500	Aspect Ratio	42.0000	Aspect Ratio	14.0000	Aspect Ratio	42.0000
Crack Size	0.5860	Crack Size	0.1415	Crack Size	0.4245	Crack Size	0.1415
$K_t (D/d)^2$	2.3837	$K_t (D/d)^2$	1.7485	$K_t (D/d)^2$	2.2131	$K_t (D/d)^2$	1.8121
Allowable SCF	2.3700	Allowable SCF	2.7800	Allowable SCF	2.3500	Allowable SCF	2.7800
SCF Ratio	0.9942	SCF Ratio	1.5889	SCF Ratio	1.0818	SCF Ratio	1.5342
Fig. 38, $K_{ts}$	1.8592	Fig. 38, $K_{ts}$	NA	Fig. 38, $K_{ts}$	NA	Fig. 38, $K_{ts}$	NA
Fig. 38, Alpha	100.0000	Fig. 38, Alpha	0.0000	Fig. 38, Alpha	0.0000	Fig. 38, Alpha	0.0000
Min. Slope	1.1918	Min. Slope	0.0000	Min. Slope	0.0000	Min. Slope	0.0000

Left

S/G 23, Pad D		S/G 23, Pad E		S/G 23, Pad F		S/G 23, Pad G	
D/d	1.0806	D/d	1.0294	D/d	1.0838	D/d	1.0294
r/d	0.1515	r/d	0.1471	r/d	0.1563	r/d	0.1429
Aspect Ratio	18.5000	Aspect Ratio	42.0000	Aspect Ratio	14.8867	Aspect Ratio	43.0000
Crack Size	0.2830	Crack Size	0.1415	Crack Size	0.4245	Crack Size	0.1415
$K_t (D/d)^2$	1.9123	$K_t (D/d)^2$	1.7485	$K_t (D/d)^2$	2.2131	$K_t (D/d)^2$	1.8121
Allowable SCF	2.4200	Allowable SCF	2.7800	Allowable SCF	2.3500	Allowable SCF	2.7800
SCF Ratio	1.2853	SCF Ratio	1.5889	SCF Ratio	1.0818	SCF Ratio	1.5342
Fig. 38, $K_{ts}$	NA	Fig. 38, $K_{ts}$	NA	Fig. 38, $K_{ts}$	NA	Fig. 38, $K_{ts}$	NA
Fig. 38, Alpha	0.0000	Fig. 38, Alpha	0.0000	Fig. 38, Alpha	0.0000	Fig. 38, Alpha	0.0000
Min. Slope	0.0000	Min. Slope	0.0000	Min. Slope	0.0000	Min. Slope	0.0000

Top

S/G 23, Pad D		S/G 23, Pad E		S/G 23, Pad F		S/G 23, Pad G	
D/d	1.0294	D/d	1.0294	D/d	1.0294	D/d	1.0294
r/d	0.1471	r/d	0.1471	r/d	0.1471	r/d	0.1429
Aspect Ratio	37.0000	Aspect Ratio	42.0000	Aspect Ratio	44.0000	Aspect Ratio	43.0000
Crack Size	0.1415	Crack Size	0.1415	Crack Size	0.1415	Crack Size	0.1415
$K_t (D/d)^2$	1.7485	$K_t (D/d)^2$	1.7485	$K_t (D/d)^2$	1.7485	$K_t (D/d)^2$	1.8121
Allowable SCF	2.7800	Allowable SCF	2.7800	Allowable SCF	2.7800	Allowable SCF	2.7800
SCF Ratio	1.5889	SCF Ratio	1.5889	SCF Ratio	1.5889	SCF Ratio	1.5342
Fig. 38, $K_{ts}$	NA	Fig. 38, $K_{ts}$	NA	Fig. 38, $K_{ts}$	NA	Fig. 38, $K_{ts}$	NA
Fig. 38, Alpha	0.0000	Fig. 38, Alpha	0.0000	Fig. 38, Alpha	0.0000	Fig. 38, Alpha	0.0000
Min. Slope	0.0000	Min. Slope	0.0000	Min. Slope	0.0000	Min. Slope	0.0000

Bottom

TABLE 5.2.2-9  
GRIND CONTOURS FOR S/G 24, WELD PADS D, E, F, G

S/G 24, Pad D		S/G 24, Pad E		S/G 24, Pad F		S/G 24, Pad G	
D/d	1.0417	D/d	NA	D/d	1.0294	D/d	NA
r/d	0.1488	r/d	NA	r/d	0.1471	r/d	NA
Aspect Ratio	36.0714	Aspect Ratio	NA	Aspect Ratio	53.0000	Aspect Ratio	NA
Crack Size	0.1981	Crack Size	NA	Crack Size	0.1415	Crack Size	NA
$K_t (D/d)^2$	1.8121	$K_t (D/d)^2$	NA	$K_t (D/d)^2$	1.7485	$K_t (D/d)^2$	NA
Allowable SCF	2.5000	Allowable SCF	NA	Allowable SCF	2.7900	Allowable SCF	NA
SCF Ratio	1.3796	SCF Ratio	NA	SCF Ratio	1.5689	SCF Ratio	NA
Fig. 38, $K_a$	NA	Fig. 38, $K_a$	NA	Fig. 38, $K_a$	NA	Fig. 38, $K_a$	NA
Fig. 38, Alpha	0.0000	Fig. 38, Alpha	NA	Fig. 38, Alpha	0.0000	Fig. 38, Alpha	NA
Min. Slope	0.0000	Min. Slope	NA	Min. Slope	0.0000	Min. Slope	NA

Right

S/G 24, Pad D		S/G 24, Pad E		S/G 24, Pad F		S/G 24, Pad G	
D/d	1.0938	D/d	1.0204	D/d	NA	D/d	NA
r/d	0.1563	r/d	0.1458	r/d	NA	r/d	NA
Aspect Ratio	20.3533	Aspect Ratio	71.5714	Aspect Ratio	NA	Aspect Ratio	NA
Crack Size	0.4245	Crack Size	0.0991	Crack Size	NA	Crack Size	NA
$K_t (D/d)^2$	2.2131	$K_t (D/d)^2$	1.7180	$K_t (D/d)^2$	NA	$K_t (D/d)^2$	NA
Allowable SCF	2.2800	Allowable SCF	3.0000	Allowable SCF	NA	Allowable SCF	NA
SCF Ratio	1.0302	SCF Ratio	1.7462	SCF Ratio	NA	SCF Ratio	NA
Fig. 38, $K_a$	NA	Fig. 38, $K_a$	NA	Fig. 38, $K_a$	NA	Fig. 38, $K_a$	NA
Fig. 38, Alpha	0.0000	Fig. 38, Alpha	0.0000	Fig. 38, Alpha	NA	Fig. 38, Alpha	NA
Min. Slope	0.0000	Min. Slope	0.0000	Min. Slope	NA	Min. Slope	NA

Left

S/G 24, Pad D		S/G 24, Pad E		S/G 24, Pad F		S/G 24, Pad G	
D/d	1.0938	D/d	1.0174	D/d	1.0204	D/d	NA
r/d	0.1563	r/d	0.1453	r/d	0.1458	r/d	NA
Aspect Ratio	22.9000	Aspect Ratio	80.6333	Aspect Ratio	70.7143	Aspect Ratio	NA
Crack Size	0.4245	Crack Size	0.0849	Crack Size	0.0991	Crack Size	NA
$K_t (D/d)^2$	2.2131	$K_t (D/d)^2$	1.7081	$K_t (D/d)^2$	1.7180	$K_t (D/d)^2$	NA
Allowable SCF	2.2500	Allowable SCF	2.6500	Allowable SCF	3.0000	Allowable SCF	NA
SCF Ratio	1.0167	SCF Ratio	1.5515	SCF Ratio	1.7462	SCF Ratio	NA
Fig. 38, $K_a$	NA	Fig. 38, $K_a$	NA	Fig. 38, $K_a$	NA	Fig. 38, $K_a$	NA
Fig. 38, Alpha	0.0000	Fig. 38, Alpha	0.0000	Fig. 38, Alpha	0.0000	Fig. 38, Alpha	NA
Min. Slope	0.0000	Min. Slope	0.0000	Min. Slope	0.0000	Min. Slope	NA

Top

S/G 24, Pad D		S/G 24, Pad E		S/G 24, Pad F		S/G 24, Pad G	
D/d	NA	D/d	1.0355	D/d	1.0808	D/d	NA
r/d	NA	r/d	0.1479	r/d	0.1515	r/d	NA
Aspect Ratio	NA	Aspect Ratio	40.4167	Aspect Ratio	25.5000	Aspect Ratio	NA
Crack Size	NA	Crack Size	0.1688	Crack Size	0.2830	Crack Size	NA
$K_t (D/d)^2$	NA	$K_t (D/d)^2$	1.8121	$K_t (D/d)^2$	1.9348	$K_t (D/d)^2$	NA
Allowable SCF	NA	Allowable SCF	2.6500	Allowable SCF	2.4200	Allowable SCF	NA
SCF Ratio	NA	SCF Ratio	1.4624	SCF Ratio	1.2508	SCF Ratio	NA
Fig. 38, $K_a$	NA	Fig. 38, $K_a$	NA	Fig. 38, $K_a$	NA	Fig. 38, $K_a$	NA
Fig. 38, Alpha	NA	Fig. 38, Alpha	0.0000	Fig. 38, Alpha	0.0000	Fig. 38, Alpha	NA
Min. Slope	NA	Min. Slope	0.0000	Min. Slope	0.0000	Min. Slope	NA

Bottom

TABLE 5.2.2-10  
INDIAN POINT 2 GRINDOUT CONTOURS  
AREAS REQUIRING WELDING TO MEET [10]1/2 CRITERION  
FOR 300 DAYS OF OPERATION FOR ABC BRACKETS AND STRAPS

S/G	Pad/Brkt	Side	Max. Depth	Min. Rad.	Comments
21	A	R	0.43	0.50	Weld Repair Required
		L	0.37	0.50	Weld Repair Required
		T	0.22	0.50	Slope not critical
	B	B	0.34	0.50	Contouring Acceptable
		R	0.42	0.50	Weld Repair Required
		L	0.27	0.50	Weld Repair Required
	C	T			No Indications
		B	0.28	0.50	Slope not critical
		R	0.24	0.50	Slope not critical
		L	0.45	0.50	Weld Repair Required
		T			No Indications
		B	0.32	0.50	Slope not critical
23	A	R	0.33	0.50	Weld Repair Required
		L	0.30	0.50	Contouring Acceptable
		T			No Indications
	B	B			Flush, No Fillet Remains
		R	0.36	0.50	Weld Repair Required
		L	0.48	0.50	Weld Repair Required
	C	T			No Indications
		B	0.48	0.50	Contouring Acceptable
		R	0.45	0.50	Weld Repair Required
		L	0.31	0.50	Slope not critical
		T	0.35	0.50	Slope not critical
	D	B	0.37	0.50	Slope not critical
		R	0.10	0.50	Slope not critical
		L	0.40	0.50	Contouring Acceptable
	E	T	0.20	0.50	Slope not critical
		B	0.10	0.50	Slope not critical
		All	0.10	0.50	Slope not critical
	F	R	0.20	0.50	Slope not critical
		L	0.30	0.50	Slope not critical
		T	0.30	0.50	Slope not critical
		B	0.10	0.50	Slope not critical
	G	All	0.10	0.50	Slope not critical



TABLE 5.2.2-10  
INDIAN POINT 2 GRINDOUT CONTOURS (Cont.)

S/G	Pad/Brkt	Side	Max. Depth	Min. Rad.	Comments
24	A	R	0.40	0.50	Weld Repair Required
		L	0.32	0.50	Weld Repair Required
		T			No Indications
		B	0.30	0.50	Slope not critical
	B	*			Bracket Must Be Repaired
		R	0.23	0.50	Slope not critical
		L	0.20	0.50	Slope not critical
		T			No Indications
	C	B	0.19	0.50	Slope not critical
		R	0.41	0.50	Weld Repair Required
		L	0.38	0.50	Weld Repair Required
		T	0.38	0.50	Slope not critical
	D	B	0.43	0.50	Contouring Acceptable
		R	0.14	0.50	Slope not critical
		L	0.30	0.50	Remove undercut, Slope not critical
		T	0.30	0.50	Slope not critical
	E	B			No Shell Grinding Indicated
		R			No Shell Grinding Indicated
		L	0.07	0.50	Slope not critical
		T	0.06	0.50	Slope not critical
	F	B	0.12	0.50	Blend/Break Corners Only
		R	0.10	0.50	Slope not critical
		L			No Shell Grinding Indicated
		T	0.07	0.50	Slope not critical
	G	B	0.20	0.50	Slope not critical
			O.K.		No Indications

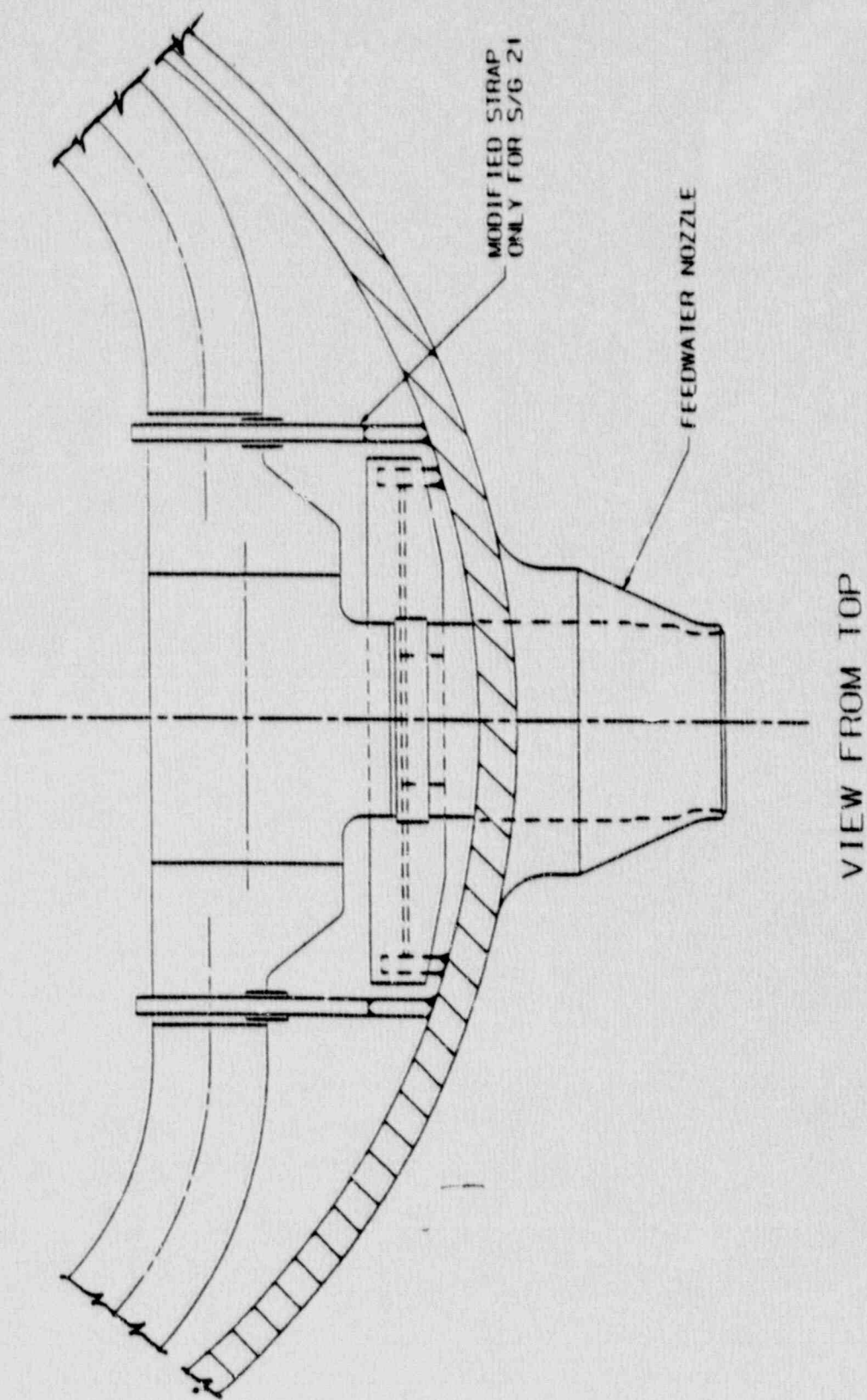


FIGURE 5.2.2-1. PLAN VIEW OF MODIFIED/RELOCATED BRACKET SUPPORT

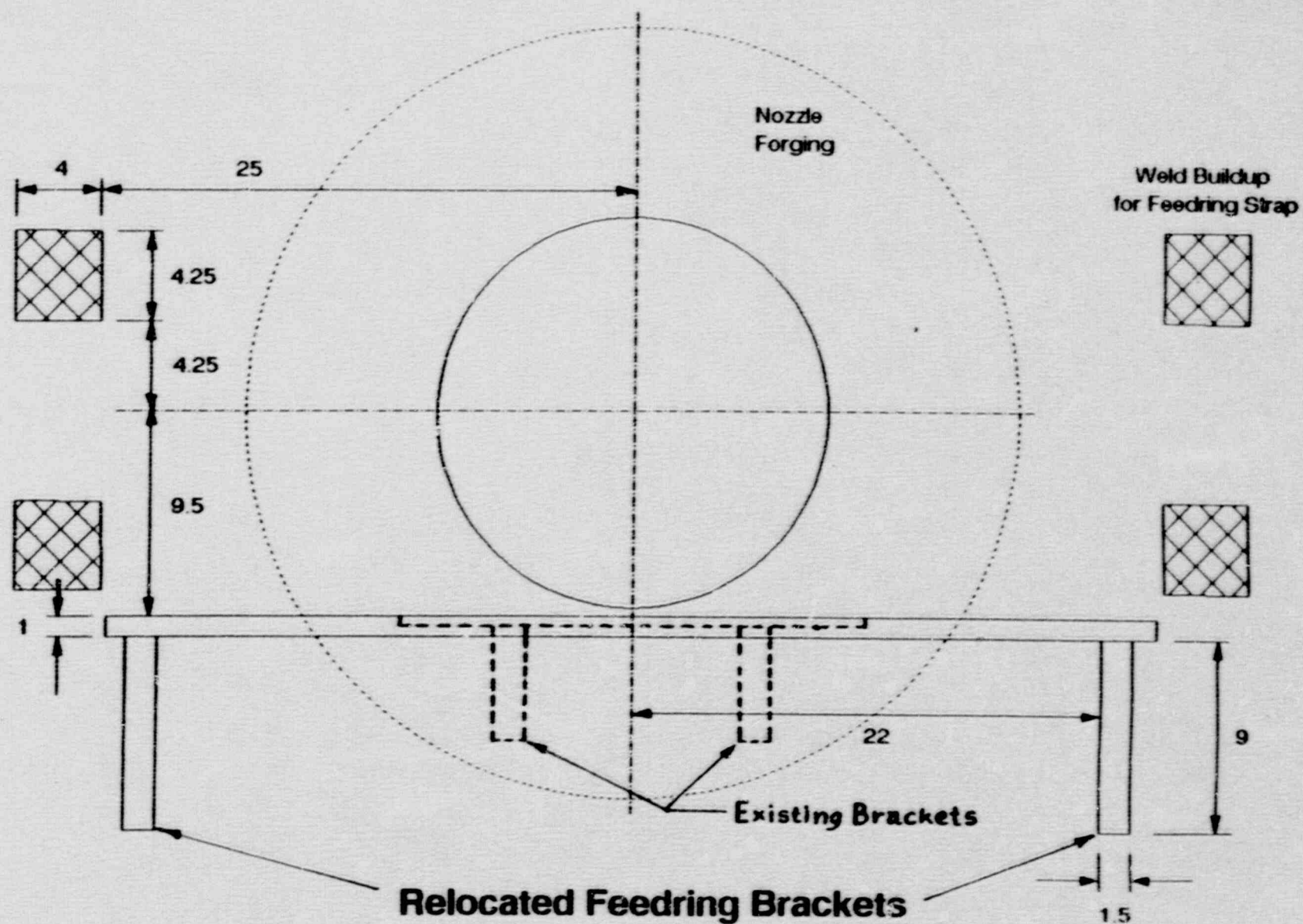


FIGURE 5.2.2-2. EXISTING & RELOCATED BRACKET SUPPORT LOCATIONS



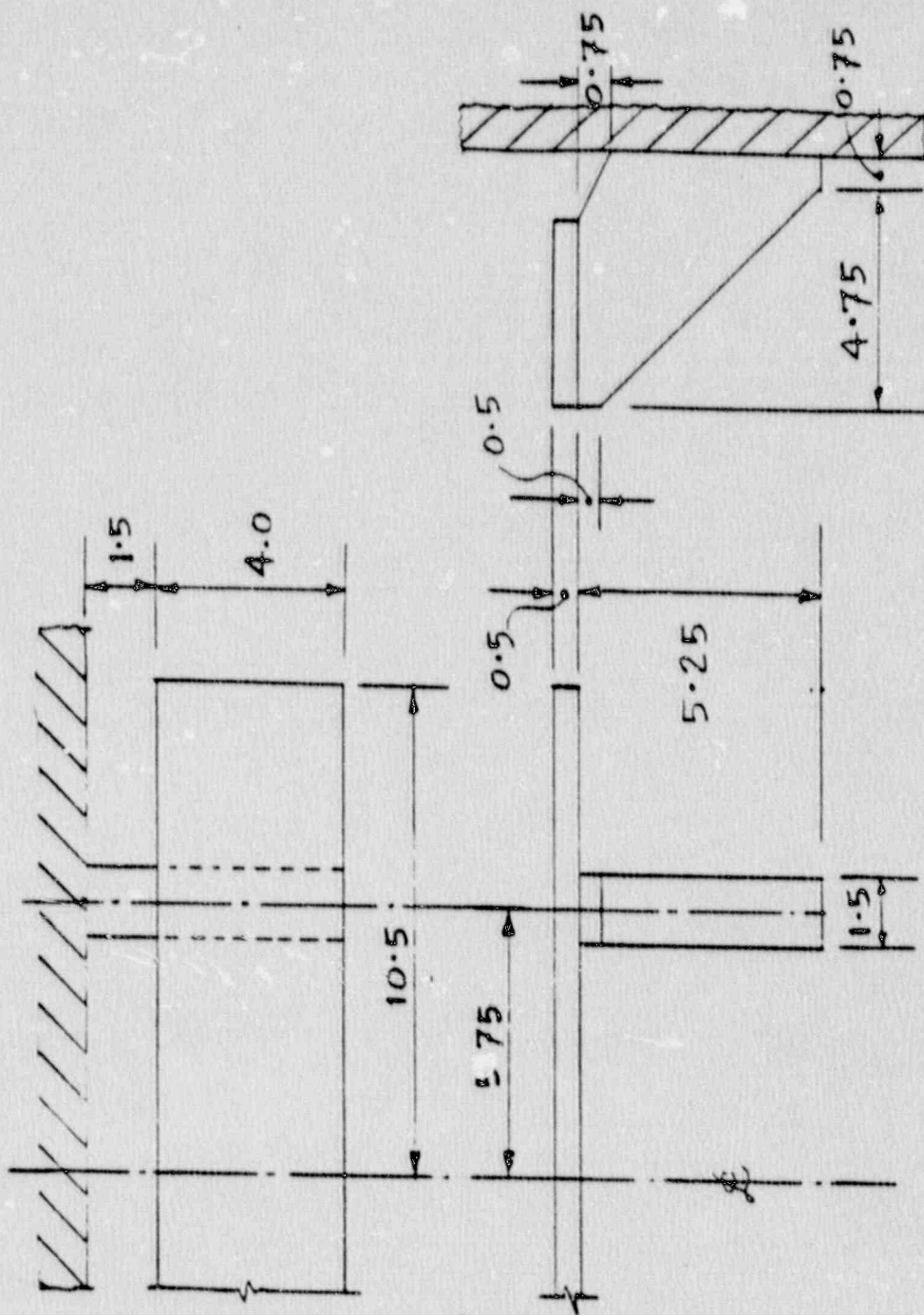


FIGURE 5.2.2-3. EXISTING BRACKET CONFIGURATION

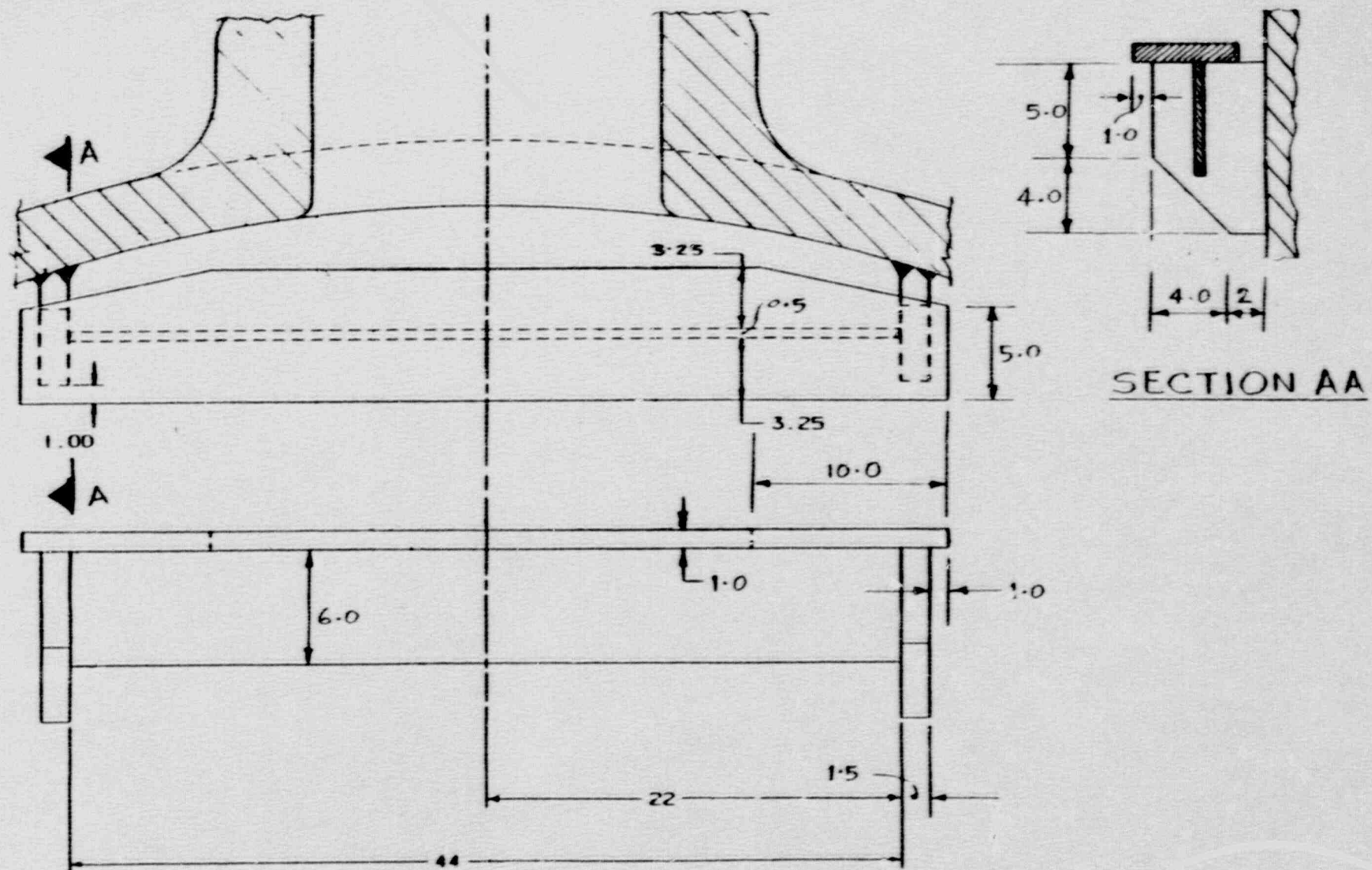
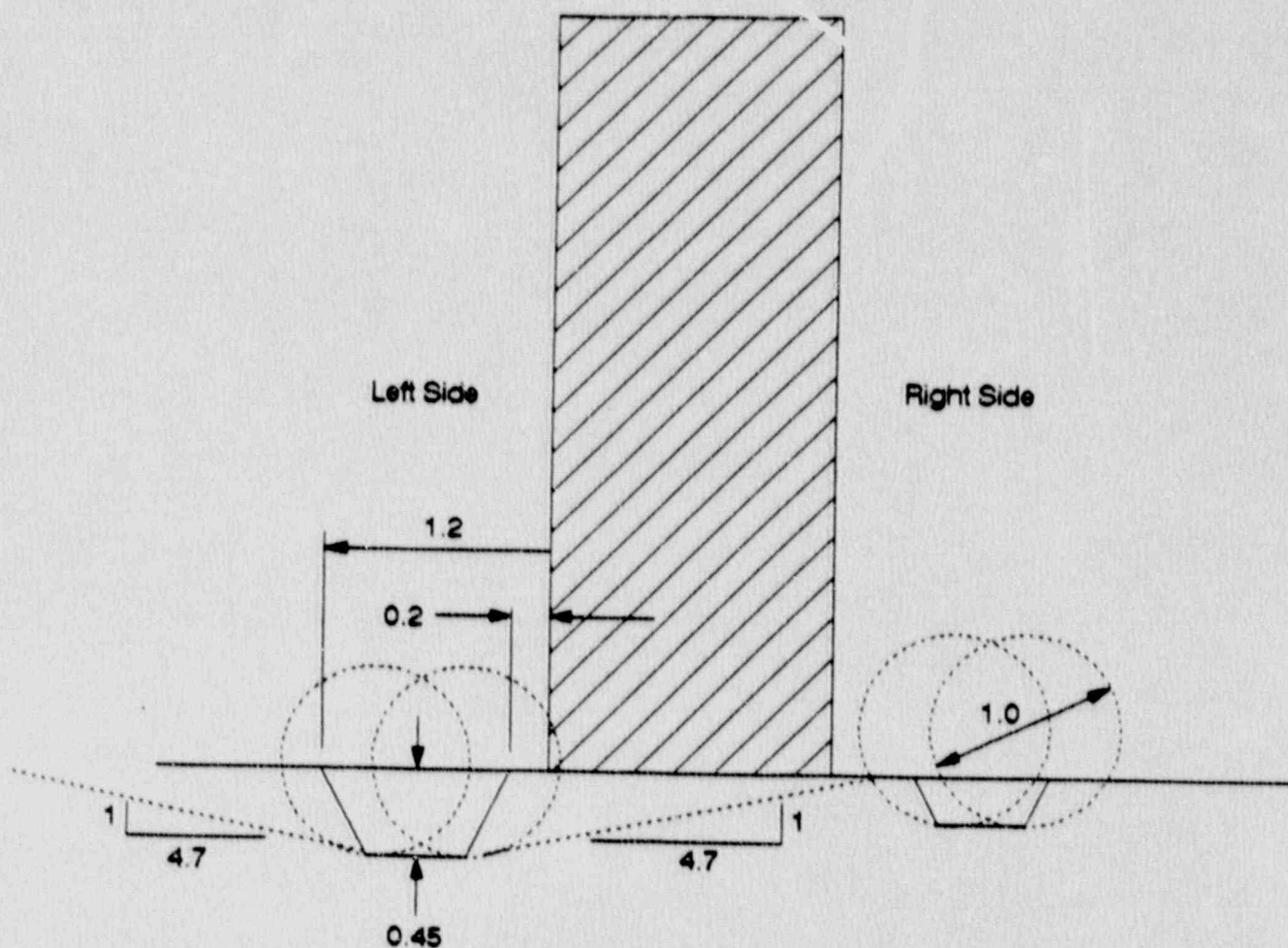


FIGURE 5.2.2-4. MODIFIED BRACKET CONFIGURATION



S/G 21, Bracket C

FIGURE 5.2.2-5. Grind Contour Acceptability for S/G 21, Bracket C



### 5.2.3 Local Grind Stress Distributions - Girth Weld and Transition Cone

A parametric evaluation was performed to determine the effects of various local grind geometries assuming different initial grind depths at the transition cone to upper shell weld. Four girth weld grind models were evaluated with grind depths of 0.50, 0.75, 1.00 and 1.25 inches. Stresses for each of these four girth weld grinds were evaluated assuming three local grinds were applied at each of two locations. The locations evaluated are: first, directly adjoining the girth weld grind, and second, approximately 12 inches below the girth weld grind. The local grinds evaluated included grind depths of 0.50, 0.65 and 0.85 inches. Figure 5.2.3-1 contains the locations evaluated. Note that the girth weld grinds occur at the transition cone to upper shell weld, while the local grinds occur below this location.

#### Adjusted Stress Distribution

As in Section 5.2.2.2, the effect of the reduced thickness of the shell after grinding on the stress distribution through the transition cone must be determined. To remove the oscillation in the stresses near the outside surface caused by the cubic variation assumed in Section 5.2.2.2, an exponential stress variation was used for the transition cone adjusted stresses.

The stress through the thickness is assumed to have the form:

$$\sigma = A_0 + A_1 e^{-by}$$

The conditions to be satisfied are:

- 1) At  $y = 0$ ,  $\sigma = SCF * S(0)$
- 2) The integral of the stress through the reduced thickness is equal to the net force on the section produced by the original stress distribution through the initial thickness.

- 3) The integral of the stress times the distance from the mid-surface through the reduced thickness is equal to the net moment about the mid-surface produced by the original stress distribution.

These result in the following equations:

$$S = A_0 + A_1$$

$$F = \int_0^t (A_0 + A_1 e^{-by}) dy$$

$$M = \int_0^t (A_0 + A_1 e^{-by})(y - t/2) dy$$

which give,

$$S = A_0 + A_1$$

$$F = A_0 t + A_1 (1 - e^{-bt})/b$$

$$M = A_1 \{1/b - t/2 - ((1+t)/b - t/2)e^{-bt}\}/b$$

These equations can be solved for  $A_0$ ,  $A_1$ , and  $b$  by iteration.

Table 5.2.3-1 contains typical distributions of stress generated for a single local grind depth (0.50 inches) for one of the four girth weld grind geometries. This table was generated for the location approximately 12 inches below the transition cone to upper shell weld grind.

#### Specific Transition Cone Local Grinds:

Upon inspection of the inside surfaces of the Indian Point 2 steam generator transition cones near the girth welds, linear indications were found which had depths and locations that could not be conservatively enveloped by the cases run during the parametric study described above. An additional

evaluation was performed for the deepest ground out region in each of the steam generators.

The procedure for calculating the adjusted stress distribution through the reduced thickness was refined as follows:

- 1) The net force and moment acting on the original thickness,  $D$ , are calculated using the original stress distribution.
- 2) The ratio of the original inside surface stress  $\sigma_0$  to the linearized inside surface stress  $(F/D - 6M/D^2)$  is determined. Let this ratio be  $C_0$ . This factor accounts for the nonlinear portion of the original stress distribution.
- 3) The thickness is reduced by the amount of the material ground away during the removal of indications. The inside surface stress with the reduced thickness,  $d$ , is given by

$$S = C_0 (r/d - 6M/d^2)$$

- 4) The inside surface stress is multiplied by stress concentration factors ranging from 1.0 to 2.5.
- 5) For each assumed stress concentration factor, the resulting stress distribution is required to have the same net force and moment acting on the reduced section as did the original stress distribution on the initial thickness.

The stress through the thickness is assumed to have the form:

$$\sigma = A_0 (D/d) + A_1 (D/d)^2 e^{-by}$$

where  $D$  is the thickness of the original transition cone wall and  $d$  is the reduced thickness after grinding.

The conditions to be satisfied are:



- 1) At  $y = 0$ ,  $\sigma = SCF * S$  (1)
- 2) The integral of the stress through the reduced thickness is equal to the net force on the section produced by the original stress distribution through the initial thickness.
- 3) The integral of the stress times the distance from the midsurface through the reduced thickness is equal to the net moment about the midsurface produced by the original stress distribution.

In equation (1) above, SCF is the applied stress concentration factor and  $S$  is the value of the stress at the inside surface as determined in item (3) above. If  $F$  is the net force on the section produced by the original stress distribution and  $M$  the net moment about the midsurface produced by the original stress distribution, the above three conditions result in:

$$S = SCF * S = A_0 (D/d) + A_1 (D/d)^2$$

$$F = \int_0^d \{A_0 (D/d) + A_1 (D/d)^2 e^{-by}\} dy$$

$$M = \int_0^d \{A_0 (D/d) + A_1 (D/d)^2 e^{-by}\} \{y - d/2\} dy$$

which give,

$$S = A_0 (D/d) + A_1 (D/d)^2 \quad (2)$$

$$F = A_0 D + A_1 (D/d)^2 (1 - e^{-bd})/b \quad (3)$$

$$M = -A_1 (D/d)^2 \{(d/2b + 1/b^2)(1 - e^{-bd}) + (d/b) e^{-bd}\} \quad (4)$$

These equations can be solved for  $A_0$ ,  $A_1$ , and  $b$  by iteration as follows:

- 1) Assume a value for  $b$

- 2) Solve (4) for  $A_1$ .
- 3) With that value of  $A_1$ , use (1) to determine  $A_0$ .
- 4) Solve (3) for  $F$ .
- 5) Compare  $F$  with the net force calculated for the original stress distribution. If they differ, modify  $b$  and repeat steps (2) - (5).

The deepest ground out regions in the transition cones for each of the Indian Point 2 steam generators were:

SG 21	0.71 inches
SG 22	0.91 inches
SG 23	0.70 inches
SG 24	1.00 inches

Table 5.2.3-2 presents the adjusted stress distributions for the deepest of these local grind geometries. Based on the fracture evaluation in Section 5.3, it is determined that a one-inch radius is required for grinding indications deeper than 0.75 inches, while a one-half inch radius is acceptable for shallower indications, with all indications having a blend slope of 2:1.

TABLE 5.2.3-1  
0.50 INCH GRIND MODEL, ASN 1 MAX GRIND DEPTH OF 0.50 INCH

**Grind = 0.50    ASN/Node = 1/274**

**Combined Stresses - FW275**

Numerical Integration

Node	Distance	Stress
274	0.0000	20.490
276	0.4150	15.298
278	0.8930	11.359
280	1.4410	8.798
282	2.0710	7.607
284	2.7940	7.735
286	3.6250	9.263

Force	Moment
7.4260	-11.9933
6.3710	-7.4558
5.5230	-3.6292
5.1676	-0.3314
5.5461	3.4442
7.0627	9.9545

Totals =      37.0964      -10.0110

Max. Grind Depth =      0.5  
Remaining Thickness =      3.125

Exponential Distribution Stress =  $A_0 + A_1 e^{-by}$

**Axial Stresses Through Remaining Thickness (ksi)**

Distance	Stress Concentration Factor		
	1.5	2.0	2.5
0.0000	30.735	40.980	51.225
0.5208	17.999	18.664	18.212
1.0417	11.958	10.674	9.395
2.0833	7.733	6.789	6.412
3.1250	6.782	6.291	6.200



TABLE 5.2.3-2

0.75 INCH GRIND MODEL, ASN 1 MAX GRIND DEPTH OF 0.50 INCH

Grind = 0.75 ASN/Node = 1/274

## Combined Stresses - FW275

Numerical Integration

Node	Distance	Stress
274	0.0000	19.105
276	0.4150	14.227
278	0.8930	10.653
280	1.4410	8.513
282	2.0710	7.804
284	2.7940	8.478
286	3.6250	10.625

Force	Moment
6.9164	-11.1708
5.9463	-6.9569
5.2515	-3.4434
5.1399	-0.3139
5.8859	3.6786
7.9373	11.2120

Totals = 37.0773 -6.9943

Max. Grind Depth = 0.5  
 Remaining Thickness = 3.125

Exponential Distribution Stress =  $A_0 + A_1 e^{-by}$ 

Axial Stresses Through Remaining Thickness (ksi)

Distance	Stress Concentration Factor		
	1.5	2.0	2.5
0.0000	28.658	38.210	47.763
0.5208	16.521	16.389	15.389
1.0417	11.512	10.276	9.299
2.0833	8.592	8.084	7.937
3.1250	8.095	7.912	7.889

TABLE 5.2.3-3  
1.00 INCH GRIND MODEL, ASN 1 MAX GRIND DEPTH OF 0.50 INCH

**Grind = 1.00 ASN/Node = 1/274**

**Combined Stresses - FW275**

Numerical Integration

Node	Distance	Stress
274	0.0000	19.456
276	0.4150	14.503
278	0.8930	10.841
280	1.4410	8.600
282	2.0710	7.773
284	2.7940	8.313
286	3.6250	10.311

Force	Moment
7.0465	-11.3807
6.0572	-7.0870
5.3268	-3.4946
5.1575	-0.3188
5.8151	3.6289
7.7383	10.9253

Totals = 37.1414 -7.7268

Max. Grind Depth = 0.5  
Remaining Thickness = 3.125

Exponential Distribution Stress =  $A_0 + A_1 e^{-by}$

**Axial Stresses Through Remaining Thickness (ksi)**

Distance	Stress Concentration Factor		
	1.5	2.0	2.5
0.0000	29.184	38.912	48.640
0.5208	16.936	17.016	16.132
1.0417	11.652	10.388	9.306
2.0833	8.389	7.773	7.572
3.1250	7.782	7.533	7.495

TABLE 5.2.3-4

1.25 INCH GRIND MODEL, ASN 1 MAX GRIND DEPTH OF 0.50 INCH

Grind = 1.25 ASN/Node = 1/274

## Combined Stresses - FW275

Numerical Integration

Node	Distance	Stress
274	0.0000	18.621
276	0.4150	13.861
278	0.8930	10.422
280	1.4410	8.435
282	2.0710	7.900
284	2.7940	8.774
286	3.6250	11.154

Force	Moment
6.7400	-10.8860
5.8036	-6.7890
5.1668	-3.3849
5.1455	-0.3084
6.0277	3.7752
8.2801	11.7042

Totals = 37.1637 -5.8889

Max. Grind Depth = 0.5  
 Remaining Thickness = 3.125

Exponential Distribution Stress =  $A_0 + A_1 e^{-by}$ 

Axial Stresses Through Remaining Thickness (ksi)

Distance	Stress Concentration Factor		
	1.5	2.0	2.5
0.0000	27.932	37.242	46.552
0.5208	15.892	15.422	14.279
1.0417	11.349	10.194	9.409
2.0833	8.988	8.641	8.563
3.1250	8.652	8.552	8.544



TABLE 5.2.3-5

### Original Stress Distribution

## Numerical Integration

Node	Distance	Stress
326	0.0000	22.255
327	0.2077	18.517
328	0.4155	15.870
329	0.6541	13.079
330	0.8927	11.266
331	1.1668	9.343
332	1.4409	8.196
333	1.7558	7.003
334	2.0707	6.393
335	2.4324	5.798
336	2.7941	5.742
337	3.2095	5.844
338	3.6250	6.710

Force	Moment
4.2349	-7.2493
3.5717	-5.3703
3.4540	-4.4265
2.9047	-3.0268
2.8246	-2.2229
2.4038	-1.2298
2.3928	-0.5222
2.1090	0.2074
2.2047	0.9614
2.0869	1.6704
2.4068	2.8639
2.6079	4.1975

Totals	33.2018	-14.1470
--------	---------	----------

IPP Transition Cone, 3/4" Girth Weld Grind  
S/G 21 - FWCYC-560

Maximum Grind Depth	0.7100	$F/D - 6M/D^2$	15.619	$D/d$	1.2406
Remaining Thickness	2.9150	$C_0$	1.425	$(D/d)^2$	1.5465
Exponential Distribution	Stress = $A_0 (D/d) + A_1 (D/d)^2 e^{-by}$		$F/d - 6M/d^2$		21.379
	Axial Stresses Through Remaining Thickness		$C_0(F/d - 6M/d^2)$		30.46349

Distance	Stress Concentration Factor						
	1.0	1.4	1.5	1.6	1.8	2.0	2.5
0.0000	30.463	42.649	45.695	48.742	54.834	60.927	76.159
0.2915	18.356	18.855	18.744	18.570	18.081	17.464	15.699
0.5830	12.990	11.658	11.325	11.009	10.441	9.965	9.135
1.0202	9.979	9.056	8.914	8.798	8.626	8.513	8.364
1.4575	9.090	8.624	8.566	8.520	8.454	8.409	8.336
1.8947	8.828	8.552	8.516	8.486	8.438	8.401	8.335
2.3320	8.751	8.540	8.508	8.481	8.436	8.401	8.335
2.9150	8.725	8.538	8.507	8.481	8.436	8.400	8.335

TABLE 5.2.3-6  
ADJUSTED STRESS DISTRIBUTION FOR S/G 22 TRANSITION CONE

Original Stress Distribution

Numerical Integration

Node	Distance	Stress
326	0.0000	22.255
327	0.2077	18.517
328	0.4155	15.870
329	0.6541	13.079
330	0.8927	11.266
331	1.1668	9.343
332	1.4409	8.196
333	1.7558	7.003
334	2.0707	6.393
335	2.4324	5.798
336	2.7941	5.742
337	3.2095	5.844
338	3.6250	6.710

Force	Moment
4.2349	-7.2493
3.5717	-5.3703
3.4540	-4.4265
2.9047	-3.0268
2.8246	-2.2229
2.4038	-1.2298
2.3928	-0.5222
2.1090	0.2074
2.2047	0.9614
2.0869	1.6704
2.4068	2.8639
2.6079	4.1975

Totals      33.2018    -14.1470

IPP Transition Cone, 3/4" Girth Weld Grind  
S/G 22 - FWCYC-560

Maximum Grind Depth	0.9100	F/D - 6M/D <sup>2</sup>	15.619	D/d	1.3352
Remaining Thickness	2.7150	C <sub>0</sub>	1.425	(D/d) <sup>2</sup>	1.7827
Exponential Distribution Stress = A <sub>0</sub> (D/d) + A <sub>1</sub> (D/d) <sup>2</sup> e <sup>-by</sup>					F/d - 6M/d <sup>2</sup> 23.744
Axial Stresses Through Remaining Thickness					C <sub>0</sub> (F/d-6M/d <sup>2</sup> )      33.83336

Distance	Stress Concentration Factor						
	1.0	1.4	1.5	1.6	1.8	2.0	2.5
0.0000	33.833	47.367	50.750	54.133	60.900	67.667	84.583
0.2715	20.211	20.854	20.752	20.579	20.070	19.409	17.469
0.5430	14.109	12.638	12.264	11.907	11.258	10.707	9.726
0.9502	10.642	9.586	9.420	9.282	9.077	8.939	8.756
1.3575	9.602	9.060	8.991	8.937	8.858	8.803	8.717
1.7647	9.291	8.969	8.927	8.892	8.836	8.793	8.716
2.1720	9.197	8.954	8.917	8.886	8.834	8.792	8.716
2.7150	9.166	8.951	8.916	8.885	8.833	8.792	8.715

TABLE 5.2.3-7  
ADJUSTED STRESS DISTRIBUTION FOR S/G 23 TRANSITION CONE

Original Stress Distribution			Numerical Integration	
Node	Distance	Stress	Force	Moment
326	0.0000	22.255	4.2349	-7.2495
327	0.2077	18.517	3.5717	-5.3703
328	0.4155	15.870	3.4540	-4.4265
329	0.6541	13.079	2.9047	-3.0268
330	0.8927	11.266	2.8246	-2.2229
331	1.1668	9.343	2.4038	-1.2298
332	1.4409	8.196	2.3928	-0.5222
333	1.7558	7.003	2.1090	0.2074
334	2.0707	6.393	2.2047	0.9614
335	2.4324	5.798	2.0869	1.6704
336	2.7941	5.742	2.4068	2.8639
337	3.2015	5.844	2.6079	4.1975
338	3.6250	6.710		

Totals                      33.2018      -14.1470

**IPP Transition Cone, 3/4" Girth Weld Grind  
S/G 23 - FWCYC-560**

Maximum Grind Depth	0.7000	$F/D - 6M/D^2$	15.619	$D/d$	1.2393
Remaining Thickness	2.9250	$C_0$	1.425	$(D/d)^2$	1.5359
				$F/d - 6M/d^2$	21.272
Exponential Distribution Stress = $A_0 (D/d) + A_1 (D/d)^2 e^{-by}$				$C_0(F/d - 3M/d^2)$	30.31084

**Axial Stresses Through Remaining Thickness**

Distance	Stress Concentration Factor						
	1.0	1.4	1.5	1.6	1.8	2.0	2.5
0.0000	30.311	42.435	45.466	48.497	54.560	60.622	75.777
0.2925	18.272	18.764	18.653	18.479	17.991	17.376	15.619
0.5850	12.939	11.613	11.282	10.968	10.404	9.930	9.107
1.0237	9.948	9.031	8.890	8.775	8.605	8.492	8.345
1.4625	9.066	8.603	8.546	8.500	8.435	8.389	8.318
1.9012	8.806	8.532	8.496	8.466	8.419	8.382	8.317
2.3400	8.729	8.520	8.489	8.462	8.417	8.382	8.317
2.9250	8.704	8.518	8.488	8.461	8.417	8.382	8.317



TABLE 5.2.3-8  
ADJUSTED STRESS DISTRIBUTION FOR S/G 24 TRANSITION CONE

Original Stress Distribution

Numerical Integration

Node	Distance	Stress
313	0.0000	21.505
314	0.2077	18.019
315	0.4155	15.407
316	0.6541	12.618
317	0.8927	10.753
318	1.1668	8.815
319	1.4409	7.732
320	1.7558	6.653
321	2.0707	6.280
322	2.4324	5.984
323	2.7941	6.251
324	3.2095	6.697
325	3.6250	7.659

Force	Moment
4.1053	-7.0269
3.4719	-5.2203
3.3437	-4.2856
2.7885	-2.9063
2.6819	-2.1113
2.2678	-1.1602
2.2647	-0.4938
2.0361	0.2020
2.2179	0.9705
2.2126	1.7746
2.6898	3.2053
2.9823	4.7996

Totals                      33.0624      -12.2524

IPP Transition Cone, 3/4" Girth Weld Grind  
S/G 24 - FWCYC-560

Maximum Grind Depth	1.0000	F/D - 6M/D <sup>2</sup>	14.715	D/d	1.3810
Remaining Thickness	2.6250	C <sub>0</sub>	1.461	(D/d) <sup>2</sup>	1.9070
				F/d - 6M/d <sup>2</sup>	23.264
Exponential Distribution Stress = A <sub>0</sub> (D/d) + A <sub>1</sub> (D/d) <sup>2</sup> e <sup>-by</sup>				C <sub>0</sub> (F/d-6M/d <sup>2</sup> )	33.99853

Axial Stresses Through Remaining Thickness

Distance	Stress Concentration Factor						
	1.0	1.4	1.5	1.6	1.8	2.0	2.5
0.0000	33.999	47.500	50.998	54.398	61.197	67.997	84.996
0.2625	20.155	20.518	20.356	20.129	19.530	18.807	16.819
0.5250	14.205	12.703	12.340	12.001	11.399	10.903	10.065
0.9187	10.984	10.024	9.881	9.765	9.597	9.487	9.345
1.3125	10.077	9.608	9.551	9.507	9.441	9.396	9.323
1.7062	9.821	9.544	9.507	9.477	9.428	9.390	9.322
2.1000	9.749	9.534	9.501	9.473	9.427	9.390	9.322
2.6250	9.726	9.532	9.501	9.473	9.427	9.390	9.322

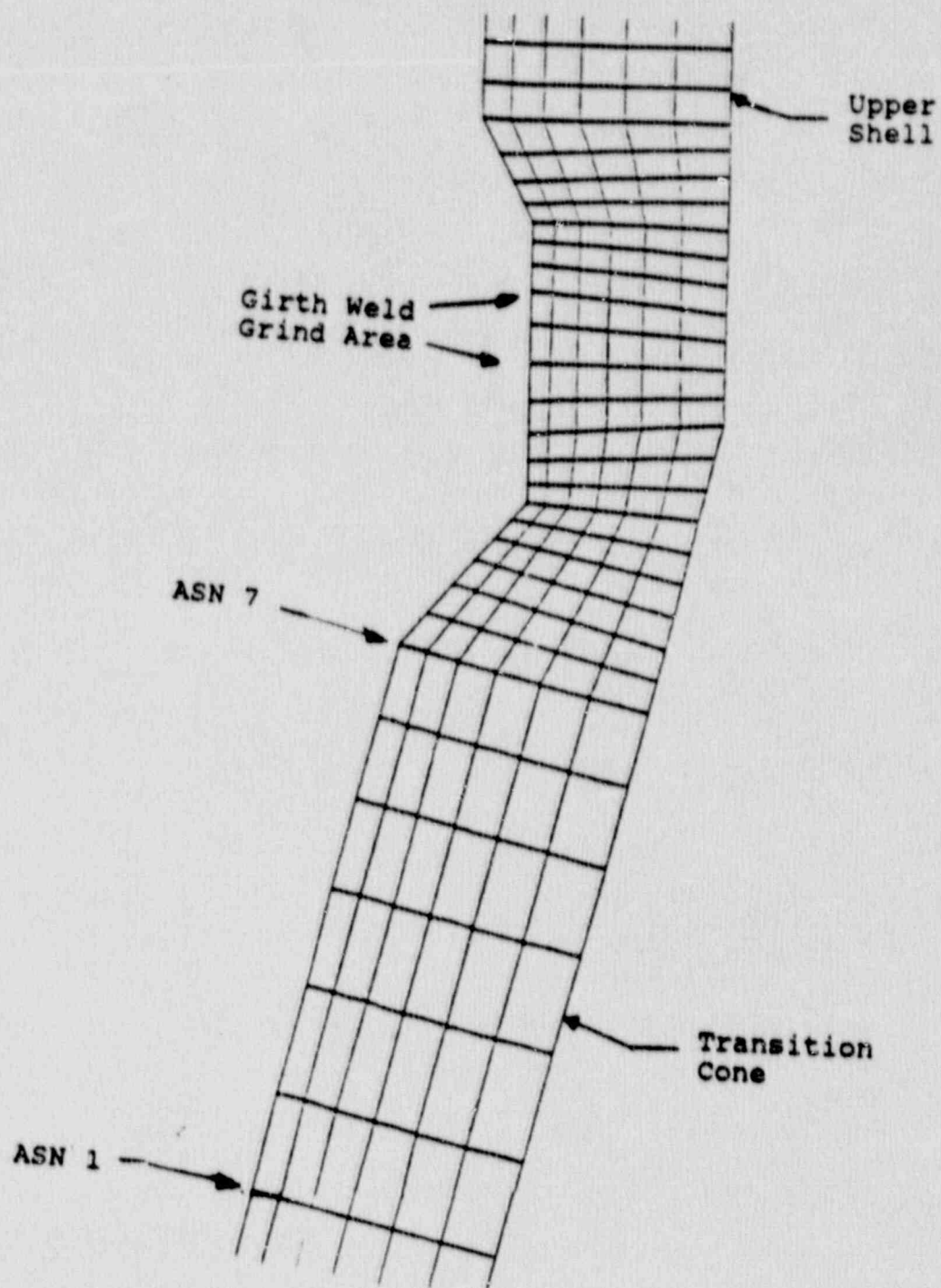


Figure 5.2.3-1  
Local Grind Evaluation Locations

### 5.3 FRACTURE MECHANICS EVALUATION

#### 5.3.1 General Approach: Acceptance Criteria

The approach used to demonstrate margin for continued operation is based on a modification of the fracture mechanics criteria of Section XI of the ASME Code. The Section XI fracture criteria are contained in paragraph IWB-3600, and normally used to justify continued operation without removal of cracks.

In this case, all cracks are being removed by grinding, which satisfies the Section XI criteria completely with no further analysis required. To further demonstrate that the steam generator integrity is expected to be maintained through the next operating cycle, the Section XI fracture criteria have been applied to the repaired configuration, to show that any cracks which might initiate and grow during the next operating cycle are within acceptable limits through the entire cycle.

Specifically, this criterion has been applied by reducing the material fracture toughness by a factor equal to the square root of 10, taken from paragraph IWB-3612 of Section XI, which applies to normal and upset operating transients. Since the governing transients do not drop the temperature of the vessel below 300°F, the fracture toughness of the material is on the upper shelf, or 200 ksi  $\sqrt{\text{in}}$ . The allowable fracture toughness then becomes 200 ksi  $\sqrt{\text{in}}$  divided by the square root of 10, or 63.2 ksi  $\sqrt{\text{in}}$ . For each of the regions in which cracking has been found, this criterion has been applied to the projected future crack growth. That is, that applied stress intensity factor for postulated flaws in each region has been calculated as a function of flaw depth, and limited to value of 63.2 ksi  $\sqrt{\text{in}}$ . The evaluations, whose results are summarized in section 5.3.7, have assumed flaws re-occur in all affected regions, with shape and orientation as found in the present inspections.



### 5.3.2 Stress Intensity Factor Calculations

The stress intensity factor was calculated using the expression of Raju and Newman (Reference 1). The stress intensity factor  $K_I$  for this case can be calculated using the actual stress profile through the wall. The stress distribution through the wall thickness is represented by a third order polynomial:

$$\sigma = \sum_{j=0}^3 A_j X^j$$

where:  $A_j = A_1, A_2, A_3, A_4$  are the coefficients of the curve fit  
 $X^j$  = the coordinate measured in the thickness direction, with  $X=0$  at the inside surface

The stress intensity factors for various ratios,  $a/c$ , ( $a$ : semi-minor axis,  $c$ : semi-major axis), for various angular locations along the crack front ( $\phi$ ), for inside and outside surface flaws of a cylinder, and for various ratios of thickness to inside radius,  $t/R$  were obtained by Raju and Newman (Reference 4). The magnification factors for the loading conditions utilized for an inside surface flaw are given in tables in the paper (Reference 4). Magnification factors for various locations around the periphery of the crack can be obtained by using an interpolation method. Stress intensity factors can be expressed by the general form:

$$K_I = \left(\frac{\pi a}{Q}\right)^{0.5} \sum_{j=0}^3 G_j(a/c, a/t, t/R, \phi) A_j a^j$$

where  $a/c$ : Ratio of crack dimensions  
 $a/t$ : Ratio of crack depth to thickness of a cylinder  
 $t/R$ : Ratio of thickness to inside radius  
 $\phi$ : Crack front location  
 $G_j = G_1, G_2, G_3, G_4$  are the influence function coefficients (from reference 4)

$$Q^{1/2} = \int_0^{\pi/2} (\cos^2 \phi + \frac{a^2}{c^2} \sin^2 \phi)^{1/2} d\phi$$

For the feedwater nozzle corner region, a separate expression was used. This  $K_I$  solution is based upon work performed by General Electric and reported in an EPRI special report (Reference 5). The geometry resembles a circular surface crack in a rounded corner, and is nearly identical to the feedwater nozzle corner. Only the  $K_I$  value at the deepest point (along the line of symmetry) is reported.

The  $K_I$  solution is written in terms of the stress distribution from the inside surface:

$$\sigma = A_0 + A_1 X + A_2 X^2 + A_3 X^3$$

$$K_I = (\pi a)^{0.5} \{ .706 A_0 + .537 \left( \frac{2a}{\pi} \right) A_1 + .448 \left( \frac{a^2}{2\pi} \right) A_2 + .393 \left( \frac{4a^3}{3\pi} \right) A_3 \}$$

This study was undertaken by General Electric to simulate a crack in a BWR feedwater nozzle, and therefore is applicable to nozzles of similar geometry. The feedwater nozzle is nearly identical in dimensions to a BWR feedwater nozzle.

An additional stress intensity factor expression was required for the fracture and fatigue crack growth analyses used in the treatment of the embedded flaw indications, as discussed in Section 5.3.8. The stress intensity factor expression of Shah and Kobayashi (Reference 6) was used. The flaw shape was set with length equal to five times the width ( $a/\ell = 0.10$ ), and the eccentricity (flaw location within the wall) was varied. This flaw shape was chosen to provide a worst case calculation of stress intensity factor for embedded flaws. The calculated crack growth was very small for this case, so no other shapes were considered necessary to analyze.

### 5.3.3 Crack Growth Rates

The mode of crack extension which is occurring in the girth weld region, and the adjacent cone region is primarily static load cracking. This finding has been discussed earlier in the metallurgical evaluation portion of this report and is further confirmed by the cracking behavior observed during the recent part-cycle of operation.

Table 5.3-1 provides a summary of the maximum crack extension measured in the depth direction at the end of the previous cycle, and at the end of the recent part-cycle. Results are summarized for each steam generator, and have been presented in terms of growth rates in inches per day. These results were obtained from reviewing all the measured crack extensions around the circumference of the girth weld and finding the maximum crack extension. It is clear from this table that the growth rate in the lead steam generator (22) is almost identical on a per-day basis for both service periods. The maximum growth rates in the other three generators have increased in the recent part cycle.

There is a dearth of experimental information on static load crack growth rates in carbon and low alloy steels under static loadings. The available information shows that growth rates are strongly dependent on the environment, especially the level of oxygen present. Since it is known that the level of oxygen present in the system was not consistent, the best approach is to use the measured crack growth rate for the maximum crack extension in each steam generator. Therefore, the maximum growth rate observed during the last two cycles of operation was used, for each individual generator.

The fatigue crack growth rate reference law used for the treatment of the embedded flaws in Section 5.3.8 was taken from Section XI of the ASME Code.

The crack growth rate reference curve for air environments is a single curve, the growth rate being only a function of applied  $\Delta K$ .

$$\frac{da}{dN} = (0.0267 \times 10^{-3}) \Delta K_I^{3.726}$$



where,  $\frac{da}{dN}$  = Crack growth rate, micro-inches/cycle

$\Delta K_I$  = stress intensity factor range, ksi  $\sqrt{\text{in}}$

$$= (K_{I_{\max}} - K_{I_{\min}})$$

#### 5.3.4 Methodology

A methodology was developed for assessing the integrity of each area for which stress corrosion cracking remains a concern and for determining the appropriate actions to be taken to permit safety and operability. This methodology encompasses general integrity evaluations, grinding limitations and grindout contouring, and weld repair. The steps, generally, are as follow:

- 1) Using the maximum growth rates found over the last two cycles of operation, which occurred during the last operating cycle (212 days), the postulated cracks for an assumed operating cycle of 300 days are obtained by multiplying the depth of the observed cracks by 300/212. Such cracks will be referred to as "reference cracks."
- 2) Obtain the stress distribution through the thickness of the wall for the load condition which produces the maximum stresses normal to the observed cracks from the appropriate finite element analysis performed previously.
- 3) Adjust the stress distribution through the thickness to account for the reduced thickness after grinding and for a range of stress concentration factors that could be introduced by the grind contour. The adjusted stress distributions have the same net force and moment acting on the reduced section as did the original stress distribution in step (2).

- 4) Perform stress intensity factor calculations for a range of aspect ratios for each of the stress distributions determined in step (3). Determine the maximum crack depths that satisfy the fracture criterion under consideration for each stress concentration factor and aspect ratio considered.
- 5) The grind geometry after contouring is assumed to be a [  $\sqrt{a/c}$  ]. The stress concentration produced by this geometry is obtained from the literature.
- 6) The crack depth from step (1) along with the appropriate aspect ratio are used to determine the allowable stress concentration factor from the results obtained in step (4). If that stress concentration factor is greater than the one determined in step (5), then the [  $\sqrt{a/c}$  ] assumed for the grind geometry is acceptable. Otherwise, a slope is specified for the sides of the notch to reduce the stress concentration factor.
- 7) The inspection reports of the grind locations and depths are then checked to determine whether the required grind contour can be performed without undercutting any adjacent structures, such as feedring support brackets. Steps (1) through (4) above apply to all regions evaluated, while steps (5) through (7), as an example, are specific to the feedring support brackets A, B, C and the feedring strap weld pads.

#### 5.3.5 Reference Crack Depth

Extensive evaluations were made of the cracking observed in the girth weld, transition cone brackets and straps after the last 212 days of operation, as determined by grinding out the cracks. The total maximum growth estimates for 300 days, which are called reference crack depths in this discussion, are listed below for the girth weld.

SG 21 : 0.51 in.

SG 22 : 0.75 in.

SG 23 : 0.39 in.

SG 24 : 0.48 in.

The reference cracks for the other steam generator regions are listed in Table 5.3-2. The crack growth rates are also given in inches per day of service. The aspect ratios in Table 5.3-2 were conservatively determined by examining the array of crack lengths and depths measured in grinding out cracks. A statistical approach was used for determining aspect ratios associated with the girth weld and transition cone as will be discussed below. Upper bound values were used at the other locations. If the fracture toughness criteria under consideration are satisfied, then 300 days of operation have been demonstrated.

#### 5.3.6 Reference Flaw Shape Determination

A detailed study was made of the surface flaws found in the girth weld and cone region, in order to make a reliable determination of the shape to be used in the analysis. The crack shape was found to be directly related to the growth behavior. Cracks which were found to be very long were also very shallow, and cracks which grew deep were not very long. A statistical evaluation was made of the 1990 data from the girth weld region, and a 99 percent upper confidence limit curve was constructed, as shown in Figure 5.3-1.

The driving force, or stress intensity factor for a flaw is strongly related to the flaw shape, with longer flaws (higher aspect ratios) having higher values of stress intensity factor for a given depth. Since we see the trend in the observed flaws is for longer flaws to be more shallow, if we want to maximize the stress intensity factor for the girth weld region, the more shallow crack extensions should be considered. The smallest crack extension for 300 days service was 0.39 inches, predicted for steam generator 23. All the other generators have larger predicted crack depths, therefore smaller aspect ratios.

Referring to figure 5.3-1, the 99 percent confidence limit on aspect ratio for a crack with depth = 0.39 inch is found to be 3.8. This aspect ratio was



increased to 4.4 to cover the largest indication found in the 1990 inspection, as also seen in Figure 5.3-1. Therefore, all postulated flaws for the girth weld for comparison with the acceptance criteria were assumed to have an aspect ratio of 4.4, for all steam generators.

The 99 percent upper confidence limit curve developed from the 1990 inspection results was also compared with the results of the 1989 inspection, and the result is shown in Figure 5.3-2. Although the scatter in the data is somewhat greater, the general behavior is very similar, and the prediction curve envelopes most of the data.

#### 5.3.7 Results for Surface Flaw Acceptability

The reference cracks are given in Table 5.3-2. The fracture toughness criteria are presented in Section 5.3.1. Stress analyses results were obtained for all the pertinent configurations, including contoured grinds for the situations where weld repairs are not made or are not made in full. These stress analyses are discussed in Section 5.2.

Fracture mechanics evaluations were performed using a range of postulated cracks and the appropriate stresses. The allowable toughness (63.2 ksi√in) was used in establishing the days of operation for the steam generator girth weld/bracket/transition cone region during the next half-cycle. The stress intensity factor calculations for each of the regions in the steam generator (except the feedwater nozzle region, Section 6.0) are summarized in Figures 5.3-3 through 5.3-7.

The results of the evaluation are summarized in Table 5.3-3. The fracture toughness criterion is satisfied for an assumed 300 days service in all areas except for the girth weld in steam generator 22 (271 days). With the extreme conservatism incorporated in the fracture toughness criterion, it is judged that an assumed 300 days of service can be accomplished without compromising safety and reliability. It should be noted that the next operating cycle is scheduled to be less than 240 days.

In order to verify the conservatism of the approach used to treat the surface flaws in the girth weld region, an evaluation of the crack growth behavior observed over the most recent two cycles was carried out. The approach used was to determine the maximum applied stress intensity factor for each flaw discovered. Since the calculated stress intensity factors are more strongly a function of crack shape than of grinding depth, the stress intensity factor results for a nominal grinding depth of 0.5 inch was used. With these results as a base, all the cracks from the 1990 inspection were plotted based on their depth and aspect ratio. The results appear in Figure 5.3-8, and show that the maximum applied stress intensity factor at the end of the 1989-90 cycle was about 52 ksi/in. This value is well below the Section XI criterion of 63.2 ksi/in, which verifies the conservatism of the approach used.

#### 5.3.8 Fracture Evaluation of Embedded Indications in the Girth Weld Region

In addition to the surface indications discussed in the above sections, a number of embedded indications were discovered during the final ultrasonic inspections of the girth weld region. These indications are summarized in Table 5.3-4, and have been subjected to a fracture mechanics evaluation, in accordance with the guidelines of Section XI, paragraph IWB 3600.

Steam Generator 22. Three indications were found in the cone region, away from any grindouts and these were plotted on Figure 5.3-9 (indications 1, 8/60 and 12). Two indications were found in the cone region, in the vicinity of grinds, number 6 in the region of a 0.375 grind and number 8/45 in the vicinity of a one-half inch grind. These have been plotted on Figure 5.3-10, the flaw chart for a one-half inch grind in the girth weld region, which is conservatively applicable to the cone region (where the stresses are lower).

Steam Generators 21 and 24. The first and third indications were assumed to be located near a one inch grind-out, for conservatism and have been plotted on Figure 5.3-11. The second indication was confirmed to be located near a one-half inch grind-out, and has been plotted on Figure 5.3-10.

In all the cases, the flaw evaluation charts were constructed following the guidelines of Section XI. The details of the chart construction are contained in Appendix A. In all cases, the embedded indications were found to be acceptable by analysis, with no repair required.



TABLE 5.3-1

CRACK GROWTH RATE DETERMINATION: GIRTH WELD

o Previous Cycle Maximum Crack Growth (388 Days)

S/G 21 : 0.30 in.

S/G 22 : 0.949

S/G 23 : 0.326

S/G 24 : 0.367

o Recent Part-Cycle Maximum Growth (212 Days)

S/G 21 : 0.360 in.

S/G 22 : 0.51 in.

S/G 23 : 0.27 in.

S/G 24 : 0.33 in.

o Maximum Crack Growth Per Day:

Previous Cycle

Recent Part Cycle

S/G 21 : 0.0008 in/day

S/G 21 : .0017 in/day

S/G 22 : 0.0024

S/G 22 : 0.0025

S/G 23 : 0.0008

S/G 23 : 0.0013

S/G 24 : 0.0009

S/G 24 : 0.0016

TABLE 5.3-2

REFERENCE CRACKS (307 DAYS OF OPERATION) FOR THE GIRTH WELD,  
TRANSITION CONE, BRACKETS AND STRAPS

<u>Steam Generator</u>	<u>Location</u>	<u>Crack Growth Rate (in/day)</u>	<u>Crack Depth (in)</u>	<u>Aspect Ratio</u>
21	Girth Weld	0.00170	0.51	4.4
22	Girth Weld	0.00250	0.75	4.4
23	Girth Weld	0.00130	0.39	4.4
24	Girth Weld	0.00160	0.48	4.4
A11	Transition Cone	0.00267	0.80	4.4
A11	All Brackets <sup>a</sup> & Straps	0.00284	0.85	20 <sup>b</sup>

a The brackets at the feedwater nozzle have been removed and new brackets installed away from the feedwater nozzle.

b This value is approximate.

TABLE 5.3-3

DAYS OF SERVICE BASED ON THE INTEGRITY EVALUATION  
FOR THE GIRTH WELD, TRANSITION CONE, BRACKETS AND STRAPS

<u>Steam Generator</u>	<u>Reference Location</u>	<u>Days of Service Based on</u>		<u>K<sub>IC</sub> = 63.2 ksi√in.</u>
		<u>Crack Depth (in.)<sup>b</sup></u>	<u>Aspect Ratio</u>	
21	Girth weld (max. grind)	0.51	4.4	>300
22	Girth weld (weld repaired to max. of 0.68 in.) <sup>a</sup>	0.75	4.4	271
23	Girth weld (max. grind depth of 1.01 in.)	0.39	4.4	>300
24	Girth weld (max. grind depth of 0.80 in.)	0.48	4.4	>300
A11	Transition cone	0.80	4.4	>300
A11	Brackets and straps (areas weld repaired to original configuration)	0.85	20	>300
A11	Brackets and straps (no weld repairs)	0.85	20	>300

<sup>a</sup> Weld repaired to return wall thickness to within 0.68 inch of original.

<sup>b</sup> Does not include the effect of mitigating actions to remove dissolved oxygen from the auxiliary feedwater.



TABLE 5.3-4

## SUMMARY OF EMBEDDED FLAW INDICATIONS, GIRTH WELD REGION

Unit/ Indication	2a	a/t	s	$\delta=s+a$	$\delta/t$	l
SG 21, #12	0.524"	0.069	0.95"	1.212"	0.319	2.5"
SG 22, #8/60	0.26"	0.034	0.22"	0.35"	0.092	3.00"
SG 22, #1	0.26"	0.034	1.35"	1.48"	0.389	7.00"
SG 22, #12	0.44"	0.058	0.22"	0.44"	0.116	2.50"
SG 22, #6	0.349"	0.046	0.218"	0.393"	0.103	2.125"
SG 22, #8/45	0.349"	0.046	0.131"	0.306"	0.081	1.25"
SG 24, #16	0.262	0.034	0.131	0.262	0.069	1.625
SG 24, #18	0.437	0.058	1.44	1.659	0.436	1.5

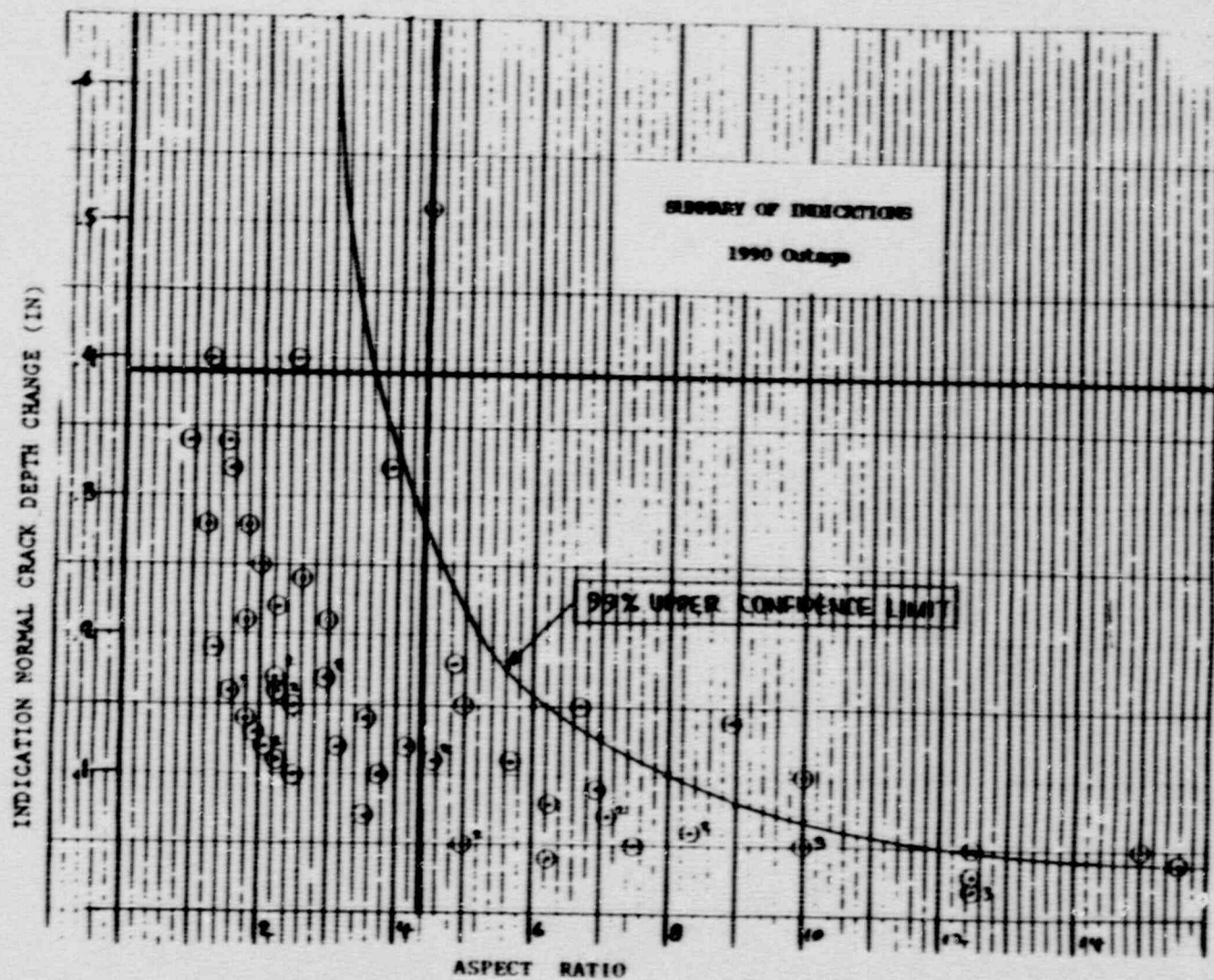


Figure 5.3-1  
Summary of Indications from the 1990 Outage, Showing the 99 Percent Upper  
Confidence Limit on Flaw Shape as a Function of Depth

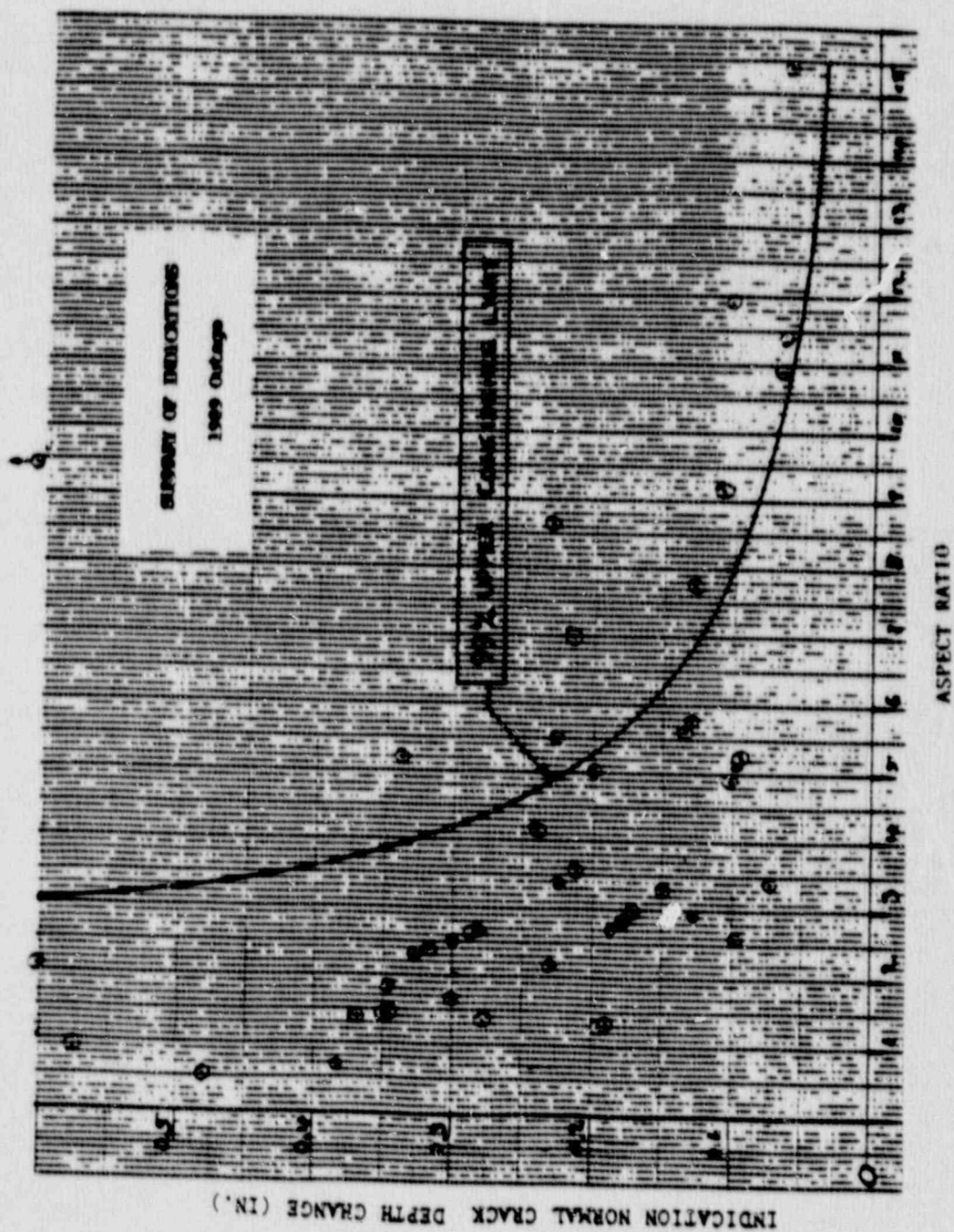


Figure 5.3-2  
Summary of Indications from the 1989 Outage, Showing Applicability  
of the 99 Percent Confidence Limit Curve from the 1990 Outage



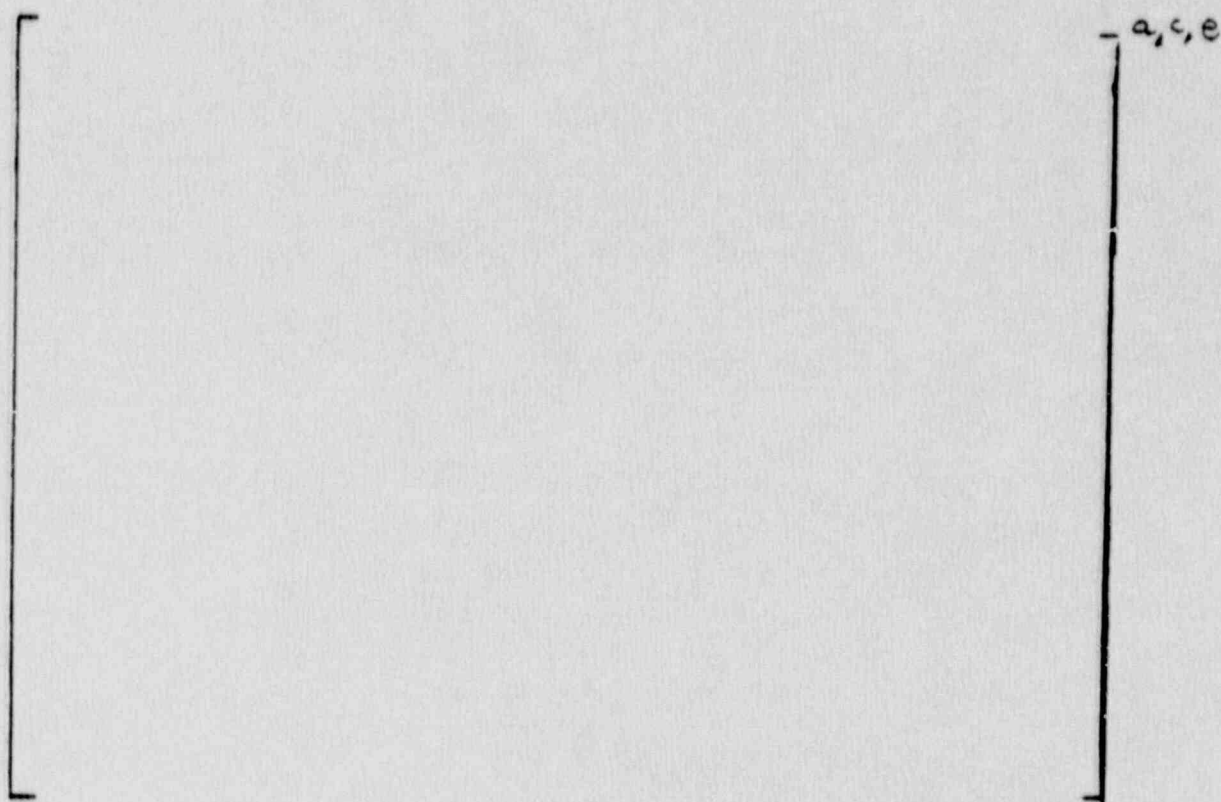


Figure 5.3-3  
Stress Intensity Factor Results, Girth Weld, 0.5 Inch Grind Depth

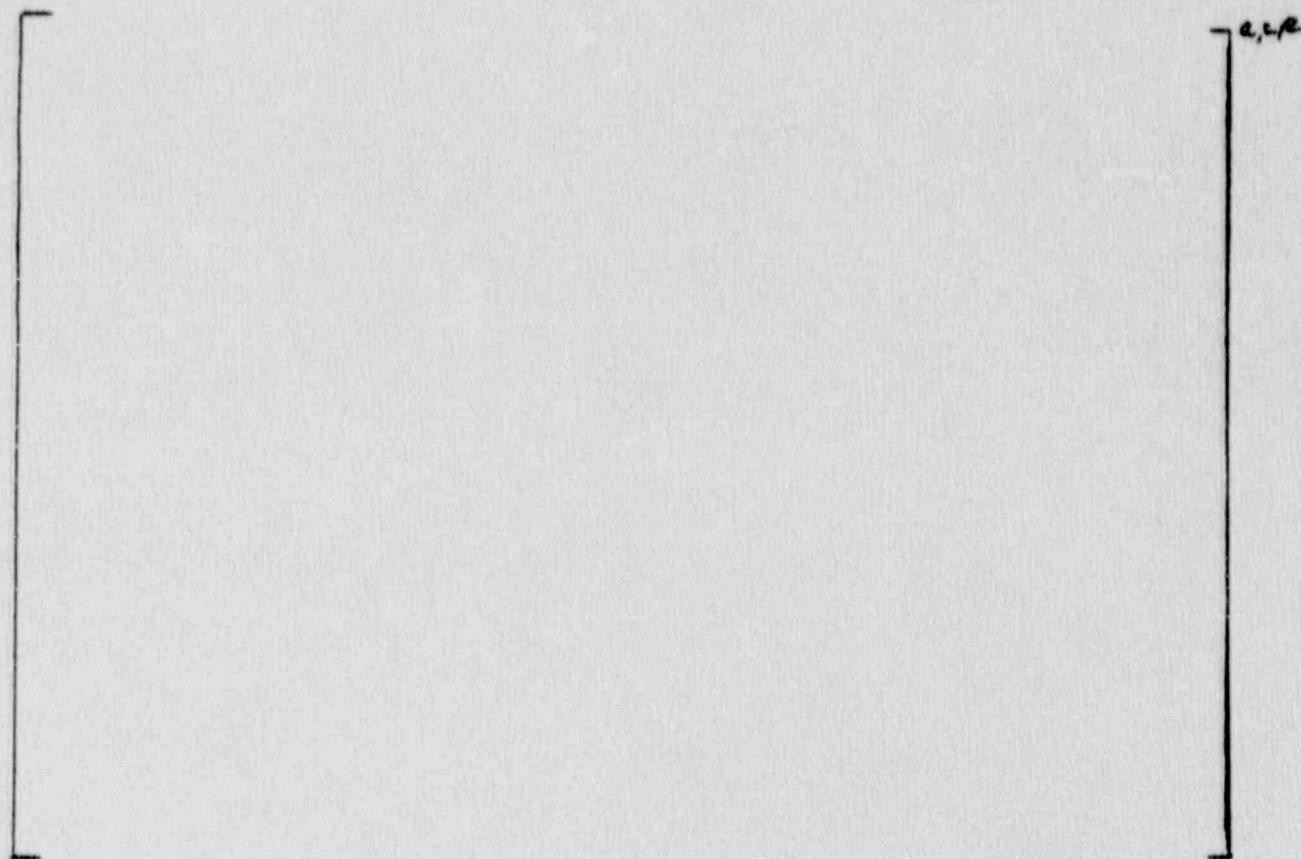


Figure 5.3-4  
Stress Intensity Factor Results, Girth Weld, 0.75 Inch Grinding Depth

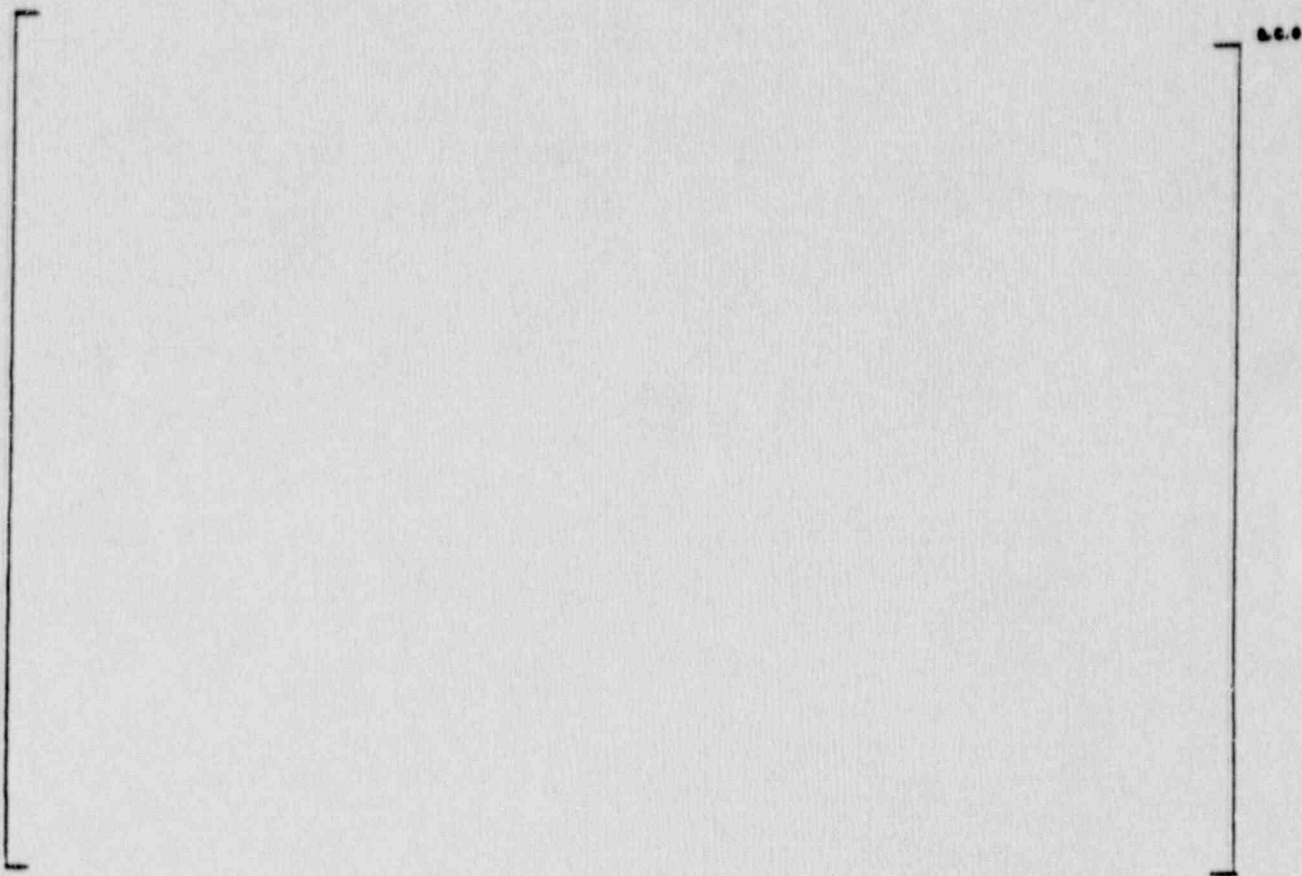


Figure 5.3-5  
Stress Intensity Factor Results, Girth Weld, 1.0 Inch Grinding Depth



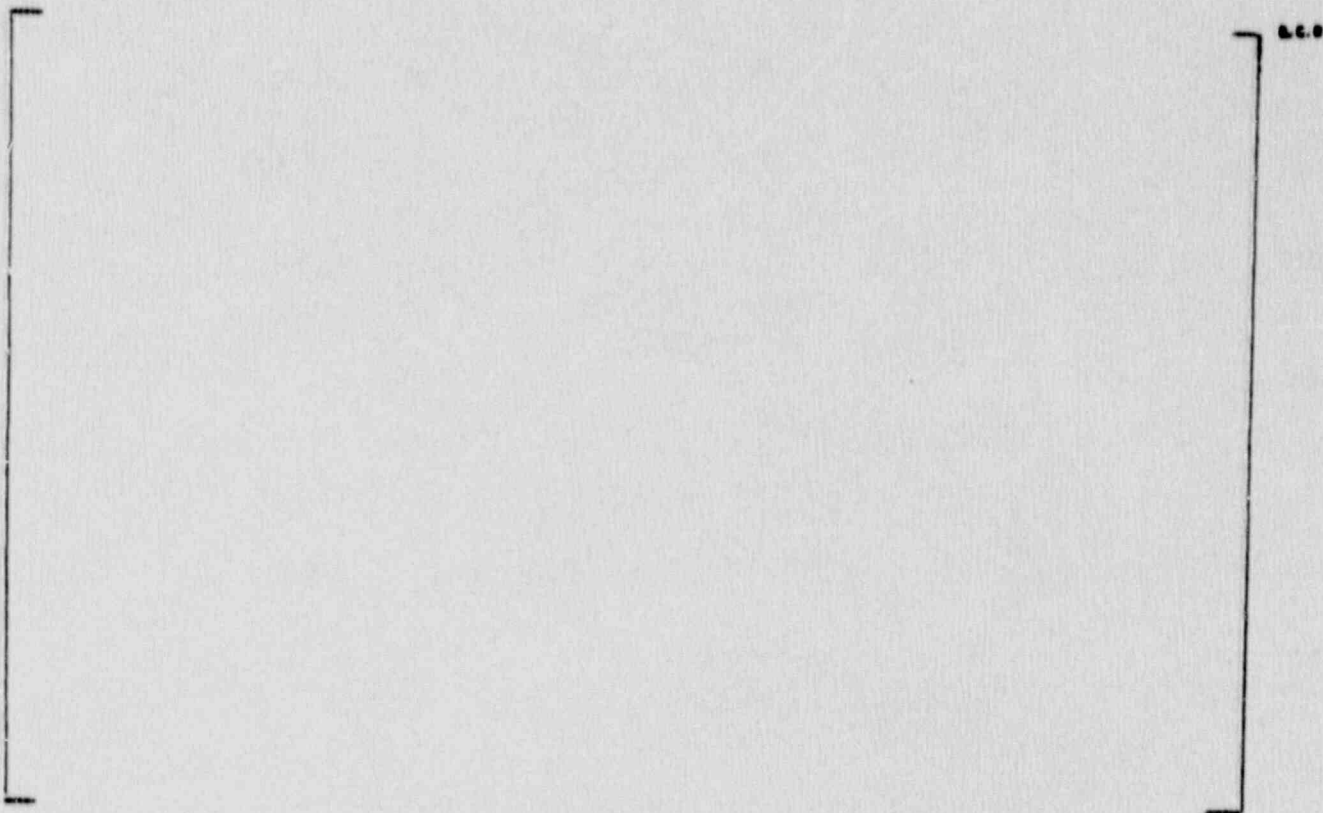


Figure 5.3-6  
Stress Intensity Factor Results, Transition Cone Region



Figure 5.3-7  
Stress Intensity Factor Results, Brackets and Strap Regions

a, c, e

Figure 5.3-8  
Determination of Applied Stress Intensity Factors for all Girth Weld Cracks  
Discovered After the 1989-90 Operating Period.



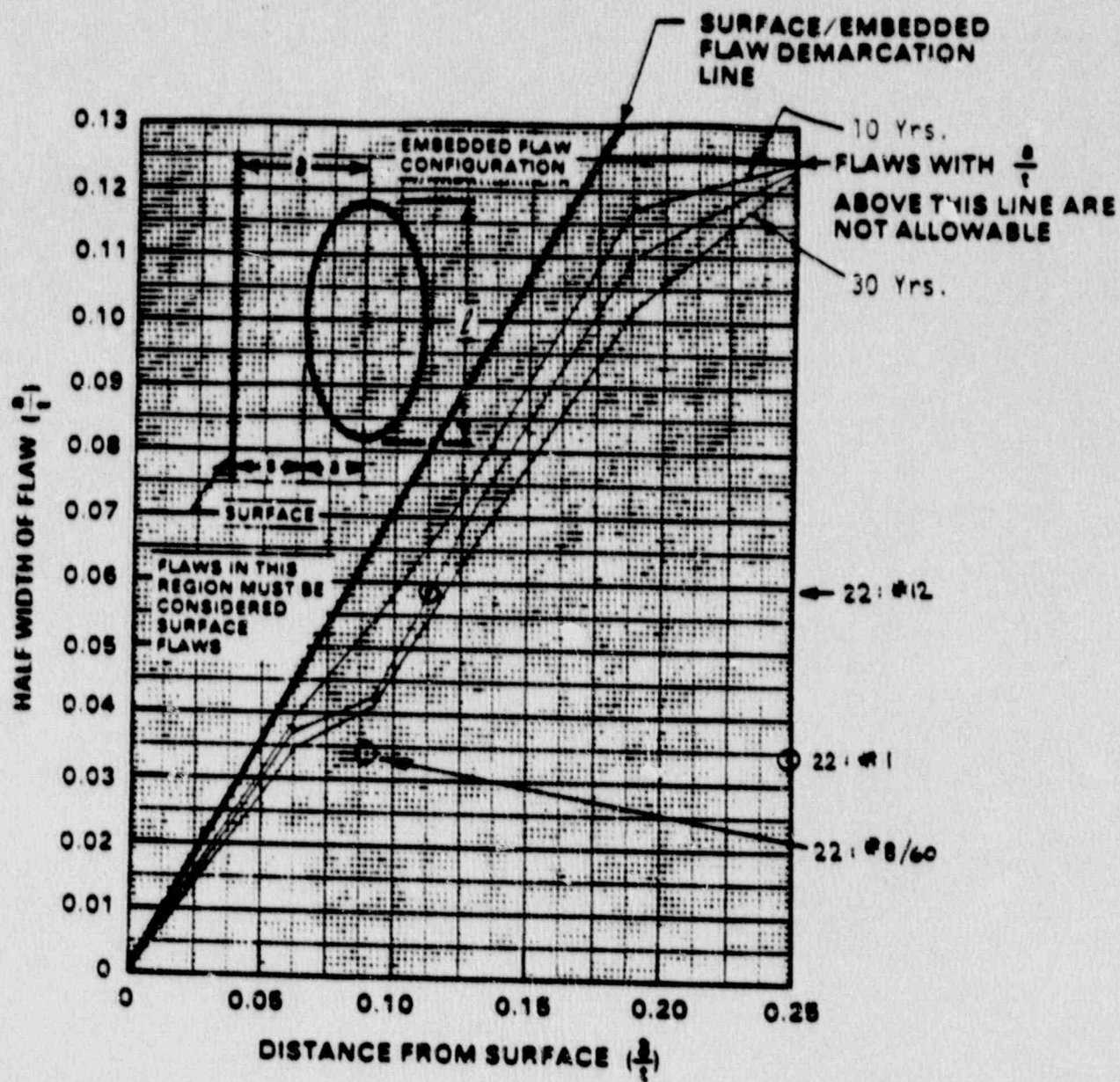


Figure 5.3-9  
Flaw Evaluation Chart for Embedded Flaws in the  
Transition Cone Regime

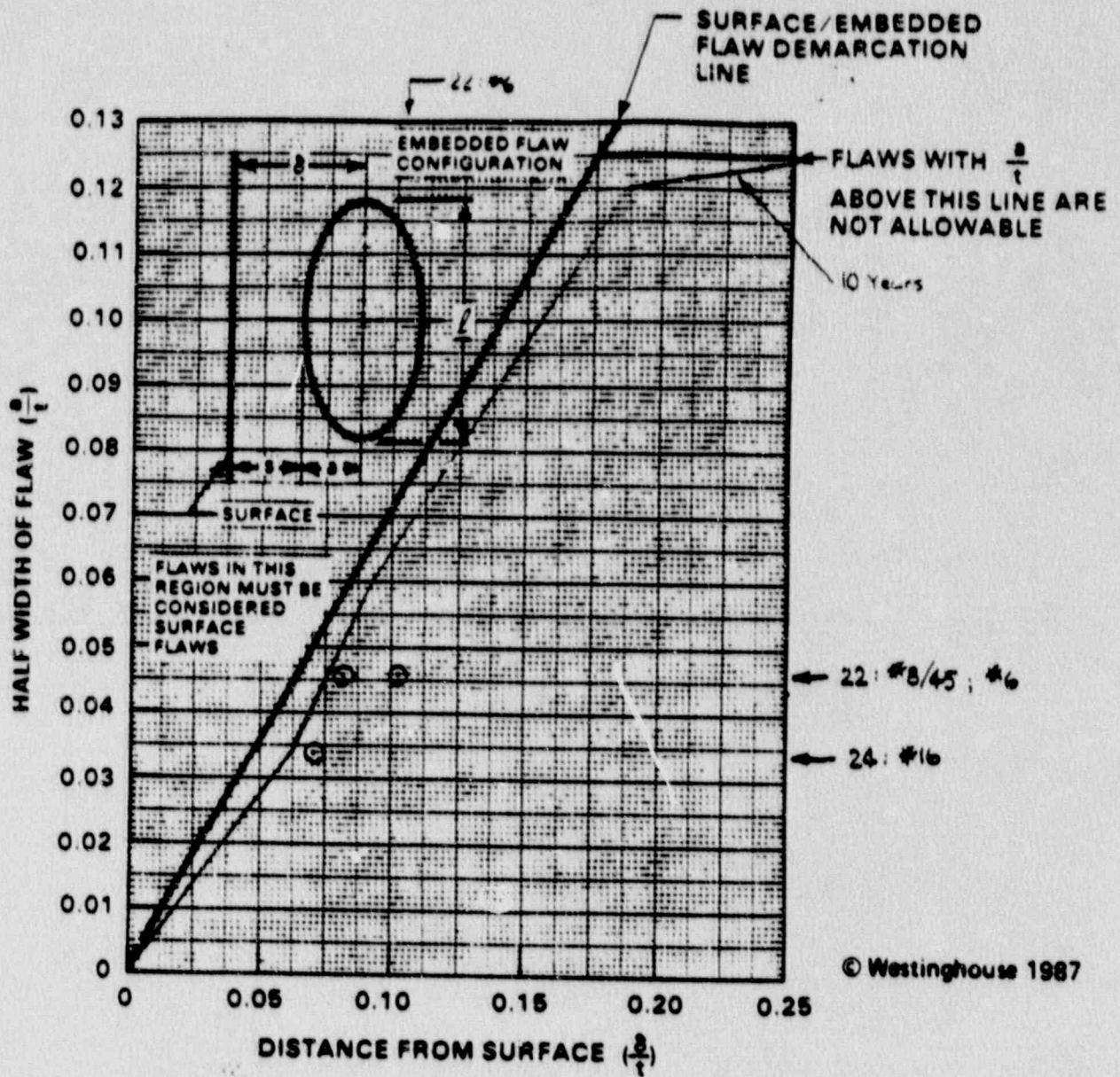


Figure 5.3-10  
Flaw Evaluation Chart for Embedded Flaws in the  
Vicinity of a 0.5 inch Deep Grind in the Girth Weld



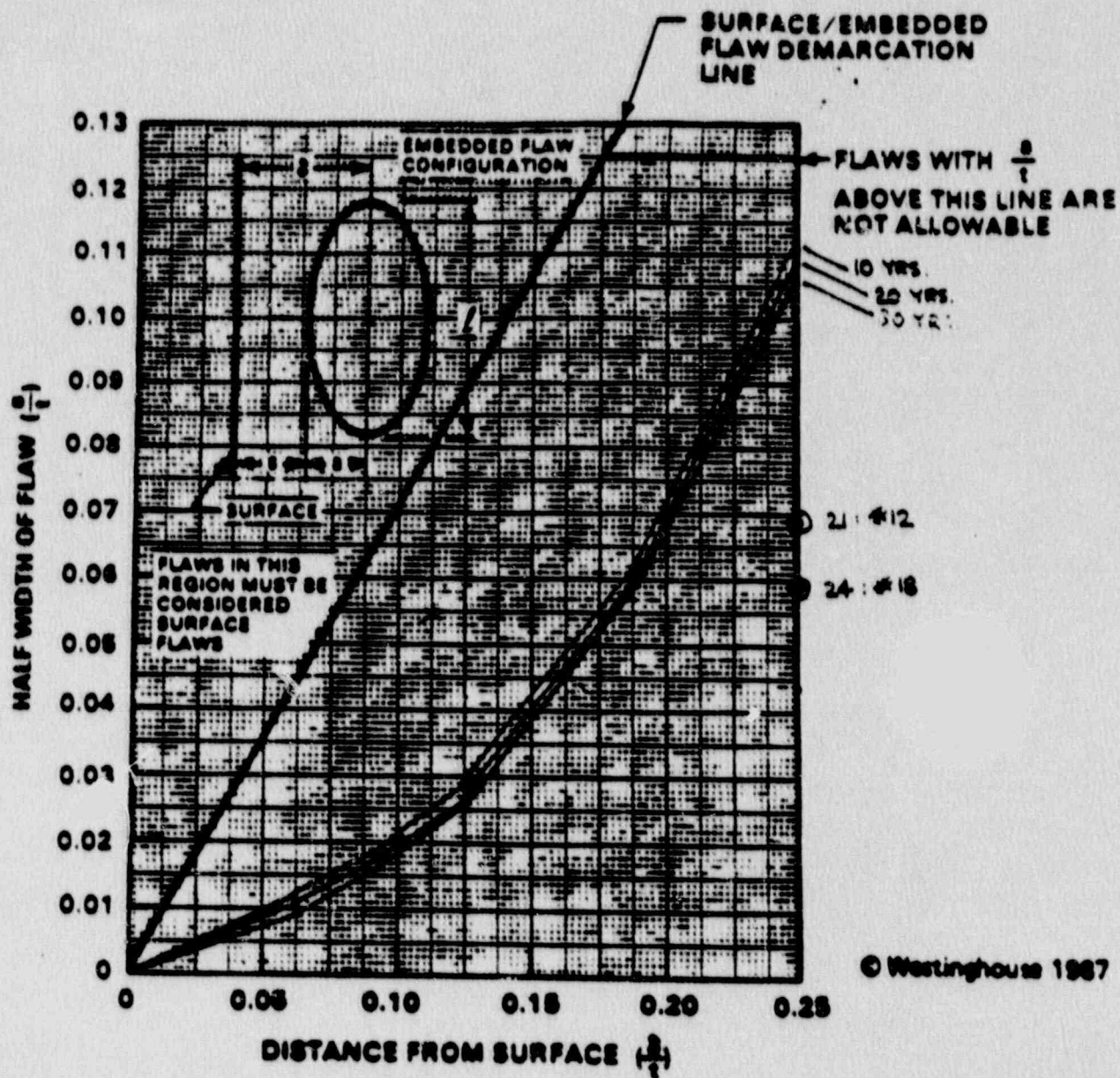


Figure 5.3-11  
Flaw Evaluation Chart for Embedded Flaws in the  
Vicinity of a 1.0 Inch Deep Grid in the Girth Weld



## 5.4 CONCLUSIONS

Detailed stress and fracture evaluations have been completed for the girth weld, transition cone, feedring brackets and straps. The result of these evaluations conclude that these regions of the steam generator in their as-repaired condition can continue to operate for the next cycle. In addition to the repairs which have been made, these regions have been evaluated to demonstrate that adequate safety margins are maintained throughout the upcoming service period, even if the surface flaws reinitiate, and propagate at the highest rates observed during the recent two cycles.

A separate evaluation was made to demonstrate the acceptability of a number of embedded flaws discovered during the final ultrasonic inspections of the girth weld region. These indications were shown to be acceptable to the criteria of Section XI without repair, using flaw evaluation charts, whose development is discussed in Appendix A.

## 5.5 REFERENCES

- 1) R. P. Wedler, Vertical Steam Generator Stress Report (for Series 44), Westinghouse Tampa Division, 4/20/69, pp. 16-1 through 16-24.
- 2) "Indian Point Unit 2 Steam Generator Girth Weld/Feedwater Nozzles Report, Spring, 1989 Outage, Consolidated Edison of New York," WCAP-12293, Rev. 2, Westinghouse Electric Corporation, ESBU, Pittsburgh, PA, October 1989.
- 3) Peterson, R. E., Stress Concentration Factors, John
- 4) Raju, I. S. and Newman, J. C., "Stress Intensity Factor Influence Coefficients for Internal and External Surface Cracks in Cylindrical Vessels" in Aspects of Fracture Mechanics in Pressure Vessels and Piping, ASME publication PVP. Vol. 58, 1982.
- 5) Marston, T. U., Editor, Flaw Evaluation Procedures: ASME Section XI, EPRI Special Report No. EPRI-NP-719-SR, August 1978.

- 6) Shah, R. C. and Kobayashi, A. S., "Stress Intensity Factor for an Elliptical Crack Under Arbitrary Loading," Engineering Fracture Mechanics, Vol. 3, 1981, pp. 71-96.

## 6.0 EVALUATION FOR FEEDWATER NOZZLE REGION

The stresses used for the evaluation of the feedwater nozzle region were taken from the 3-D finite element model developed for the analysis of the feedwater nozzle cracks during the Spring, 1989 outage (Reference 1). Figure 6.0-1 shows two views of the finite element model, and Figure 6.0-2 gives an enlarged view of the feedwater nozzle region along with the locations of analysis sections on the shell face and along the bottom of the nozzle bore evaluated in Reference 1. The sections to follow describe the thermal boundary conditions used in that analysis, list the resulting stresses at key locations, and present the fracture mechanics methodology and results.

All indications in the nozzle forging were removed by grinding and filled in with weld metal to restore the surface to its original contours with the exception of a few shallow indications in the inner bore. These were removed by light grinding. Thus the analyses described in the following sections are used for backup and to confirm the ability of the feedwater nozzle region to withstand an assumed 300 days of operation.



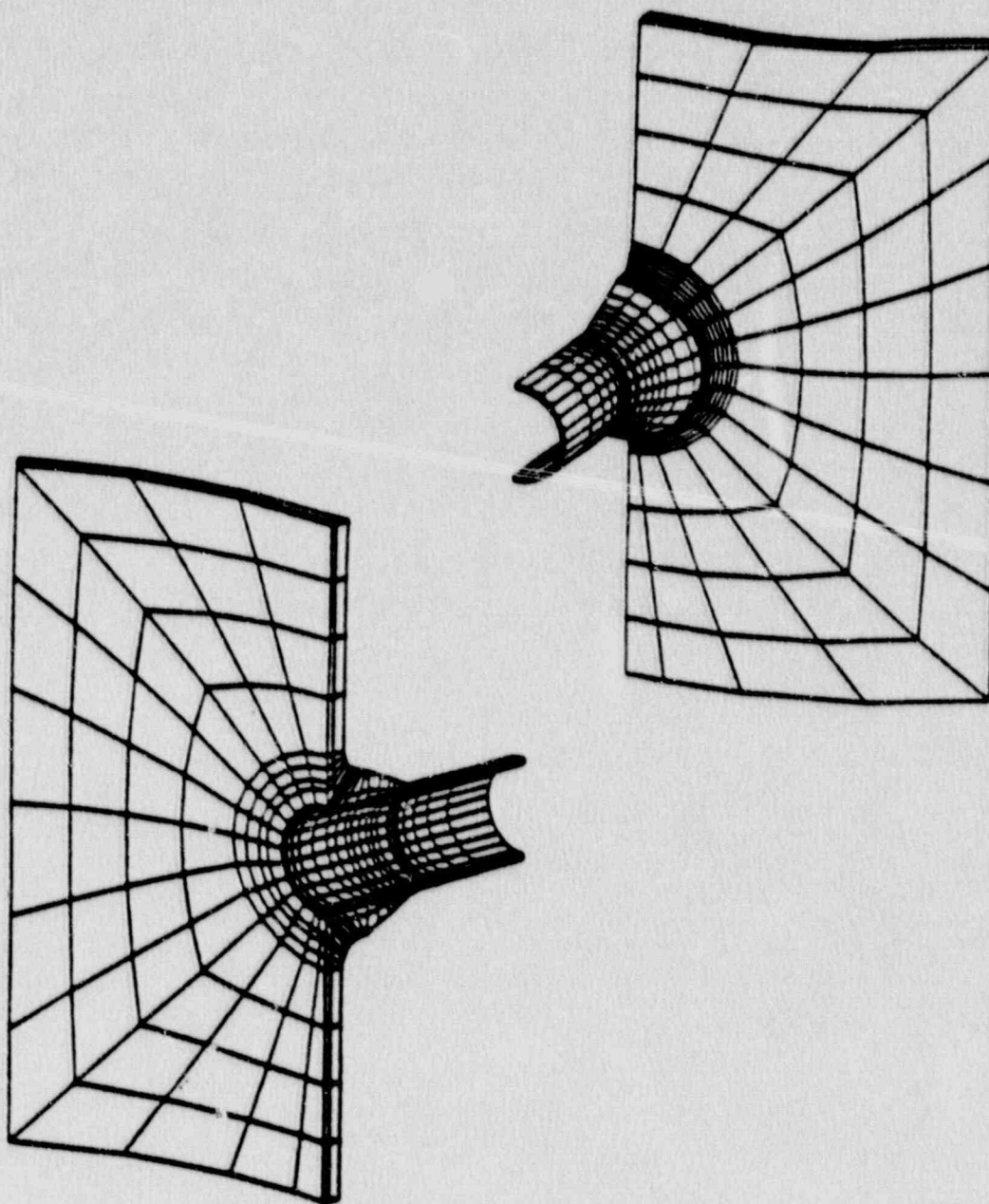


Figure 6.0-1  
Feedwater Nozzle Finite Element Model

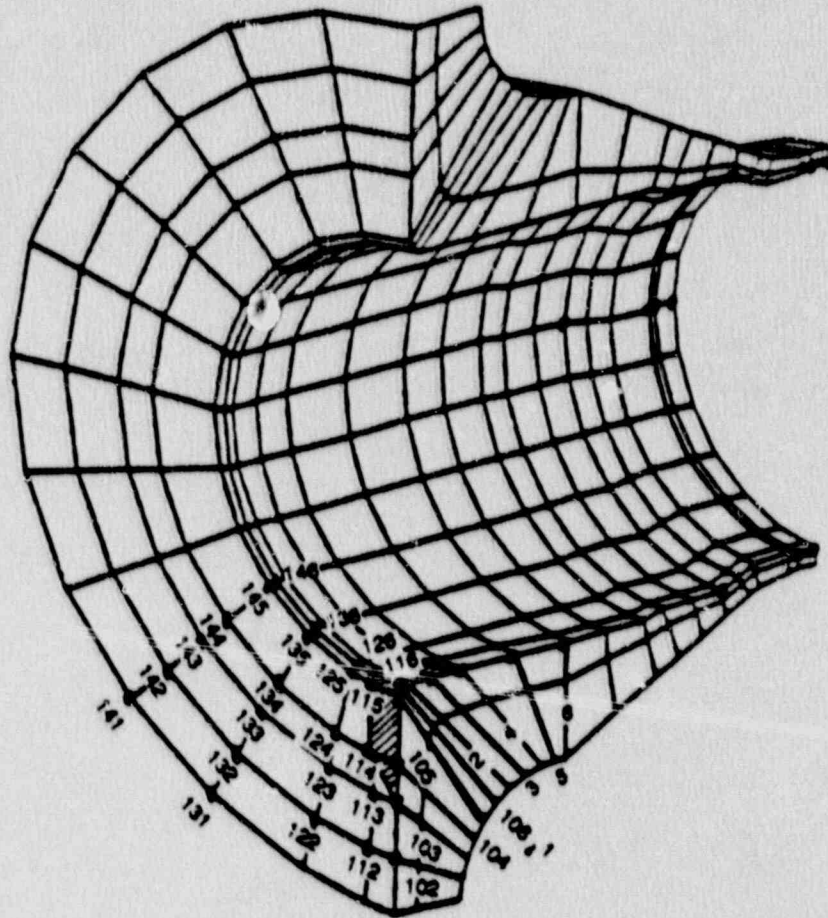


Figure 6.0-2  
Analysis Section Locations

## 6.1 THERMAL HYDRAULICS

The unit loads applied to the finite element model were pressure, 6 thermal stratification profiles (representing feedwater cycling during hot standby), and steady state conditions from two system transients (Plant Loading and Loss of Power). Since the main area of concern was the knuckle region and shell face of the nozzle, and the thermal sleeve protects these areas from direct contact with the full flow of the feedwater, feedwater thermal transients were not considered. Pipe loads have little effect on the knuckle region of the nozzle and were also not considered.

Figures 6.1-1 and 6.1-2 show the fluid temperatures within the nozzle for each of the six stratification profiles (T1 through T6). The cross-hatched areas indicate the location of the interface between the hot and cold fluids. These profiles are based on data obtained from five operating plants during hot standby operation for the feedwater line cracking investigation performed during 1979-1980 (Reference 2). Hot standby operation is a no-load condition with the secondary side of the steam generator at 547°F. During this condition, feedwater injection from the condensate storage tank raises the water level from the lower control point to the upper control point. Repeating this injection constitutes "feedwater cycling" during hot standby. Conservatively, it is assumed in the following fracture mechanics evaluation (Section 6.3) that "feedwater cycling" during hot standby is any hot standby operation with feedwater cycling with the reactor coolant system at or above 200°F.

The thermal sleeve was installed inside the feedwater nozzle with a small clearance slip fit at its end. With no seal between the sleeve and nozzle, a leak path exists between the liner and nozzle, allowing some of the feedwater to flow into the annulus between the two components. This bypass flow becomes more pronounced as the feedwater temperature decreases. Figure 6.1-3 shows the elements in the finite element models assumed to be exposed to this bypass flow for each of the stratification profiles.

The different heat transfer regions of the feedwater nozzle are identified on Figure 6.1-4. The film coefficients as a function of nozzle and fluid



temperatures are given in Table 6.1-1 for the thermal stratification profiles in each of these regions. The film coefficients for the 0-100% power and loss of power transients are given in Table 6.1-2. The film coefficients at the end of each of these transients were the ones used for the steady state thermal solutions.

Table 6.1-1  
Film Coefficients for Thermal Stratification

**REGION 2 FILM COEFFICIENTS \***

Fluid Temp	Nozzle Temperature					
	547	450	350	250	150	70
70	83.51	80.79	75.15	65.51	48.78	16.48
150	102.10	98.00	89.41	74.18	24.96	50.49
250	110.50	104.90	91.85	33.34	76.59	74.39
350	110.60	101.30	39.11	93.38	96.16	92.17
450	102.50	42.05	102.30	109.30	109.10	105.10
500	92.13	93.68	109.50	114.30	113.70	109.90
535	73.14	101.60	112.90	116.90	116.20	112.60

**REGION 3 FILM COEFFICIENTS**

Fluid Temp	Nozzle Temperature					
	547	450	350	250	150	70
70	141.60	139.30	136.10	131.80	125.70	115.70
150	201.40	198.20	193.30	185.80	169.10	185.00
250	243.10	239.30	232.60	216.30	236.10	245.20
350	264.30	259.10	244.50	264.30	275.70	283.10
450	270.40	257.90	277.10	288.70	298.10	304.70
500	267.70	271.10	284.60	295.00	303.80	310.00
535	262.50	275.50	287.40	297.10	305.50	311.50

**REGION 4 FILM COEFFICIENTS**

Fluid Temp	Nozzle Temperature					
	547	450	350	250	150	70
70	188.90	182.50	175.00	166.20	154.70	137.90
150	311.20	297.80	281.40	260.60	222.40	255.00
250	417.50	395.70	367.30	315.10	366.60	390.10
350	478.50	446.00	385.00	445.20	478.80	500.30
450	492.30	428.40	492.70	528.70	557.00	576.60
500	478.50	479.10	522.50	554.00	580.00	598.30
535	456.50	498.10	535.30	564.00	588.30	605.60

\* Region 1 same as Region 2.

Table 6.1-2  
Film Coefficients for System Thermal Transients  
Plant Loading at 100 Percent Power

PLANT LOADING \*

TIME	REGION 2	REGION 3	REGION 4
0	99.50	209.80	336.20
200	108.20	240.90	408.90
400	123.30	327.00	682.90
600	127.40	373.40	903.40
800	128.70	407.20	1119.00
1000	128.70	442.80	1430.00
1050	126.50	447.40	1482.00
1200	126.90	451.70	1529.00
1400	126.60	448.50	1494.00

LOSS OF POWER \*

TIME	REGION 2	REGION 3	REGION 4
0.0	126.80	450.60	1517.00
2.5	126.80	450.60	1517.00
5.0	120.80	392.20	1022.00
7.5	74.88	164.10	243.90
60.0	84.30	191.80	295.90
90.0	92.41	196.20	310.10
120.0	89.56	174.30	260.50
150.0	68.24	110.30	140.20
200.0	68.24	110.30	140.20
250.0	68.24	110.30	140.20
300.0	68.24	110.30	140.20

\* Region 1 same as Region 2.



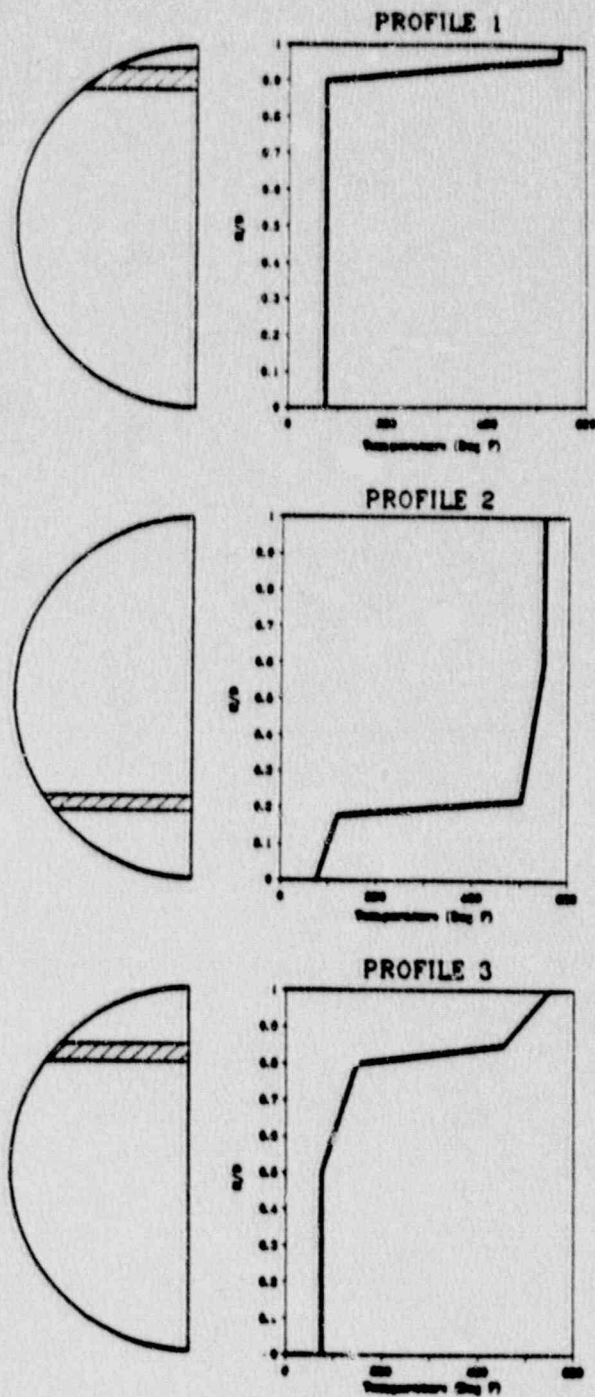


Figure 6.1-1  
Thermal Stratification Profiles 1-3

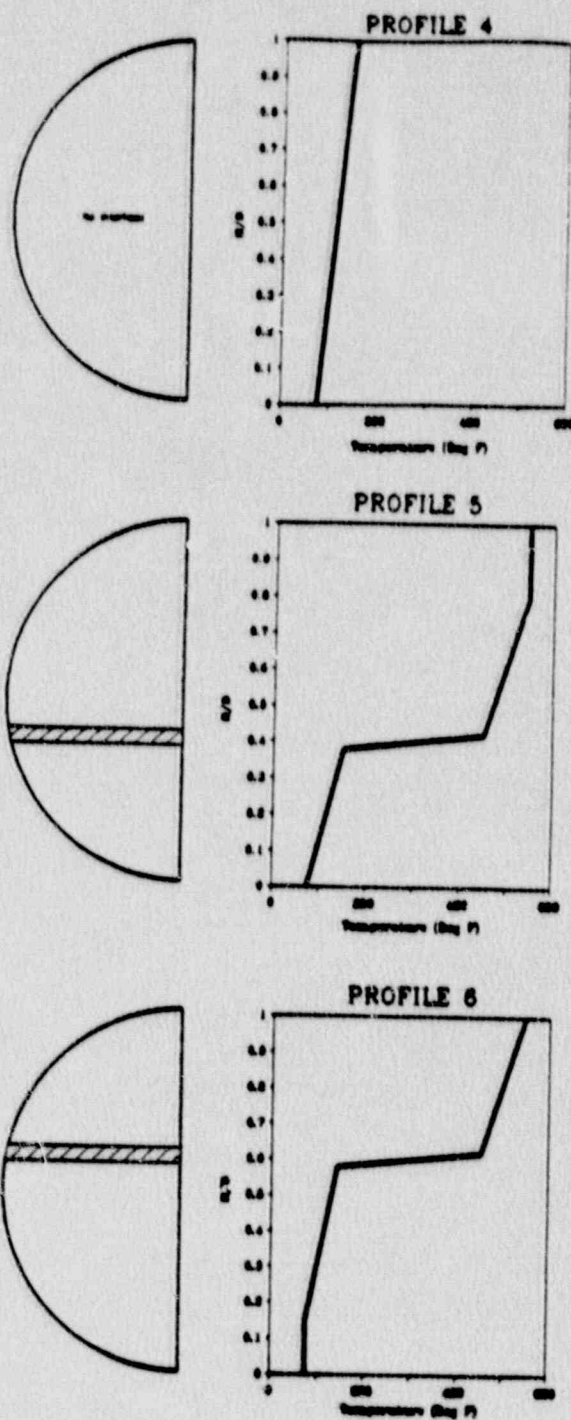
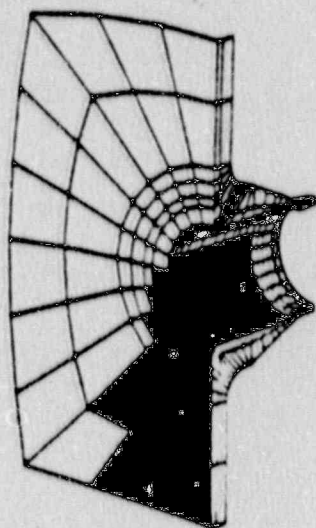
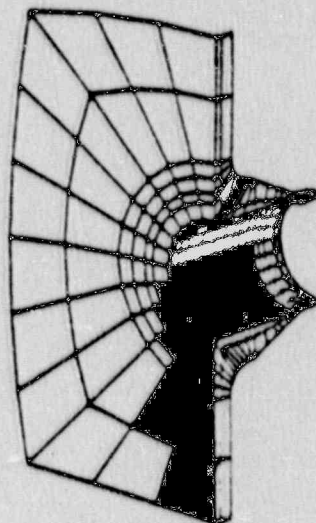


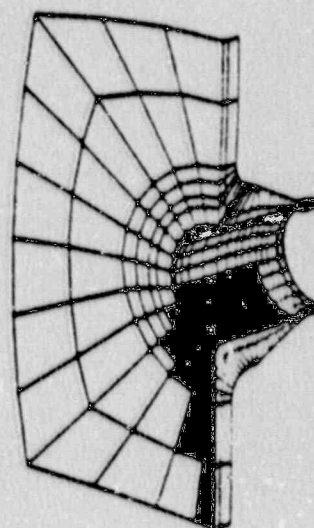
Figure 6.1-2  
Thermal Stratification Profiles 4-6



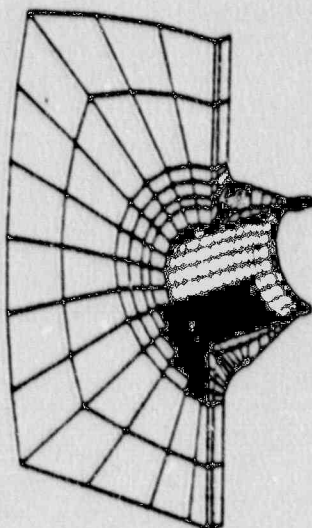
Profile 4



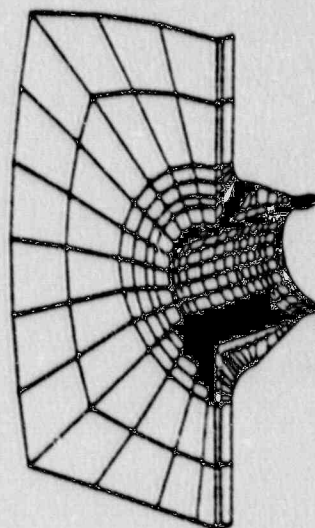
Profile 1



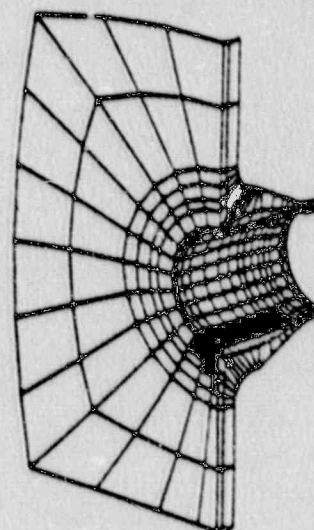
Profile 3



Profile 6



Profile 5



Profile 2

Figure 6.1-3  
Bypass Flow Through Sleeve/Nozzle Annulus During Stratification





## 6.2 STRESS ANALYSIS

Stresses used in the fracture analyses of Section 6.3 for various locations near the feedwater nozzle are described in the following subsections.

### 6.2.1 Feeding Support Brackets

Figure 6.2-1 is a sketch of the feeding supports in the vicinity of the feedwater nozzle. The support brackets are welded to the shell face of the nozzle forging. Since extensive cracking had been found around these brackets in all four steam generators, they were removed and relocated as described in Section 5.2.2.1. All indications were removed by grinding and filled in with weld metal to restore the surface to the original contours. Stresses from the feedwater nozzle model of Reference 1 are thus appropriate for use in the fracture evaluation. Table 6.2-1 lists the maximum stress components for the analysis sections of Figure 6.0-2 near the support brackets. Of these, ASN's 123, 124, 133, and 134 are the closest. The one with the highest stresses (ASN 134) was used for the fracture analysis.

### 6.2.2 Feedwater Nozzle Bore and Counterbore

All indications in the nozzle bore were prepared by grinding and filled in with weld metal to restore the surface to the original contours. Stresses from the feedwater nozzle model of Reference 1 are thus appropriate for use in the fracture evaluation. Table 6.2-2 lists the maximum stress components for the analysis sections of Figure 6.0-2 along the bottom of the nozzle bore from the knuckle to the start of the land supporting the thermal sleeve. ASN's 1 and 2 are through the knuckle of the nozzle, while ASN's 3 through 6 progress outward along the bore. The stresses for ASN 1 were used to evaluate the knuckle, and the ASN 3 stresses were used for the nozzle bore evaluation.

Following the repair of the nozzles on Steam Generators 21 and 23, two indications were found on the inside surface near the end of the thermal sleeve at the bottom of the nozzle, one in each steam generator. These indications were removed by light grinding and blending. The stresses in

those regions were adjusted to account for the small decrease in thickness of the section. The governing grindout was 0.080 inch deep. Following the same procedure as described in Section 5.2, the stress distribution through the reduced thickness for this case was obtained for a series of stress concentration factors ranging from 1.0 to 2.5. These are presented in Table 6.2-3 along with the results of the supporting calculations.

Axial stress for the nozzle counterbore was taken from Table 11.7.4 of Reference 2 to address the circumferential cracking found in this region. The value of 34.725 ksi corresponds to the maximum axial tensile stress produced by thermal stratification for a nozzle with a straight pipe attached. At the counterbore the axial stress is virtually constant through the thickness.



Table 6.2-1. IPP Feedwater Nozzle Shell Face Stresses

ASN	Surface Node	Load Condition	Distance	Hoop Stress (ksi)
122	2115	T6-425*	0.000	63.363
			0.655	55.088
			1.310	49.476
			2.619	34.899
			3.929	23.069
123	2515	T6-404	0.000	71.017
			0.825	63.229
			1.650	54.215
			3.299	35.742
			4.949	19.228
124	2915	T6-404	0.000	79.661
			0.962	69.372
			1.924	56.368
			3.848	37.336
			5.772	12.445
125	3315	T5-424	0.000	106.753
			1.292	89.766
			2.584	71.442
			5.168	40.664
			7.752	7.607
132	2105	T6-425	0.000	63.190
			0.637	53.656
			1.274	44.327
			2.548	31.587
			3.822	15.751
133	2505	T6-425	0.000	75.370
			0.796	64.079
			1.593	54.456
			3.186	34.649
			4.779	14.634
134	2905	T6-425	0.000	83.386
			0.932	73.442
			1.864	59.259
			3.728	37.390
			5.592	10.563
135	3305	T6-425	0.0000	102.141
			1.261	87.501
			2.521	69.700
			5.043	40.951
			7.564	9.100

\* T6-425 designates profile T6 with a 425°F temperature difference between hot and cold layers.

Table 6.2-2. IPP Feedwater Nozzle Bore Stresses

ASN	Surface Node	Load Condition	Distance	Hoop Stress (ksi)
1	3735	T5-424*	0.000	106.544
			1.320	88.730
			2.639	70.717
			5.279	39.487
			7.918	6.070
2	4135	T5-424	0.000	103.063
			1.318	86.671
			2.637	68.180
			5.274	35.500
			7.911	1.716
3	4535	T5-424	0.000	92.339
			1.220	75.744
			2.439	58.594
			4.878	28.472
			7.317	-4.548
4	4935	T5-424	0.000	80.146
			1.107	62.769
			2.213	47.476
			4.426	19.408
			6.639	-7.826
5	5335	T2-440	0.000	59.277
			0.918	43.490
			1.837	31.689
			3.674	10.074
			5.510	-5.555
6	5735	T5-424	0.000	36.056
			0.833	23.785
			1.667	15.464
			3.333	0.672
			5.000	-6.907

\* T6-424 designates profile T6 with a 424°F temperature difference between hot and cold layers.

Table 6.2-3. Adjusted Stress Distribution for Nozzle Bore Repair

Original Stress Distribution			Numerical Integration	
Node	Distance	Stress (ksi)	Force	Moment
7735	0.0000	49.280	7.5562	-3.5429
7734	0.1850	32.409	4.7466	-1.3557
7733	0.3700	18.906	3.2701	-0.2297
7732	0.7400	-1.2	-3.9429	-1.6740
Totals			11.6300	-6.8023

IPP FW Nozzle, ASN 214  
T2-360 Deg

Maximum Grind Depth      0.08  
Remaining Thickness      1.03

Exponential Distribution Stress =  $A_0 + A_1 e^{-by}$

Axial Stresses Through Remaining Thickness

Distance	Stress Concentration Factor			
	1.0	1.5	2.0	2.5
0.0000	49.280	73.920	98.560	123.200
0.1717	33.387	47.497	61.587	75.670
0.3433	19.962	25.334	30.685	36.027
0.6867	-0.957	-8.848	-16.734	-24.618
1.0300	-15.884	-32.895	-49.861	-66.808



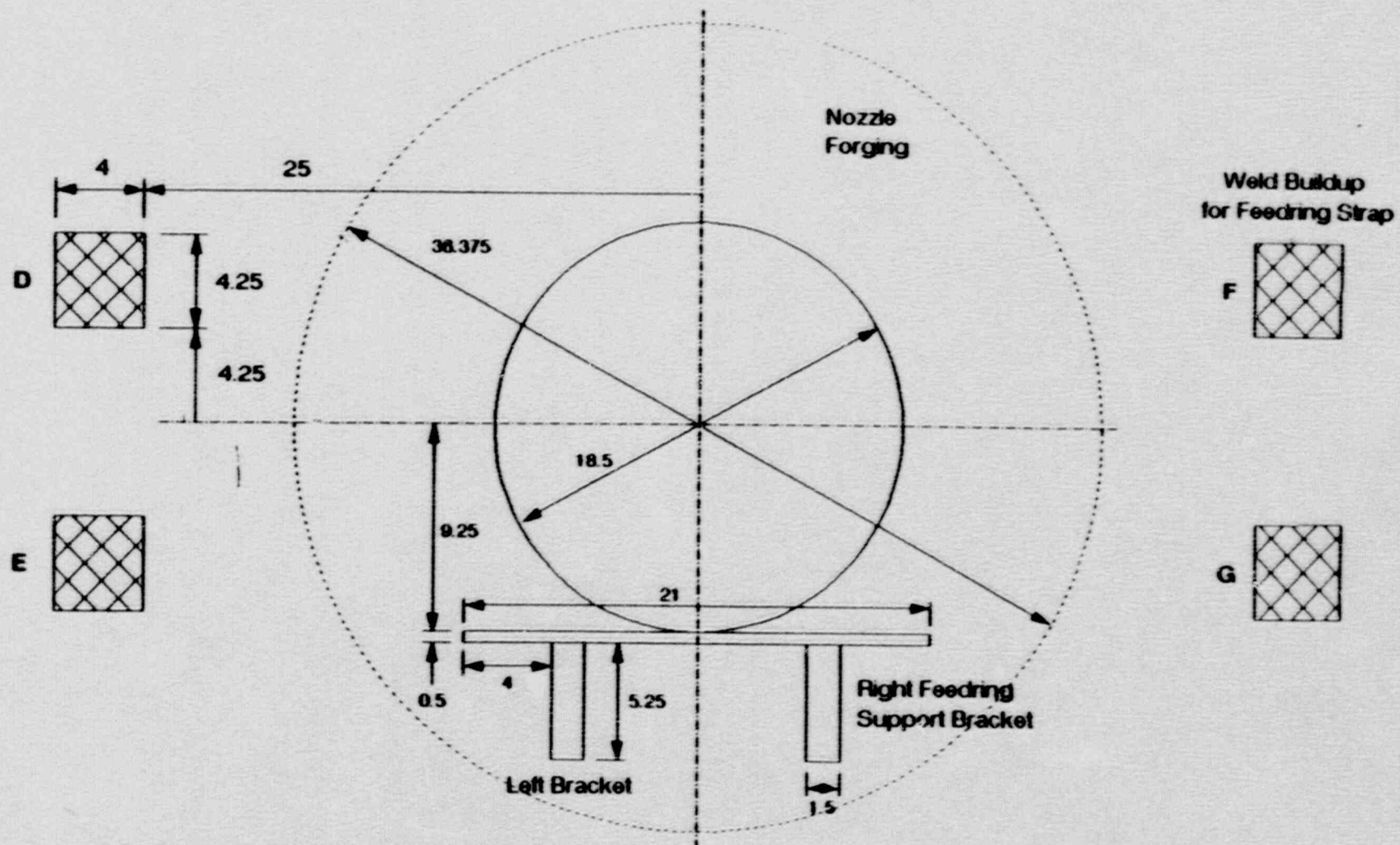


Figure 6.2-1  
Feeding Support Geometry at Nozzle

## 6.3 FRACTURE MECHANICS EVALUATION

### 6.3.1 Source of Cracking

Cracks have been found in the feedwater nozzle faces adjacent to the feeding support brackets, in the feedwater nozzle faces between bracket welds, in the knuckles and bores and at the feedwater nozzle counterbores. These general regions are identified in Figure 6.3-1.

At the welds of the feedwater nozzle brackets, it is judged that stress corrosion cracking is a large contributor to the crack extension. All the conditions for stress corrosion cracking exist in addition to a fatigue component due to bypass flow during the feedwater cycling at hot standby. However, the nozzle brackets have been removed and new brackets placed away from the feedwater nozzle. Since the potential for stress corrosion cracking would still exist for these brackets, they now fall under the category of "brackets and straps (areas weld repaired to original configurations)," the integrity of which has been previously addressed in Section 5.0 (see Table 5.3-3).

The cracking at the remaining locations of the feedwater nozzle are judged to be due to corrosion fatigue as confirmed by the boat sample removed from a nozzle bore (see Section 3.0). The root cause of the cracking in the shell face, knuckle and bore is judged to be predominantly thermal striping (high cycle fatigue) due to bypass flow behind the thermal sleeve as indicated in Figure 6.3-2. Thermal stratification (low cycle fatigue) is judged to be the dominant loading for the counterbore based on prior experience. These loads occur during the feedwater cycling at hot standby. The mechanisms are summarized in Figure 6.3-3.

All the cracks in the feedwater nozzle regions have been ground out. Weld repair was used to restore all the grinds to within tolerances of original dimensions. However, following the repair of the nozzles on Steam Generators 21 and 23, two indications were found on the inside surface near the end of the thermal sleeve at the bottom of the nozzle, one in each Steam Generators. As discussed in Section 6.2.2, the governing grindout was 0.080 inch deep.

This grind out location is conservatively enveloped by the analysis of the bore as discussed later.

### 6.3.2 Service at Hot Standby

In the section above feedwater cycling at hot standby is identified as the source of the observed corrosion fatigue. The service experience at hot standby is reviewed in Table 6.3-1. It should be noted that the recorded times include the time for start-up and associated pressure testing. For analysis purposes, four days at hot standby were used as the average time associated with startup and pressure testing. This assumption is consistent with recent operating experiences, minimizes the time and therefore maximizes the crack growth rate used in the analysis. Given in Table 6.3-1 is a summary of times at hot standby with feedwater cycling ~~also~~ and times for both start-up with associated pressure test and feedwater cycling. This table thus provides the time frame for which the corrosion fatigue cracking discussed above occurs. More specifically it provides the basis for estimating crack growth rates as discussed below.

### 6.3.3 Crack Growth Rates at Hot Standby With Feedwater Cycling

Failure by fatigue of a component consists of two stages - crack incubation without crack formation and crack extension to failure. The cycles of crack extension in some cases may be but a small portion of the total cycles, a ratio of 1 to 10 not being unreasonable for high cycle fatigue. This trend is somewhat reversed for low cycle fatigue.

For this evaluation it is conservatively assumed that the cycles associated with crack extension both by high cycle and low cycle fatigue make up only [ ]a,c of the total number of cycles [ ]a,c. In the counterbore and nozzle bore the crack initiation and propagation are considered to be the result of feedwater cycling at hot standby for the service life to date of the plant. On the other hand, for the cracking found in areas in which previously no cracks were found or in which cracks were ground out, it is assumed that they have grown to the depth observed in the



four days at hot standby with feedwater cycling experienced in the just completed one-half cycle.

For those locations where the service life to date can be associated with the corrosion fatigue crack growth, the hours for which the crack has been growing is [ ]a,c (i.e., [ ]a,c or [ ]a,c

The cracks associated with the bore and counterbore are postulated to have reached their observed depths over [ ]a,c at hot standby with feedwater cycling while the recently observed cracks at the nozzle face between the bracket welds and the knuckle cracks are postulated to have reached their observed depths in just four days at hot standby with feedwater cycling. Thus the crack growth rates in these areas can be expressed in inch/DHSB where DHSB is day at hot standby with feedwater cycling. The rates at the four nozzle regions of interest are given in Table 6.3-2.

#### 6.3.4 The Alternative Fracture Toughness Criteria

As confirmed by boat sample examination (see Section 3.0), the mechanism of cracking is cyclic corrosion fatigue typically with actual cracking occurring after a substantial incubation period of cycling. All of the cracks have been removed and repairs have been made as appropriate.

The fracture criterion applied to the situation wherein stress corrosion cracking is the crack extension method is that of IWB 3612 of Section XI of the ASME Code. For the case at hand (i.e., cyclic fatigue), however, it is unduly speculative to hypothesize, for purposes of imposing a fracture criterion, that cracks would reappear and grow during the remainder of the current cycle. A more realistic fracture criterion is described below.

It must be recognized that failure by flaw instability for the cases at hand at operating temperature will be by ductile tearing and not brittle fracture. By applying an arbitrary brittle fracture K criterion such as  $K_{Ic} = 200 \text{ ksi } \sqrt{\text{in.}}$ , advantage is not taken of the much higher K values (as obtained from J-integral values) that would exist for limited stable crack extension. It is also recognized that a fatigue mechanism dominates the

crack extension of interest here, such a mechanism being reasonably well understood and quantifiable.

A fracture toughness criterion for the nozzle face, knuckle and bore is first investigated.

A data base for upper shelf Charpy impact energy vs.  $K_{Ic}$  as a lower bound value is given in Reference 3. Because of the plasticity occurring during the fracture toughness tests, the lower bound  $K_{Ic}$  so determined is size dependent. Thus that part of the data base applicable to the nozzle face, knuckle and bore is the data from specimens between 3 and 4 inches in thickness, consistent with the minimum thickness of the steam generator of 3.5 inches. The appropriate data base is given in Table 6.3-3. As may be seen over 50% of the material involved was either 302B steel or 302B steel nickel modified (i.e., A533B steel). All heats were typical of the steel making practice in the 1960's. Charpy impact energy values vary between 35 and 124 ft. lbs. while the measured  $K_{Ic}$  values range from 153 to 399 ksi√in.

A linear regression analysis was performed on the data of Table 6.3-3 and a plot of the fit is given in Figure 6.3-4. The fit is quite definitive with the standard error on the mean being 18.6 ksi√in. (i.e., less than 12.5% of the least  $K_{Ic}$  of the data base). The  $K_{Ic}$  vs. Charpy energy relationship is:

$$K_{Ic} = 56.955 + 2.6126 C_v, \text{ (ksi } \sqrt{\text{in.}}, \text{ ft-lbs)} \quad (6.3-1)$$

where  $C_v$  is Charpy impact energy.

The Certified Materials Tests Reports (CMTRs) were examined for the feedwater nozzles. Charpy impact energy tests of 10°F were required for each heat. At operating temperature the Charpy energy would be greater. A total of 12 Charpy energies at 10°F were available and are given in Table 6.3-4. The lowest Charpy datum (i.e., 55 ft-lbs) was used to establish the attendant  $K_{Ic}$  based on the above correlation at the lower 99% confidence limit (i.e., a value three standard errors less than the estimate of the mean). The  $K_{Ic}$  so determined is 145 ksi√in.

A similar evaluation as above was made to determine the appropriate  $K_{IC}$  to use for the minimum counterbore thickness of 0.688 in. Data from Reference 3 of specimens with thicknesses only between 0.394 in. and 1 in. were used in the correlation and are given in Table 6.3-5. A plot of the fit is given in Figure 6.3-5. The standard error on the mean was 22.67 ksi√in. The  $K_{IC}$  versus Charpy energy relationship is:

$$K_{IC} = 74.362 + 1.5788 C_v, \text{ (ksi}\sqrt{\text{in.}}, \text{ ft-lbs)} \quad (6.3-2)$$

where  $C_v$  is Charpy impact energy.

Again the lowest Charpy datum (i.e., 55 ft-lbs) of Table 6.3-4 was used to determine the  $K_{IC}$  estimate at the lower 99% confidence limit. The value so obtained is 93 ksi√in.

In summary, the material specific statistically based 99% lower confidence limit  $K_{IC}$  for the thicker section of the nozzle forging is 145 ksi√in. This is the value to be used for evaluating the face, knuckle and bore of the feedwater nozzle. For the counterbore the  $K_{IC}$  to be used is 93 ksi√in.

The fracture toughness is conservative not only because the 99% confidence limits are used in establishing the value from the correlation but also because the Charpy impact data from the CMTRs were obtained at 10°F, undoubtedly in the transition temperature region of the material. At operating temperatures Charpy impact values approaching or exceeding 100 ft-lbs are anticipated; however, only the fracture toughnesses confirmed by actual data are used. The overall conservatisms are reviewed in Table 6.3-6. Based on these conservatisms the above fracture criteria are fully justified.

#### 6.3.5 Stability Evaluation of the Nozzle Region

Cracks are not expected to initiate by cyclic corrosion fatigue in the near term; however, for purposes of analyses cracking is postulated to occur immediately when subjected to feedwater cycling. This is a very conservative assumption.



As previously discussed this integrity evaluation is in terms of the number of allowable days at hot standby, not the days during power operation. Using the finite element through-wall stress results of Section 6.2 and the aspect ratios given in Table 6.3-2 for each location, parametric calculations of stress intensity factors at various crack depths were made to determine the allowable crack depths satisfying the appropriate fracture toughness criteria. Plots of the various parametric studies are given in Figures 6.3-6 through 6.3-9. The critical crack depths are given in Table 6.3-7. Such crack depths divided by the appropriate crack growth rate in inch/DHSB (see Table 6.3-2) give the number of days of hot standby. The associated days at hot standby are also given in Table 6.3-7.

TABLE 6.3-1

HOT STANDBY HOURS FOR INDIAN POINT UNIT 2

(a) Startup, Pressure Test and Feedwater Cycling:

Total Time to Date: 9950 hours

Average Number of Days at Hot Standby:

To Date:	25 days/year
Last Full Cycle:	14 days/year
Last Half Cycle:	14 days/year

(b) Feedwater Cycling Only:

Total Time to Date: 8990 hours

Average Number of Days at Hot Standby:

To Date:	23 days/year
Last Full Cycle:	11 days/year
Last Half Cycle:	7 days/year

TABLE 6.3-2

## CRACK GROWTH RATES FOR THE NOZZLE REGION

<u>Steam Generator</u>	<u>Location</u>	Days at Hot Standby (DHSB)	Crack Depth	Aspect Ratio	Crack Growth Rate (in./DHSB) a,c,e
A11	Nozzle-Face	4.0	0.290	10	0.0725
A11	Knuckle	4.0	0.130	NAA	0.0325
A11	Knuckle	18.75	0.400 <sup>b</sup>	NA	0.0213
21	Bore	18.75	0.198	10	0.0106
22	Bore	18.75	0.295	10	0.0157
23	Bore	18.75	0.217	10	0.0116
24	Bore	18.75	0.347	10	0.0185
21	Counterbore <sup>c</sup>	18.75	0.318	100	0.0170
22	Counterbore	18.75	0.338	100	0.0180
23	Counterbore	18.75	0.200	100	0.0107
24	Counterbore	18.75	0.270	100	0.0144

a Not applicable

b Upper bound value based on grindout during 1989 outage

c Nozzle-to-pipe joint



TABLE 6.3-3

LOWER BOUND  $K_{Ic}$  VALUES FROM THREE AND FOUR INCH  
THICK SPECIMENS AND CORRESPONDING CHARPY IMPACT DATA

Material	Orientation	Test Temp (°F)	Charpy Shelf (ft-lbs)	Lower Bound $K_{Ic}$ (Thickness) (ksi $\sqrt{in(in)}$ )
A533 Grade B Class 1 Plate	Longitudinal	200	118	369(3)
A533 Grade B Class 1 Plate	Longitudinal	550	105	293(3)
A533 Grade B Class 1 Plate	Transverse	200	85	282(3)
A533 Grade B Class 1 Plate	Transverse	550	80	240(3)
A533 Grade B Class 1 Plate	Transverse	200	81	278(4)
A508 Class 2 Forging	Circumferential	200	83	280(4)
A508 Class 2 Forging	Circumferential	130	88	307(4)
A508 Class 2 Weldment	With Weld	200	124	399(4)
A302 Grade B Plate	Transverse	200	35	153(4)
Ni-Cr-Mo Rotor	Circumferential	250	58	202(4), 214(4)

TABLE 6.3-4

AVAILABLE CHARPY DATA FROM CERTIFIED MATERIALS  
TEST REPORT

TEST TEMPERATURE: 10°F

CHARPY ENERGY (FT-LBS)

86	64	70	64
70.5	64	78.5	55
72.5	64	75	55

NOTE: The Least Value, 55 ft-lbs, Was Used to Estimate  $K_{Ic}$  At the 99% Lower Confidence Limit

TABLE 6.3-5  
LOWER BOUND  $K_{Ic}$  VALUES FOR 0.394 AND 1-INCH  
THICK SPECIMENS AND CORRESPONDING CHARPY IMPACT DATA

Material	Orientation	Test Temp (°F)	Charpy Shelf (ft-lbs)	LowerBound $K_{Ic}$ (Thickness) (ksi $\sqrt{in(in)}$ )
A533 Grade B Class 1 Plate	Longitudinal	200	118	248(1), 261(1)
A533 Grade B Class 1 Plate	Longitudinal	550	105	232(1), 210(1)
A533 Grade B Class 1 Plate	Transverse	200	85	253(1)
A533 Grade B Class 1 Plate	Transverse	550	80	204(1)
A533 Grade B Class 1 Plate	Transverse	200	81	228(.394), 209(.394), 244(1)
A508 Class 2 Forging	Circumferential	200	83	209(.85)
A508 Class 2 Forging	Circumferential	200	88	220(.85)
A508 Class 2 Weldment	With Weld	200	124	223(.85), 285(.85)
A533 Grade B Class 1 Weldment	With Weld	200	150	305(1)
A302 Grade B Plate	Transverse	200	35	131(.394), 119(.394) 103(.394), 120(.394)
Ni-Cr-Mo Rotor Forging	Axial	550	58	178(1), 171(1), 123(1)
A516 Grade 70 Plate	Longitudinal	440	87	221(1)
A516 Grade 70 Weldment	With Weld	200	96	237(1)
A516 Grade 70 Weldment	With Weld	440	88	221(1)

<sup>a</sup>A discussed in Referenced 1, the data base is limited to 35 ft-lbs and above.



TABLE 6.3-6

CONSERVATISMS IN THE FRACTURE TOUGHNESS  $K_{Ic}$  CRITERIA

- o Lower Bound Size Dependent Fracture Toughness Values Used In the Correlations
- o Correlation Is Based on Upper Shelf Values Where Transitional Variability Is Of No Concern
- o Least Charpy Energy Obtained at 10°F Used To Estimate  $K_{Ic}$
- o The Applicable Charpy Energy Would Be The One At Operating Temperature (>300°F) And Would Probably be Around 100 ft-lbs or Over
- o The  $K_{Ic}$  Criteria Are Determined At The 99% Lower Confidence Limit

TABLE 6.3-7

CALCULATED DAYS AT HOT STANDBY BASED  
ON THE INTEGRITY EVALUATION

<u>Steam Generator</u>	<u>Location</u>	<u>Allowable Crack Depth (in)</u>	<u>Aspect Ratio</u>	<u>Crack Growth Rate (in/DHSB)</u>	<u>Calculated Days at Hot Standby With Feedwater Cycling<sup>d</sup></u>
A11	Nozzle-Face	[			a, c, e
A11	Knuckle				
A11	Knuckle <sup>b</sup>				
21	Bore				
22	Bore				
23	Bore				
24	Bore				
21	Counterbore <sup>c</sup>				
22	Counterbore <sup>c</sup>				
23	Counterbore <sup>c</sup>				
24	Counterbore <sup>c</sup>				

a Not applicable

b Upper bound of

c Nozzle-to-pipe joint

d Not calendar days but equivalent days with feedwater cycling

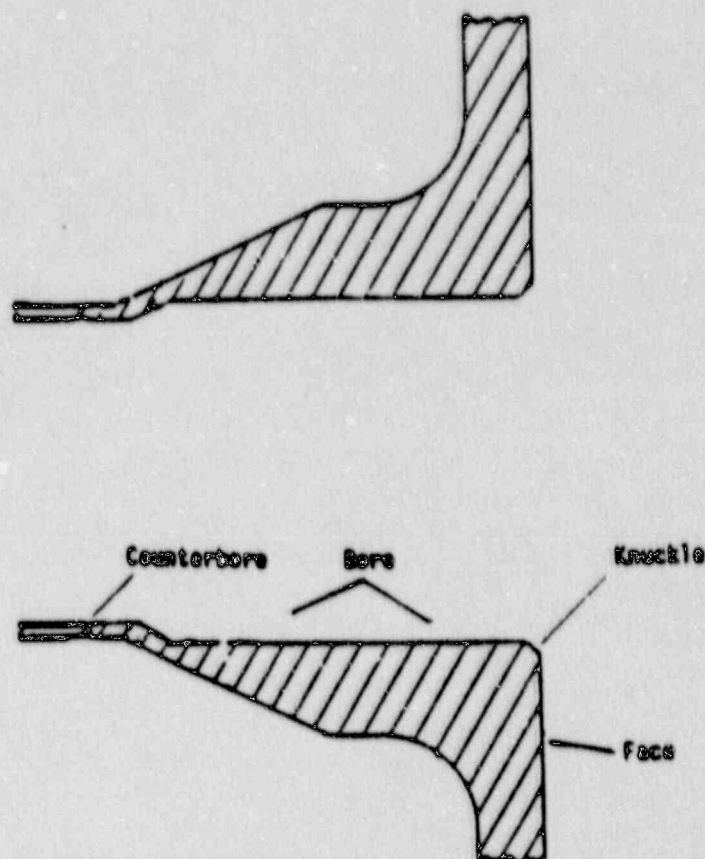


Figure 6.3-1  
Feedwater Nozzle Showing the Four Locations Analyzed



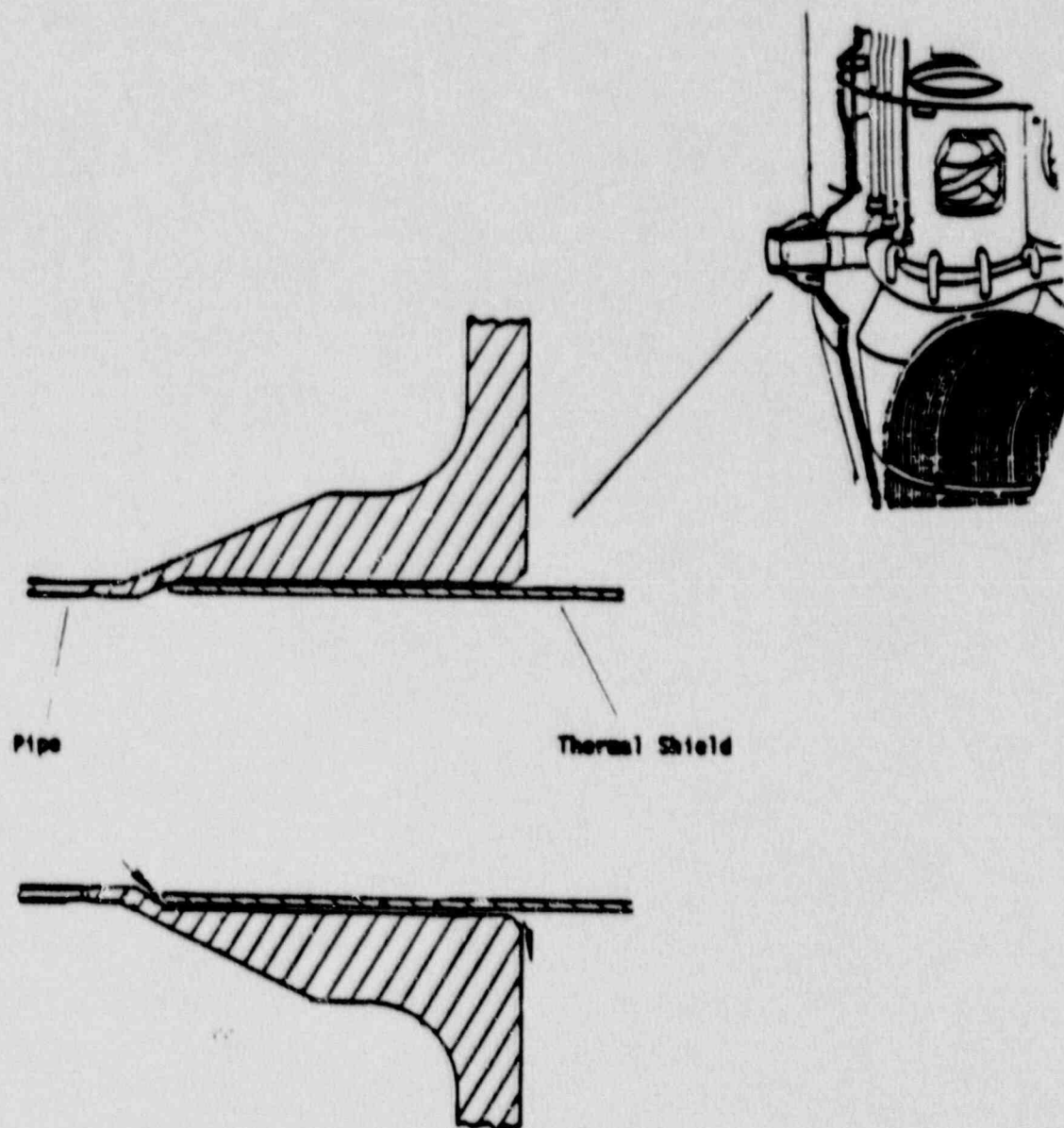


Figure 6.3-2  
Feedwater Nozzle With Thermal Shield Showing Bypass Flow

SCC - Stress Corrosion Cracking

CF - Corrosion Fatigue

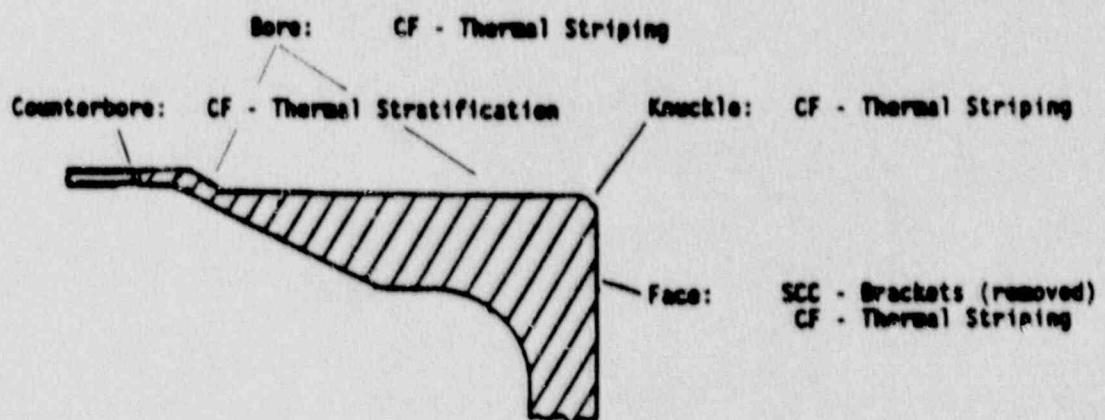
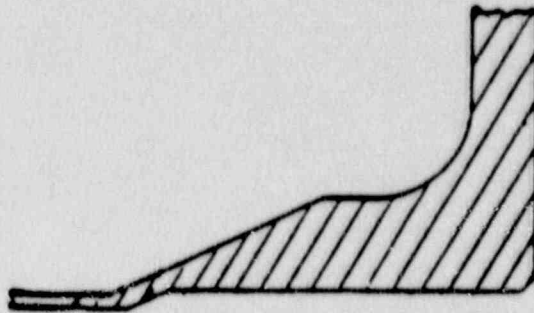


Figure 6.3-3  
Feedwater Nozzle Showing the Predominant Loading  
and Mode of Crack Propagation at Each Location

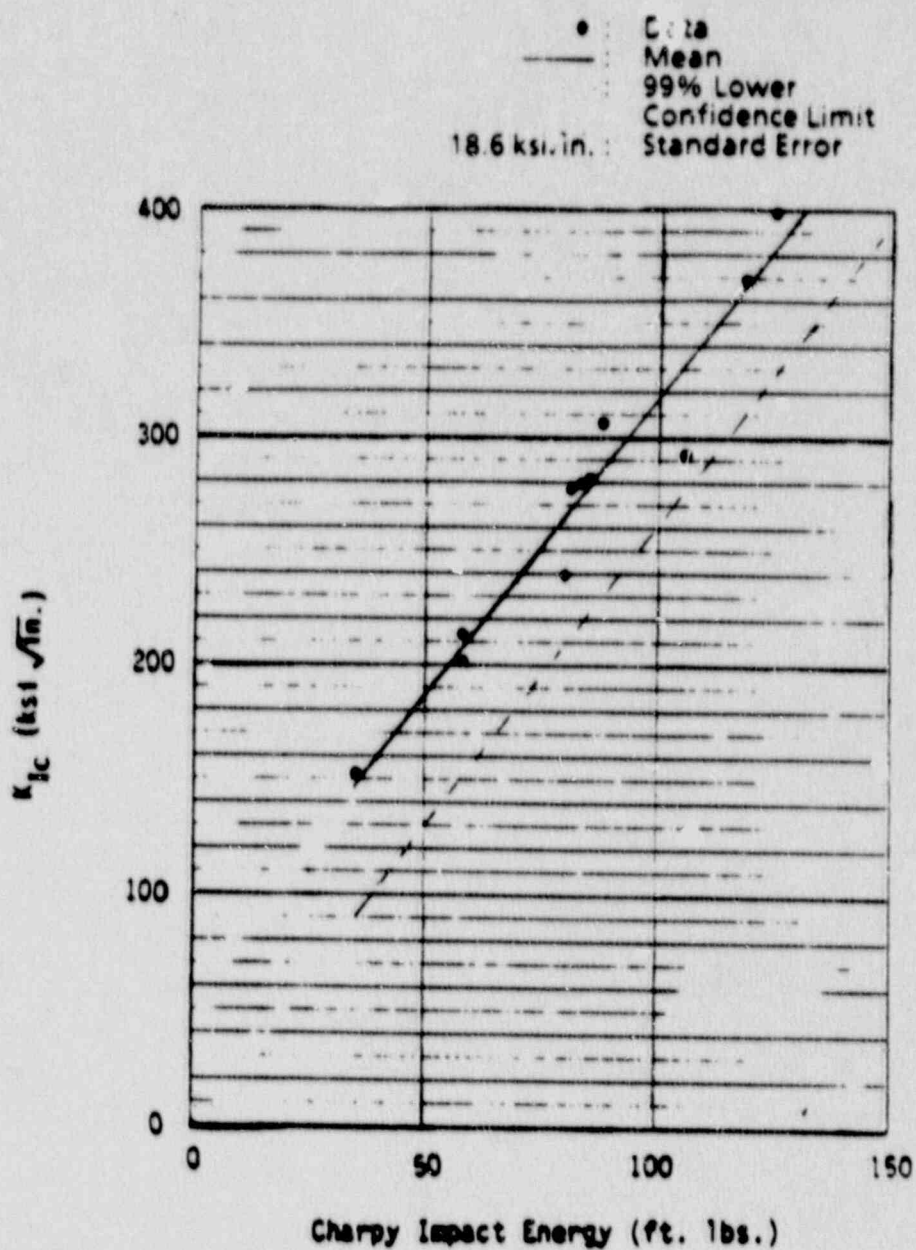


Figure 6.3-4  
 Correlation of  $K_{Ic}$  With Charpy Energy Showing the 99% Lower Confidence Limit for Application at Face, Knuckle and Bore



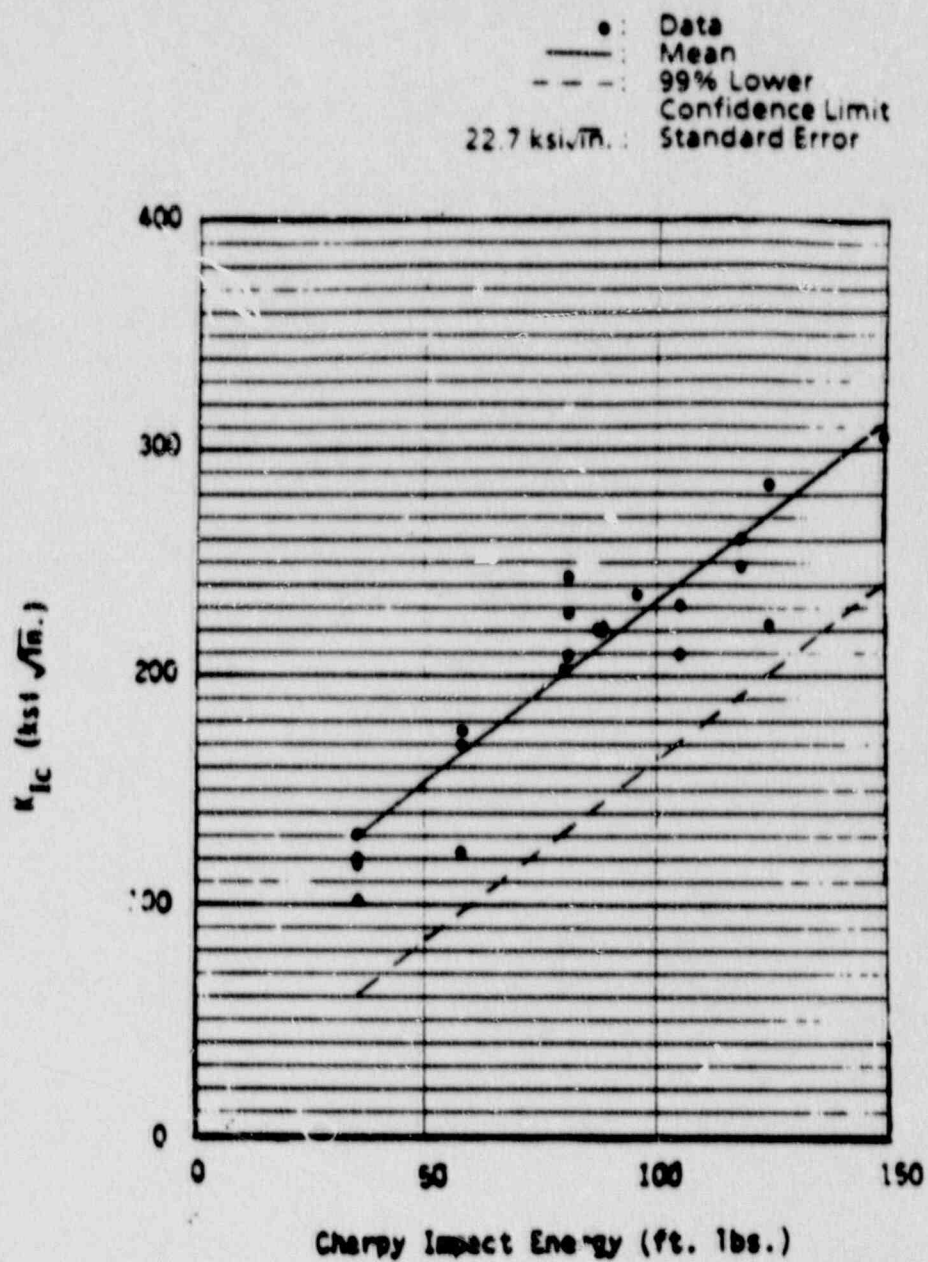


Figure 6.3-5  
 Correlation of  $K_{Ic}$  With Charpy Energy Showing the 99%  
 Lower Confidence Limit for Application at Counterbore

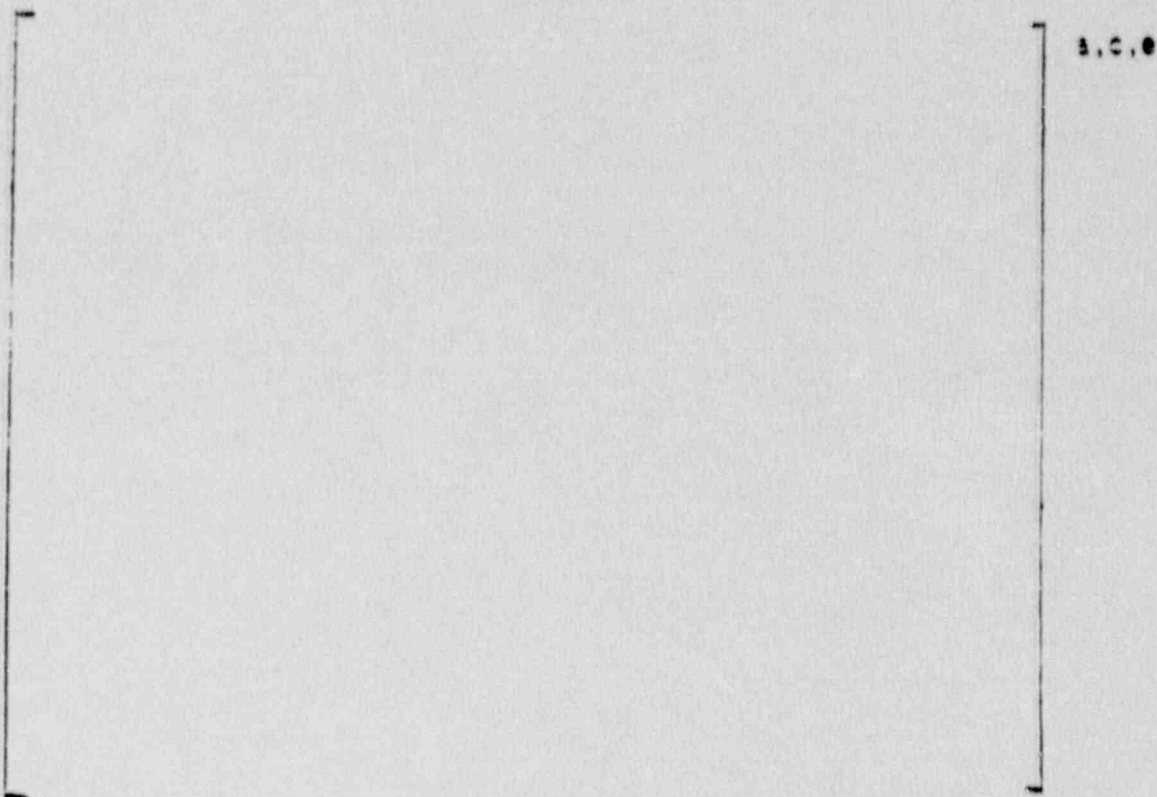


Figure 6.3-6  
Stress Intensity Factor as a Function of Flaw Depth  
With Aspect Ratio of 10 at the Feedwater Nozzle Face



Figure 6.3-7  
Stress Intensity Factor as a Function of Flaw Depth  
at the Feedwater Nozzle Knuckle





Figure 6.3-8  
Stress Intensity Factor as a Function of Flaw Depth  
With Aspect Ratio of 10 at the Feedwater Nozzle Bore



Figure 6.3-9  
Stress Intensity Factor as a Function of Flaw Depth With  
Aspect Ratio of 100 at the Feedwater Nozzle Counterbore

#### 6.4 DISCUSSION AND CONCLUSIONS

Extensive thermal hydraulic evaluations have been performed and are summarized for the application at hand. Stress analyses for the various feedwater nozzle locations have been performed and worst case scenarios are defined.

The major source of cracking in the feedwater face (without brackets), knuckle and bore has been identified as a corrosion fatigue by thermal striping occurring during feedwater cycling at hot standby with by-pass flow behind the thermal sleeve. Cracking at the counterbore is attributed to thermal stratification.

An evaluation of service at hot standby with feedwater cycling in conjunction with inspection results allowed crack growth rates to be conservatively established at each location in terms of days at hot standby. As seen in Table 6.3-2 the greatest crack growth rate was found to be at the feedwater nozzle face. Crack growth rates were available for each steam generator in the bore and counterbore. The rates were reasonably consistent.

The mechanism of crack propagation in the feedwater nozzle region is corrosion fatigue which involves an initial period of no growth followed by crack initiation and extension. All cracks have been removed and the original configuration restored with the exception noted in Section 6.3.1. Since fatigue is a long term reasonably well-understood mechanism, treating it in the same manner as stress corrosion cracking (see Section 5.0) is not warranted. Instead  $K_{IC}$  vs. Charpy energy correlations were established. Conservative component specific Charpy energies at 10°F were used to establish  $K_{IC}$  values at the lower 99% confidence limit.

Cracking is not expected to occur by cyclic corrosion fatigue in the near term. However, fracture mechanics analyses were performed based on the very conservative postulation that cracks initiate immediately when subjected to feedwater cycling.



With fracture criteria (i.e.,  $K_{IC}$ ) established, critical flaw sizes were determined using fracture mechanics. Specifically, projected crack growth was restricted so that the applied  $K$  remains below the  $K_{IC}$  criteria. Such crack growths divided by the associated crack growth rates gave the number of days at hot standby with feedwater cycling as shown in Table 6.3-7.

It is concluded that based on the recent operating experience at Indian Point Unit 2, in excess of 300 days of operation is attainable without postulated crack depths exceeding calculated values for the feedwater nozzle regions.

## 6.5 REFERENCES

- 1) "Indian Point Unit 2 Steam Generator Girth Weld/Feedwater Nozzles Report, Spring, 1989 Outage, Consolidated Edison of New York," WCAP-12293, Rev. 2, Westinghouse Electric Corporation, ESBU, Pittsburgh, PA, October 1989.
- 2) White, D. H., et al, "Investigation of Feedwater Line Cracking in Pressurized Water Reactor Plants," WCAP-9693, Westinghouse NTD, Pittsburgh, PA, June, 1980.
- 3) Witt, F. J., Relationships Between Charpy Impact Shelf Energies and Upper Shelf  $K_{IC}$  Values for Reactor Pressure Vessel Steels, Int. J. Pres. Ves. and Piping 11 (1983), pp. 47-63.

## 7.0 REPAIR AND MITIGATING ACTIONS

Based on the results of the evaluations described above, the actions taken have been either to restore the geometry to the original or modified configuration (nozzle area feed ring support) by repair welding using the temper bead technique or to remove the indications by grinding and blending. Specific repair actions are described below for each affected region.

### 7.1 GIRTH WELD

All indications located by MT in the girth weld and the region below the girth have been removed by grinding. Acceptance criteria for the grind out was:

1. MT Clear
2. Minimum 0.5 inch radius
3. 2:1 taper on slope of grind out

Further, 9 areas were weld repaired in Steam Generator 22 to restore all ground areas to a depth of 0.68 inch or less. Welding was performed using the temper bead technique, as provided by Code Case N432. The location of weld areas are identified on the maps in Appendix B.

### 7.2 FEEDRING SUPPORTS

#### 7.2.1 Thermal Sleeve Support Bracket

The Indian Point 2 steam generator feedring is supported just inside of the feedwater nozzle by a bracket that contacts the feedring thermal sleeve. Indications were discovered in some components and welds as described in Section 2.2. Because of the extent of the indications and grinding required to remove them, the original support brackets were removed completely and replaced.

The steam generator feedring replacement thermal sleeve support brackets consist of components, some of which were welded directly to the steam

generator shell. The design of the thermal sleeve support brackets parallel the original bracket closely. The principal parts of each support bracket are:

- o Two Brackets (that are welded to the steam generator shell)
- o One Shelf (that rests on the gussets and supports the thermal sleeve)
- o One Shelf Support (that serves to stiffen the shelf along its length).
- o One Shim (that fills the gap between the shelf and thermal sleeve)
- o One U-Bend Bracket (that holds the thermal sleeve against the shelf).

The replacement bracket is shown in Figures 7.2-1 and 7.2-2. The principal changes to the feedring thermal sleeve bracket, compared with the originally installed bracket, are shelf length increase, addition of a shelf support and support bracket relocation to avoid welding on the feedwater nozzle forging.

The design and fabrication of the bracket gussets is in accordance with the ASME B & PV Code Section III 1983 Edition, 1985 Winter Addenda. Results of structural analysis of the replacement bracket is contained in Section 5.2.2.1.

The material used for the bracket gussets is:

Material Specification: SA-516, Grade 70  
Armco Steel Co. Heat No.: 88095

The material for the other bracket components is carbon steel to ASTM A108 Grade 1018, ASTM A576 Grade 1018 and/or AISI 1018. This material is equivalent to that used for the original components.

#### 7.2.2 Horizontal U-Strap (S/G 21)

Horizontal U-Straps are used in three of the Indian Point 2 steam generators to position the feedring horizontally with respect to the steam generator



shell at the feedwater nozzle location. In Steam Generator 21, however, this horizontal positioning was accomplished through the support bracket. Because the original support bracket was removed (see Section 7.2.1) the horizontal positioning function was lost. Therefore, new horizontal U-Straps were installed to provide this positioning.

The steam generator feedring horizontal U-Straps that were installed in Steam Generator 21 consist of components, some of which are welded directly to the steam generator shell. The design of the horizontal U-Straps parallels the horizontal U-Straps in the other three steam generators closely. The principal parts are:

- o Two Horizontal U-Straps (that extend from the feedring at the two reducers to the steam generator shell).
- o Two Retainer Blocks (that are welded inside the U-Straps close to the feedring).

The horizontal U-Straps in Steam Generator 21 are shown in Figures 7.2-1 and 7.2-3. The principal difference between these U-Straps and those installed in the other three steam generators are the fabrication of the ends of the U-Straps (approximately 6 inches long) from an ASME Code material. This is to permit welding of the ends of the U-Straps directly to the steam generator shell, and not to weld buildups as was done in the other three steam generators.

The design and fabrication of the end pieces of the horizontal U-Straps is in accordance with the ASME B & PV Code Section III 1983 Edition, 1985 Winter Addenda.

The material used for the end portions of the horizontal U-Straps (in Steam Generator 21) is:

Material Specification: SA-516, Grade 70  
Armco Steel Co. Heat No.: 88095

The material for the other horizontal U-Strap components is carbon steel to ASTM A108 Grade 1018, ASTM A576 Grade 1018 and/or AISI 1018. This material is equivalent to that used for the original components.

### 7.2.3 Feeding A-B-C Supports

Each feeding support consists of the following components:

- o One transition Bar (that is welded to the steam generator shell).
- o One Bracket (that is welded to the transition bar)
- o One Bracket Bar (that rests on the gusset and supports the feeding.)
- o One J-Bracket (A & B locations) or One U-Bracket (C location) (that holds the feeding against the Gusset Bar).

Figure 7.2-4 shows the transition bar, bracket and bracket bar welded together and to the steam generator shell.

Indications detected during the inspection described in Section 2.3 were removed by grinding. The ground regions were repair welded as described in Section 5.2.2.2.

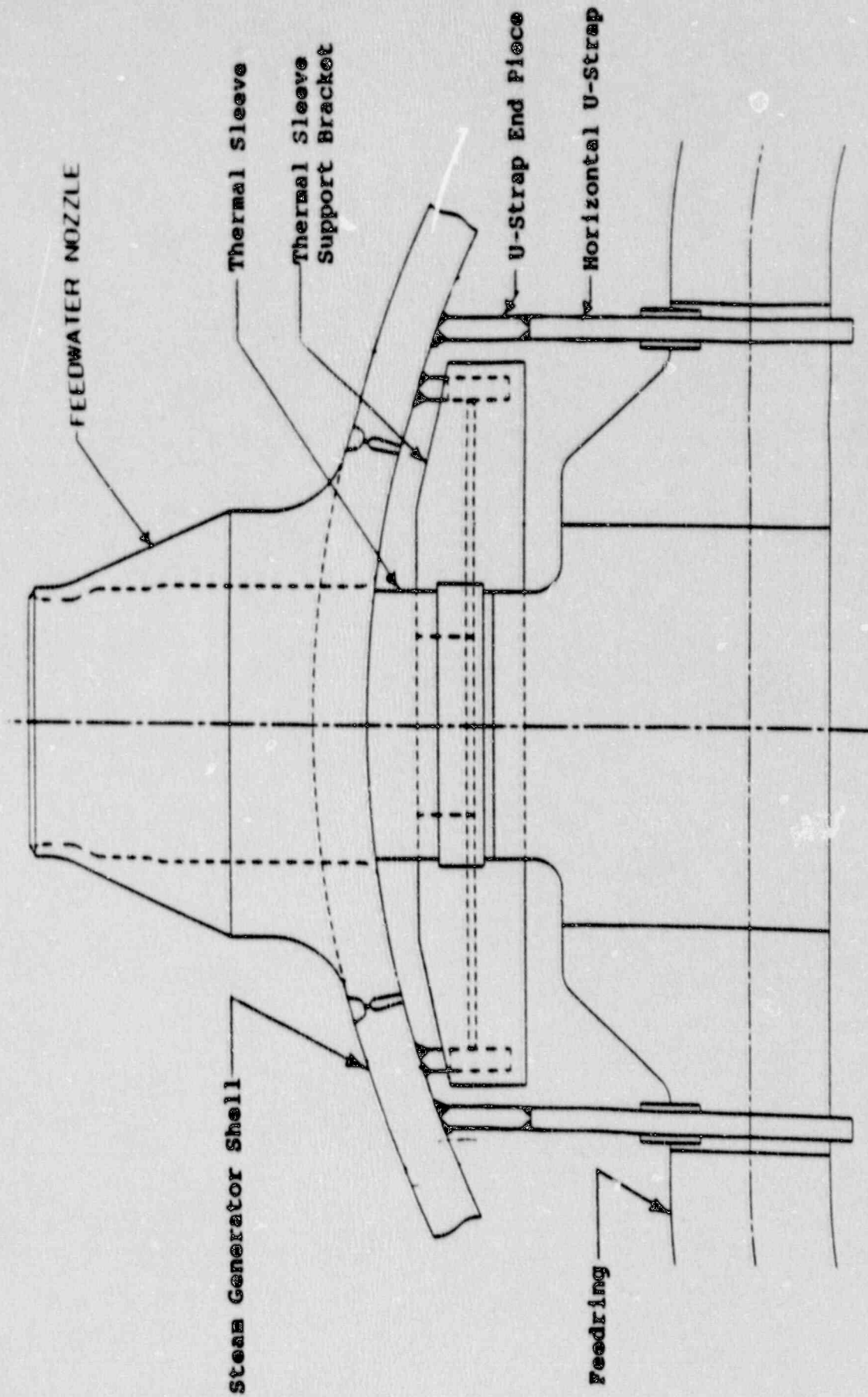


Figure 1.2-1  
Feeding Thermal Sleeve Support Bracket and  
Horizontal U-Strap (S/G 21) - Plan View



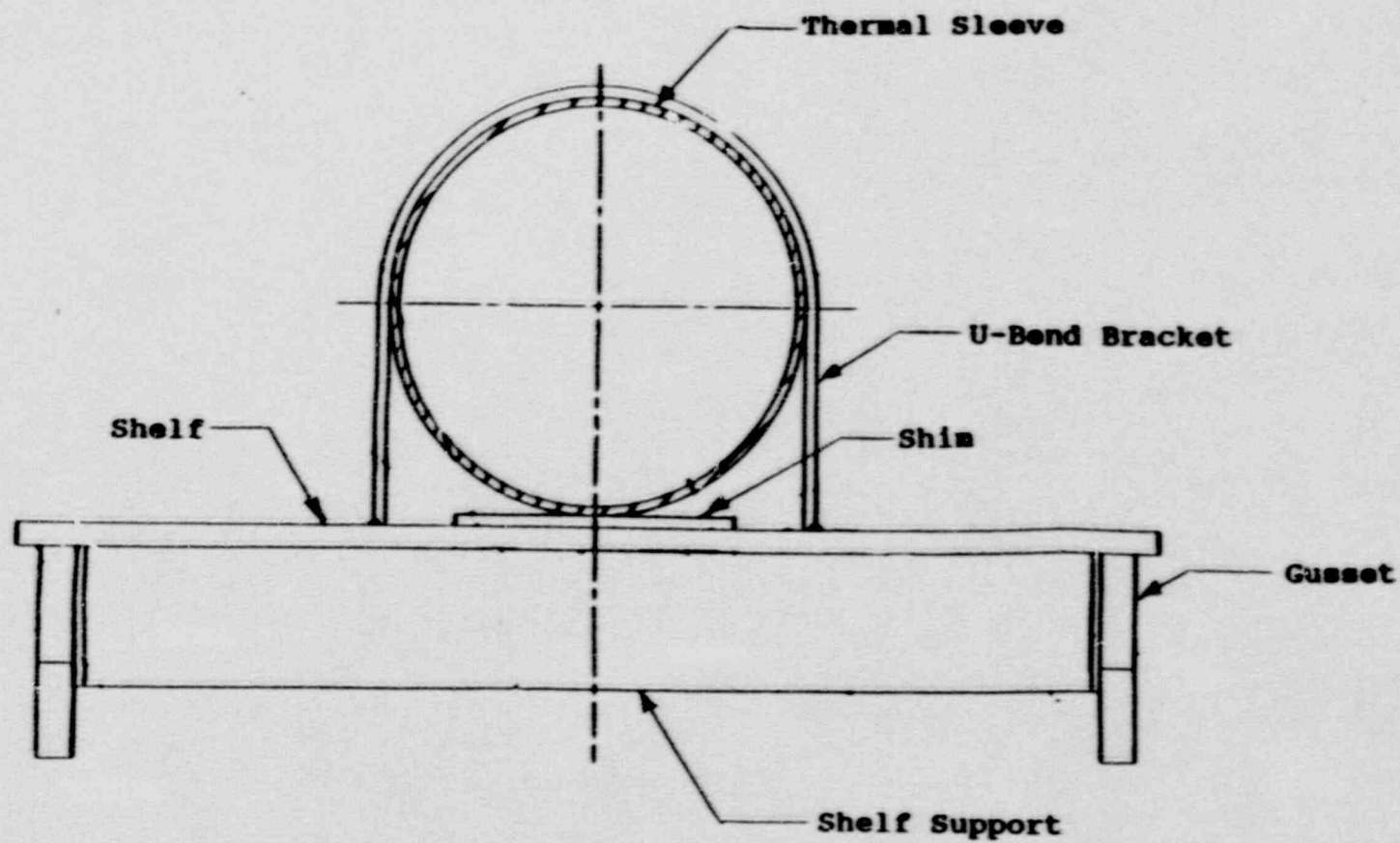


Figure 7.2-2  
Feeding Thermal Sleeve Support Bracket - Elevation

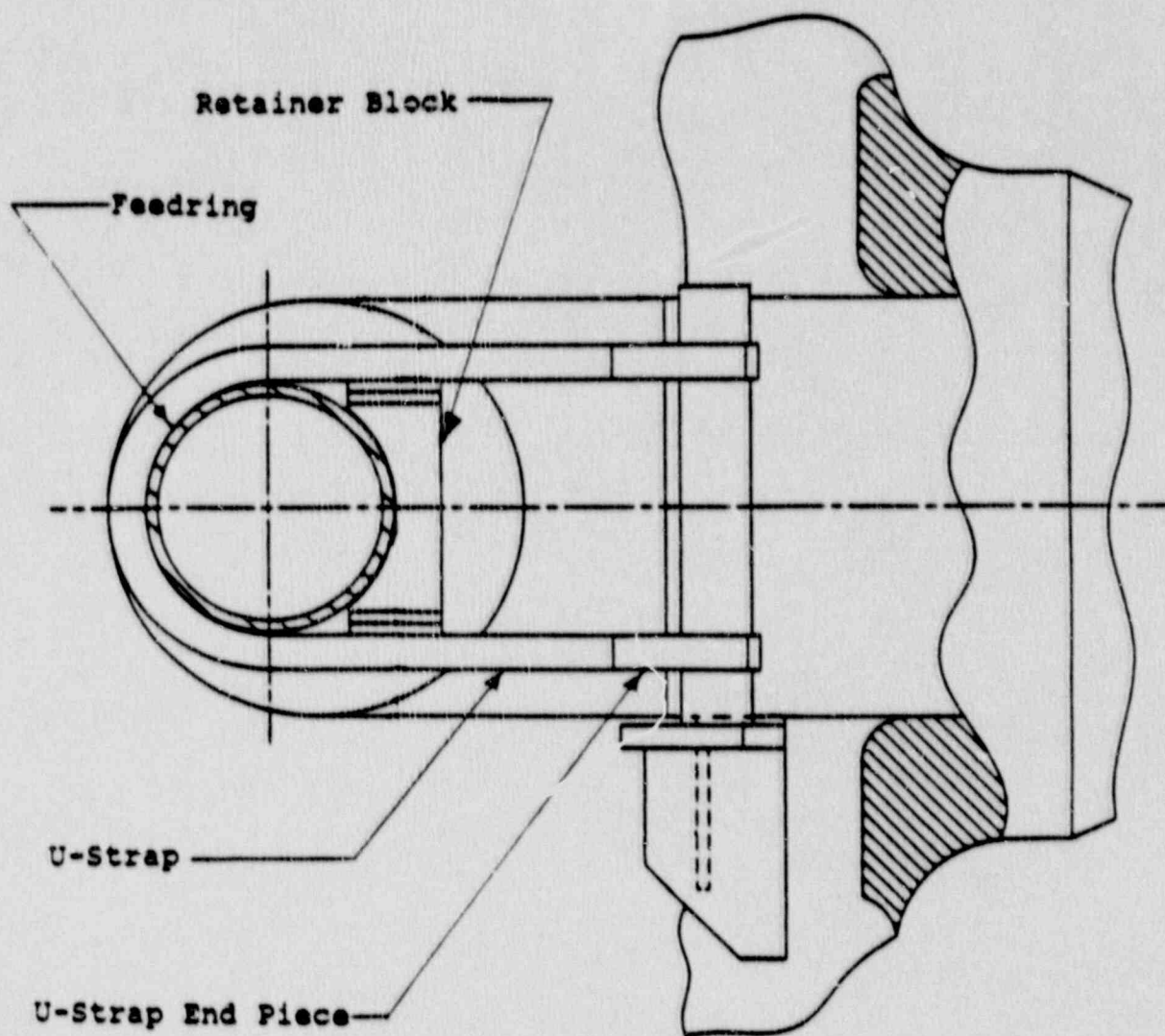


Figure 7.2-3  
Horizontal U-Strap (S/G 21) - Elevation

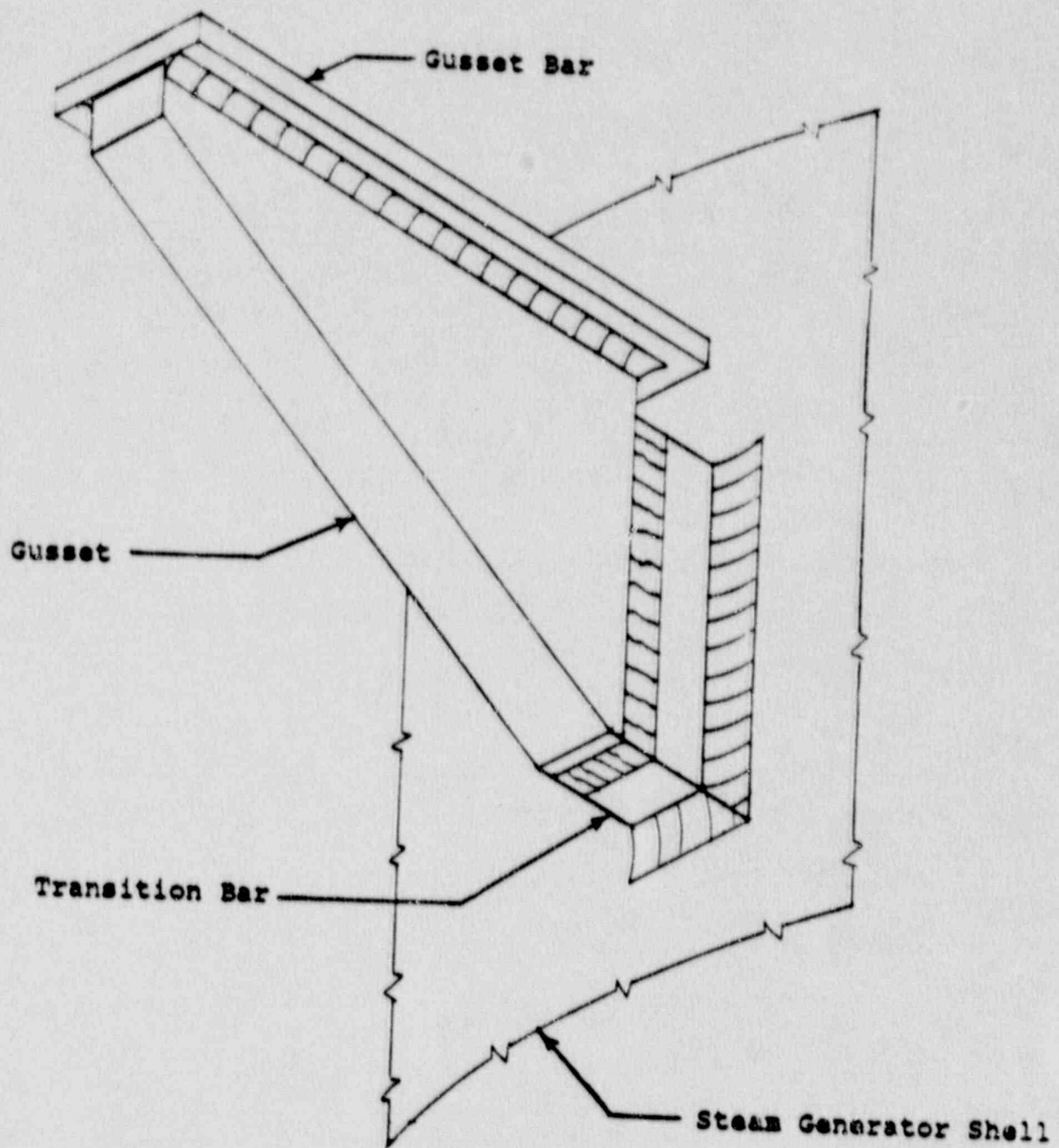


Figure 7.2-4  
Feeding A-B-C Support - isometric View



### 7.3 FEEDWATER NOZZLE REGION

The feedwater pipe, feedwater nozzle/pipe joint (counterbore), the nozzle inner bore, the knuckle region (inner radius) and the shell face of the nozzle forging just below the knuckle have been restored to the original design configuration by replacement or repair welding. Two small grindout areas in the nozzle bores were left as is discussed in Section 6.2.2.

All indications in the feedwater nozzle region were removed by hand grinding until MT clear. In order to ensure removal of all cracks in the nozzle bore, the feed ring thermal sleeve was removed. Once indication free, the nozzle bore and face were weld repaired by using the temper bead technique. The nozzle/pipe joint was repair welded from the I.D. by automatic GTAW.

After the completion of weld repairs, the nozzle and nozzle/pipe joint was final finished via a boring bar. The nozzle face was hand contoured to original dimensions. Finally, the centering pads on the O.D. of the thermal sleeve were built up with weld metal and machined to reduce the sleeve to nozzle clearance to design values. This was intended to reduce the possibility of flow induced vibration of the thermal sleeve.

### 7.4 NEAR TERM MITIGATING ACTIONS

During the mid-cycle outage, a nitrogen gas blanketing system was installed for the Condensate Storage Tank. The main source of nitrogen is provided by a liquid nitrogen trailer. The nitrogen blanketing will prevent the water in the CST from becoming saturated with oxygen. It is thought that reduction of oxygen will reduce an environment which may be conducive to pitting during injection of auxiliary feedwater when the unit is in service.

The feedring support adjacent to the feedwater nozzle has been redesigned to allow locating the brackets that are welded to the shell in a lower stressed region and to minimize the potential for cold bypass flow below the liner which can cause thermally induced loadings on the brackets. The stiffness of the bracket support for the feedring has been retained to avoid any vibration induced loadings of the feedring. The potential seismic loadings on any of

the feedring supports is well within the capability of the supports to meet ASME Code allowables.

The feedwater pipe, feedwater nozzle/pipe joint (counterbore), the nozzle inner bore, the knuckle region (inner radius) and the shell face of the nozzle forging just below the knuckle have all been restored to the original design configuration by repair welding.

Wet layup procedures have been modified to reflect a nitrogen sparging gas to displace air within the steam generators for future outages.

## 8.0 FUTURE PLANS

### 8.1 GENERAL

The cracking which has been observed in the girth weld and nearby shell, nozzles and support brackets, is the result of a combination of corrosion fatigue and stress corrosion cracking. The fatigue loading and steady state loads are the result of operating conditions and the corrosion is mainly caused by condensate storage tank, condenser and feedwater heater design and materials selection, which have contributed to oxygen and copper concentrations. Measures have been taken and are being taken to reduce or eliminate the adverse internal steam generator environmental conditions. Reduction of oxygen, coupled with the thorough examinations and extensive repairs performed during this outage on the girth weld, nozzles and support brackets, is expected to minimize the recurrence of cracking during the next cycle of operation compared to prior cycles. Nonetheless, Con Edison is preparing to reinspect during the 1991 refueling outage and to take appropriate measures based on the inspection results.

In addition, Con Edison with the assistance of industry experts in the field of metallurgy and engineering mechanics, will continue to investigate the contributions of various causative mechanisms and the potential impact of remedial approaches. Specifically, metallurgical testing programs at the M.I.T. Laboratory will be pursued to identify threshold levels associated with various parameters related to stress, temperature, environment and material which are believed to be contributing to the mechanisms of pitting and cracking in the basemetal, welds and heat affected zones.

### 8.2 INSPECTION PROGRAM FOR 1991 REFUELING OUTAGE

1. Inspect by MT all steam generators girthwelds including the repaired area up to nominally 7 inches below the centerline of the girth weld. Inspect by UT a band 360 degrees from 7" below the centerline to 14" below centerline of girth weld in SG 22. If indications are found, inspect all steam generators.



2. Inspect by MT feed ring brackets and bracket welds in all steam generators.
3. Inspect by UT one nozzle knuckle and accessible nozzle areas. If indications are found that extend into the inaccessible bore area, pull thermal sleeve from the nozzle and inspect bore by MT. If indications are found, inspect nozzle bores in all steam generators.
4. Inspect by MT or PT lower 180 degrees of all nozzle knuckles. If indications are found, inspect 360 degrees of all steam generator nozzle knuckles. If indications are found extending into the inaccessible bore area, pull thermal sleeve from nozzle and proceed as per 3 above.
5. Radiograph one nozzle-to-pipe weld and compare with as left radiographs. If indications are found, inspect the nozzle-to-pipe welds in all steam generators.
6. Inspect by UT an area in the feed pipe from the nozzle-to-pipe weld to one foot out in SG 22. If indications are found, inspect horizontal runs to the first elbow for all steam generators.
7. Inspect by MT or PT the upper 8 inch handhole in SG 23, hillside port in SGs 22 and 23, one-6 in. handhole, manway and one 3/4 in. upper and lower level instrument tap penetration. If indications are found, inspect all like components to the ones showing indication.

### 8.3 ACTIONS

If the 1991 inspection shows a recurrence of cracking similar to that experienced during the most recent period of operation, Consolidated Edison will develop an appropriate action plan which will include one or more of the following:

1. Implement repairs to provide for uninterrupted operation between refueling cycles. These repairs could include:

- a. Machining a 360 degree band up to 6 in. wide and 1 in. deep in the girth weld and build up to original contour, or machine finish to a smooth surface a band 2 feet wide centering on the girth weld - 360°.
  - b. Resurface the feedwater nozzle bores by machining to a depth of 1/2 in. and weld back to original contour.
  - c. Eliminate bypass flow in the feedwater nozzle.
  - d. Install new feedwater ring header brackets.
2. During subsequent outages, and continuing until the existing steam generators are retired from service, Con Edison will perform such inspections and repairs as may be necessary to comply with the applicable provisions of ASME B&PV Code prior to return to service.

#### 8.4 CONDENSER AND FEEDWATER HEATER CHANGE OUT

1. During the upcoming operating period corrosion product transport survey will be conducted.

2. During 1991 Refueling Outage:

The tubing of one condenser will be changed from Admiralty tubing to titanium tubing.

3. During 1993 Refueling Outage:

The remaining Admiralty condensers will be replaced with titanium and the remaining feedwater heaters will also be changed from copper alloy tubing to stainless steel tubing.

## 8.5 LONG RANGE PLANNING

Consolidated Edison will continue to evaluate and monitor the causal mechanisms for the existing cracking, as well as the safety, man-rem, cost, unit reliability and unit availability considerations associated with continued operation with the existing steam generators contrasted with steam generator replacement. These issues will be reassessed following evaluation of steam generator condition as ascertained during the 1991 outage.

In addition, Con Edison has initiated advanced planning for full reactor coolant loop decontamination (fuel removed) for possible implementation during the 1993 outage. If determined to be feasible and effective, decontamination would reduce source term, thereby reducing routine worker exposure as well as potential exposure at such time when the existing steam generators are retired.



## 9.0 SUMMARY AND CONCLUSIONS

The inspection and subsequent repair and analysis has been performed to demonstrate continued operation of Indian Point Unit 2. The inspection program was expanded until all areas containing potential indications were enveloped. Subsequent repair activities removed all indications, and, where applicable, the ground areas were restored to original geometry by welding.

The approach used to demonstrate adequate margin in the steam generator girth weld for continued operation is based on a modification of the fracture mechanics criteria of Section XI of the ASME Code. The Section XI fracture criteria found in paragraph IWB 3600 are normally used to justify continued operation without removal of cracks. In this case, all indications have been removed by grinding and some grind-out areas have been partially restored by welding.

The repair of the indications observed in the feedwater nozzle area was accomplished by grinding and restoring to original geometry by welding. To further address the indications seen in the HAZ of the feedring brackets near the nozzle, the brackets were redesigned to relocate them to a more favorable position. The nozzle indications are caused by thermal striping and stratification during cold water injection. Results of the evaluation of the boat sample removed from SG 24 nozzle showed the cracking mechanism to be corrosion fatigue. Visual examination showed significant surface pitting with shallow cracks linking the pits.

Continued operation of the unit following removal of all indications in the girth weld, nozzle and feedring support brackets has been justified. All repaired areas exhibiting susceptibility to stress corrosion cracking have been evaluated against the ASME Section XI fracture criteria which is normally used to justify continued operation without removal of the indications. The corrosion fatigue mechanisms of the feedwater nozzle was evaluated using very conservative component fracture specific criteria. All cracks have been removed by grinding and where applicable the ground areas have been restored to original geometry by welding. Considering the conservatism applied throughout the activities, it is judged that operation

to the next refueling cycle is justified. The justification for continued operation assumes that the indications will initiate and continue to grow at the same rate as in the previous cycle. It is believed that the actions to remove the dissolved oxygen from the auxiliary feedwater currently being implemented will significantly retard the process of pitting, crack initiation and growth.

APPENDIX A  
EMBEDDED FLAW EVALUATION

1.0 SCOPE OF EVALUATION

Embedded flaw evaluations were performed for the upper shell to cone weld region. This section describes the development of the embedded flaw charts for that region.

2.0 EMBEDDED VS. SURFACE FLAWS

According to IWA-3300 of the ASME Code Section XI, a flaw is defined as embedded, as shown in Figure A-1, whenever,

$$S \geq 0.4 a \quad (A-1)$$

where

S - the minimum distance from the flaw edge to the nearest vessel wall surface

a - the embedded flaw depth, (defined as the semi-minor axis of the elliptical flaw.)

The parameter  $\delta$  has been defined in this document to facilitate the use of the charts.  $\delta$  is defined as the distance from the centerline of the flaw to the surface of the vessel. Therefore,  $\delta = S + a$ . Substituting into the proximity limit in equation A-1 gives a limiting definition of  $\delta$  as a function of a, for the proximity limit.

$$a = \delta - S \quad (A-2)$$

$$\delta \geq 1.4 a \quad (A-3)$$

Therefore, the limit for a flaw to be considered embedded is  $a_0 = 0.714 \delta$ .



### 3.0 CODE CRITERIA

The criteria used in most of the cases for embedded flaws are of IWB-3612 of Code Section XI. Namely,

$$K_I < \frac{K_{Ia}}{\sqrt{10}} \text{ For normal conditions (upset \& test conditions inclusive) (A-4)}$$

$$K_I < \frac{K_{Ic}}{\sqrt{2}} \text{ For faulted conditions (emergency conditions inclusive) (A-5)}$$

where

$K_I$  = The maximum applied stress intensity factor for the flaw size  $a_f$  to which a detected flaw will grow, during the period of evaluation, which must be at least until the next inspection.

$K_{Ia}$  = Fracture toughness based on crack arrest for the corresponding crack tip temperature.

$K_{Ic}$  = Fracture toughness based on fracture initiation for the corresponding crack tip temperature.

The above two criteria must both be met. Here only the most limiting results have been used as the basis of the flaw evaluation charts.

### 4.0 BASIC DATA

In view of the criteria based on stress intensity factor, three basic groups of data are needed for construction of embedded flaw evaluation charts. They are:  $a_f$ , driving force ( $K_I$ ), and fracture toughness ( $K_{Ia}$  and  $K_{Ic}$ ).

$K_{Ic}$  and  $K_{Ia}$  are the initiation and arrest fracture toughness (respectively) of the vessel material at which the flaw is located. They can be calculated by formulas:

$$K_{Ic} = 33.2 + 2.806 \exp. [0.02(T-RTNDT + 100^{\circ}F)] \quad (A-6)$$

and

$$K_{Ia} = 26.8 + 1.233 \exp. [0.0145(T-RTNDT + 160^{\circ}F)] \quad (A-7)$$

$K_I$  is the maximum stress intensity factor for the embedded flaw of interest. The methods used for determining the stress intensity factors for embedded flaws have been referenced in Section 5.3.2.

$K_I$  used in the determination of the flaw evaluation charts is the maximum stress intensity factor of the embedded flaw under evaluation. It is important to note that the flaw size used for the calculation of  $K_I$  is not the flaw size detected by inservice inspection. Instead, it is the calculated flaw size which is projected to grow from the flaw size detected by inservice inspection. That means that the embedded flaw size used for the calculation of  $K_I$  had to be determined by using fatigue crack growth results, similar to the approach used for surface flaw evaluation, as illustrated in the previous section.

However, the fatigue crack growth for an embedded flaw (even after 30 years of additional service life) is very small in comparison with that of a surface flaw with the same initial depth. Consequently, in the evaluations, the measured flaw size has been used for evaluation by the charts independent of the service period\* because fatigue has little or no influence for embedded flaws as discussed below. This simplifies the evaluation procedure without sacrificing the accuracy of the results. A detailed justification of this conclusion is provided in the next section.

---

\* This conclusion holds for the range of flaw sizes acceptable by the rules of Section XI, IWB-3600. It would not necessarily hold for very large flaws of the order of 50 percent of the vessel wall thickness.

## 5.0 TYPICAL EMBEDDED FLAW EVALUATION CHART

The details of the procedures for the construction of an embedded flaw evaluation chart are provided in the next section.

In this section, instructions for developing a chart are provided by going through a typical chart, step by step. This would help the users to become familiar with the characteristics of each part of the chart, and make it easier to apply. This example utilizes the surface/embedded flaw demarcation criteria of the code, as discussed earlier.

Following are the highlights of auxiliary charts used to construct the embedded flaw evaluation chart for the transition cone region.

1. The abscissa of the chart in Figures A5-3, A5-4, and A5-5 represents the flaw depth  $a$ , of the embedded flaw.
2. As defined by code, embedded flaws with a depth less than  $a_0 = 0.714 \delta$  should be considered as embedded flaws. Any embedded flaws beyond the domain of  $a_0 = 0.714 \delta$ , should be evaluated by means of surface flaw charts instead.
3. A key parameter for evaluating an embedded flaw is  $\delta$ , the distance between the centerline of the embedded flaw and the nearest surface of the steam generator wall.

A range of  $\delta$  between  $1/16t$  and  $1/4t$  has been considered in constructing Figures A5-3, A5-4, and A5-5.

4. For each specific value of  $\delta$ , such as  $1/8t$ ,  $3/16t$ ,  $1/4t$ , etc., a family of curves were plotted for a range of  $a/\ell$  values ranging from .333 to .100. For any specific flaw depth  $a$  at the abscissa, a corresponding value  $K_I$  at the ordinate can be found in Figures 5-3 through 5-5, for any distance to the surface,  $\delta$ .



5. The range of  $a/\ell$  values from 0.333 to 0.10 was chosen to encompass the range of flaws which might be detected. For the upper shell to cone region, fracture results are independent of the aspect ratio, as will be discussed further below.
6. In developing this specific chart, the code acceptance limit line of  $K_{Ia}/\sqrt{10}$  as a function of flaw depth is shown in Figures A-3 through A-5.
7. The intersection of the  $K_I$  curve with the code acceptance limit line is the maximum flaw size acceptable by code for the specific curve, in accordance with the  $K_I \leq K_{Ia}/\sqrt{10}$  from IWB-3612.
8. In view of Figures A-3 through A-5, it is seen that some of the curves intersect with the code acceptance limit line. That means that, up to a distance of  $\delta = 1/4 t$  ( $= 0.875"$ ), some embedded flaws are not acceptable by the code criteria so long as their depth is within the domain of  $a_0 = 0.714 \delta$ .
9. The maximum acceptable flaw size can be found from the chart by determining the abscissa of the intersection points. Namely, for  $\delta = 0.25 t$ ,

<u><math>a/\ell</math></u>	<u>Maximum Acceptable Flaw Depth <math>a^*(in.)</math></u>
.100	0.437
.167	0.437 ( $= a_0 = 0.437$ )
.333	0.437

10. The maximum acceptable embedded flaw size for  $\delta = 1/4 t$  has been depicted in Figure A-2. This simple flaw evaluation chart,

\* Maximum Acceptable Flaw Depth  $a$  is set at  $1/8 t$ , based on engineering judgement, to limit the allowable through-wall penetration to 25 percent of the wall thickness.

described in the following paragraph, is the type to be used for evaluation.

This embedded flaw evaluation chart, constructed for the transition cone region of the steam generators, is presented in Figure A-2 and instructions given for its use in Section A.7.

#### 5.0 PROCEDURE FOR THE CONSTRUCTION OF EMBEDDED FLAW EVALUATION CHARTS

This section shows how an embedded flaw evaluation chart was constructed for the transition cone region during the governing transient which is the feedwater cycling transient. The example here is for the case of RTNDT = 30°F. Charts were also constructed for the upper shell to cone girth weld, for two different grinding depths, as seen in section 5.3.8 of the main body of this report.

##### Step 1

Calculate  $K_I$  values for embedded flaws of various size, various aspect ratios, and at various distances underneath the surface. In total, 135 cases were analyzed by closed form stress intensity factor expressions.

##### Step 2

The  $K_I$  results of the 135 cases were plotted in Figures A-3 through A-5.

##### Step 3

Determine the allowable flaw size, from  $a_c/10$  or  $K_I \leq K_{Ia}/\sqrt{10}$  criteria as determined by Figures A-3 through A-5. Similar results could be obtained for the emergency/faulted conditions, but they are not governing, so they have not been included here.

## 7.0 EVALUATION PROCEDURE

The evaluation procedures contained in ASME Section XI are clearly specified in paragraph IWB-3600. Use of the evaluation charts herein follows these procedures directly, but the steps are greatly simplified.

Once the indication is discovered, it must be characterized as to its location, length ( $\ell$ ) and depth dimension ( $a$  for surface flaws,  $2a$  for embedded flaws), including its distance from the inside surface ( $S$ ) for embedded indications. This characterization is discussed in further detail in paragraph IWA-3000 of Section XI.

The following parameters must be calculated from the above dimensions to use the charts (see Figure A-1):

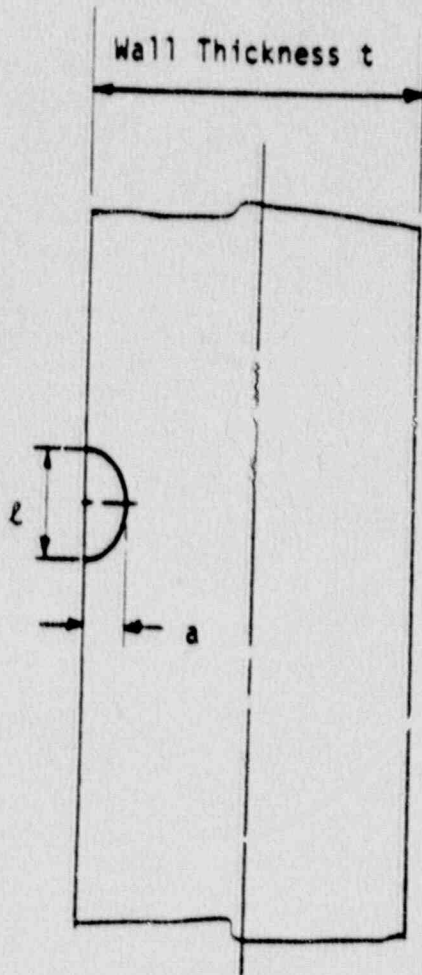
- o Flaw Shape parameter,  $a/\ell$
- o Flaw depth parameter,  $a/t$
- o Surface proximity parameter (for embedded flaws only),  $\delta/t$

where

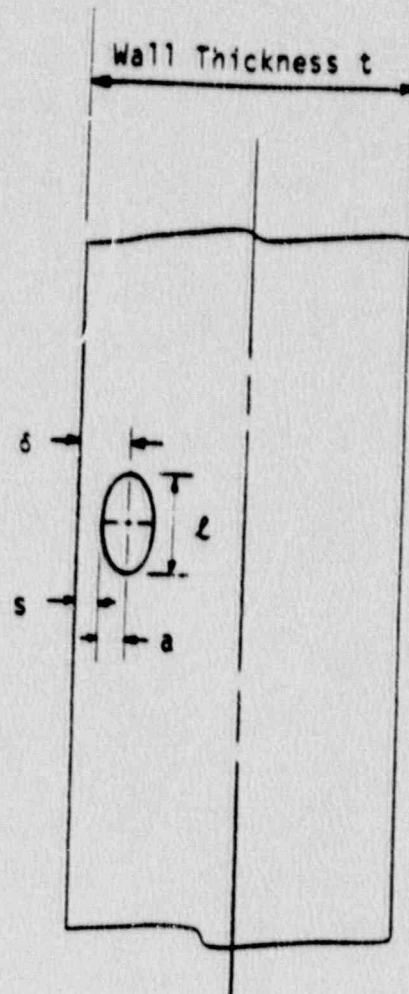
- $t$  = wall thickness of region where indication is located
- $\ell$  = length of indication
- $a$  = depth of surface flaw; or half depth of embedded flaw in the width direction
- $\delta$  = distance from flaw centerline to surface (for embedded flaws only) ( $\delta = s + a$ )
- $s$  = smallest distance from edge of embedded flaw to surface

This procedure has been followed to evaluate the indications discovered in the ultrasonic inspection of the girth weld and cone region, and the results are shown in Section 5.3.8 of the main body of the report.





TYPICAL SURFACE FLAW INDICATION



TYPICAL EMBEDDED FLAW INDICATION

Figure A -1  
Embedded vs. Surface Flaw

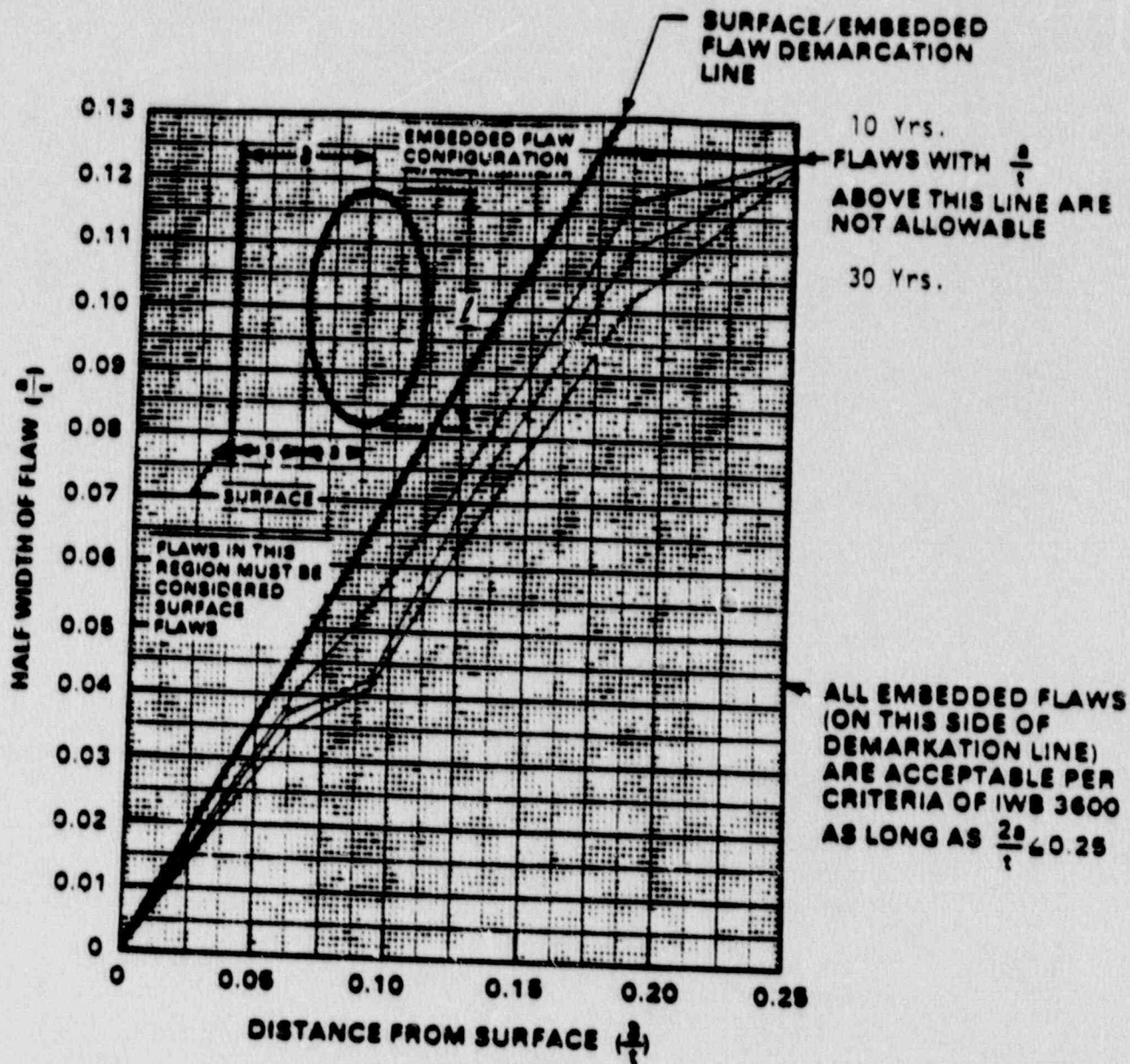


Figure A -2

Embedded Flaw Evaluation Chart for Circumferential Indications in the Cone Region

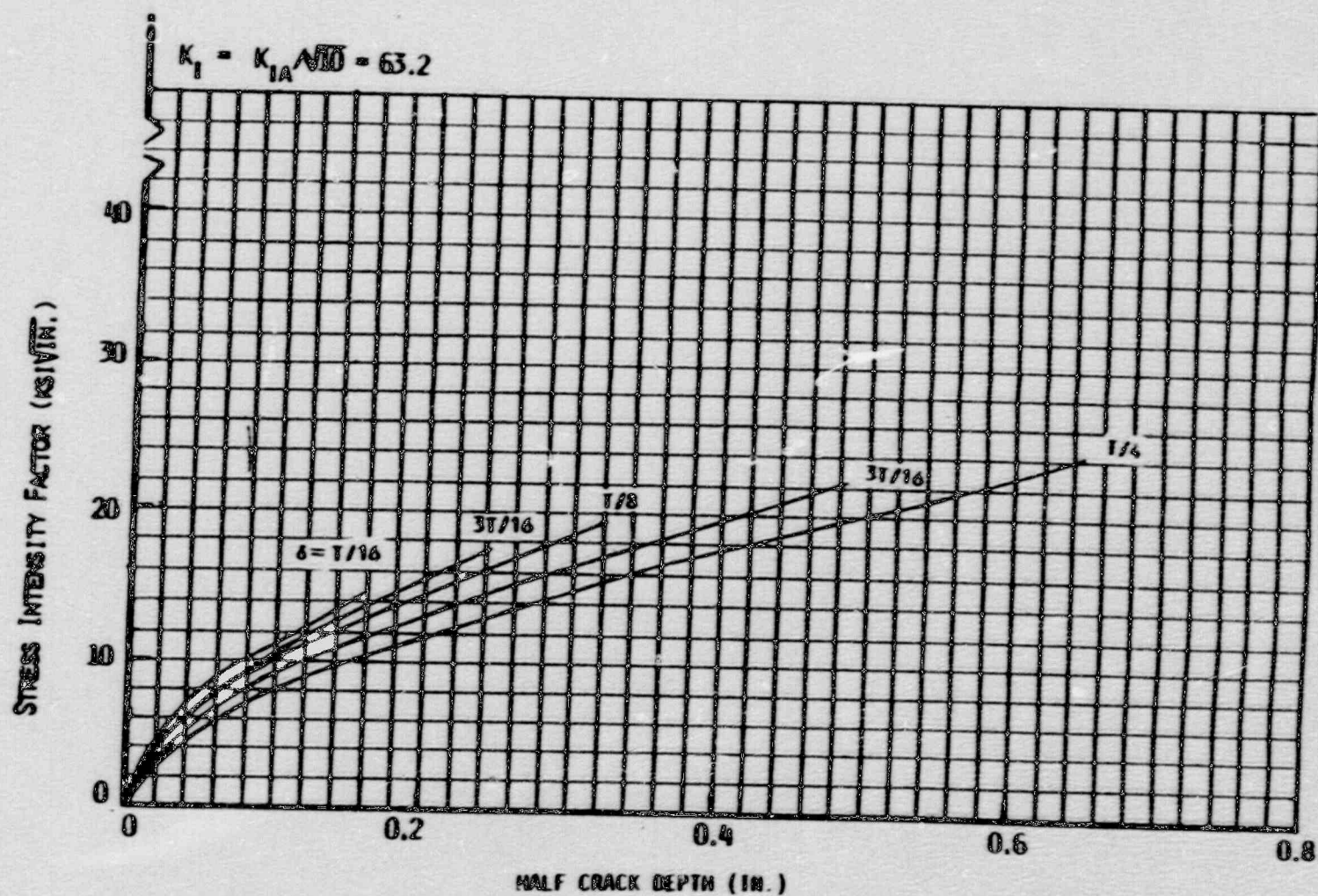


Figure A-3

Stress Intensity Factor Plots for  $a/t = 0.333$   
 Used in Construction of Embedded Flaw Charts - Cone Region



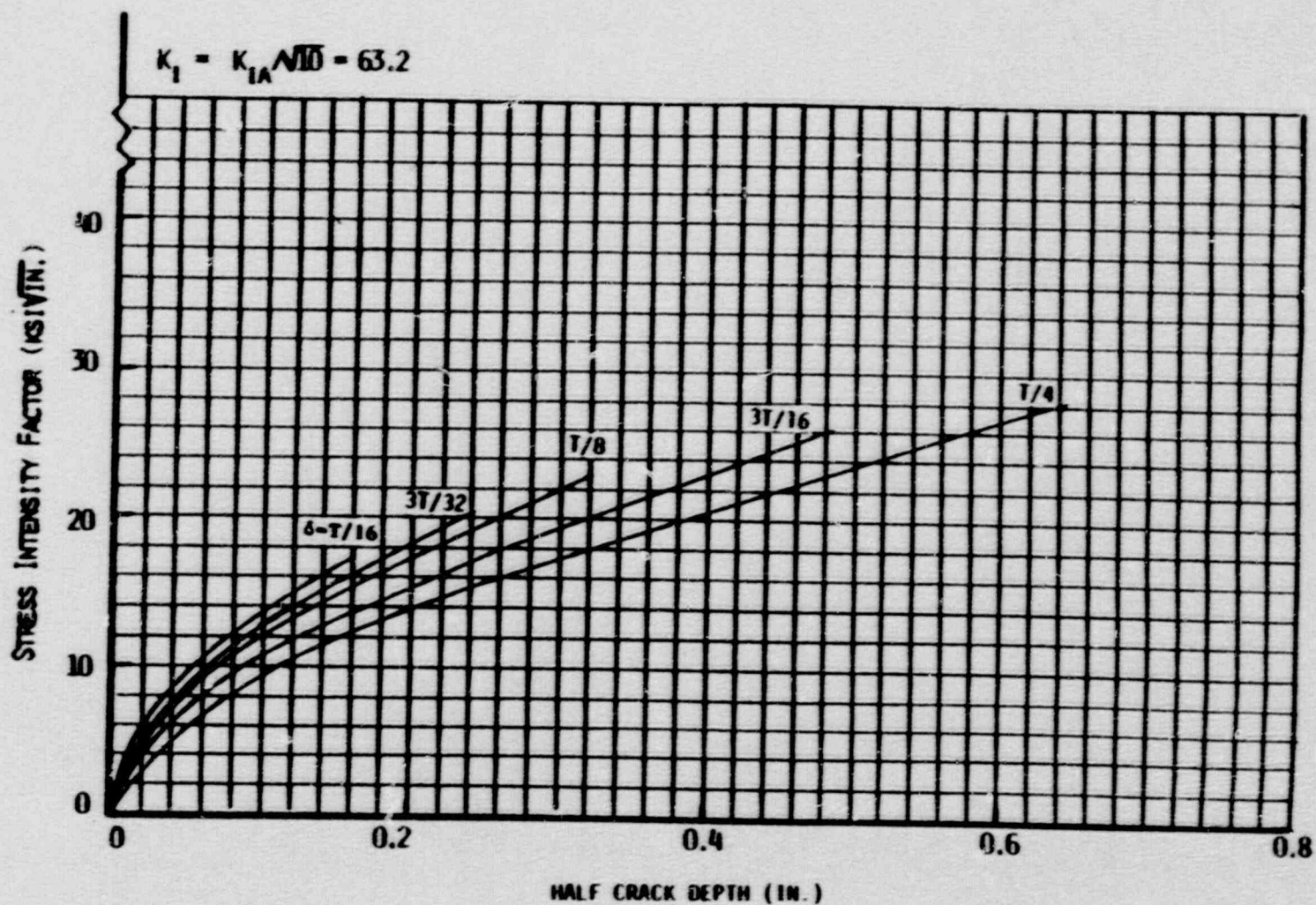


Figure A -4

Stress Intensity Factor Plots for  $a/t = 0.1667$   
 Used in Construction of Flaw Evaluation Charts - Cone Region

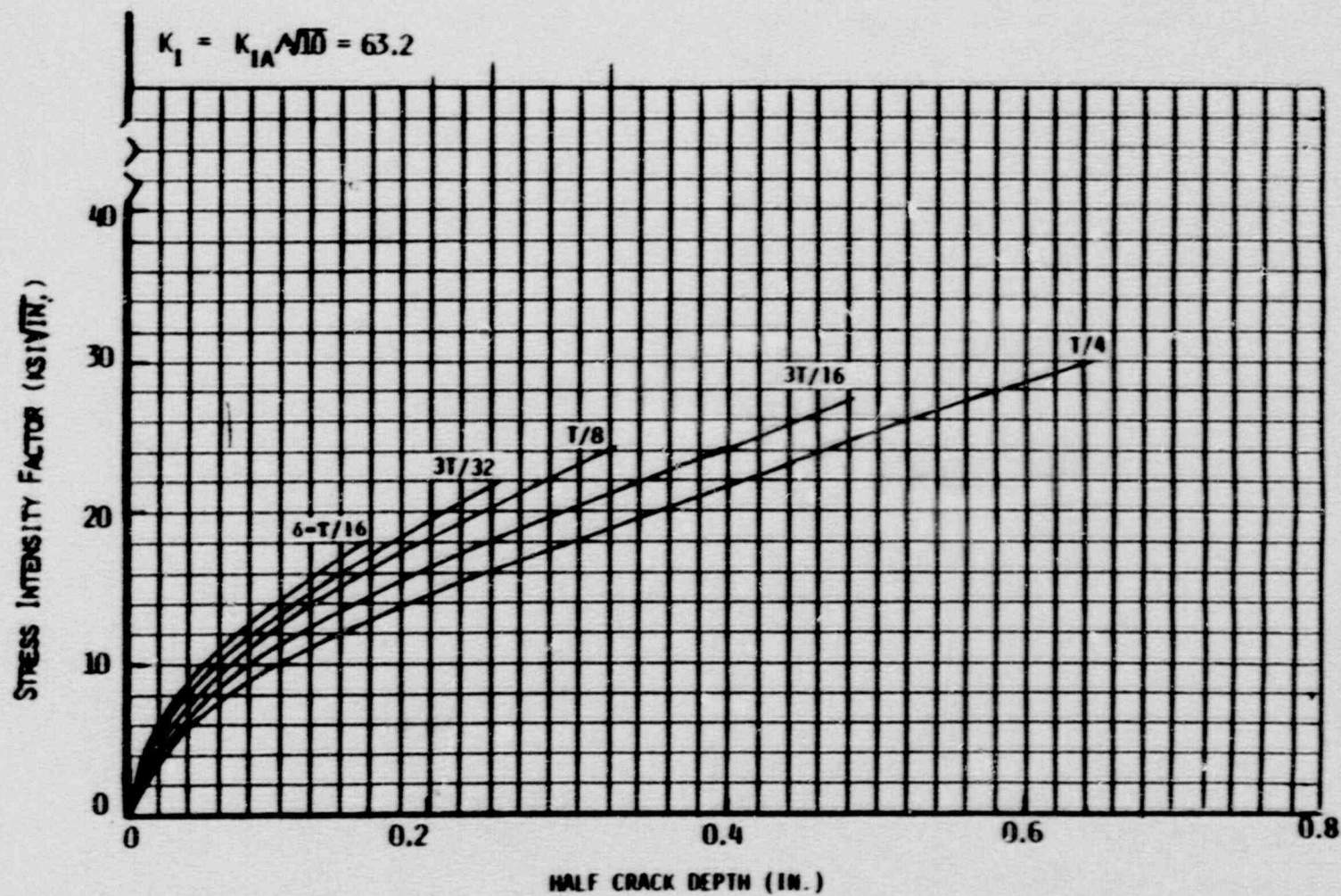


Figure A -5

Stress Intensity Factor Plots for  $a/t = 0.10$   
 Used in Construction of Flaw Evaluation Charts - Cone Region

APPENDIX B  
GIRTH WELD INSPECTION DATA



1990 OUTAGE  
GIRTH WELD INDICATIONS

SG 21 (FINAL)

ZONE NO.	IND. NO.	END OF IND. FROM		IND. LENGTH	DEPTH		IND. LOCATION	REMARKS
		ZONE LINE	HOR. REF.		FINAL NORMAL	GROWTH		
		in.	in.	in.	in.	in.		
1	1	0.50	9.00	0.38	0.76	0.34	C-89	
	2	12.25	9.75	0.38	0.24	0.18	0	
	3	19.00	10.00	0.38	0.23	0.16	0	
	4	30.50	10.13	0.50	0.29	0.17	0	
	5	41.50	8.63	0.25	0.11	0.19	0	
2	1	10.00	10.13	0.63	0.42	0.05	0	
	2	18.00	9.75	0.63	0.57	0.04	0	
	3	27.50	10.00	0.50	0.50	0.32	C-89	
	4	29.50	8.75	0.25	0.15	0.16	0	
	5	38.00	9.13	0.38	0.51	0.17	0	
3	1	2.00	9.50	0.63	0.50	0.21	S-89	
	2	7.25	9.25	1.50	0.29	0.22	S-89	
	3	27.50	9.50	0.50	0.18	0.17	0	
	4	34.13	9.50	0.38	0.14	0.15	0	
4	1	2.63	8.25	0.25	0.11	0.11	0	
	2	4.25	8.63	0.25	0.09	0.16	0	
	3	16.38	8.63	0.25	0.14	0.14	0	
	4	39.00	8.63	0.38	0.15	0.05	0	
5	1	1.50	8.50	0.25	0.12	0.10	0	
	2	13.50	9.25	0.50	0.11	0.08	0	
	3	31.50	9.25	0.25	0.16	0.16	0	
	4	41.00	9.25	0.38	0.16	0.17	0	
6	1	34.00	9.00	0.25	0.13	0.11	0	
7	1	21.00	9.00	0.25	0.11	0.05	0	
	2	21.50	9.00	0.25	0.07	0.02	0	
	3	37.00	9.00	0.25	0.10	0.13	0	
8	1	23.88	9.00	0.50	0.25	0.17	0	
	2	27.00	9.00	1.00	0.10	0.03	0	
	3	29.00	9.00	0.25	0.09	0.02	S-89	
	4	39.50	9.00	0.50	0.17	0.11	S-89	
9	1	5.50	9.00	0.25	0.09	0.07	0	
	2	12.00	9.50	0.25	0.34	0.12	0	
	3	18.50	9.25	0.50	0.36	0.12	0	
	4	25.00	9.25	0.75	0.09	0.02	0	
	5	38.50	9.00	0.63	0.14	0.09	0	

1990 OUTAGE  
GIRTH WELD INDICATIONS

SG 21 (FINAL)

ZONE NO.	IND. NO.	END OF IND. FROM		IND. LENGTH	DEPTH		IND. LOCATION	REMARKS
		ZONE LINE	HOR. REF.		FINAL NORMAL	GROWTH		
		in.	in.	in.	in.	in.		
10	1	18.25	9.00	0.25	0.12	0.02	0	
	2	23.75	9.00	0.25	0.57	0.48	S-89	BOAT (Indication Depth 0.36)
	3	38.00	9.38	0.50	0.22	0.11	S-89	
12	1	19.25	10.50	0.38	0.34	0.03	0	
	2	32.25	9.00	0.50	0.22	0.14	S-89	
	3	37.00	9.25	0.88	0.68	0.17	S-89	
	4	40.00	9.00	2.00	0.74	0.02	C-89	

TRANSITION - 9 1/4 IN. BELOW REF. LINE

C - CRACK

S - SLOPE

O - ORIGINAL

6/21/90

ZONE 11 REPORTED NO INDICATIONS BY MT INSP.  
AVERAGE GROWTH 0.11 IN.

1990 OUTAGE  
GIRTH WELD INDICATIONS

SG 22 (FINAL)

ZONE NO.	IND. NO.	END OF IND. FROM		IND. LENGTH	DEPTH		IND. LOCATION	REMARKS
		ZONE LINE in.	HORIZ. REF. in.		FINAL in.	GROWTH in.		
2	1	11.00	10.00	0.50	0.55	0.07	O	
	2	20.00	9.50	0.50	0.65	0.05	O	
	3	28.50	8.00	4.25	0.17	0.03	O	
	4	28.50	10.00	4.25	0.64	0.40	O	
	5	35.50	9.50	0.50	0.66	0.06	C-87	
5	1	13.00	9.00	1.25	0.06	0.00	C-87	
	2	24.00	8.00	7.00	0.44	0.29	S-89	
	3	34.50	9.00	0.50	1.06	0.28	S-89	
6	1	5.00	8.00	2.50	0.89	0.02	S-87	
	2	9.75	8.75	0.50	0.48	0.25	S-87	
	3	35.00	7.50	2.25	1.22	0.51	S-87	
7	1	9.50	5.75	1.00	0.18	0.00	S-87	
8	1	16.50	9.75	0.25	0.67	0.00	C-87	
9	1	31.00	5.50	1.25	-0.24	0.00	O	
	2	41.50	7.50	1.25	-0.36	0.00	O	
10	1	7.25	8.25	0.13	-0.30	0.00	S-87	
	2	10.00	7.75	0.13	-0.55	0.00	S-87	
	3	25.75	6.75	0.25	-0.24	0.00	S-87	
	4	28.50	7.00	0.25	-0.24	0.00	S-87	
	5	30.25	6.75	0.25	0.00	0.00	S-87	
	6	32.75	6.75	0.50	-0.24	0.00	S-87	
11	1	36.00	8.75	0.50	0.23	0.05	O	
	2	29.00-32.00	6.50	1.00	0.70	0.10	S-87	GROUPED 4 INDICATION

TRANSITION 7 IN. BELOW REF. LINE

C - CRACK

S - SLOPE

O - ORIGINAL

6/21/90

ZONES 1,3,4,11,12 REPORTED NO INDICATIONS BY MT INSP.  
AVERAGE GROWTH 0.09 IN.



1990 OUTAGE  
GIRTH WELD INDICATIONS

SG 23 (FINAL)

ZONE NO.	IND. NO.	END OF IND. FROM		IND. LENGTH	DEPTH		IND. LOCATION	REMARKS
		ZONE LINE	HORIZ. REF.		FINAL	GROWTH		
		in.	in.	in.	in.	in.		
3	1	13.00	9.00	0.25	-0.39	0.05	C	
	2	29.00	6.90	0.50	0.69	0.07	S-87	
5	1	10.00	8.50	3.50	0.21	0.17	O	
7	1	14.00	8.50	0.75	0.12	0.15	O	
	2	17.75	7.62	1.00	0.16	0.15	O	
	3	21.75	8.63	0.50	-0.26	0.06	O	
	4	27.25	8.00	1.00	-0.14	0.00	O	
	5	33.75	9.50	0.63	0.10	0.03	O	
8	1	3.50	7.00	0.25	0.09	0.00	C-87	
	2	13.25	6.80	0.75	-0.03	0.03	O	
	3	17.25	7.50	0.63	-0.03	0.03	O	
10	1	6.00	6.75	0.63	0.07	0.11	S-87	
11	1	8.00	6.50	0.25	0.20	0.04	C-87	
12	1	17.00	8.00	0.31	-0.18	0.27	O	

TRANSITION 8 IN. BELOW REF. LINE

C - CRACK

S - SLOPE

O - ORIGINAL

6/24/90

ZONES 1,2,4,6,9 REPORTED NO INDICATIONS BY MT INSP.  
AVERAGE GROWTH 0.08 IN.

1990 OUTAGE  
GIRTH WELD INDICATIONS

SG 24 (FINAL)

ZONE NO.	IND. NO.	END OF IND. FROM		IND. LENGTH	DEPTH		IND. LOCATION	REMARKS
		ZONE LINE	HORIZ. REF.		FINAL	GROWTH		
		in.	in.	in.	in.	in.		
1	1	11.50	10.00	0.38	-0.00	0.10	0	
	2	34.75	8.38	1.25	0.28	0.32	0	
2	1	21.00	7.38	3.88	0.24	0.16	0	
3	1	37.50	9.00	0.63	0.77	0.24	S-87	
4	1	2.50	6.88	0.25	0.11	0.12	0	
	2	2.75	8.50	0.75	0.39	0.05	0	
	3	41.25	6.75	2.50	0.05	0.10	0	
5	1	34.00	6.25	0.36	0.16	0.20	0	
6	1	11.00	5.50	0.50	0.25	0.33	0	
8	1	40.00	5.75	0.25	0.12	0.01	0	

TRANSITION 7 IN. BELOW REF. LINE

C - CRACK

S - SLOPE

O - ORIGINAL

6/21/90

ZONES 7,9,10,11,12 REPORTED NO INDICATIONS BY MT INSP.  
AVERAGE GROWTH 0.17 IN.

1990 OUTAGE  
ABOVE & BELOW GIRTH WELD  
90 24

ZONE NO.	IND NO.	END OF IND. FROM		IND LENGTH	GROWTH	REMARKS
		ZONE LINE	H.R. REF.			
		in.	in	in.	in.	
4	A	5.75	12.00	1.13	0.51	
	B	8.00	14.75	1.88	0.50	
5	A	7.25	14.00	3.38	0.52	
6	A	6.25	15.63	3.50	0.30	
9	A	18.00	2-3	5.00	0.57	ABOVE GIRTH WELD
	B	35.00	3.00	1.75	0.73	ABOVE GIRTH WELD
10	A	18.75	2.50	1.25	0.14	ABOVE GIRTH WELD
	B	23.25	2.00	0.50	0.06	ABOVE GIRTH WELD
11	A	40.00	16.25	0.38	0.71	
	B	40.00	16.50	1.25	0.71	
	C	37.25	15.88	1.25	0.71	

TRANSITION 9 1/4 in. BELOW REF LINE

6/25/90

ZONES 1,2,3,6,7,&12 REPORTED NO INDICATIONS BY MT INSP.

AVERAGE GROWTH 0.50 in.



1990 OUTAGE  
BELOW GIRTH WELD  
SG 22

ZONE NO.	IND NO.	END OF IND. FROM		IND LENGTH	GROWTH	REMARKS
		ZONE LINE	HOR. REF			
		in.	in.	in.	in.	
1	A	0.00	16.00	4.00	0.39	
	B	10.00	13.00	4.50	0.51	
	C	21.00	14.00	2.75	0.45	
	D	25.00	13.50	3.00	0.45	
	E	26.00	14.00	2.00	0.45	
	F	28.00	14.00	2.50	0.45	
	G	30.50	14.25	1.50	0.45	
	H	33.00	13.50	2.50	0.54	
	I	38.00	13.00	1.25	0.82	
2	A	0.00	14.00	2.25	0.82	
	B	1.00	13.25	1.50	0.82	
	C	10.00	13.50	6.00	0.78	
	D	18.00	15.50	7.00	0.91	
	E	29.00	13.50	3.00	0.70	
	F	31.50	14.00	3.00	0.70	
3	A	1.50	12.00	2.75	0.48	
4	A	1.50	14.50	3.00	0.93	
5	A	7.00	15.00	3.00	0.20	
7	A	38.50	15.00	3.00	0.47	
	B	38.50	13.00	2.00	0.54	
	C	39.00	13.00	2.00	0.54	
8	A	7.50	15.00	6.25	0.35	
	B	20.00	14.50	2.75	0.57	
	C	22.50	15.25	2.25	0.34	
	D	35.75	12.50	2.00	0.51	
	E	36.25	14.50	2.38	0.54	BOAT
9	A	7.00	14.00	1.50	0.40	
	B	10.25	14.00	0.50	0.42	
	C	11.00	13.50	0.88	0.46	
	D	11.00	14.00	0.63	0.40	
	E	12.25	14.00	1.50	0.38	
	F	21.75	14.00	4.00	0.42	

1990 OUTAGE  
BELOW GIRTH WELD  
SG 22

ZONE NO.	IND NO.	END OF IND. FROM		IND LENGTH	GROWTH	REMARKS
		ZONE LINE	HOR. REF.			
		in.	in.	in.	in.	
10	A	1.00	14.00	2.00	0.46	
	B	2.75	14.25	1.75	0.45	
	C	5.25	13-14.25	1.50	0.43	
	D	29.25	14.00	1.00	0.33	
	E	30.25	14.25	0.25	0.53	
	F	30.50	14.00	3.00	0.50	
11	A	26.00	13.00	0.50	0.14	
	B	37.25	12.50	1.50	0.21	
	C	38.50	13.00	1.50	0.26	

TRANSITION 7 in. BELOW REF LINE

6/25/90

ZONES 6, & 12 REPORT NO INDICATIONS BY MT INSP.

AVERAGE GROWTH 0.49 IN.

1990 OUTAGE  
BELOW GIRTH WELD  
SG 23

ZONE NO.	IND NO.	END OF IND. FROM		IND LENGTH	GROWTH	REMARKS
		ZONE LINE	HOR. REF.			
1	A	19.00	16.50	4.00	0.49	
	B	19.00	17.50	4.00	0.49	
	C	22.00	12.75	2.00	0.12	
2	A	16.00	15.00	1.00	0.43	
	B	18.00	15.00	2.50	0.63	
4	A	19.00	15.00	1.50	0.55	
	B	20.50	15.50	1.50	0.55	
	C	23.00	15.50	1.00	0.55	
5	A	27.00	14.50	1.00	0.50	
7	A	34.50	15.75	2.00	0.70	CONT. IN ZONE 8
10	A	26.50	15.75	1.00	0.22	
	B	26.50	15.00	1.25	0.22	
11	A	32.00	14.75	2.00	0.39	
11	B	41.25	15.00	1.50	0.38	CONT. IN ZONE 12
12	A	10.00	15.00	1.75	0.32	

TRANSITION B in. BELOW REF LINE

06/25/90

ZONES 3, 6, 8, & 9 REPORTED NO INDICATIONS BY HT INSP.

AVERAGE GROWTH 0.39 in.



1990 OUTAGE  
BELOW GIRTH WELD  
SC 24

ZONE NO.	IND NO.	END OF IND. FROM		IND LENGTH	GROWTH	REMARKS
		ZONE LINE	HOR. REF.			
		in.	in.	in.	in.	
4	A	19.00	13.50	2.00	0.30	
5	A	10.00	14.50	3.00	1.00	
9	A	31.00	14.50	6.00	0.10	
10	A	30.00	14.50	1.25	0.35	
10	B	41.50	14.50	1.00	0.32	CONT. IN ZONE 11
12	A	4.00	14.00	2.25	0.35	
	B	6.00	14.50	0.75	0.35	

TRANSITION 7 in. BELOW REF LINE

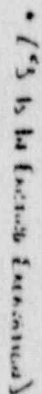
6/25/90

ZONES 1,2,3,6,7,8,11 REPORTED NO INDICATIONS BY HT IWSP.

AVERAGE GROWTH

0.40 in.

APPENDIX C  
GIRTH WELD INDICATION MAPS



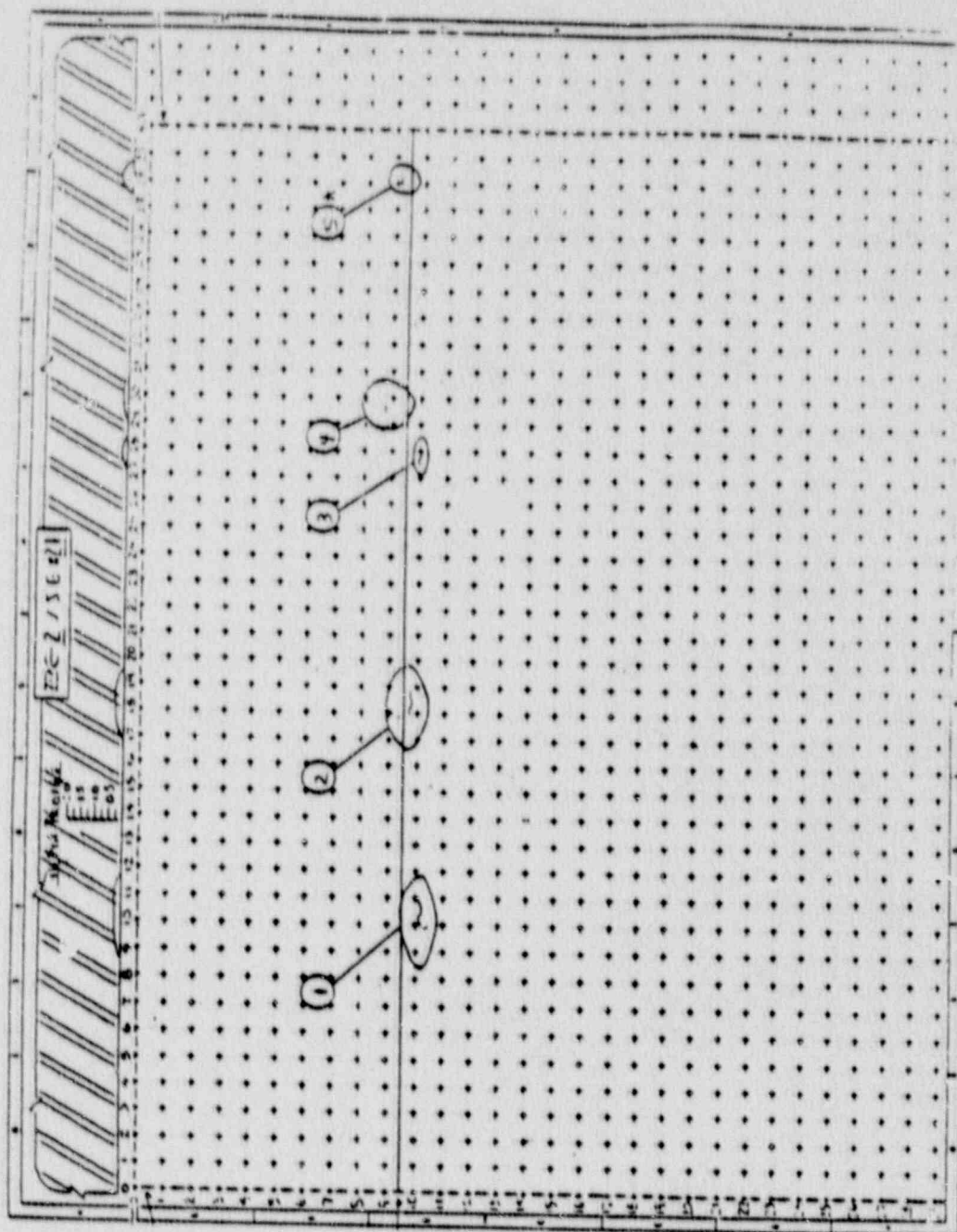
INDICATION AND EXCAVATION MAP  
ZONE 1, S.G. #21

ZONE 1, S.G. #21



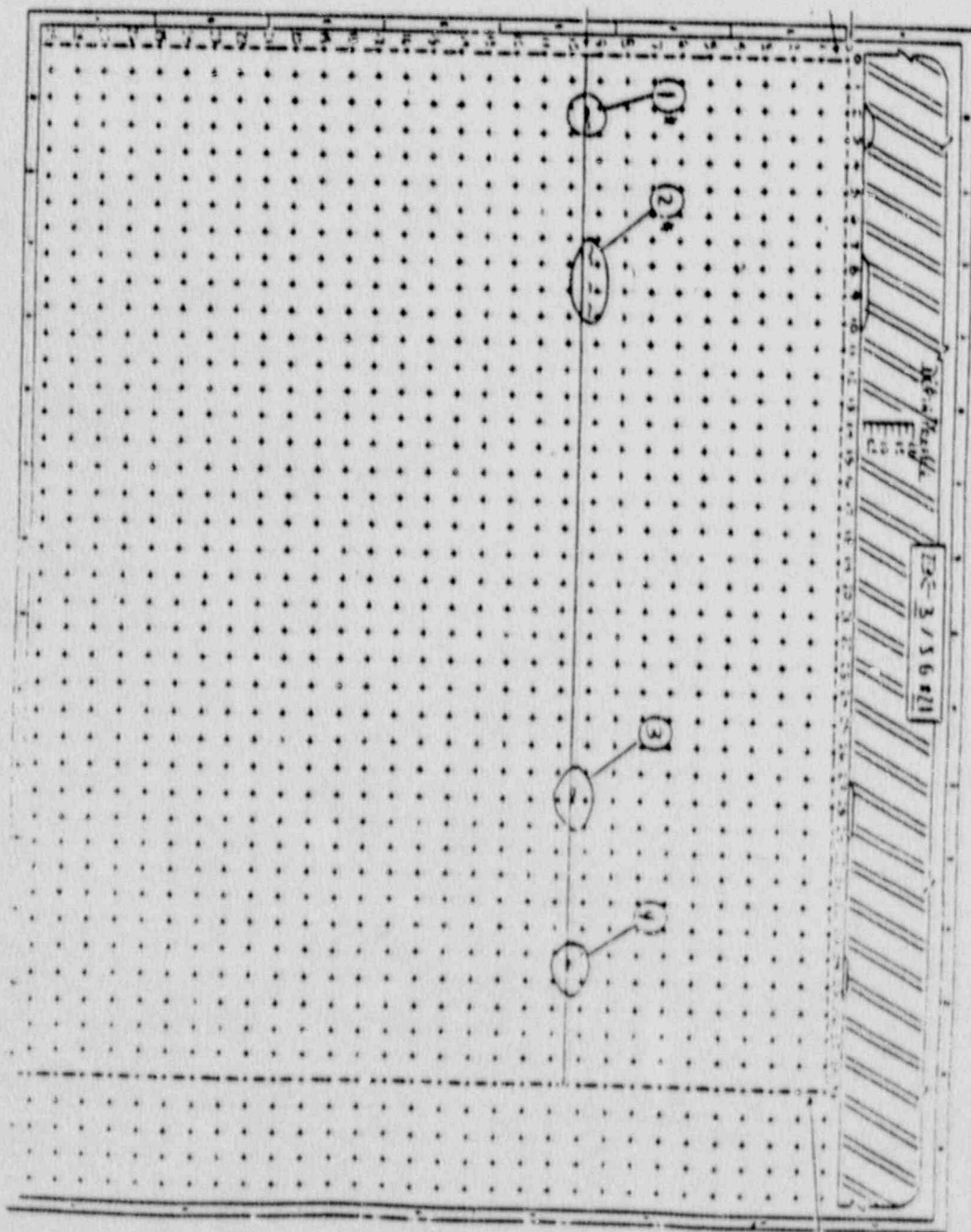
# INDICATION AND EXCAVATION MAP

Z. 2, S.G. #21

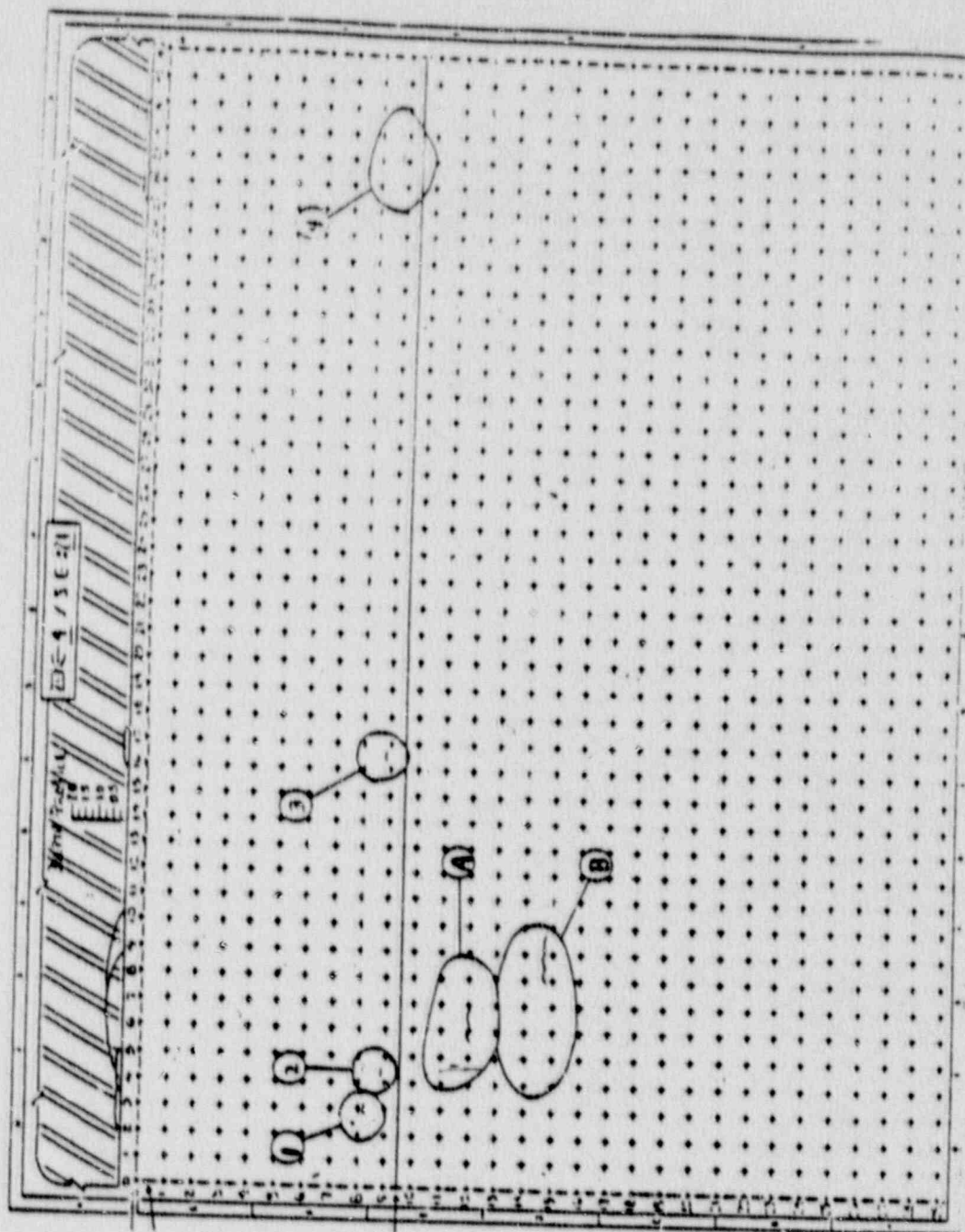


# INDICATION AND EXCAVATION MAP

ZONE 3, S.G. #21

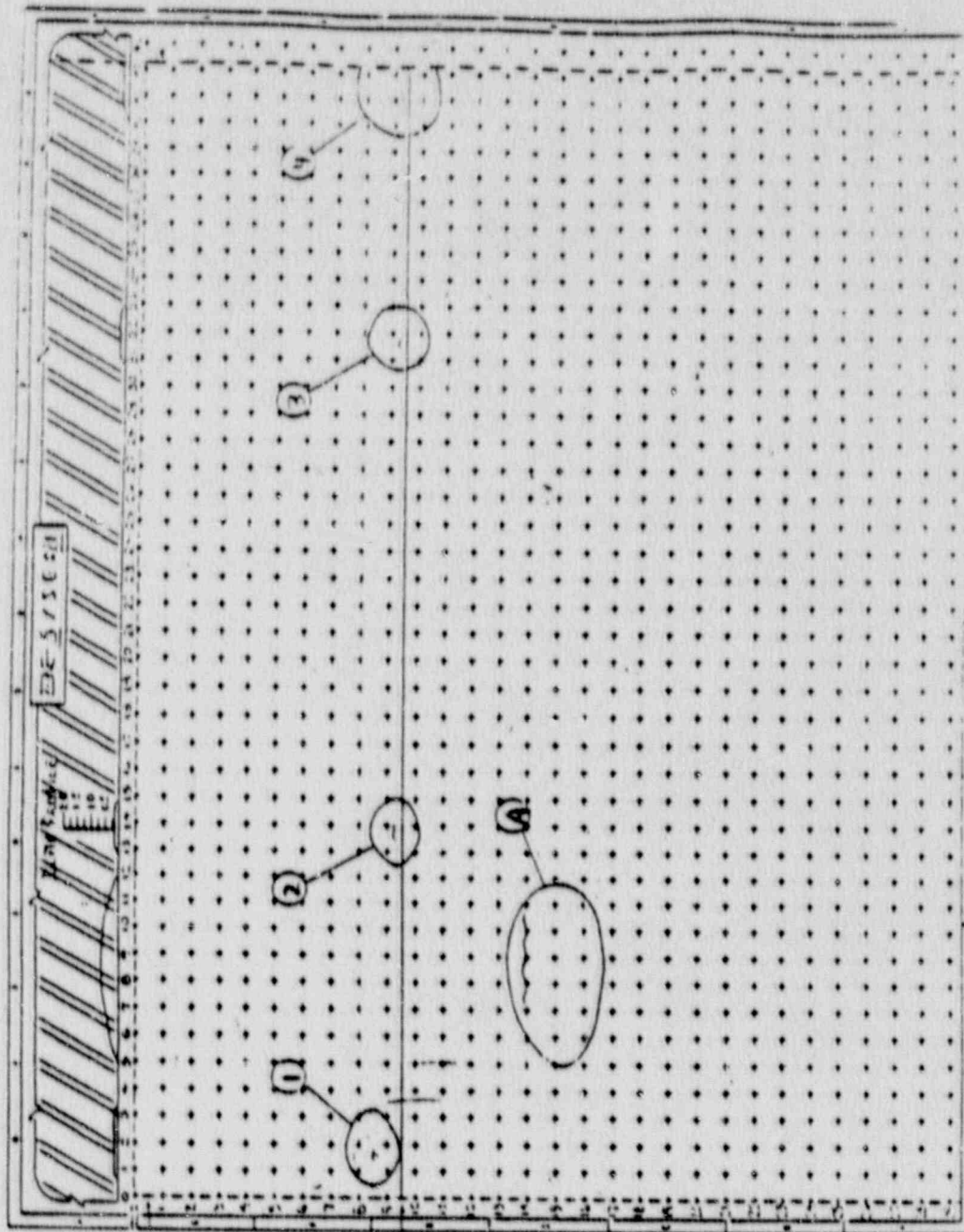


INDICATION AND EXCAVATION MAP  
 ZONE 4, S.G. #21

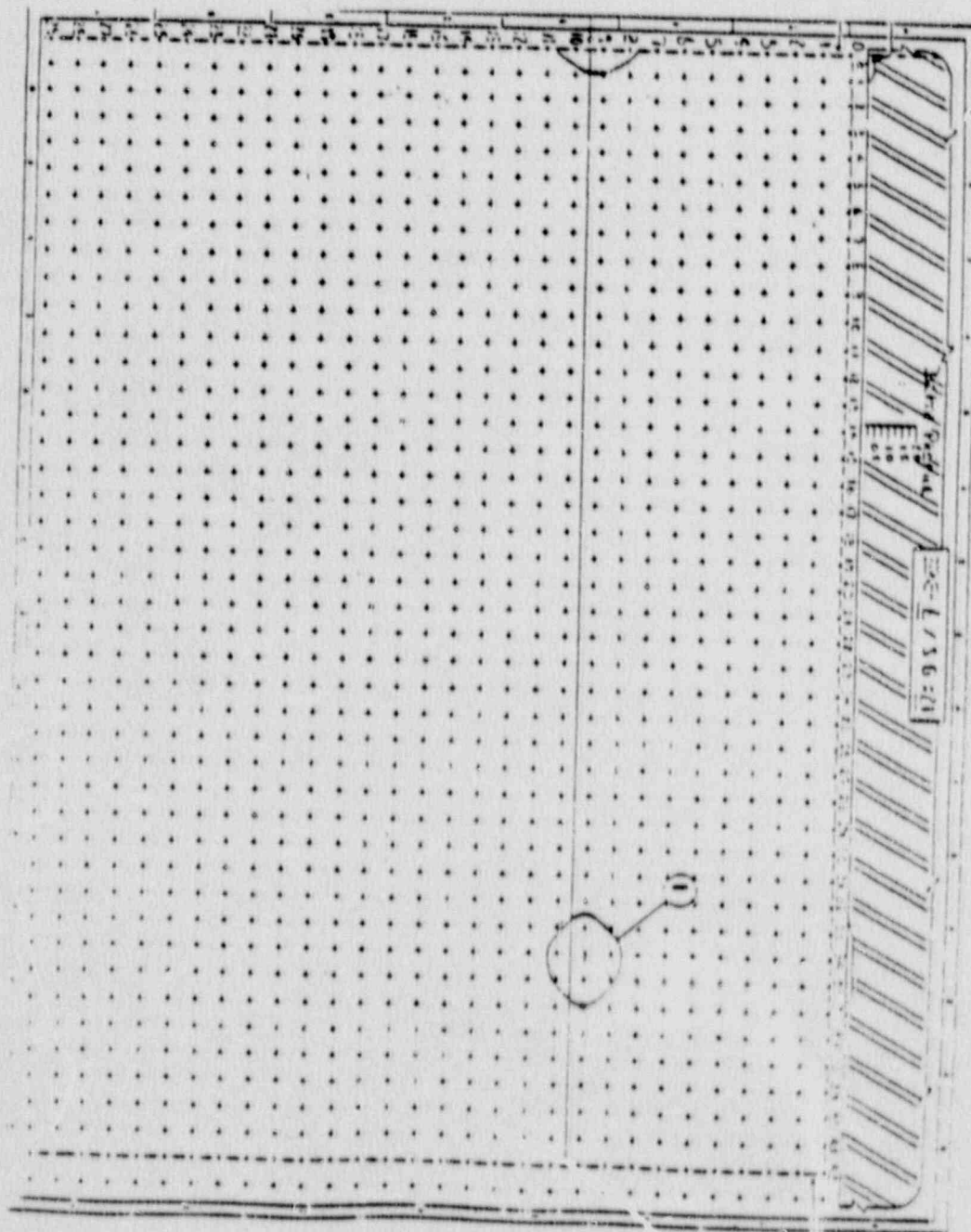


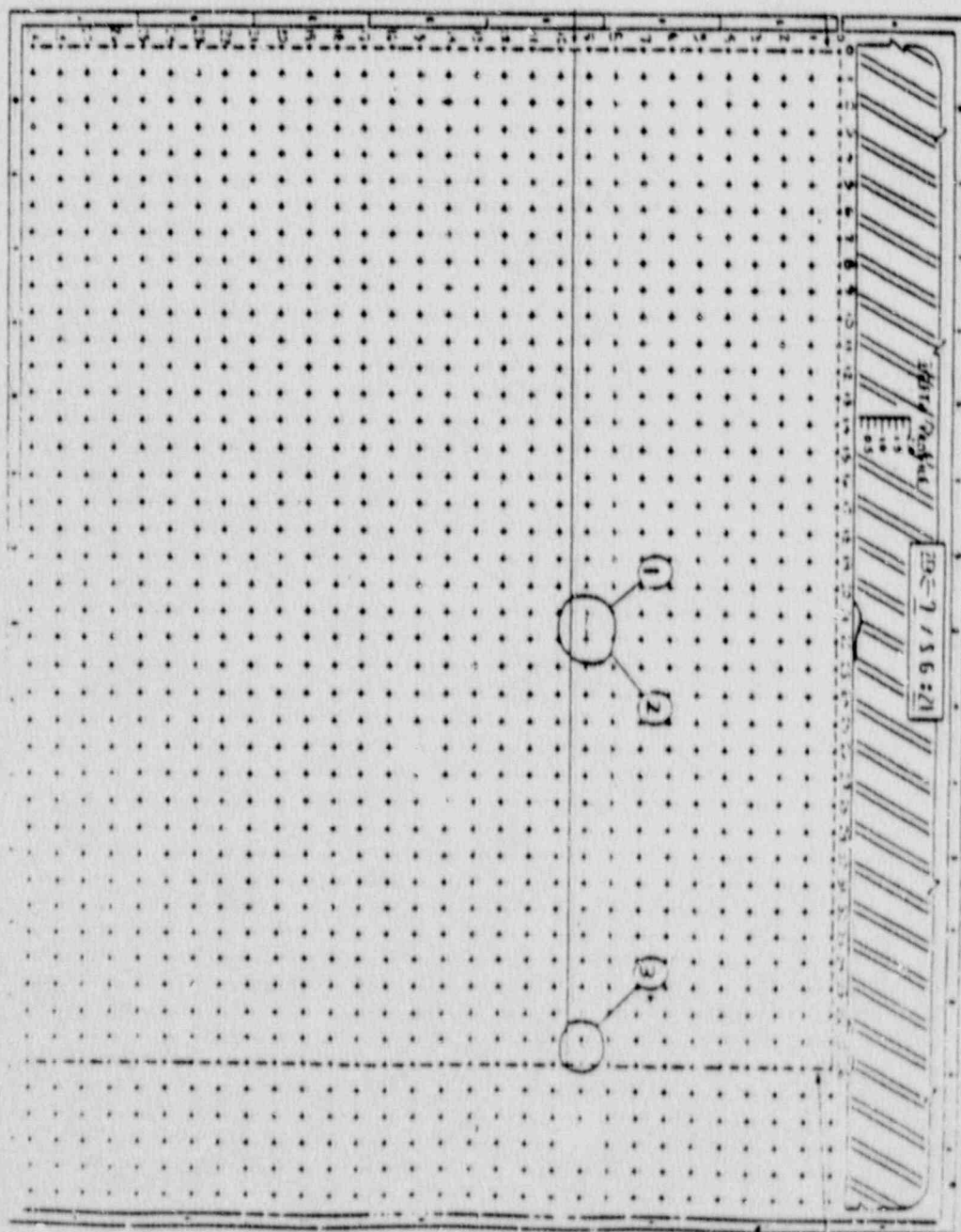


INDICATION AND EXCAVATION MAP  
 ZONE 5, S.G. #21



# INDICATION AND EXCAVATION MAP ZONE 6, S.G. #21

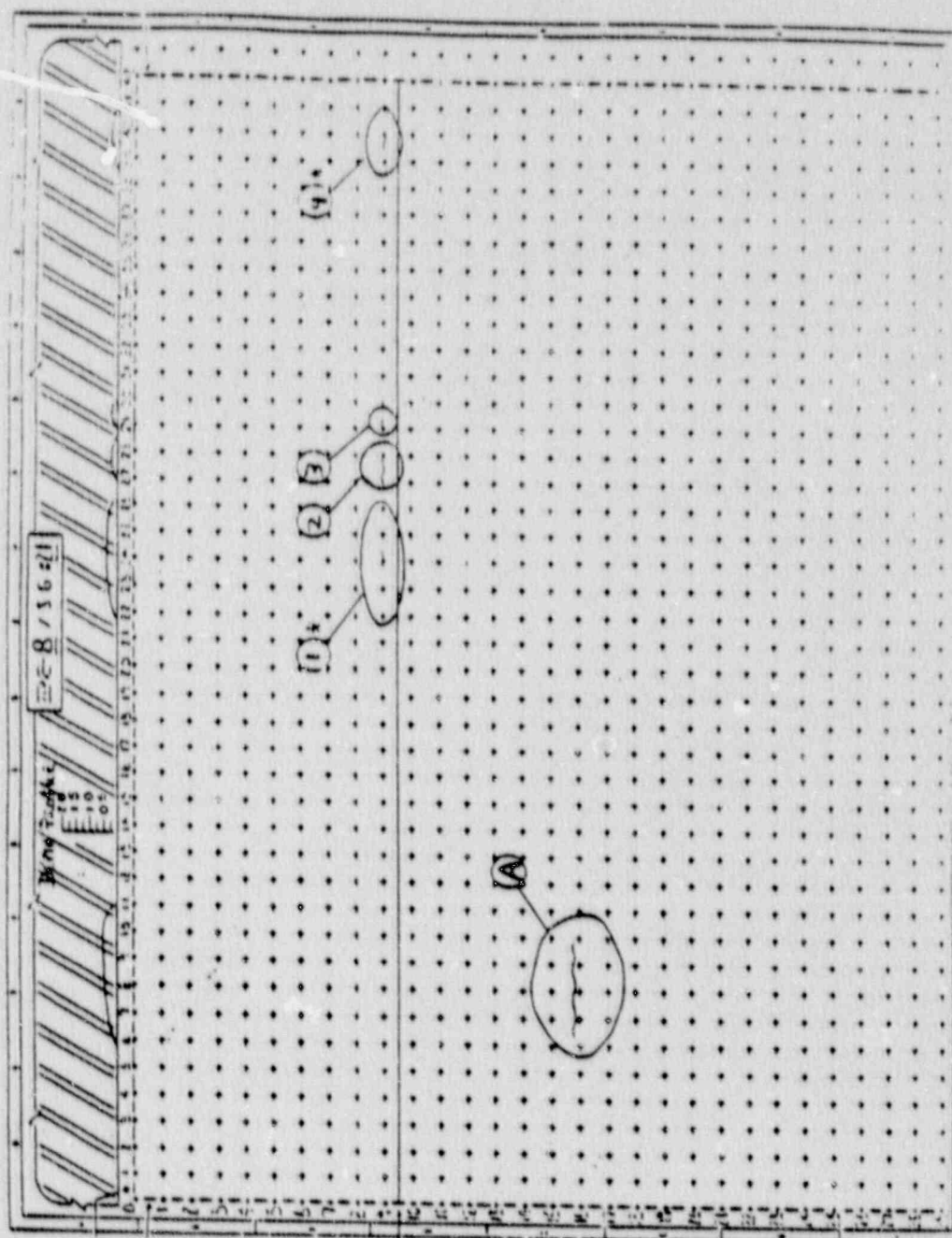




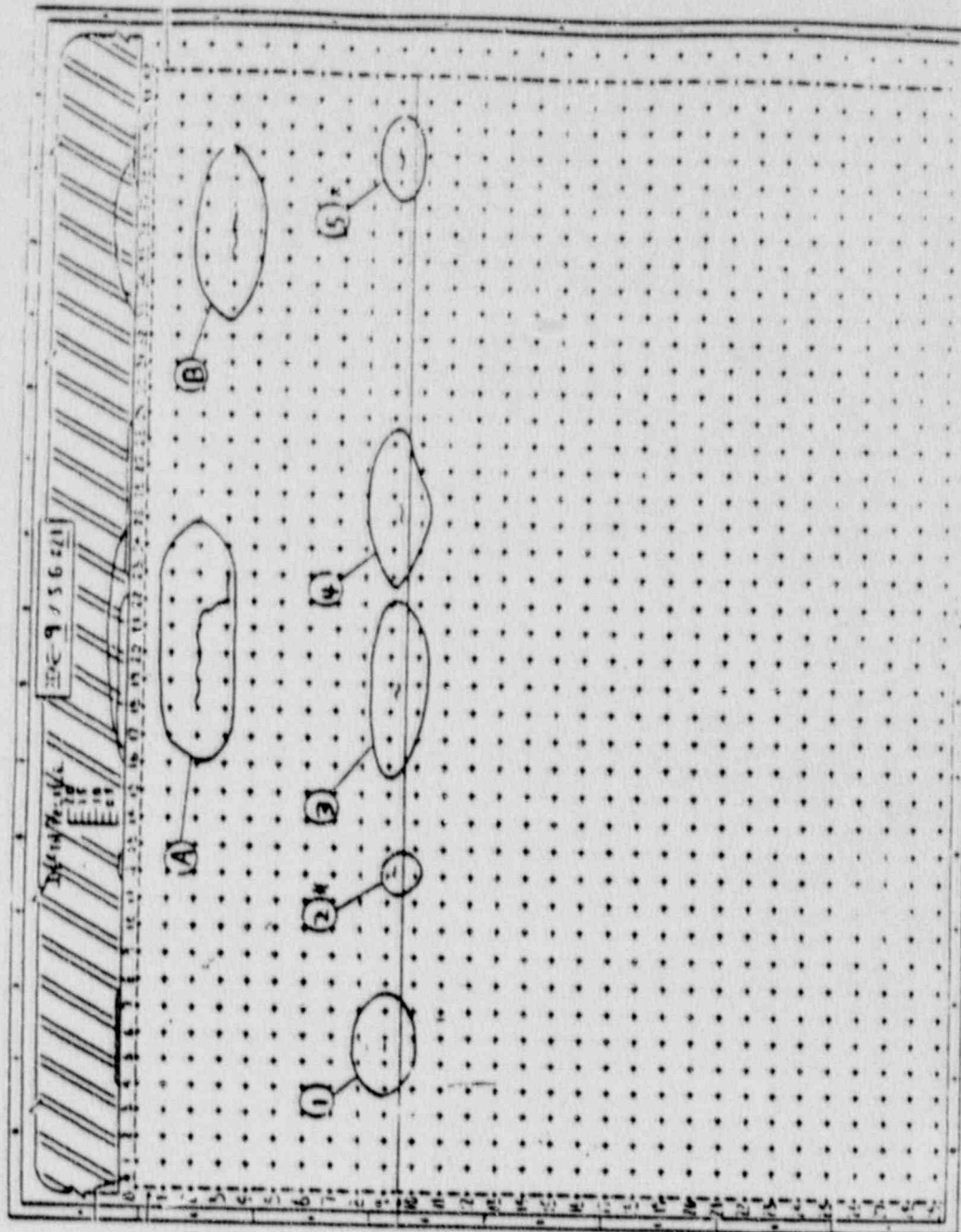
INDICATION AND EXCAVATION MAP  
ZONE 7, S.G. #21

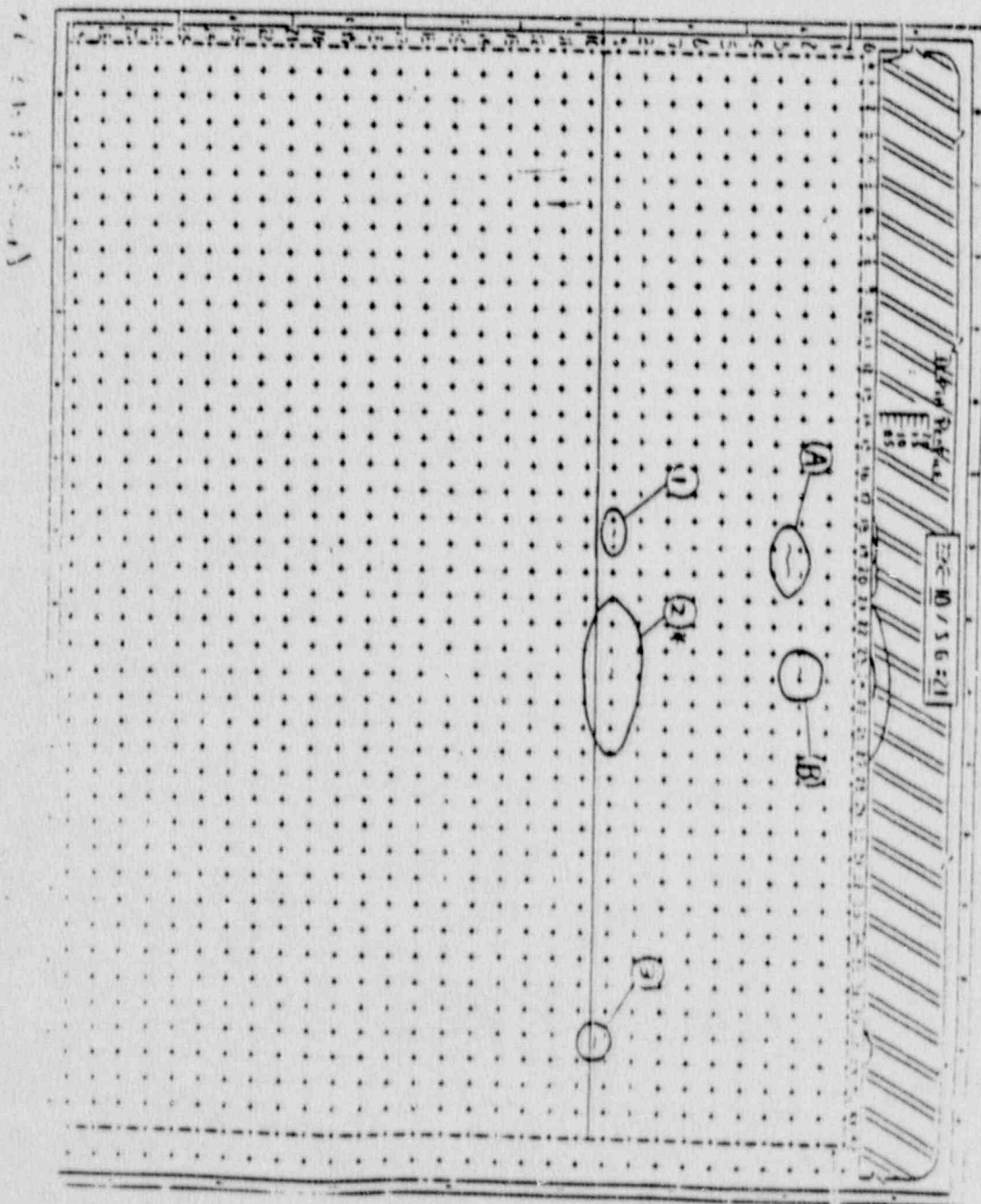


ZONE 8, S.G. #21



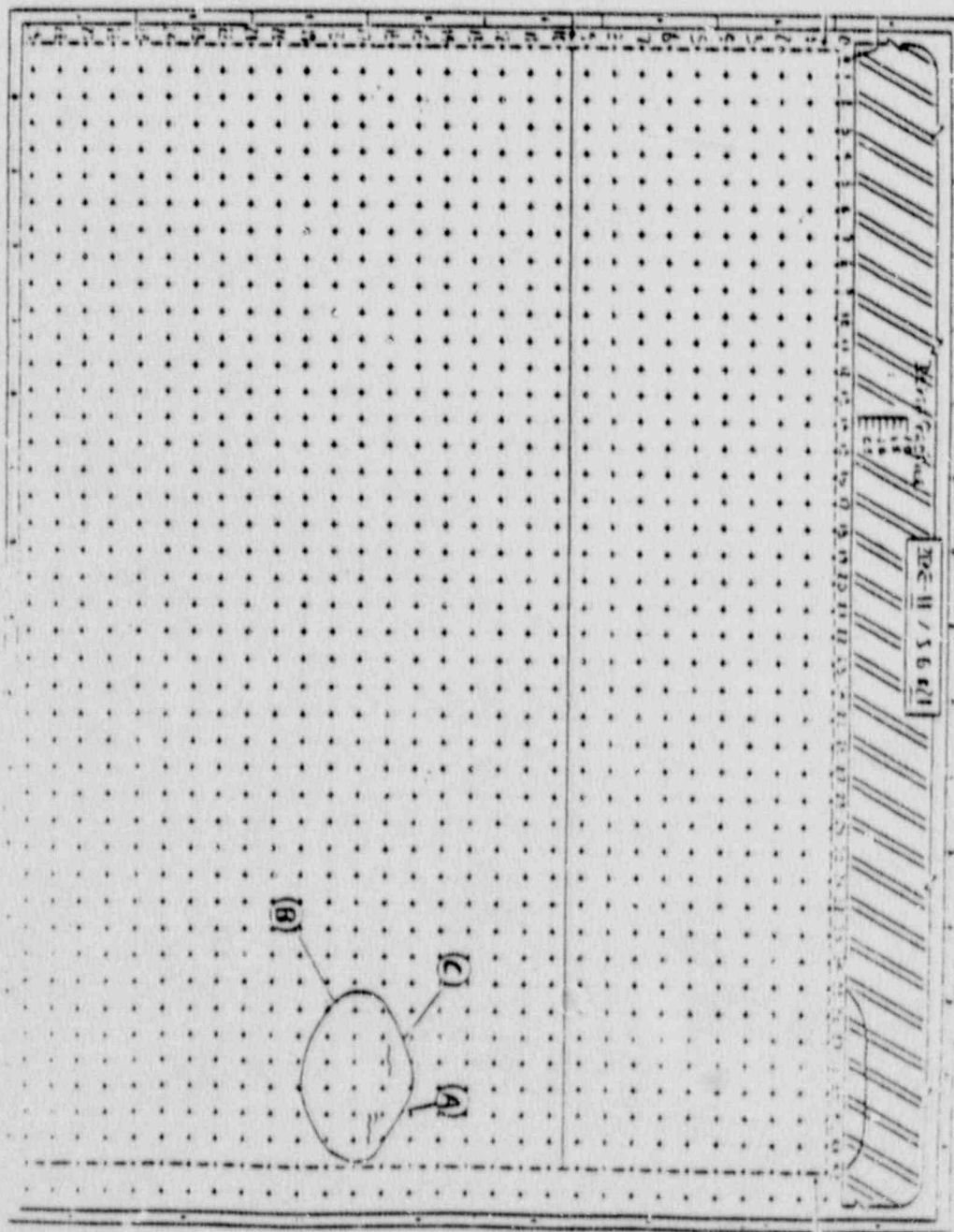
INDICATION AND EXCAVATION MAP  
 ZONE 9, S.G. #21





INDICATION AND EXCAVATION MAP  
ZONE 10, S.G. #21

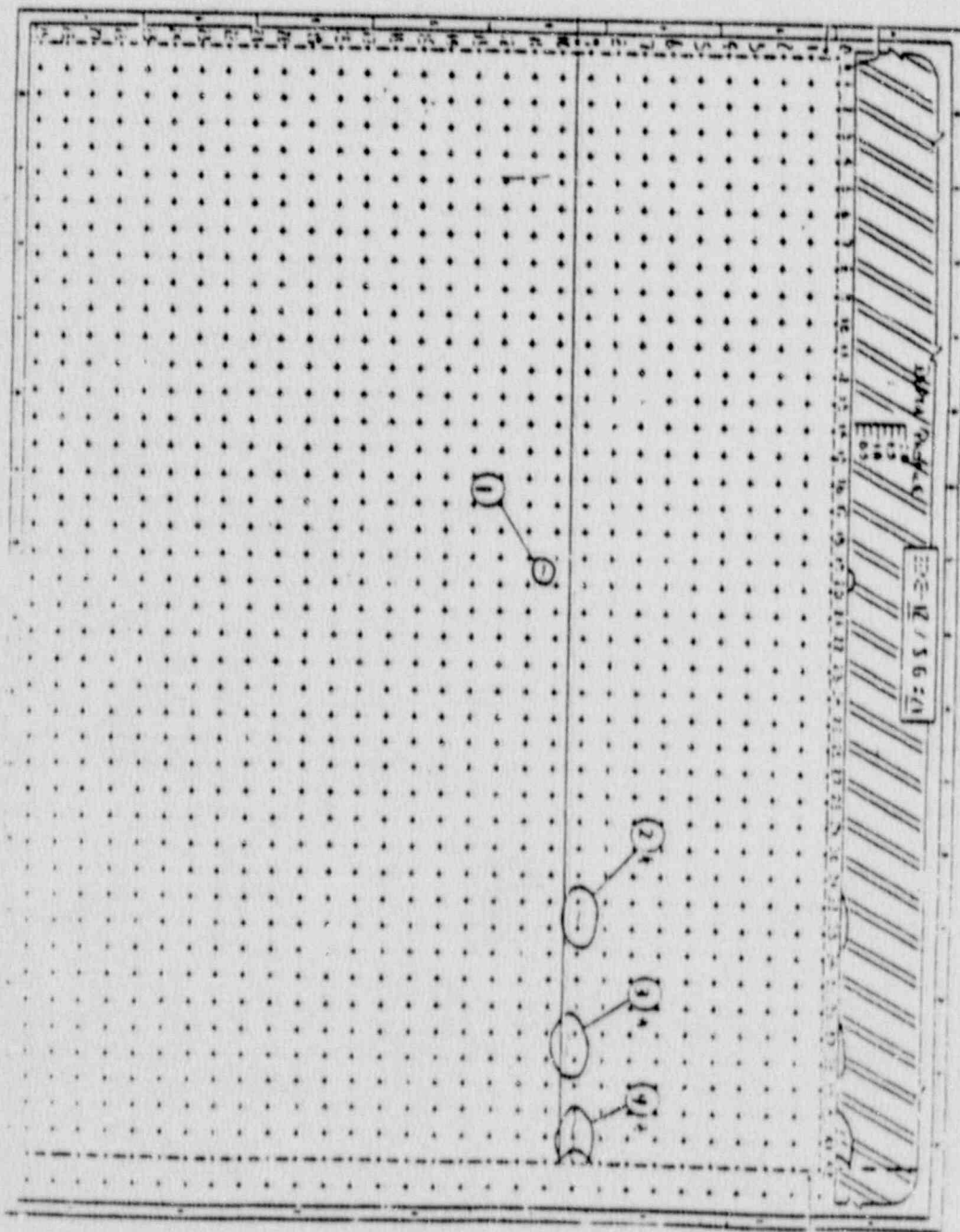




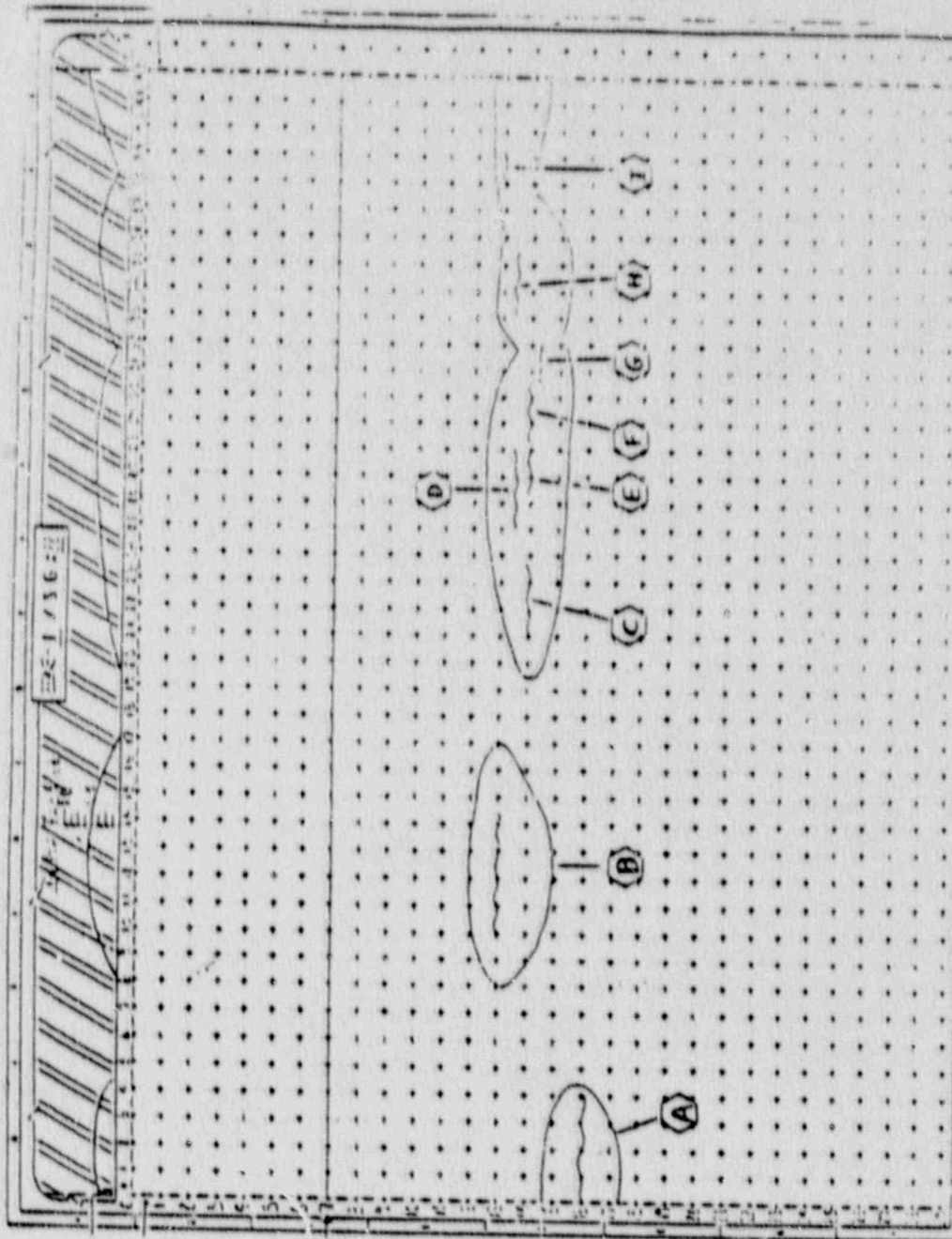
INDICATION AND EXCAVATION MAP  
ZONE II, S.G. #21

# INDICATION AND EXCAVATION MAP

ZONE 12, S.G. #21

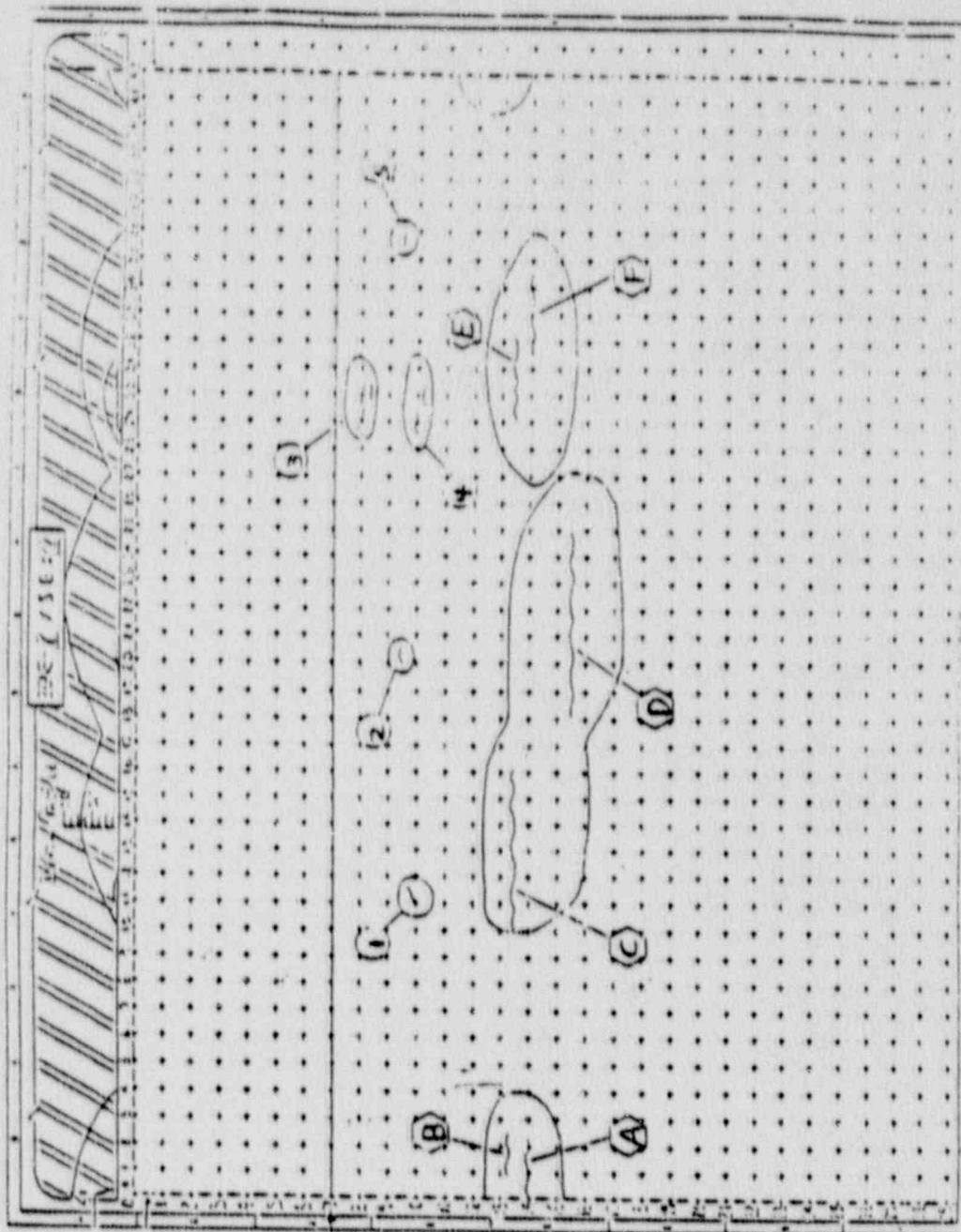


CRACKS, EXCAVATIONS AND WSI WELDS  
 ZONE 1, S.G. #22

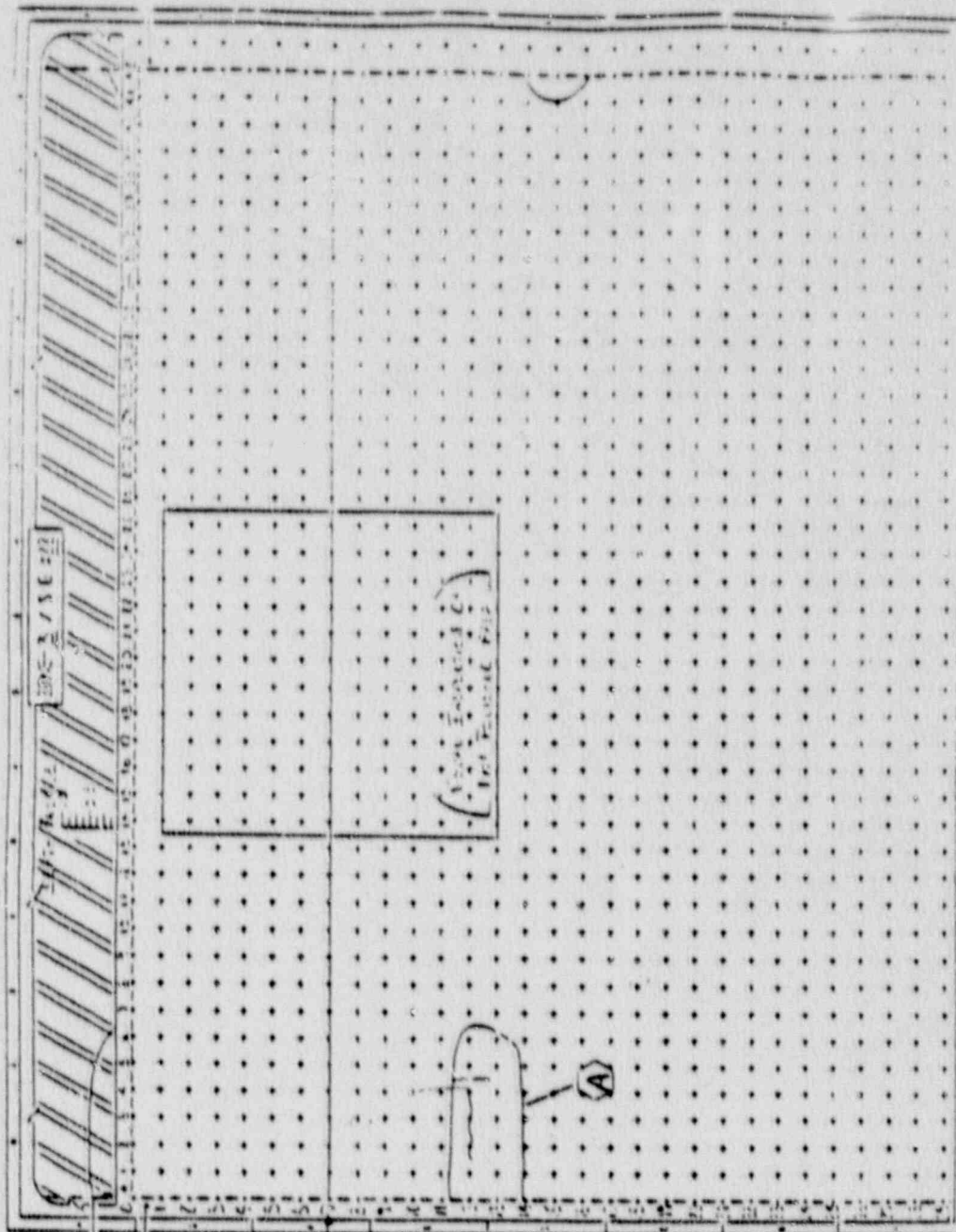




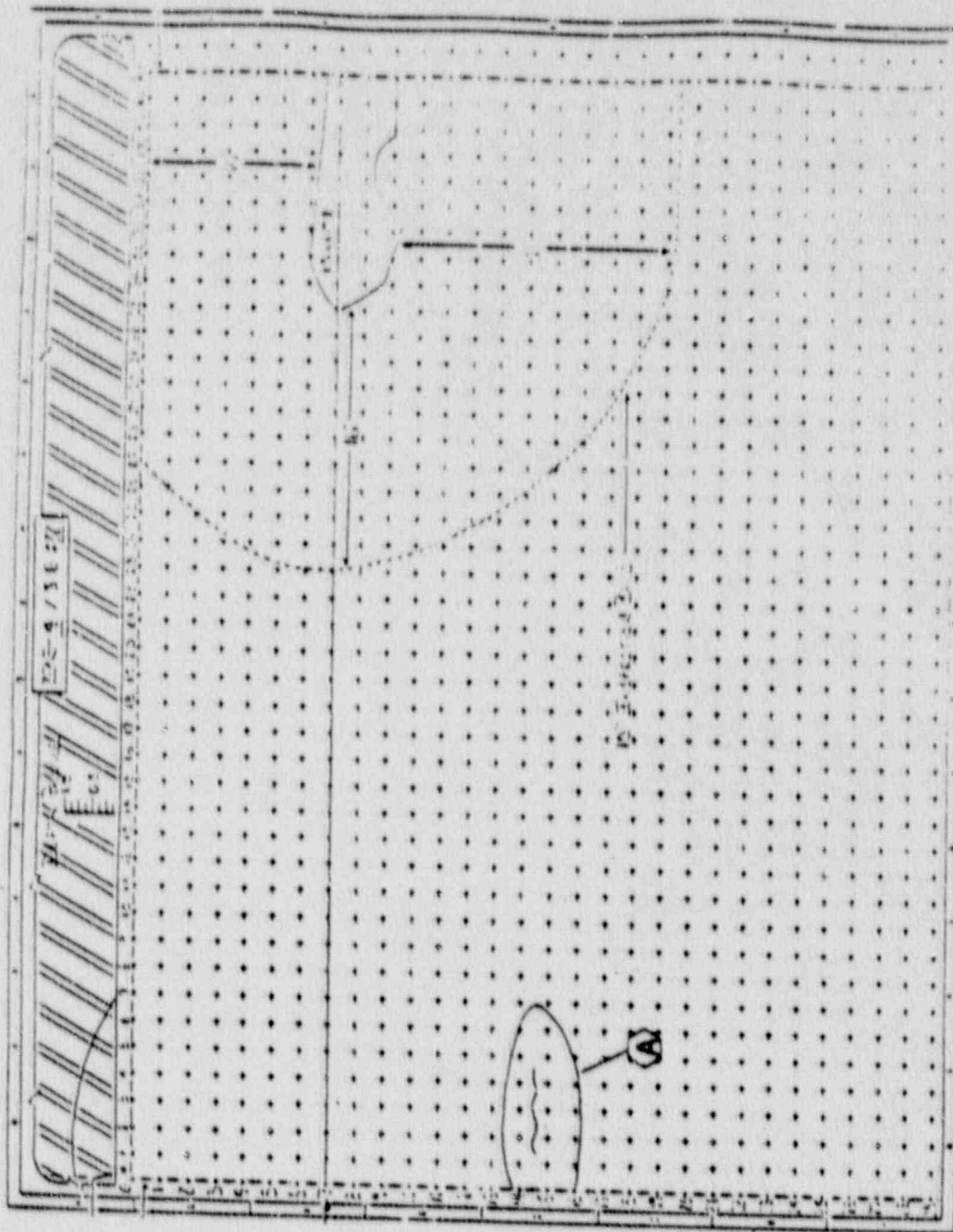
CRACKS, EXCAVATIONS AND WSI WELDS  
 ZONE 2, S.G. #22



ZONE 3, S.G. #22

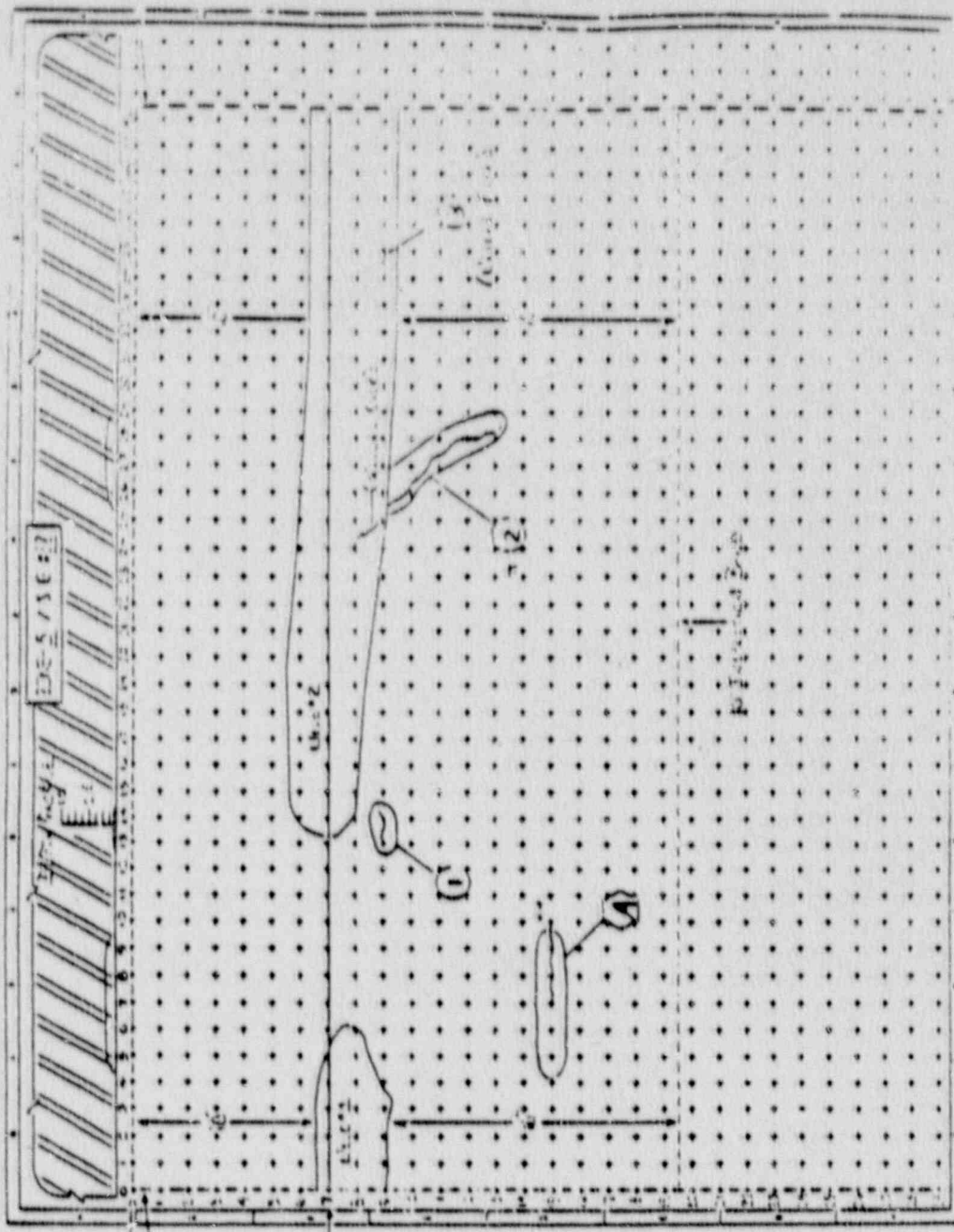


CRACKS, EXCAVATIONS AND WSI WELDS  
ZONE 4, S.G. #22

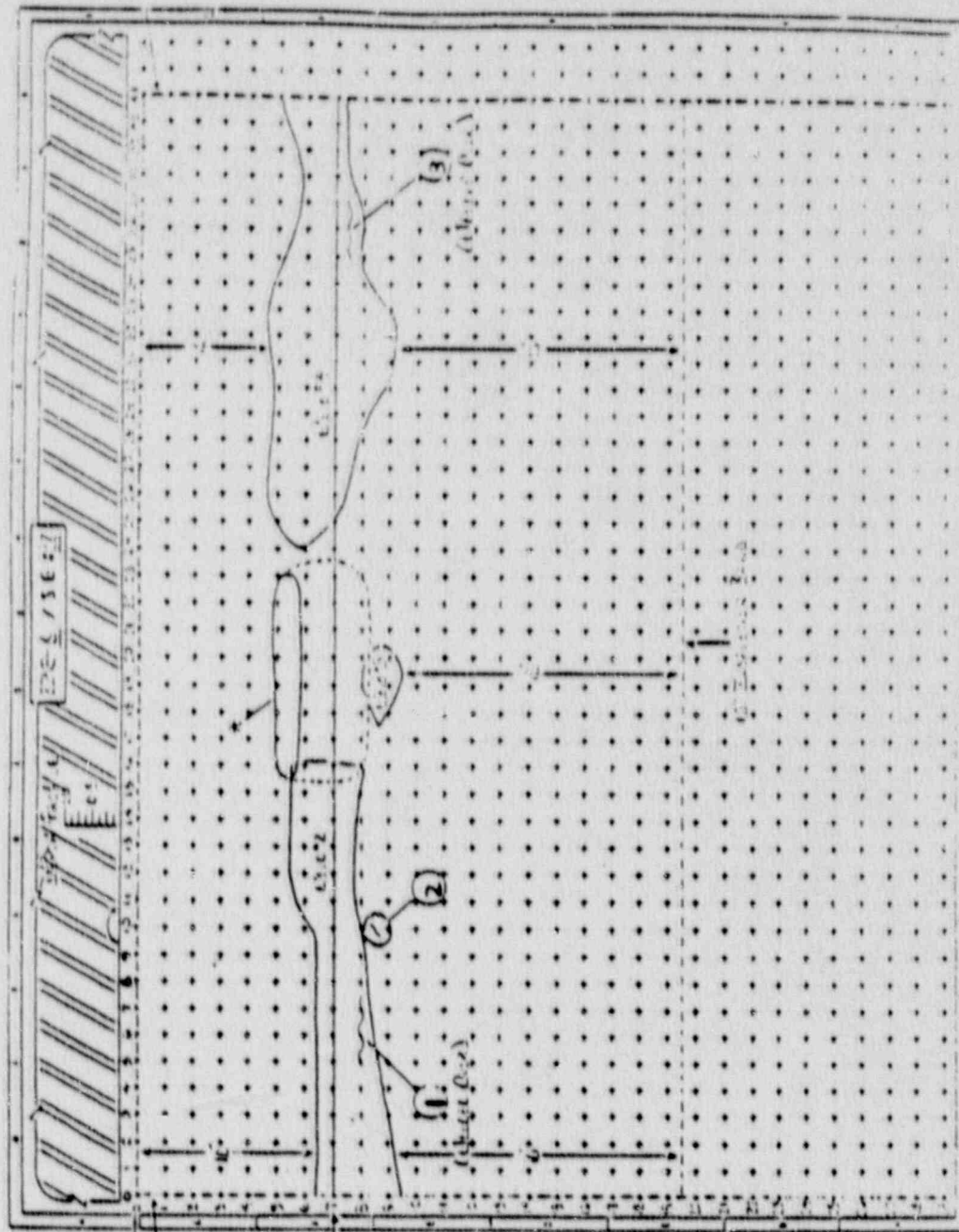




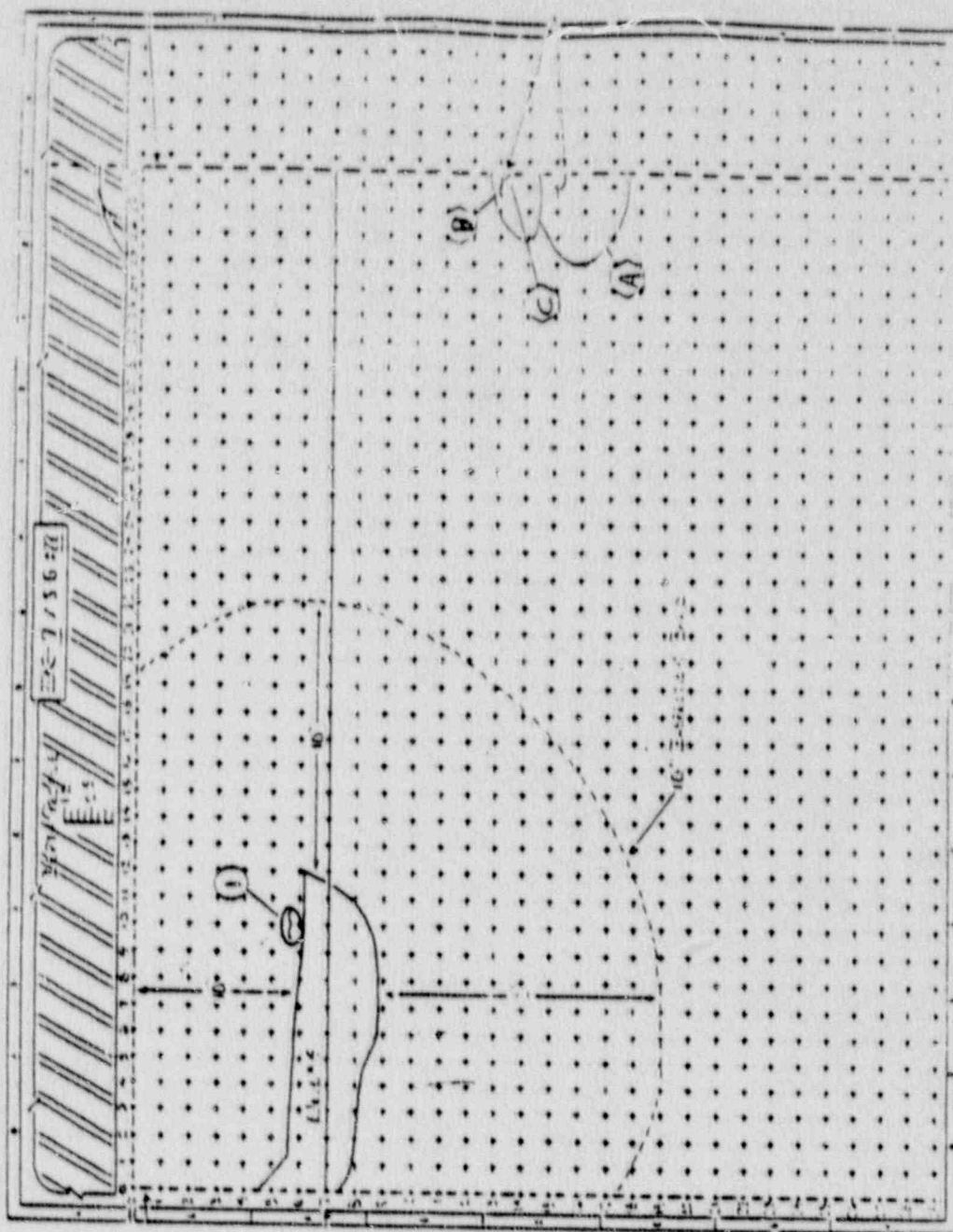
CRACKS, EXCAVATIONS AND WSI WELDS  
 ZONE 5, S.G. #22



CRACKS, EXCAVATIONS AND WSI WELDS  
 ZONE 6, S.G. #22

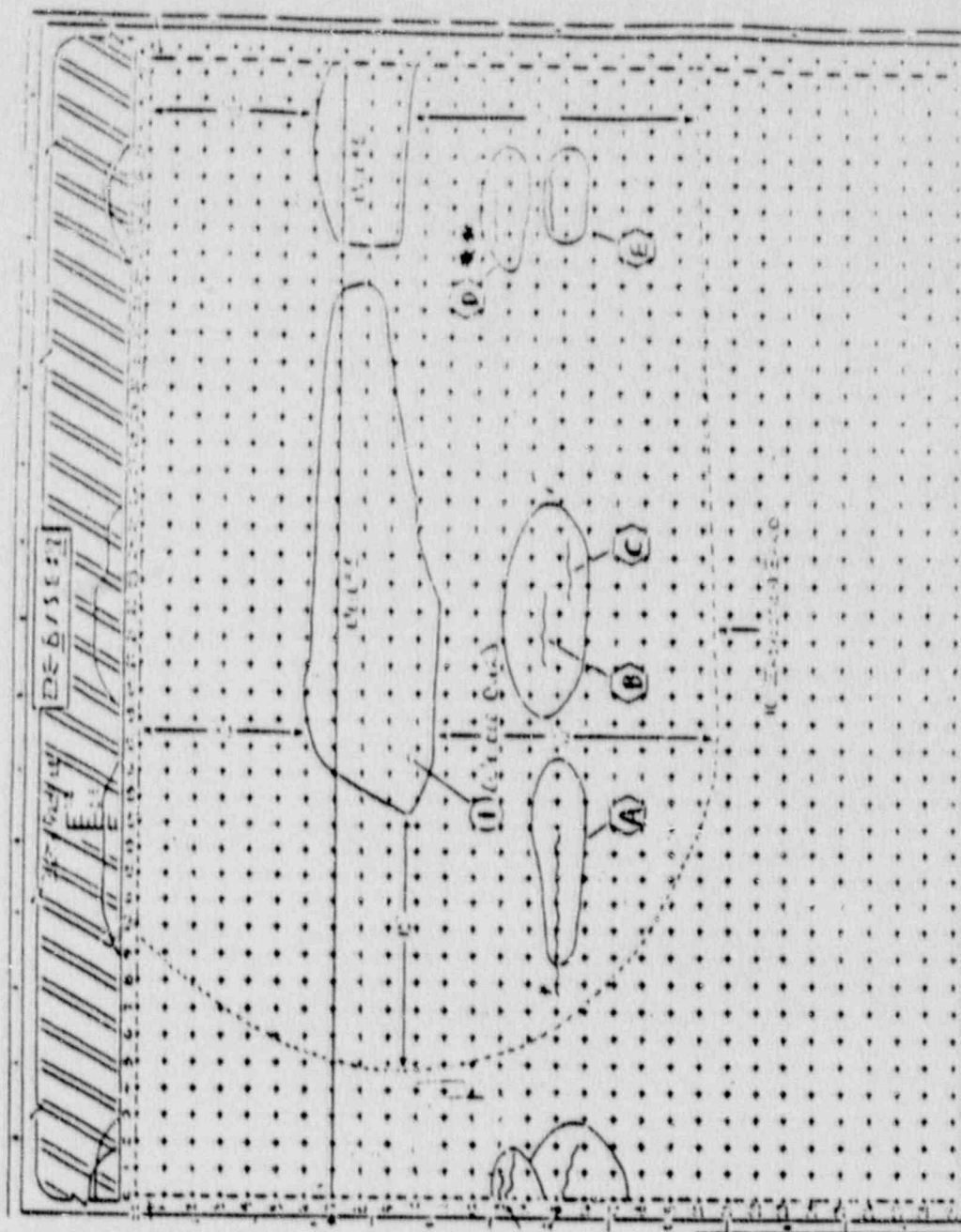


CRACKS, EXCAVATIONS AND WSI WELDS  
 ZONE 7, S.G. #22

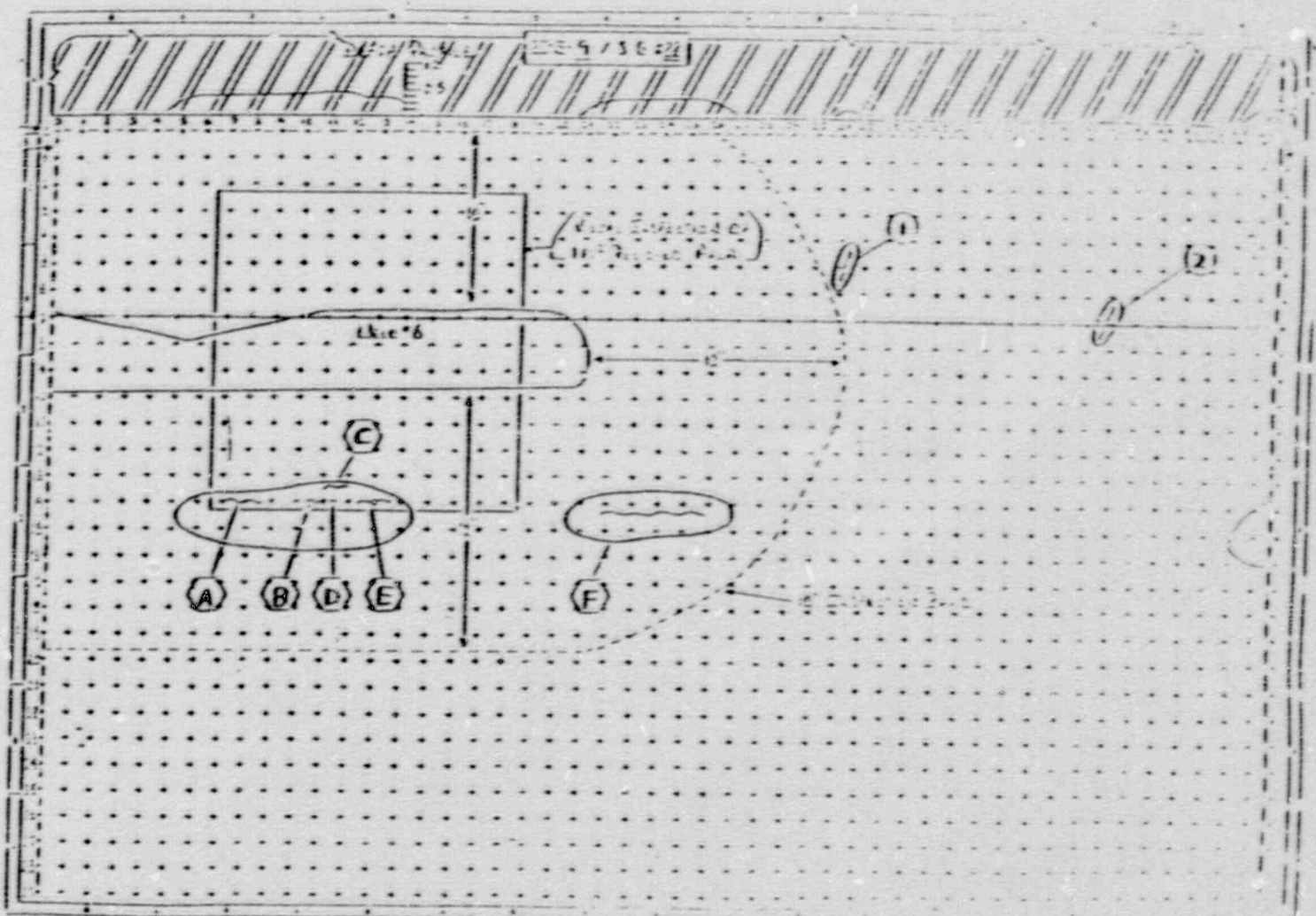




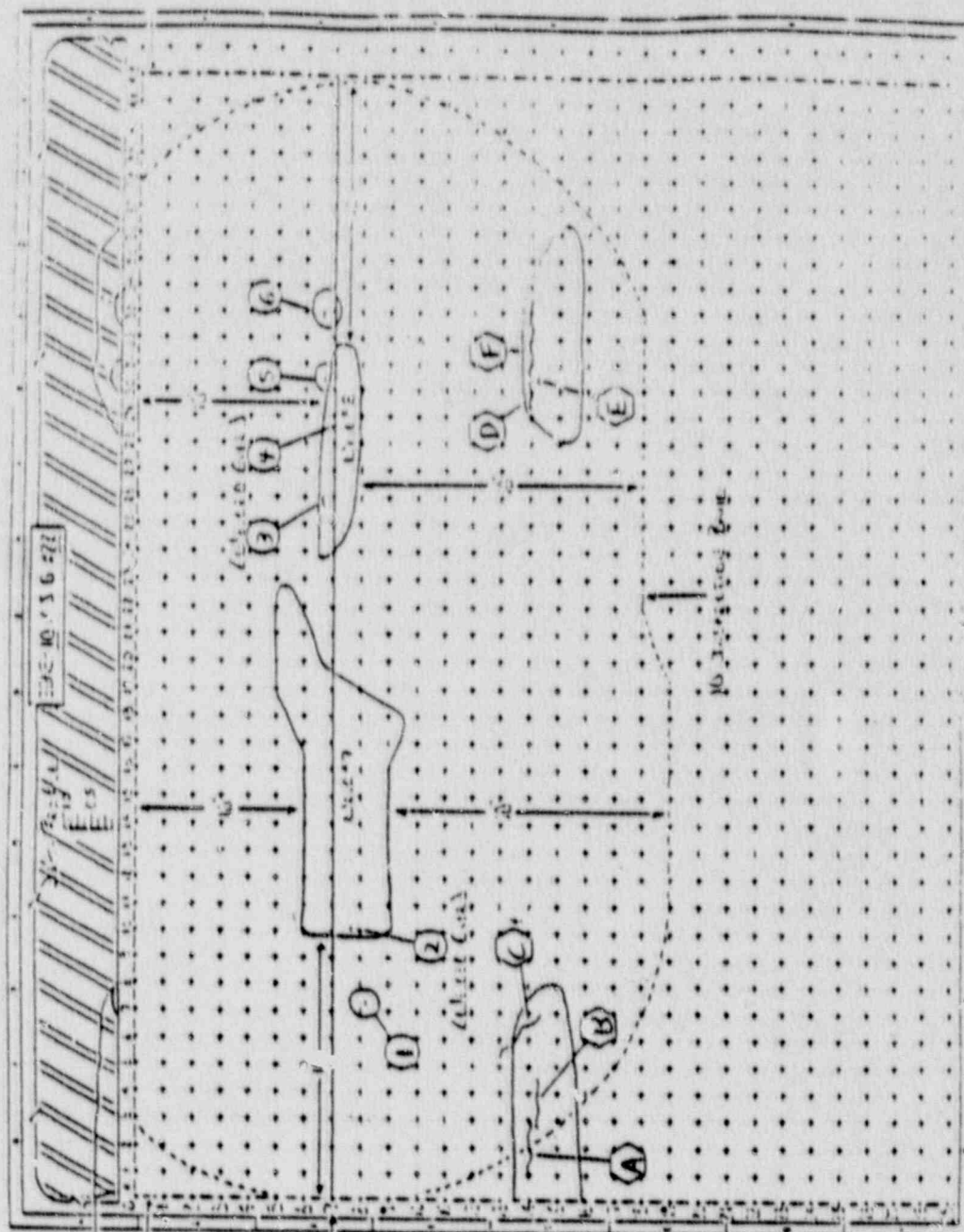
CRACKS, EXCAVATIONS AND WSI WELDS  
 ZONE B, S.G. #22



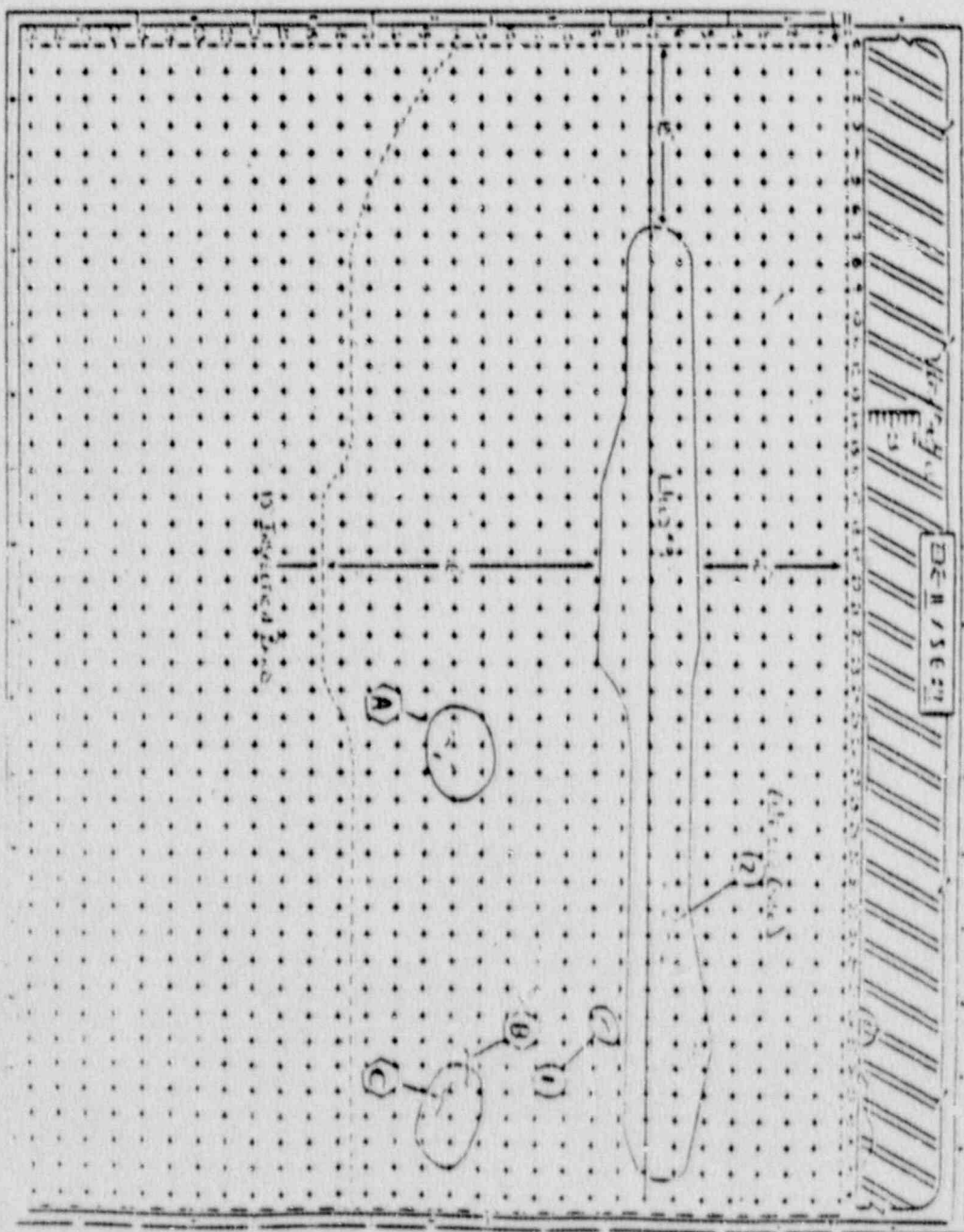
CRACKS, EXCAVATIONS AND WSI WELDS  
 ZONE 9, S.G. #22



CRACKS, EXCAVATIONS AND WSI WELDS  
 ZONE 10, S.G. #22

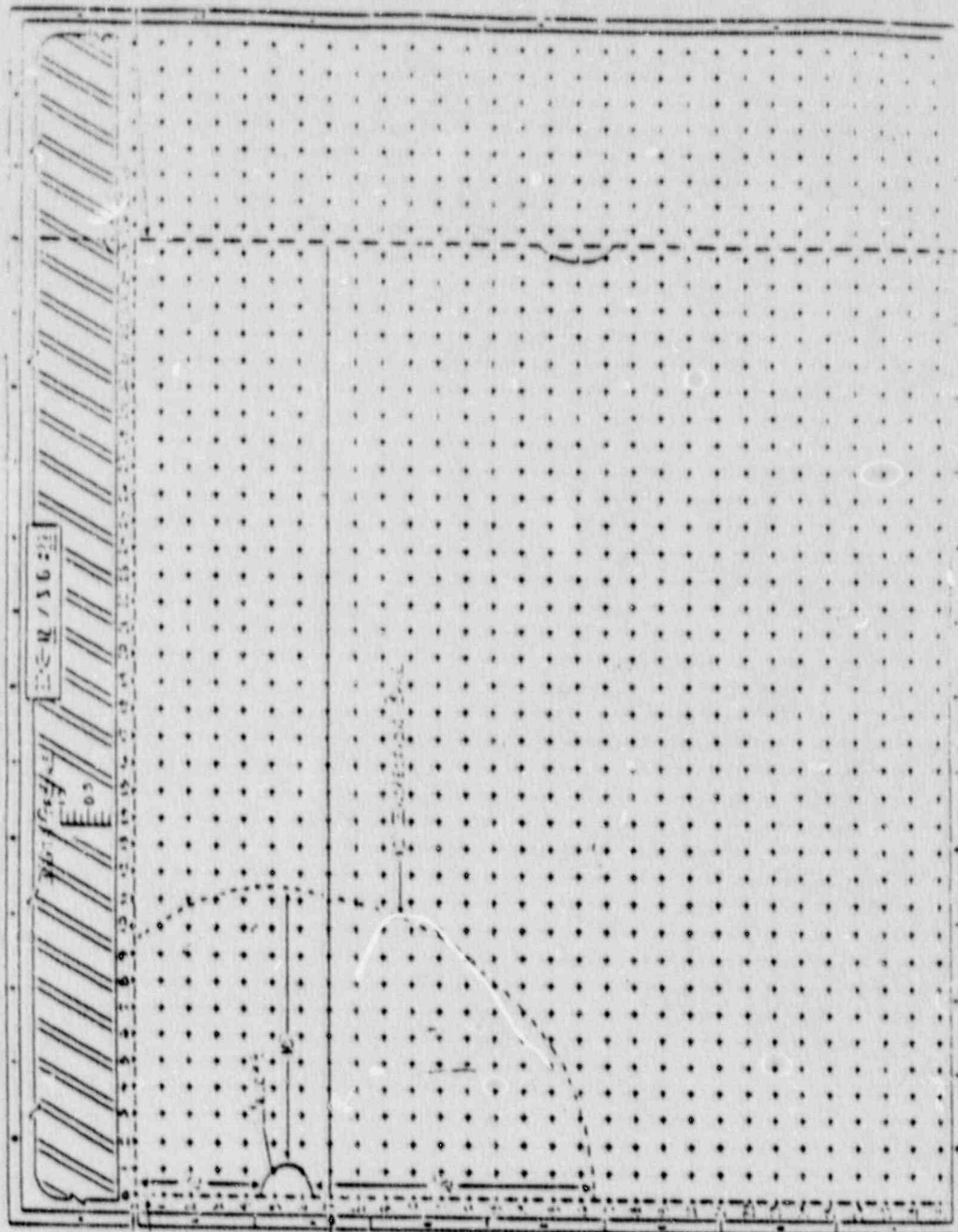




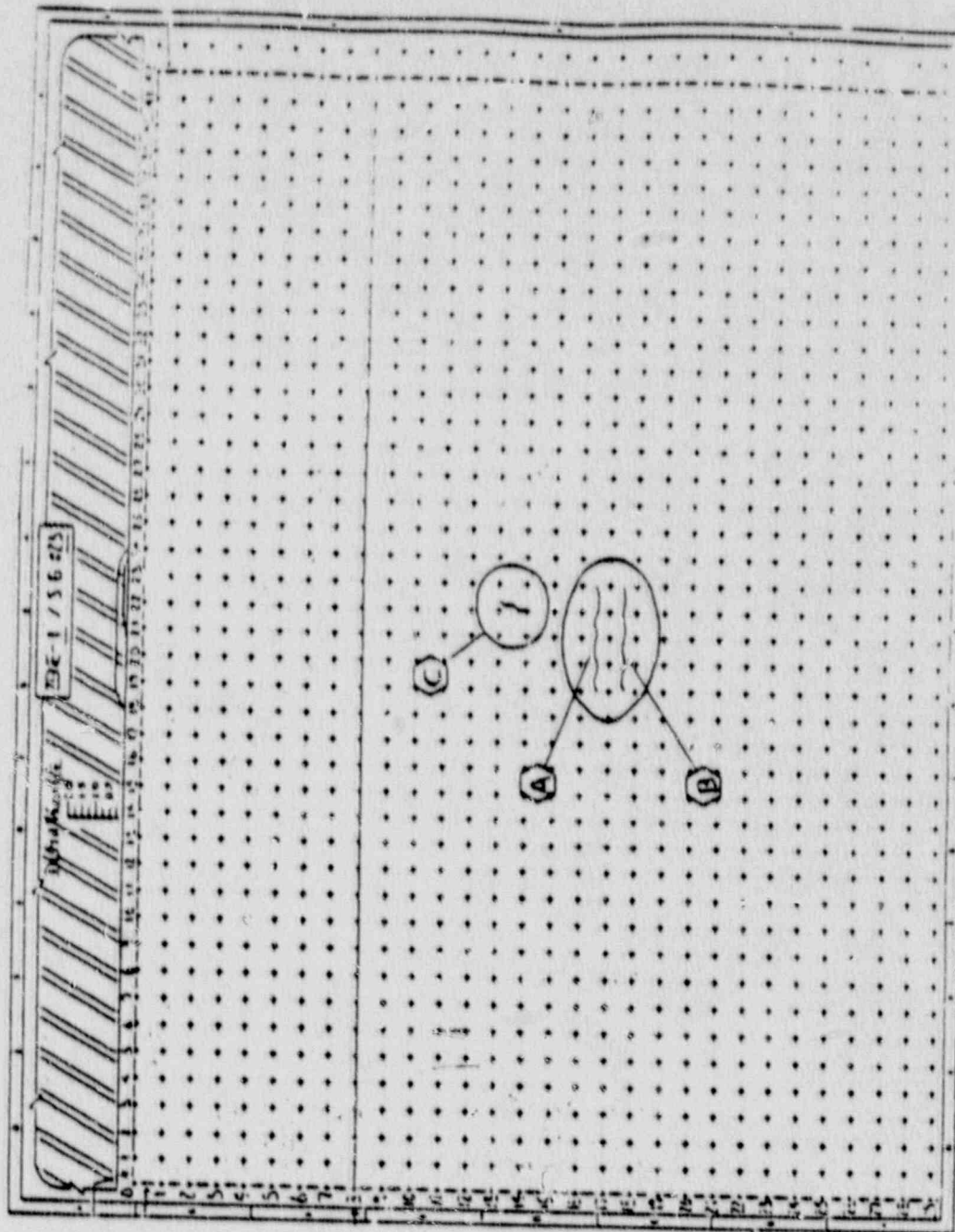


CRACKS, EXCAVATIONS AND WSI WELDS  
ZONE 11, S.G. #22

CRACKS, EXCAVATIONS AND WSI WELDS  
ZONE 12, S.G. #22

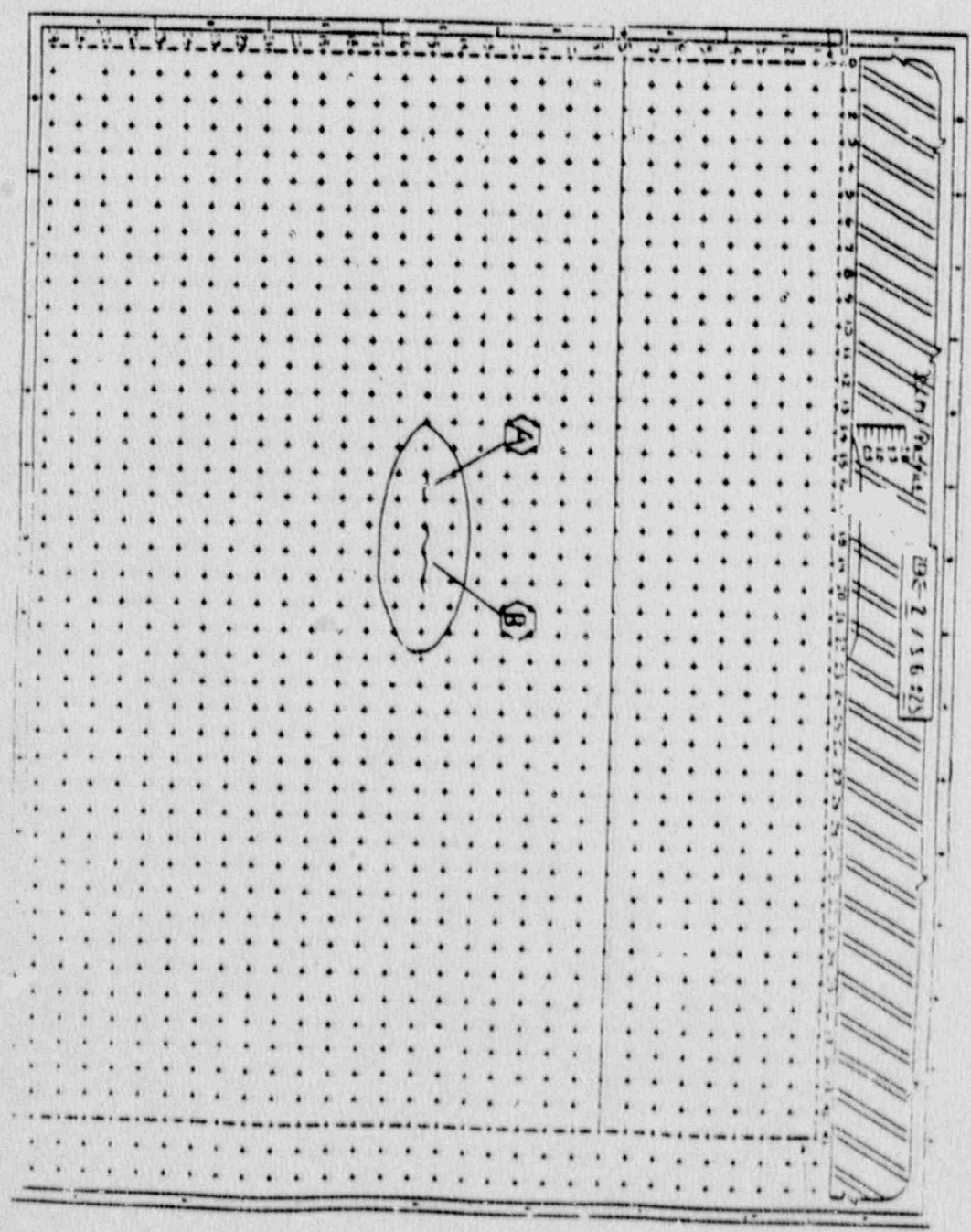


INDICATION AND EXCAVATION MAP  
ZONE 1, S.G. #23

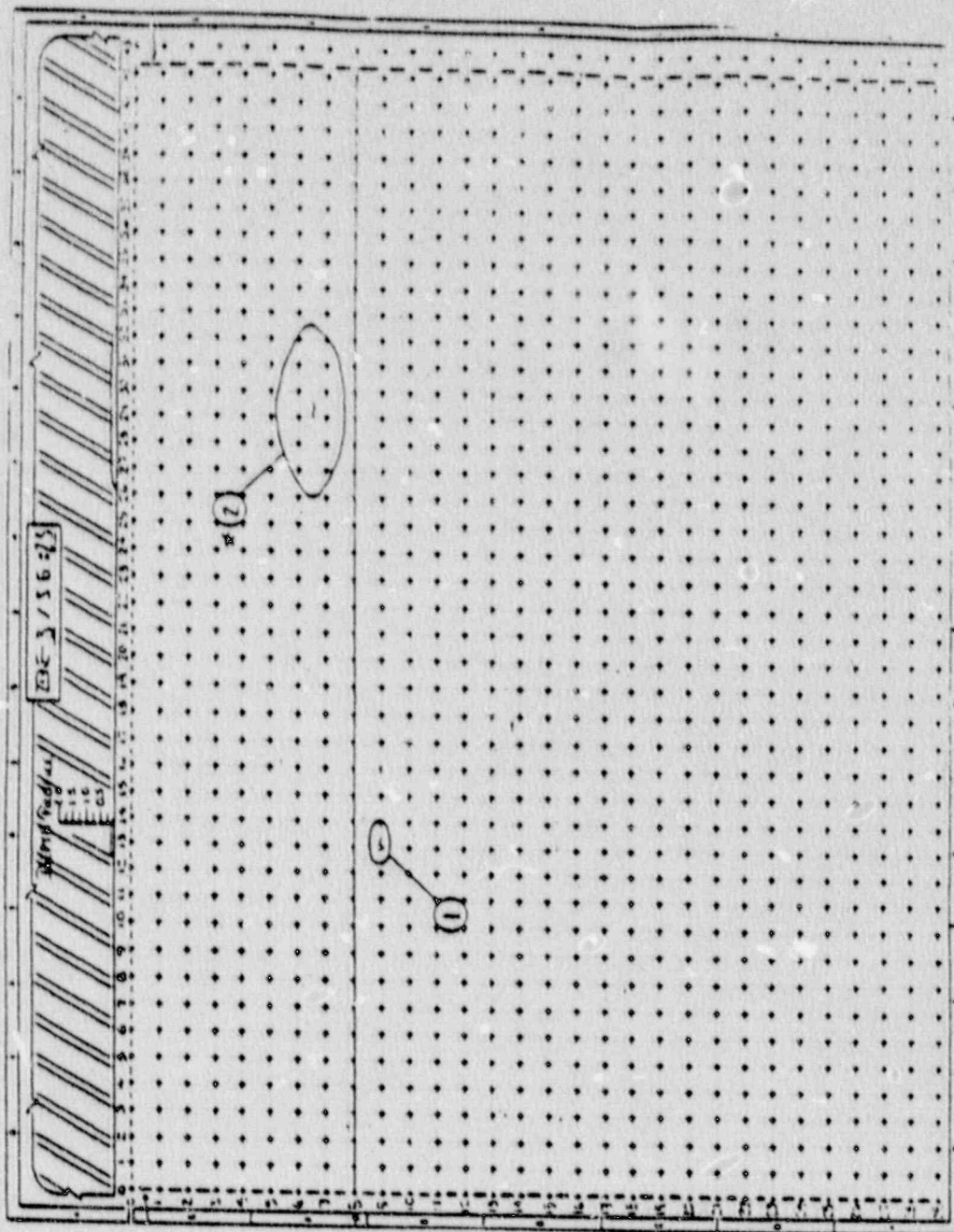




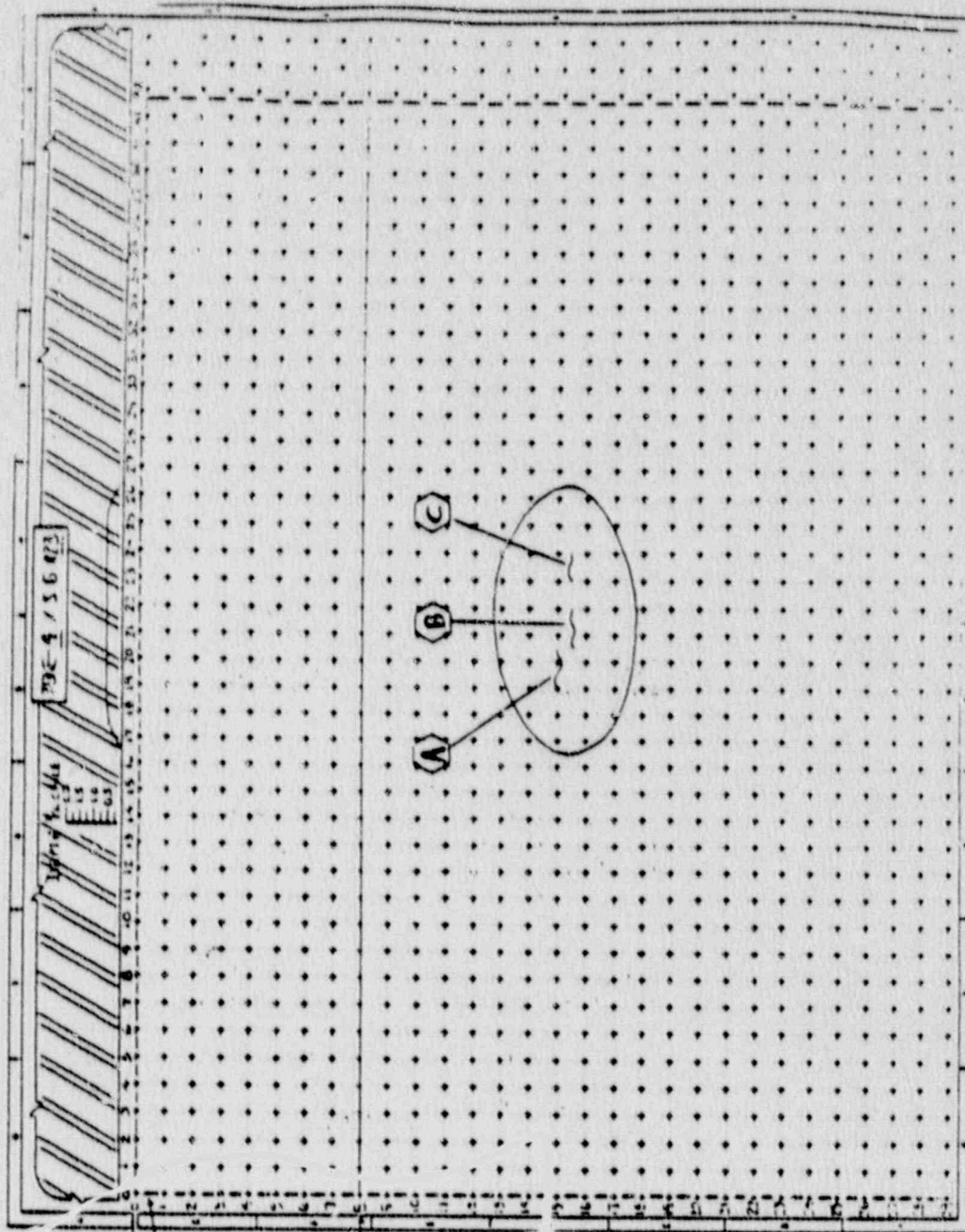
# INDICATION AND EXCAVATION MAP ZONE 2, S.G. #23



INDICATION AND EXCAVATION MAP  
ZONE 3, S.G. #23



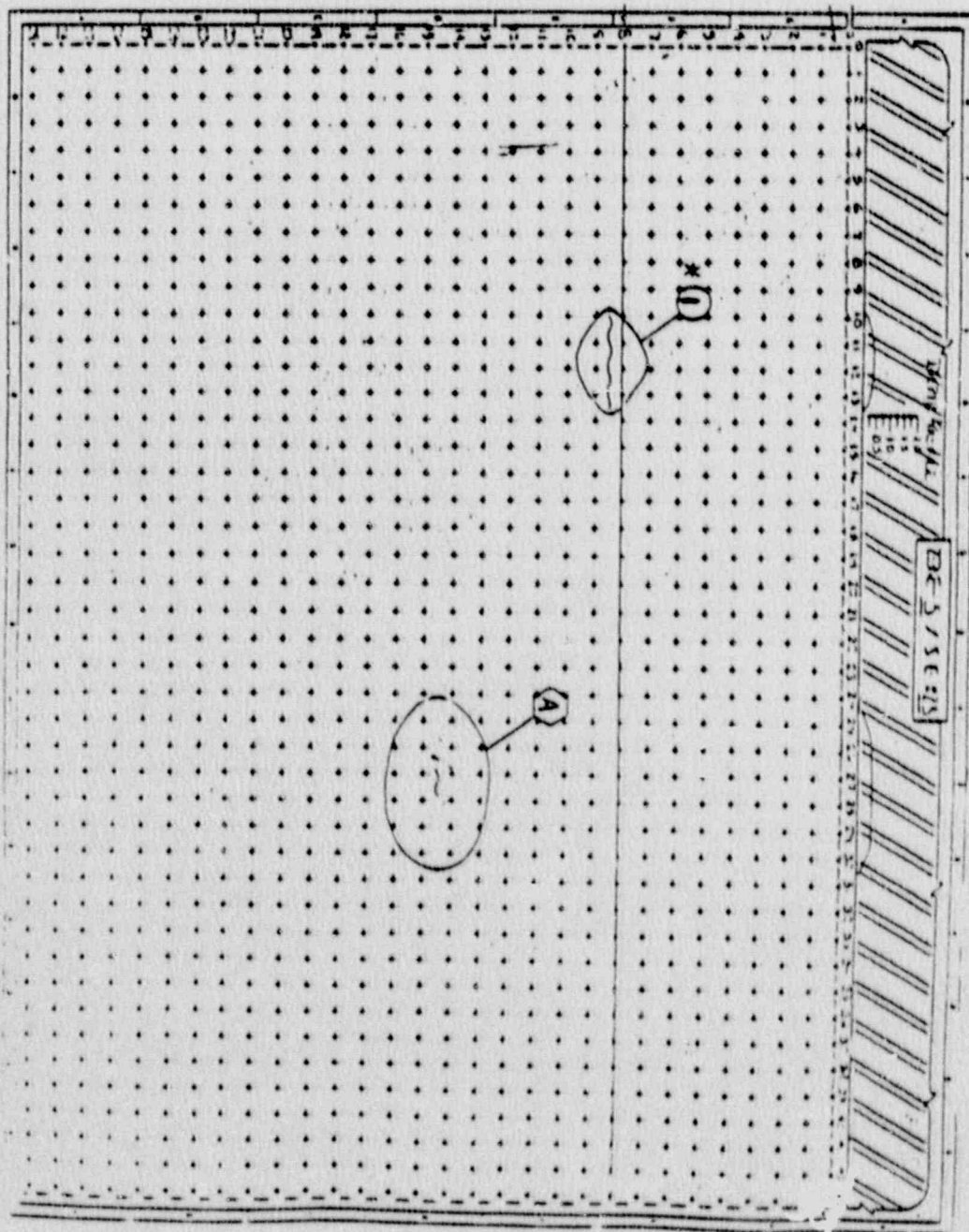
INDICATION AND EXCAVATION MAP  
 ZONE 4, S.G. #23



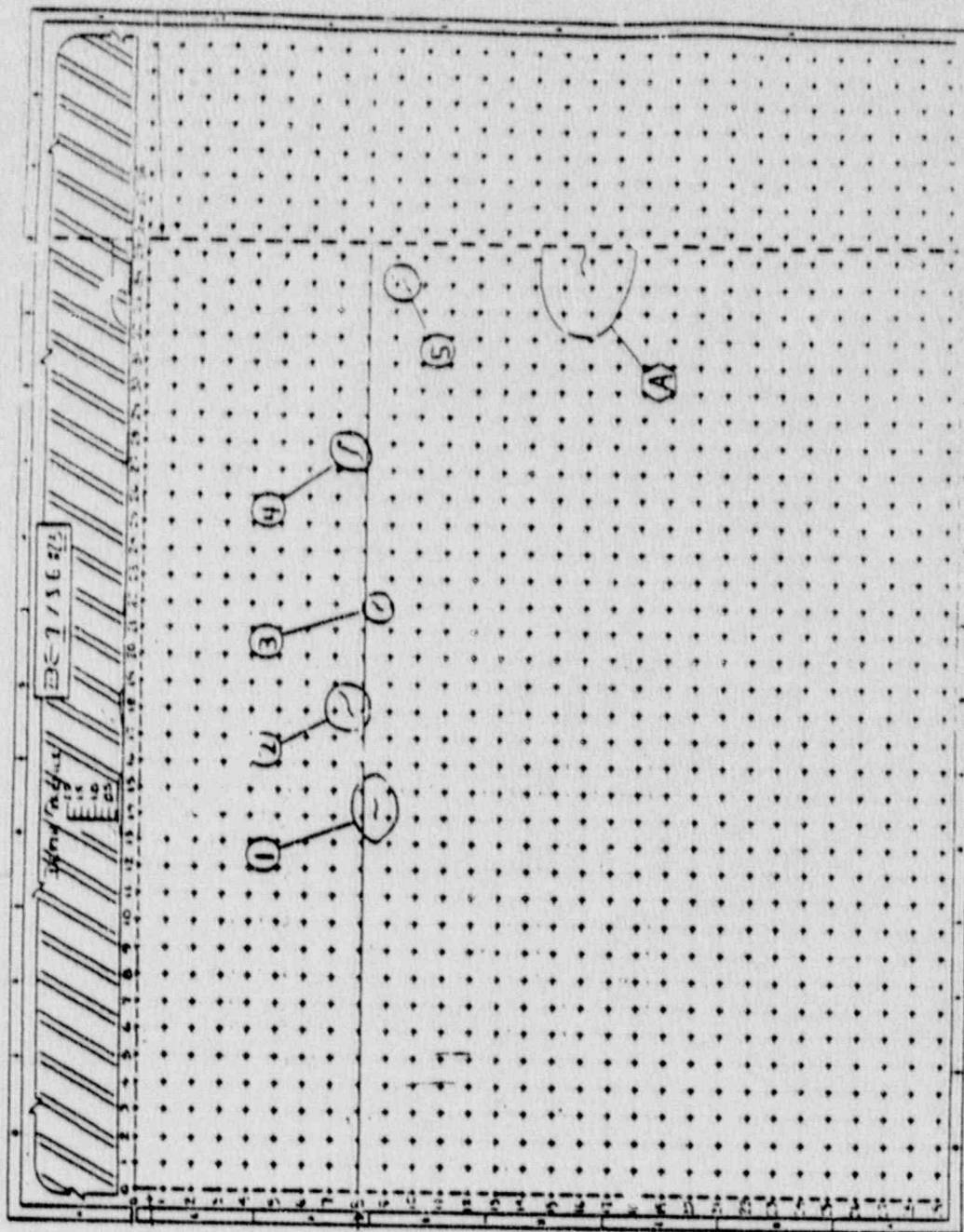


# INDICATION AND EXCAVATION MAP

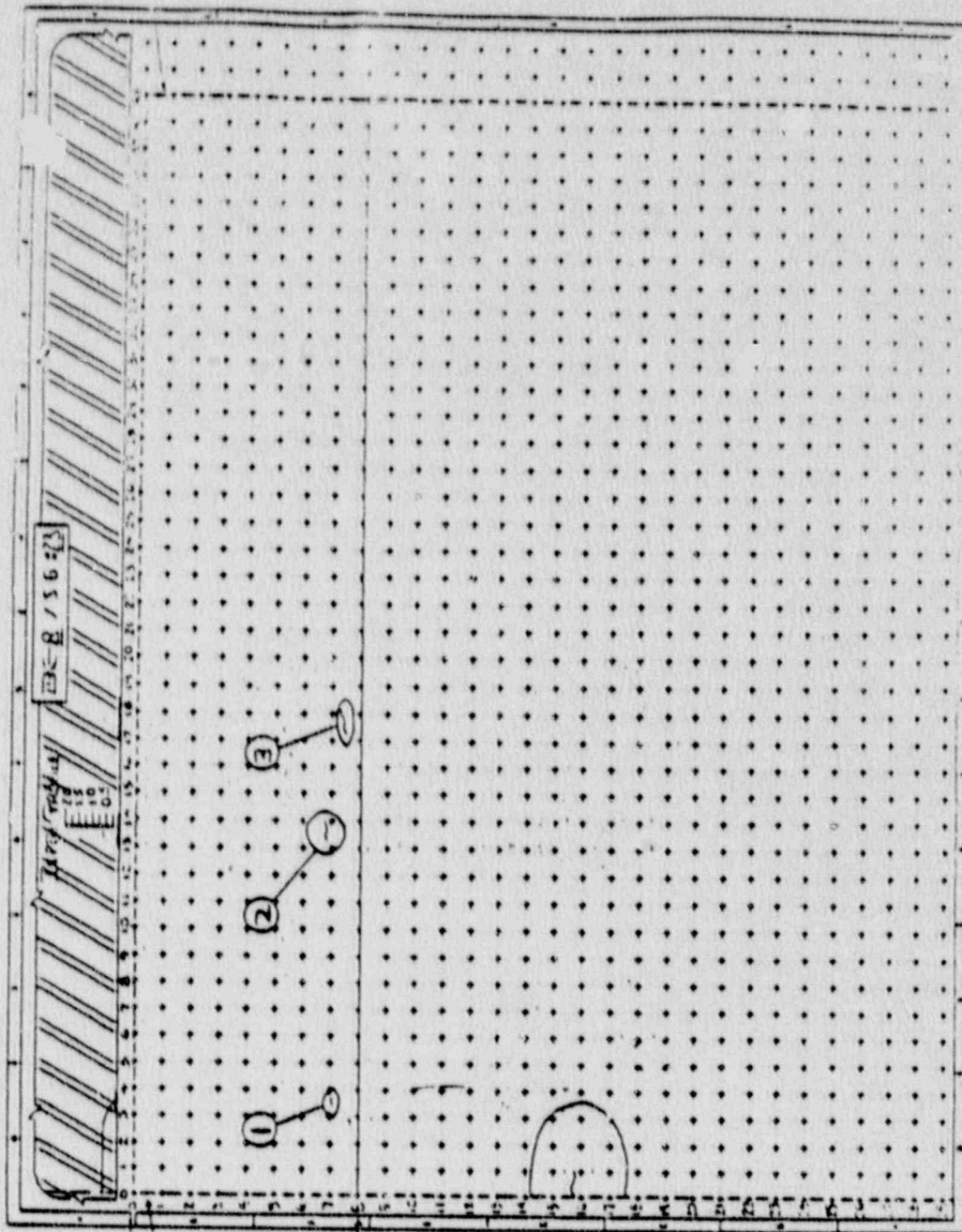
ZONE 5, S.G. #23



INDICATION AND EXCAVATION MAP  
 ZONE 7, S.G. #23

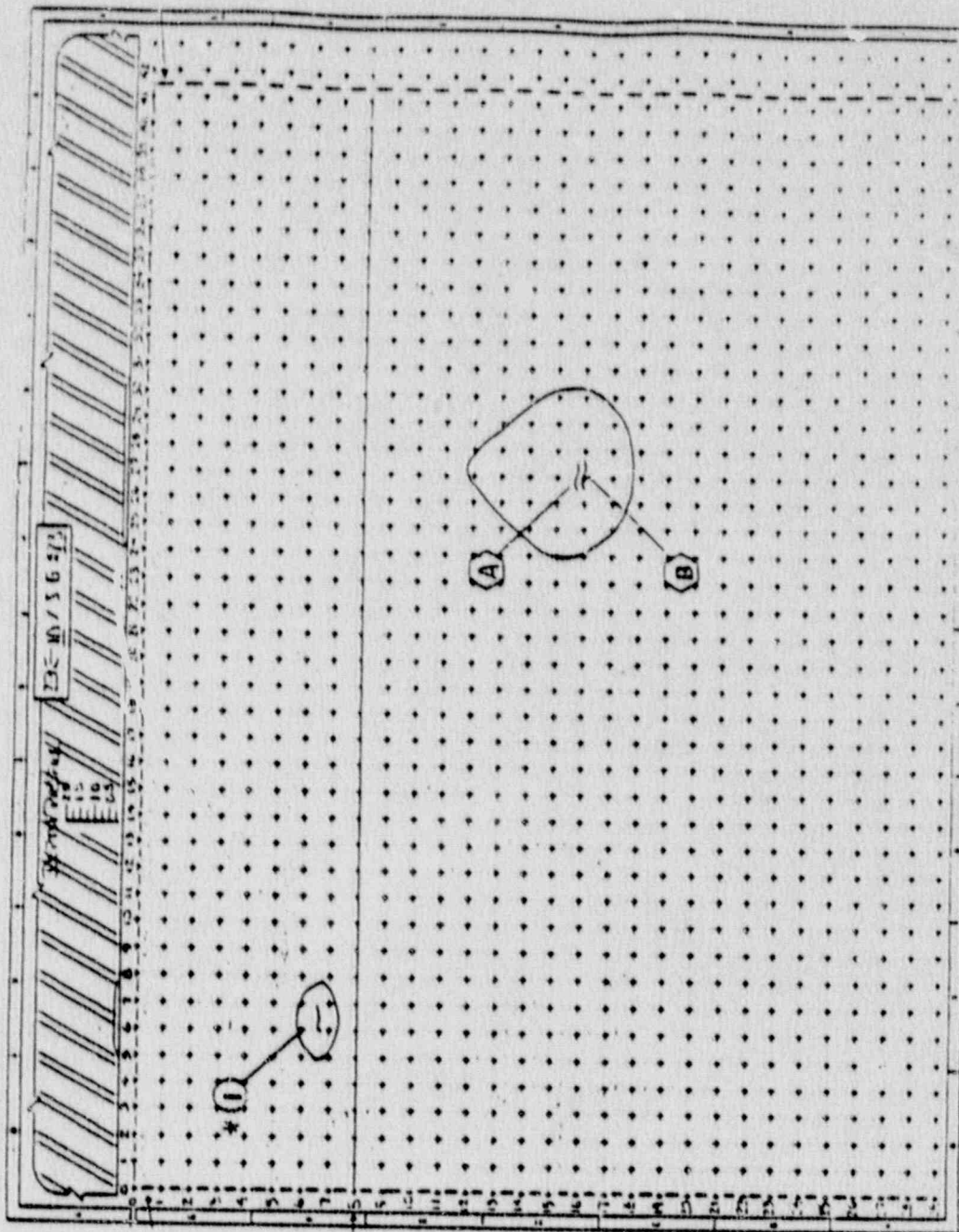


INDICATION AND EXCAVATION MAP  
 ZONE 8, S.G. #23

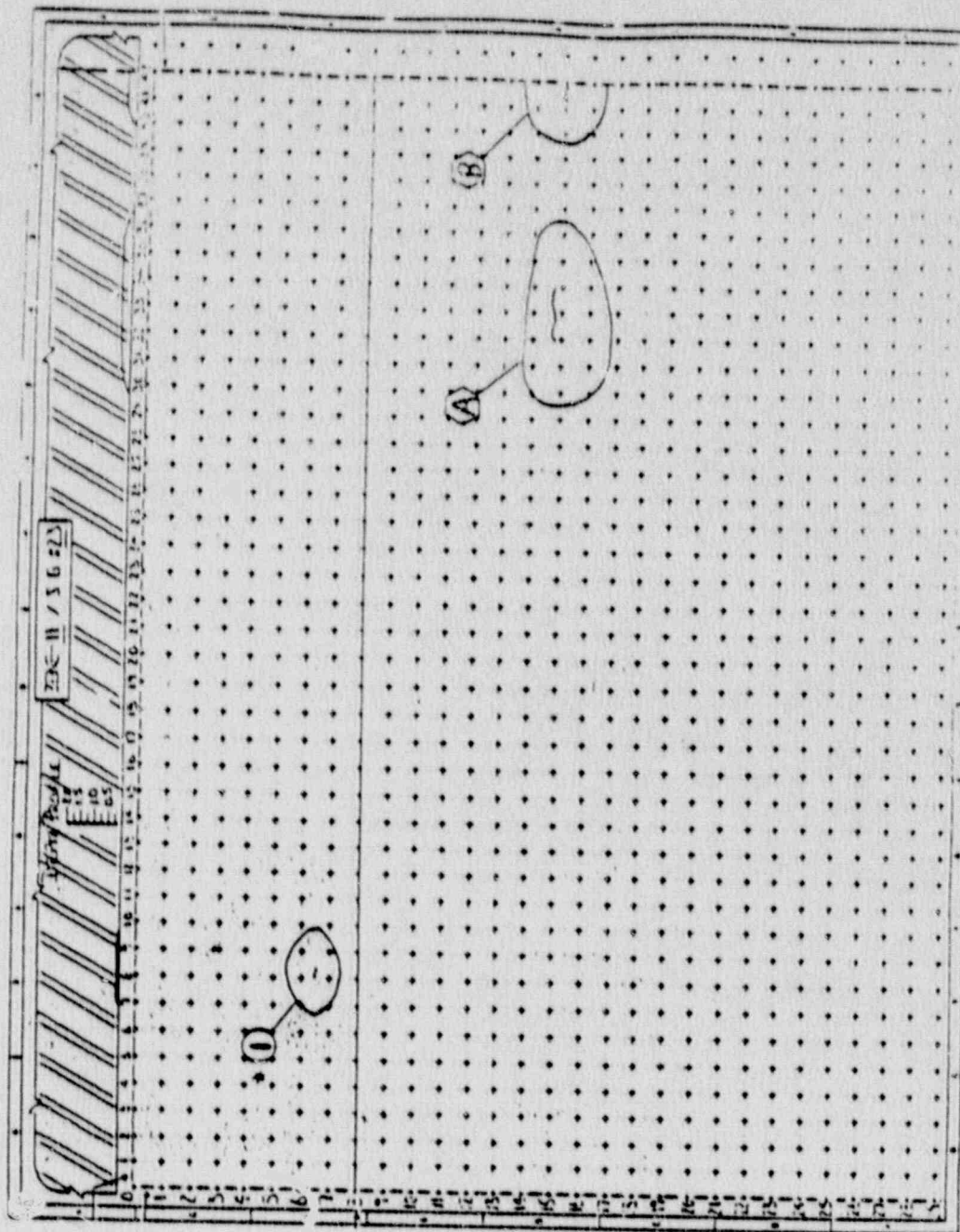




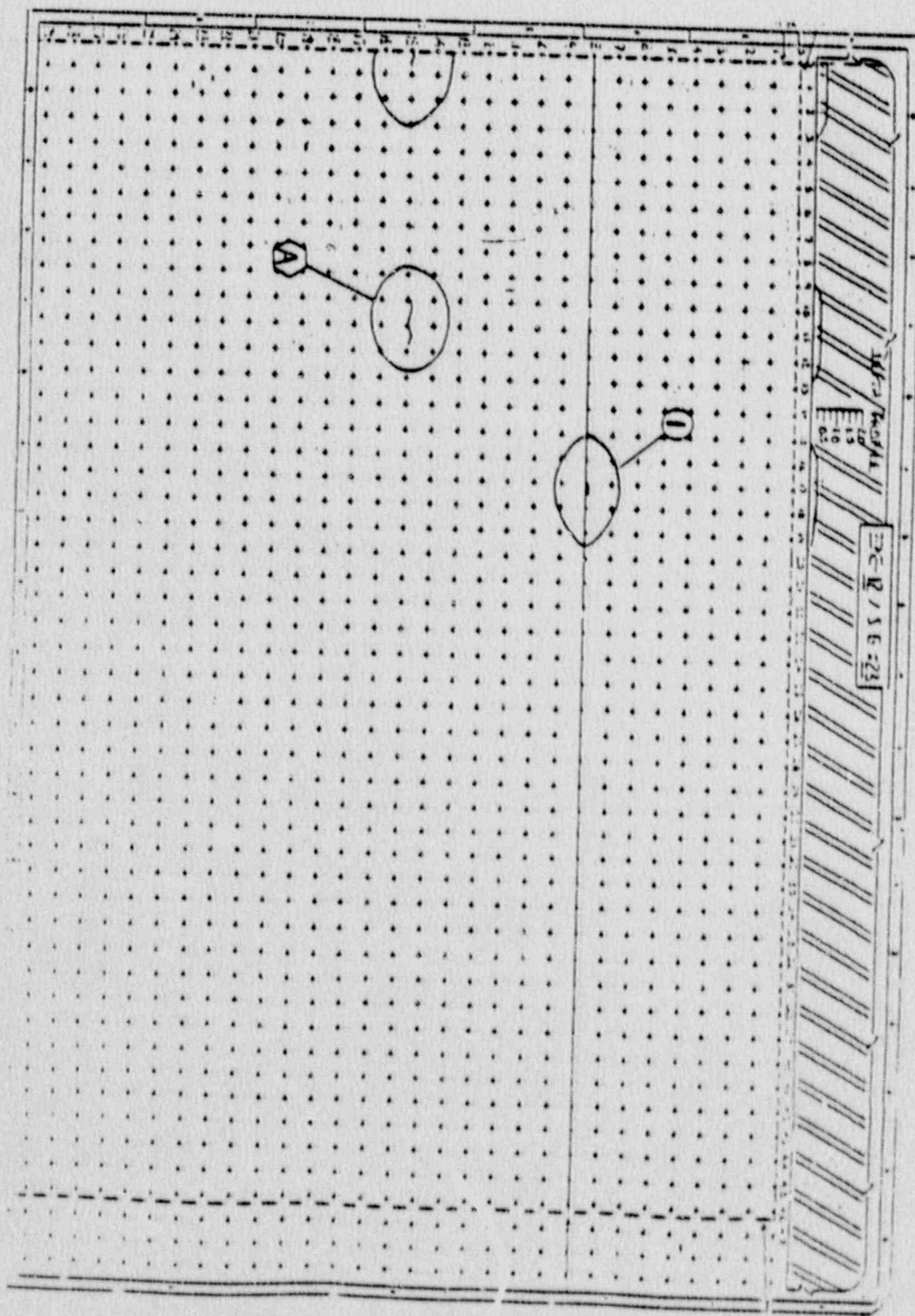
INDICATION AND EXCAVATION MAP  
 ZONE 10, S.G. #23



INDICATION AND EXCAVATION MAP  
 ZONE 11, S.G. #23

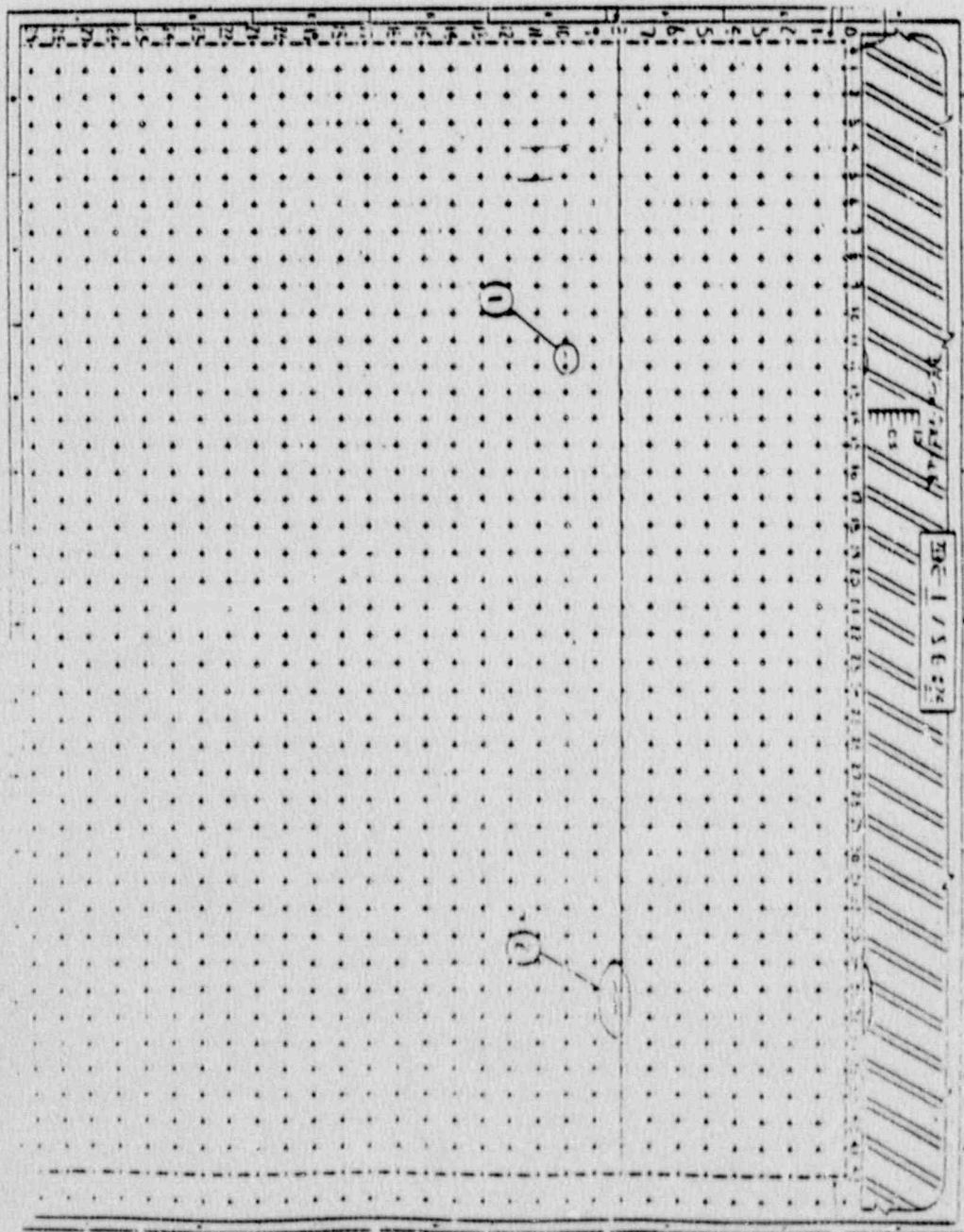


# INDICATION AND EXCAVATION MAP ZONE 12, S.G. #23

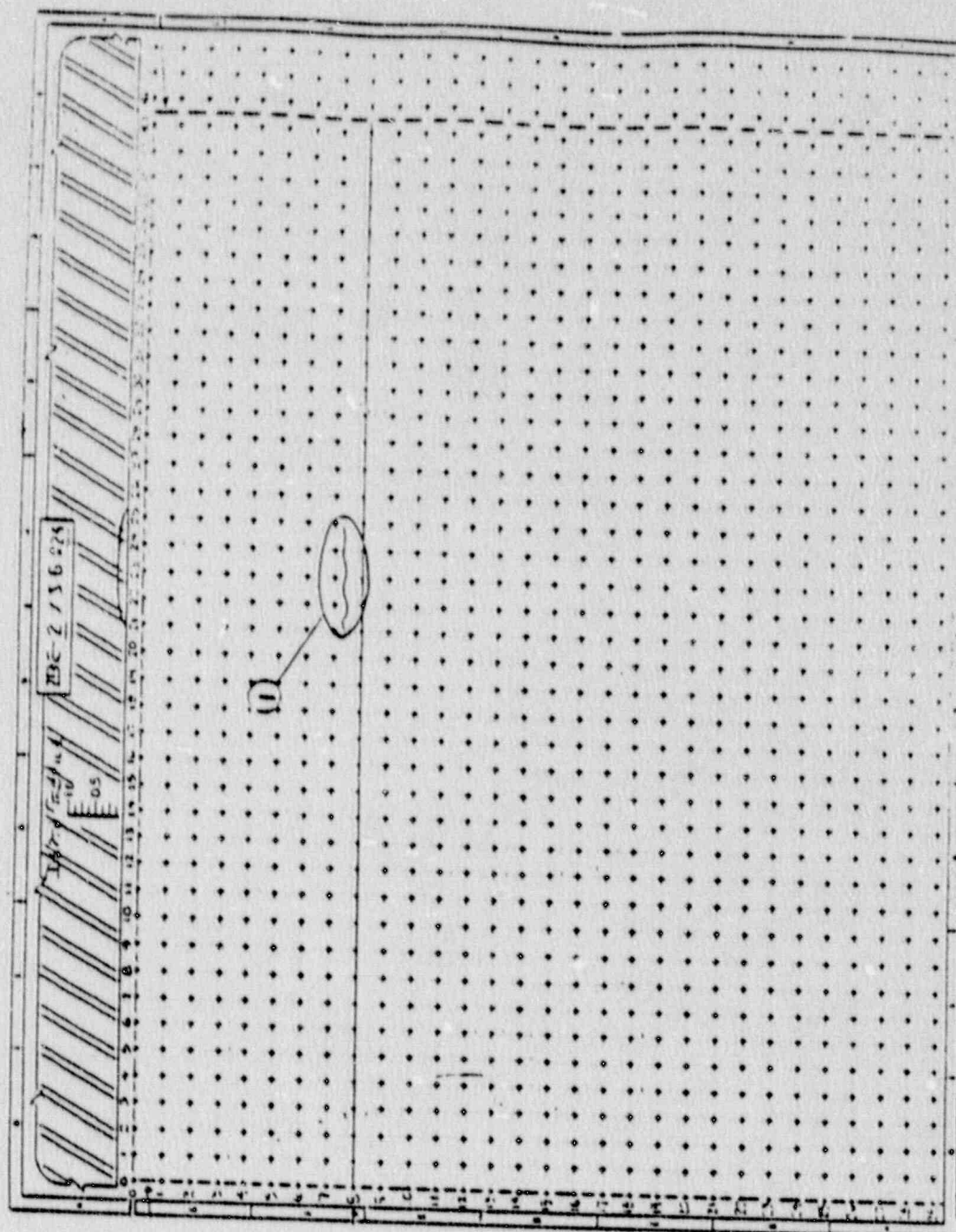




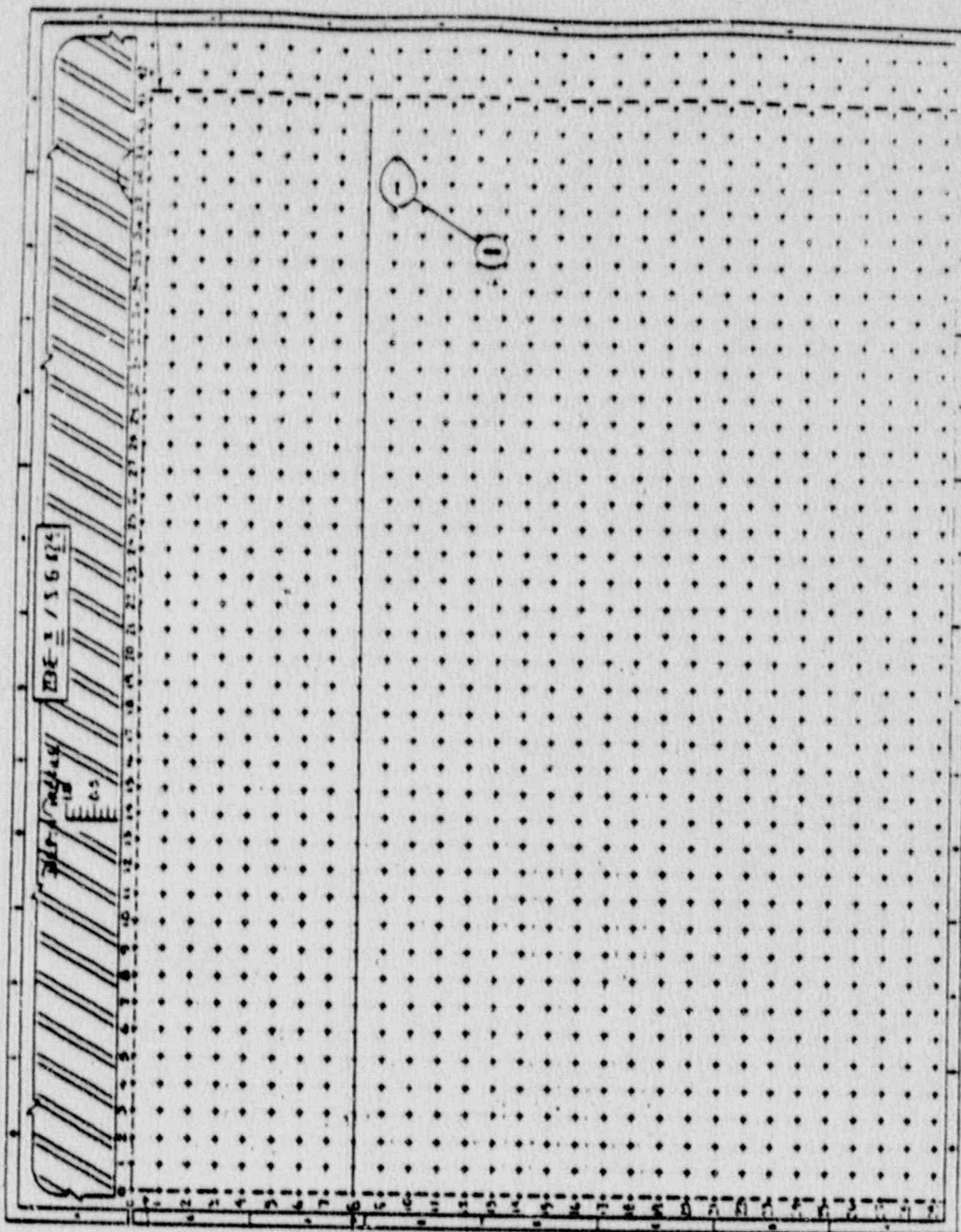
# INDICATION AND EXCAVATION MAP ZONE 1, S.G. #24



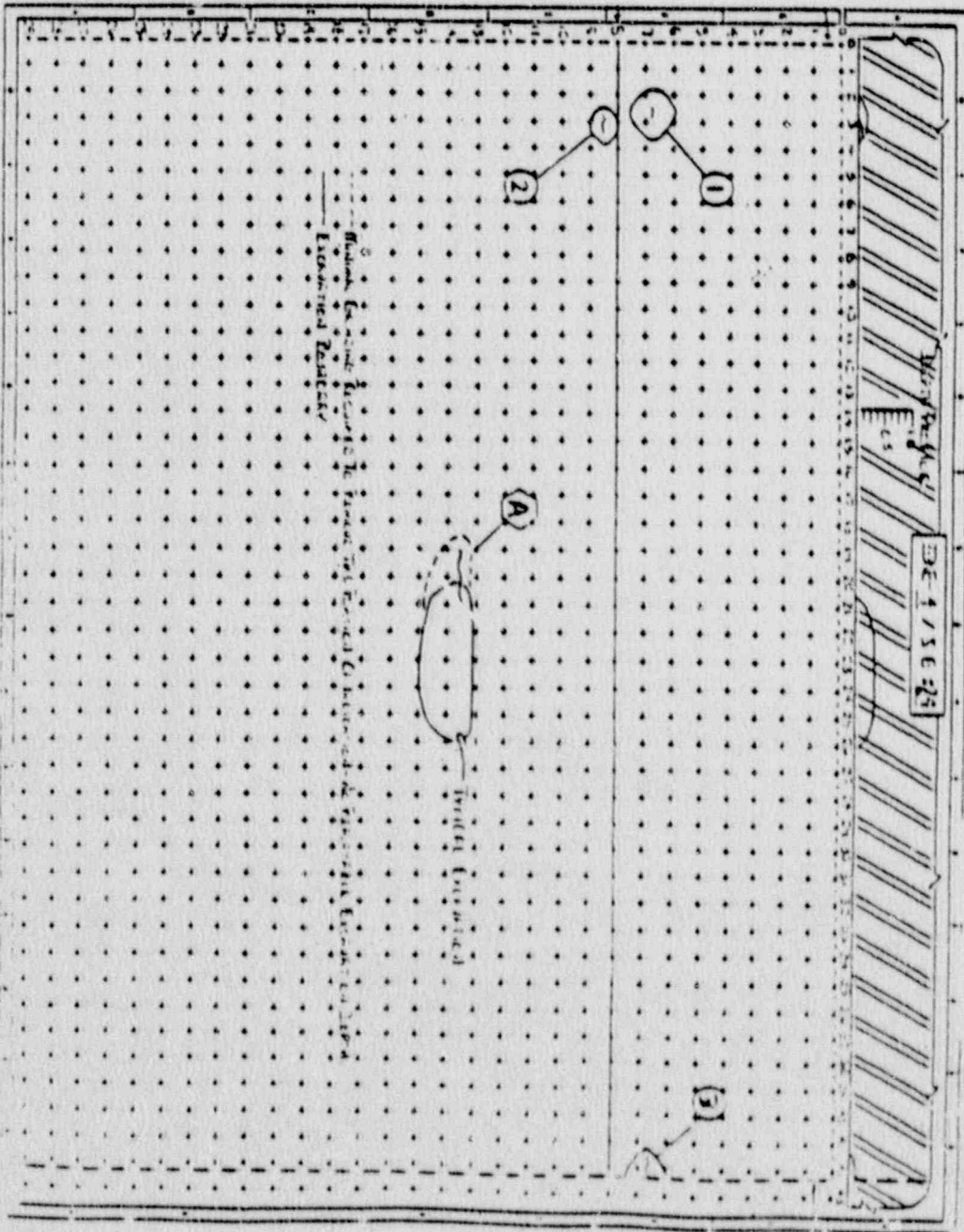
INDICATION AND EXCAVATION MAP  
 ZONE 2, S.G. #24



INDICATION AND EXCAVATION MAP  
 ZONE 3, S.G. #24

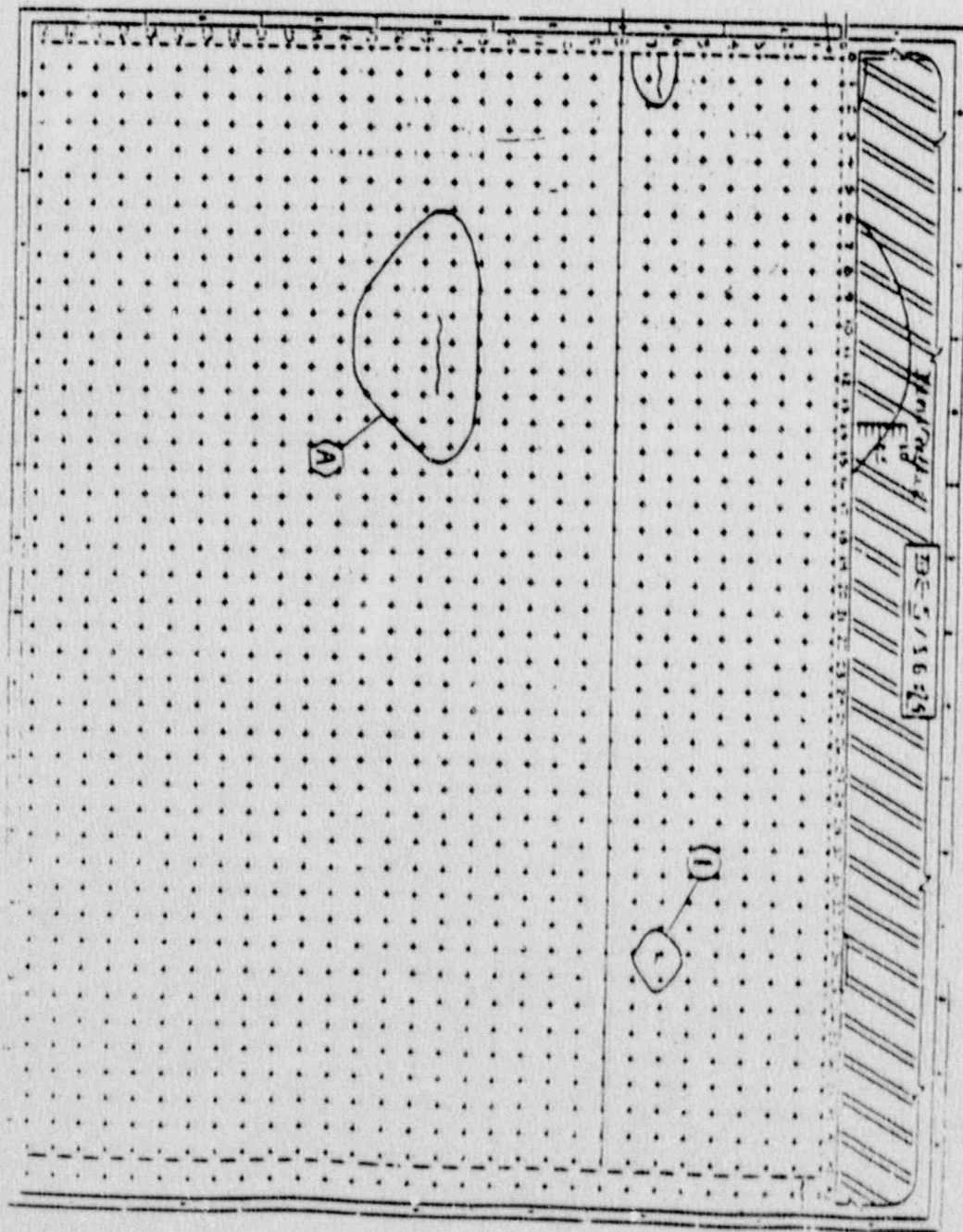






INDICATION AND EXCAVATION MAP  
ZONE 4, S.G. #24

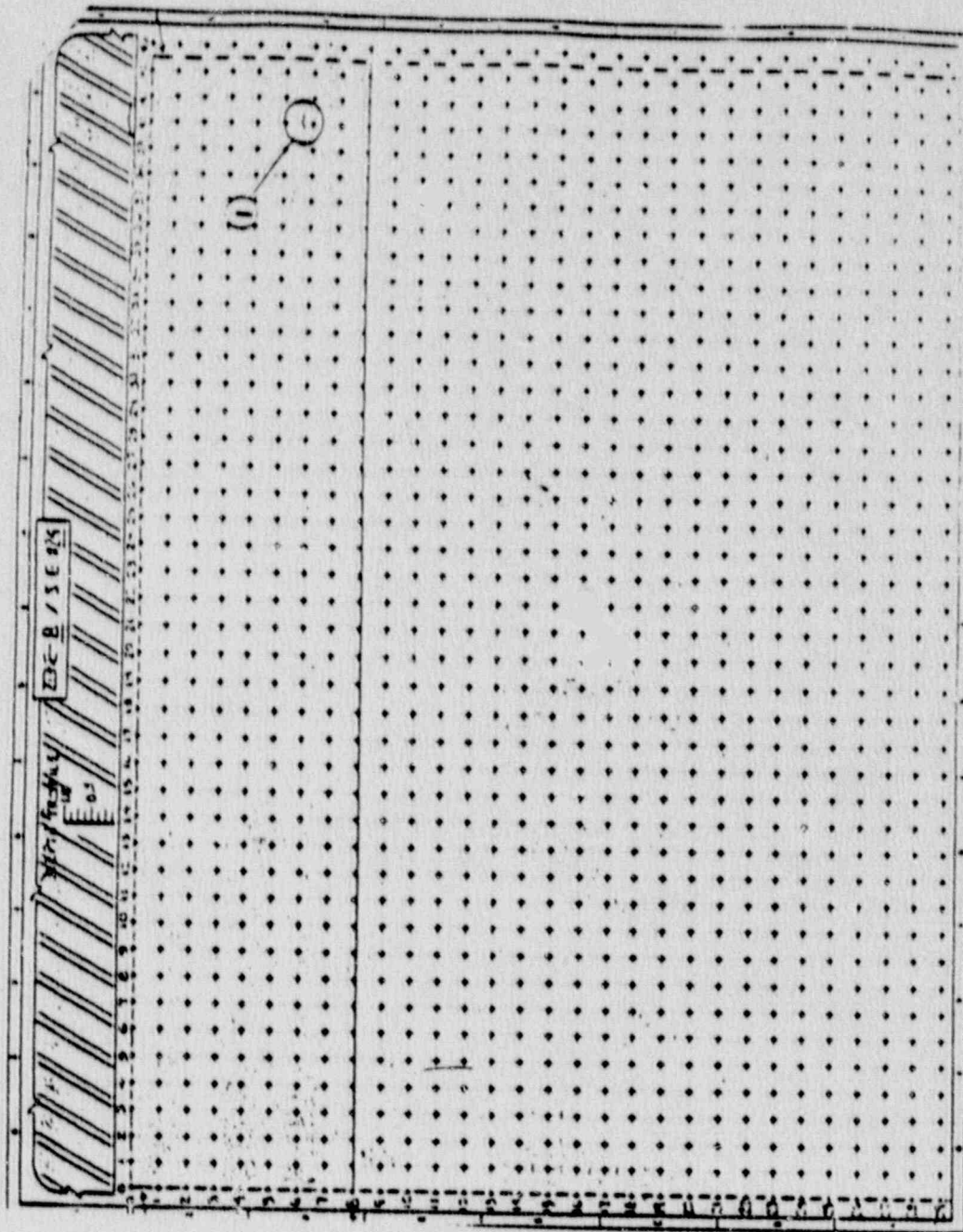
INDICATION AND EXCAVATION MAP  
 ZONE 5, S.G. #24



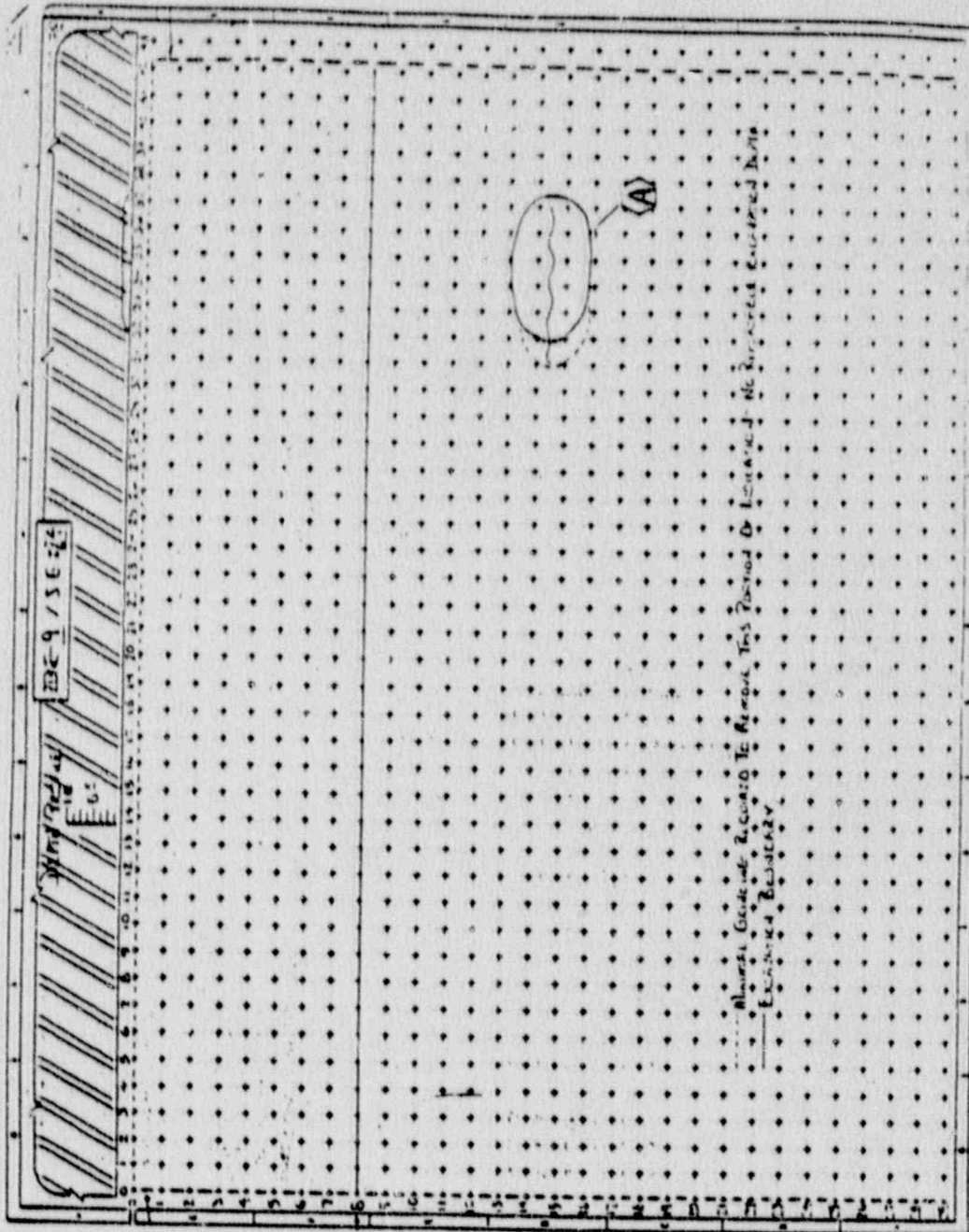
[illegible]



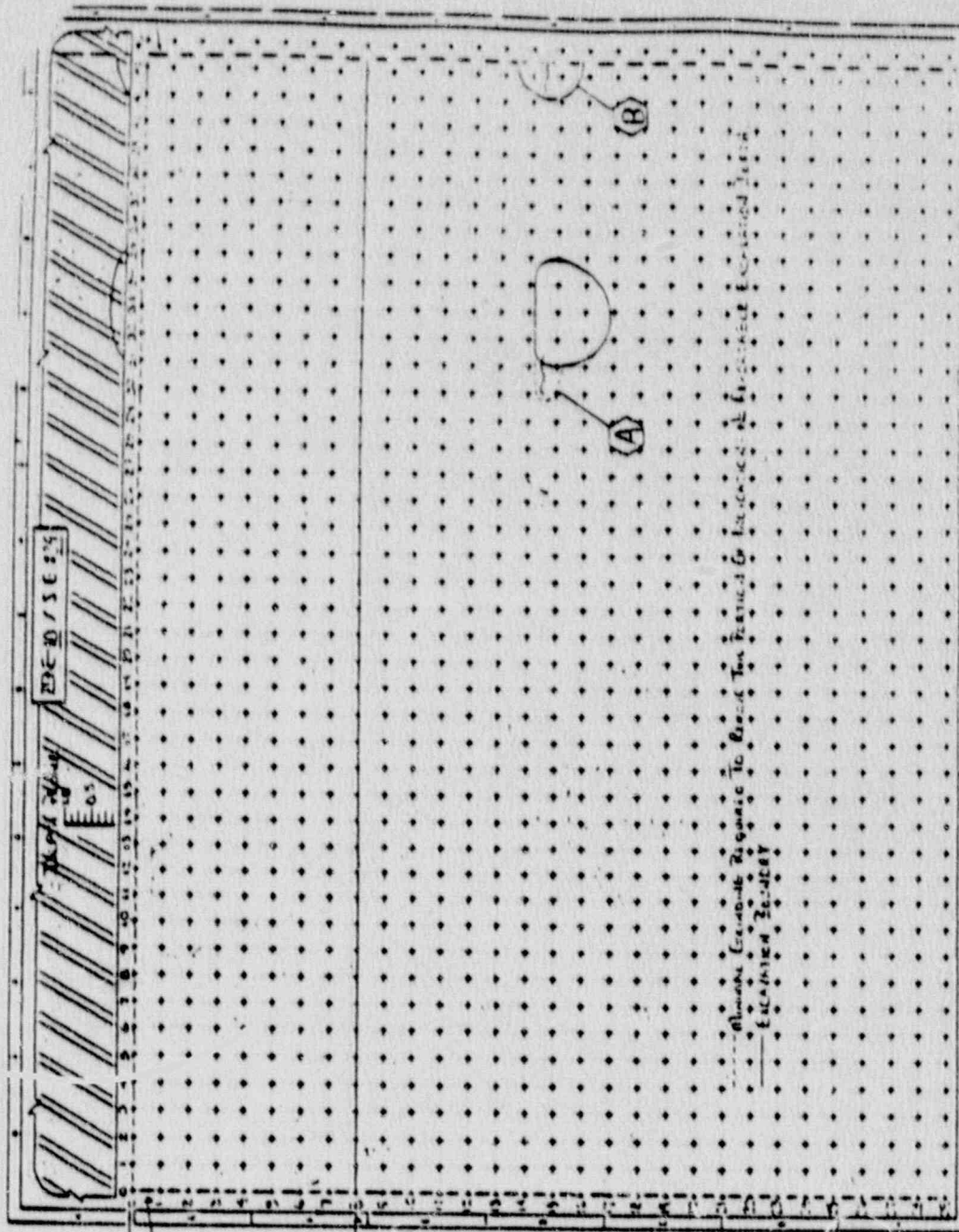
INDICATION AND EXCAVATION MAP  
 ZONE 8, S.G. #24



INDICATION AND EXCAVATION MAP  
 ZONE 9, S.G. #24

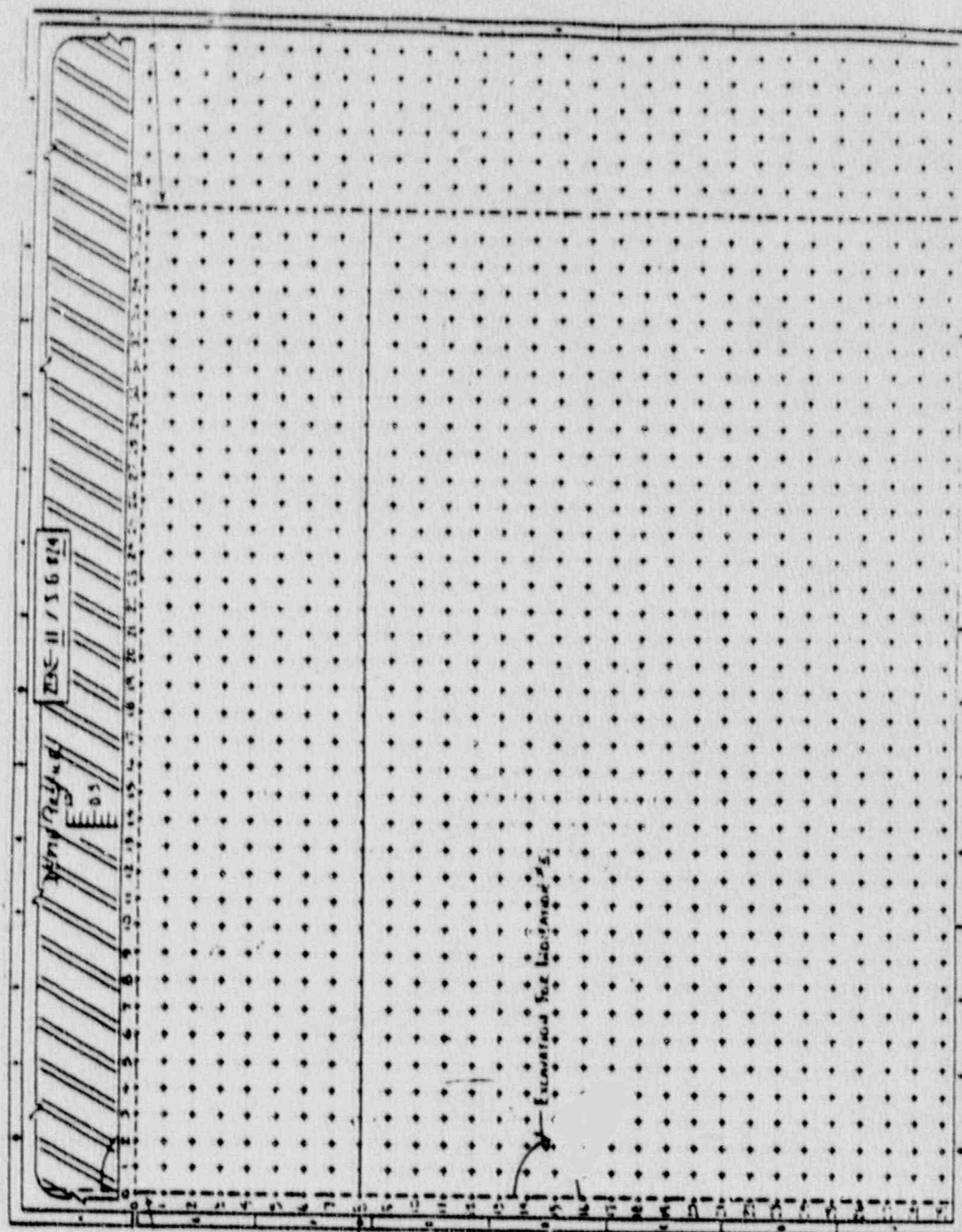


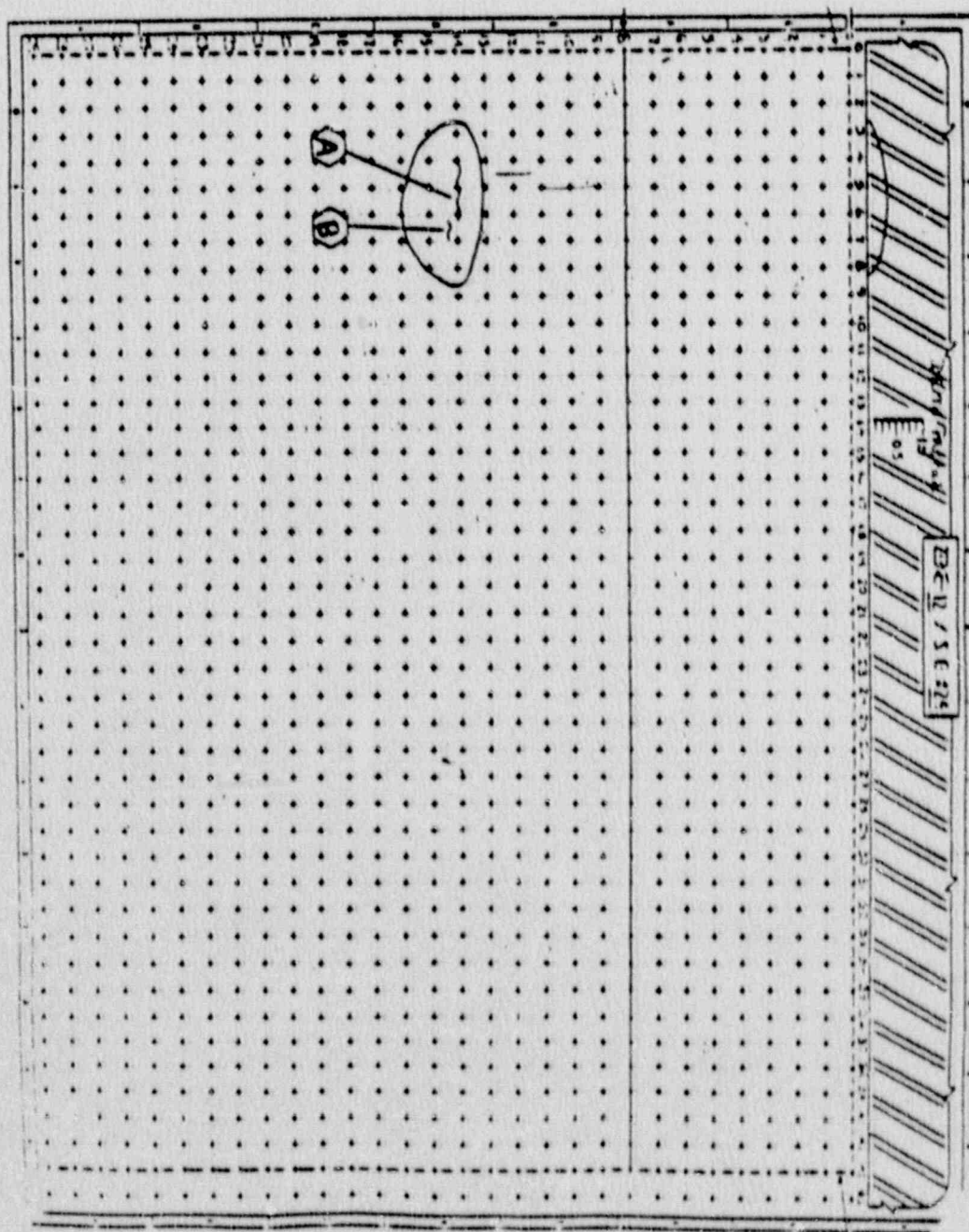
INDICATION AND EXCAVATION MAP  
 ZONE 10, S.G. #24





INDICATION AND EXCAVATION MAP  
 ZONE 11, S.G. #24





INDICATION AND EXCAVATION MAP  
ZONE 12, S.G. #24

RECONSTRUCTION OF THE CLASS

APPENDIX D  
FEEDRING SUPPORT INSPECTION DATA



TABLE 1  
SUPPORT DIMENSIONS

NOZZLE AREA SUPPORTS

SIZE

LEFT, RIGHT

4 1/2" x 1 1/2"

A, B, C

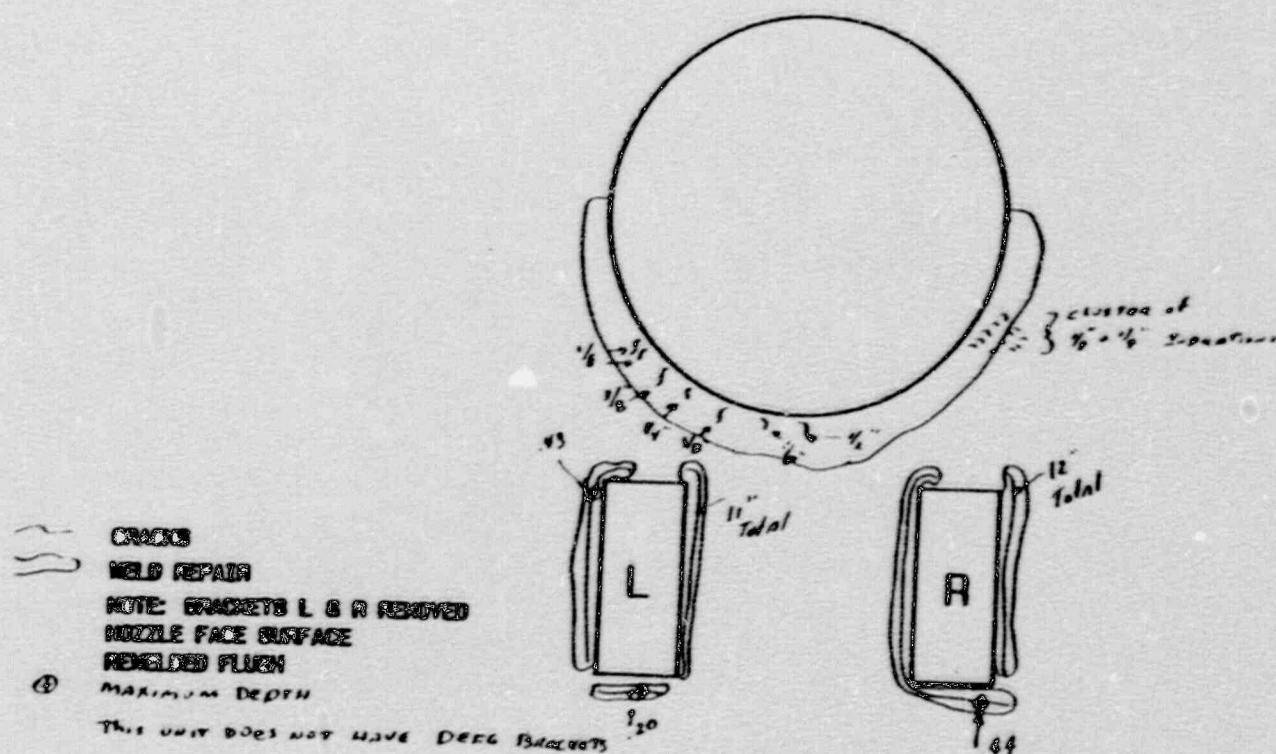
6.0" x 2 1/2"

D, E, F, G

4.0" x 4.0"

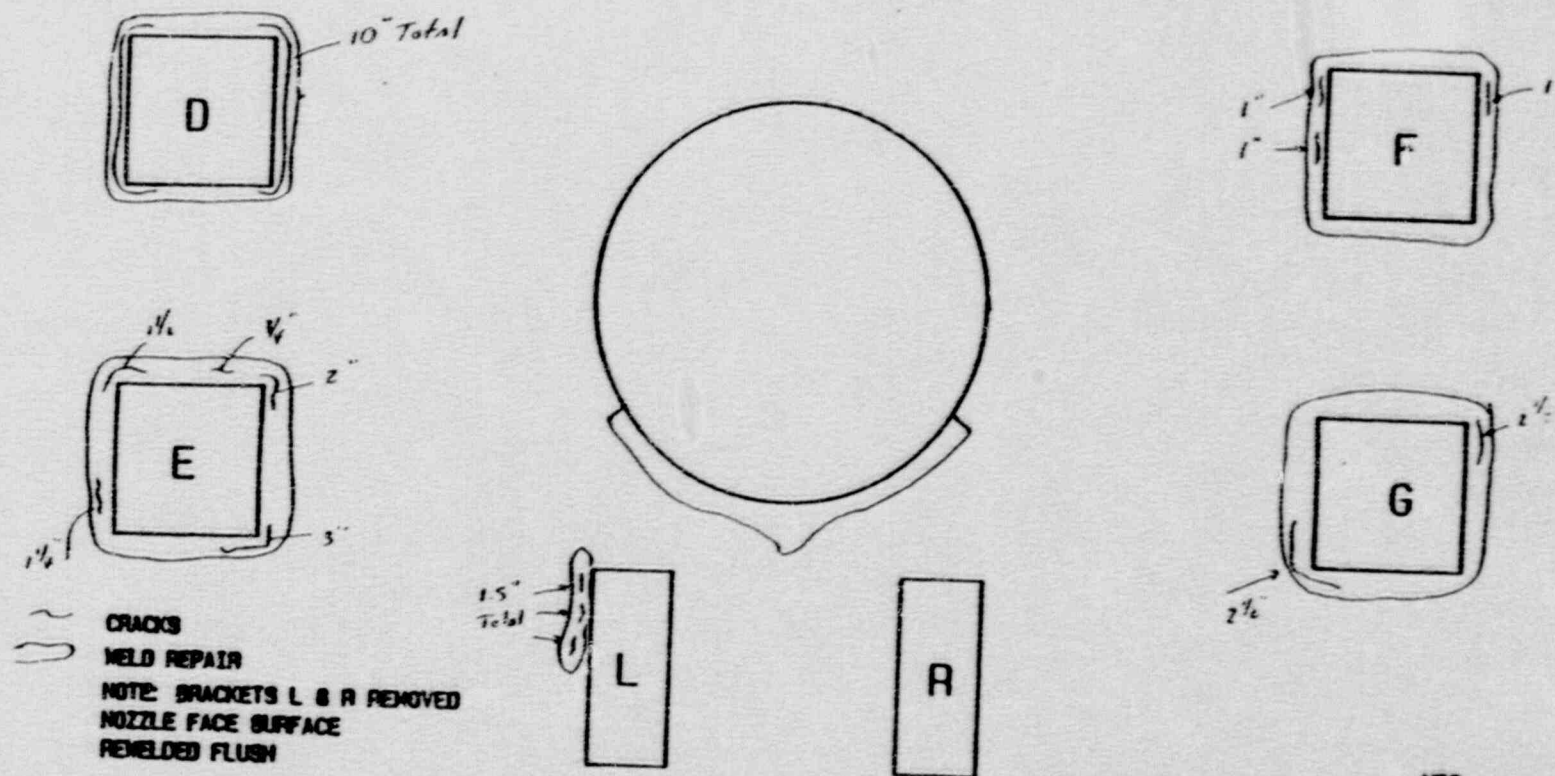
APPENDIX E  
FEEDRING SUPPORT GRINDING AND REPAIR MAPS

# INDIAN POINT 2 STEAM GENERATOR #1 NOZZLE AREA SUPPORTS



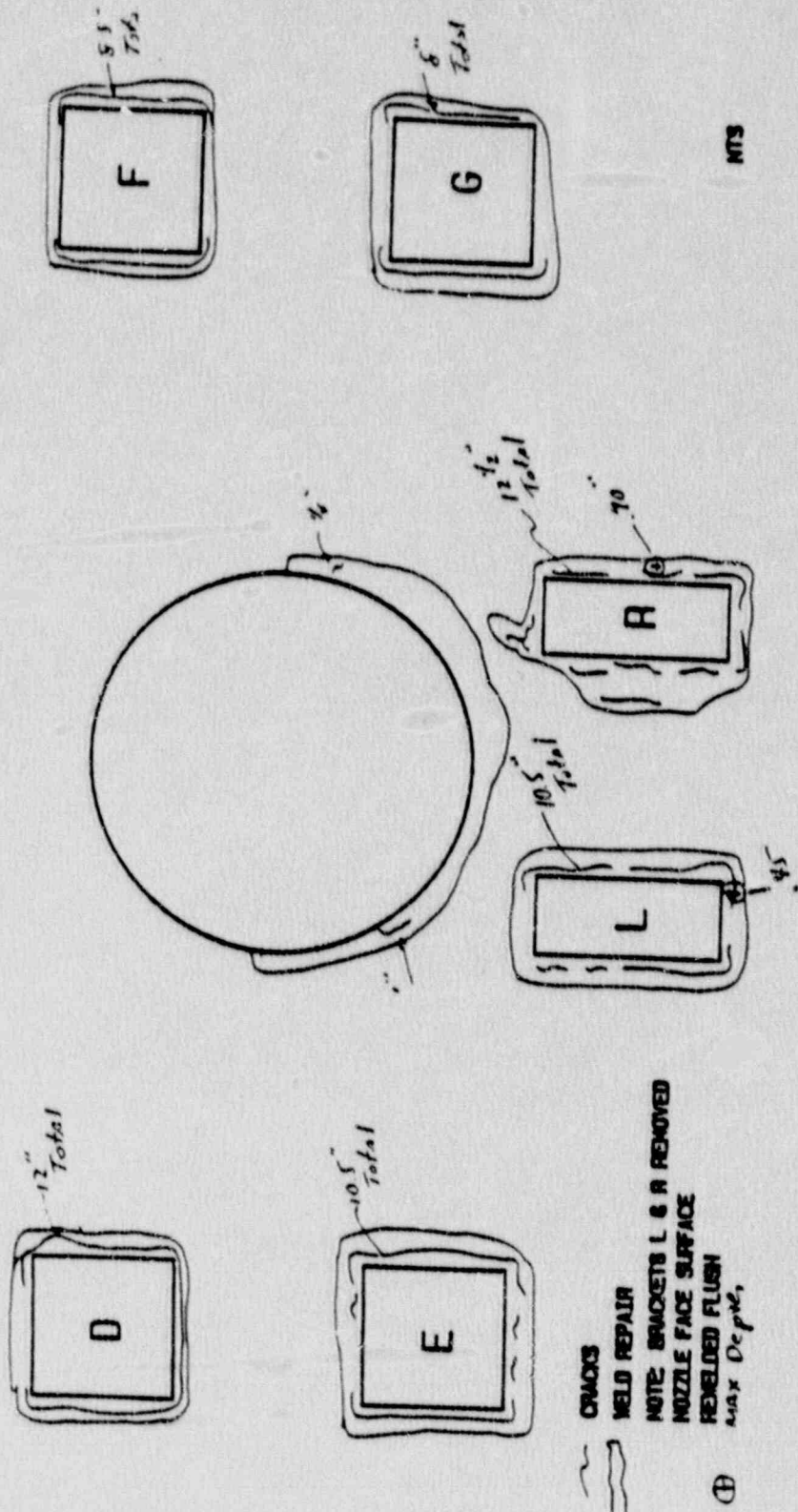


# INDIAN POINT 2 STEAM GENERATOR 22 NOZZLE AREA SUPPORTS



NTS

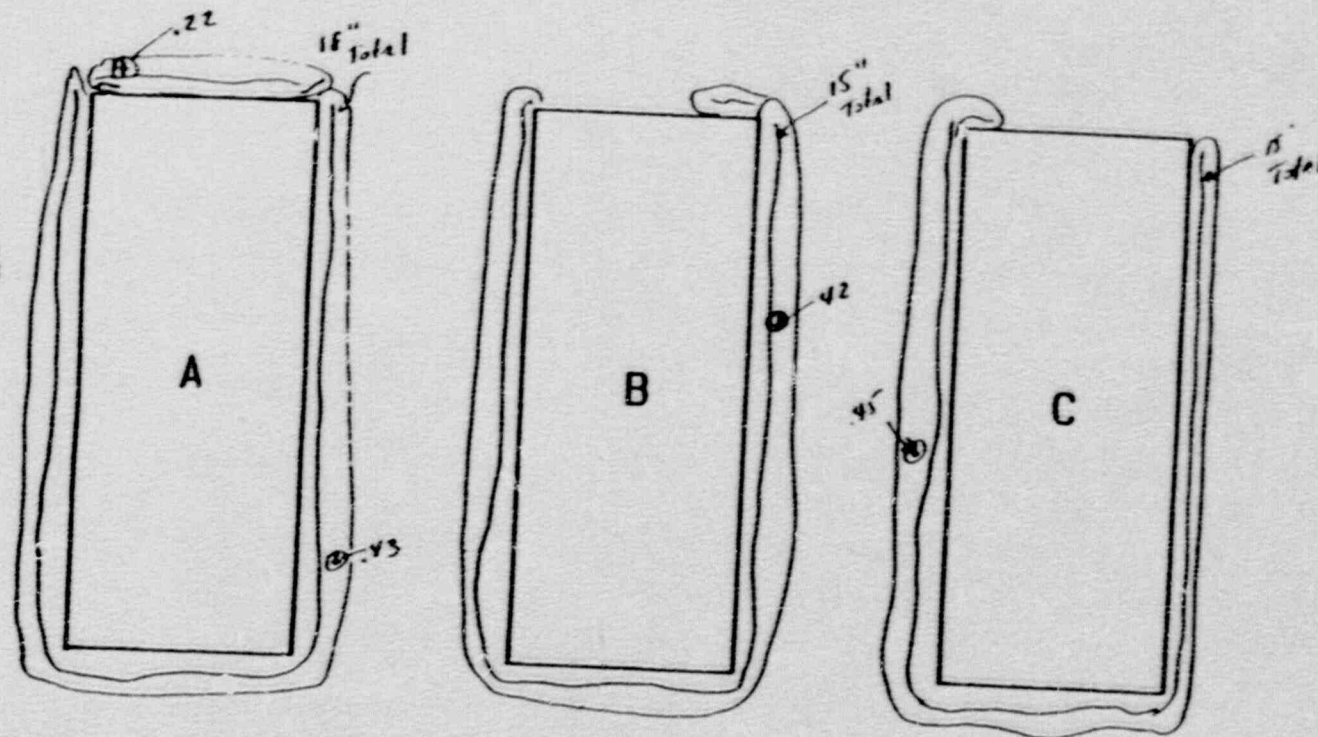
# INDIAN POINT 2 STEAM GENERATOR 23 NOZZLE AREA SUPPORTS





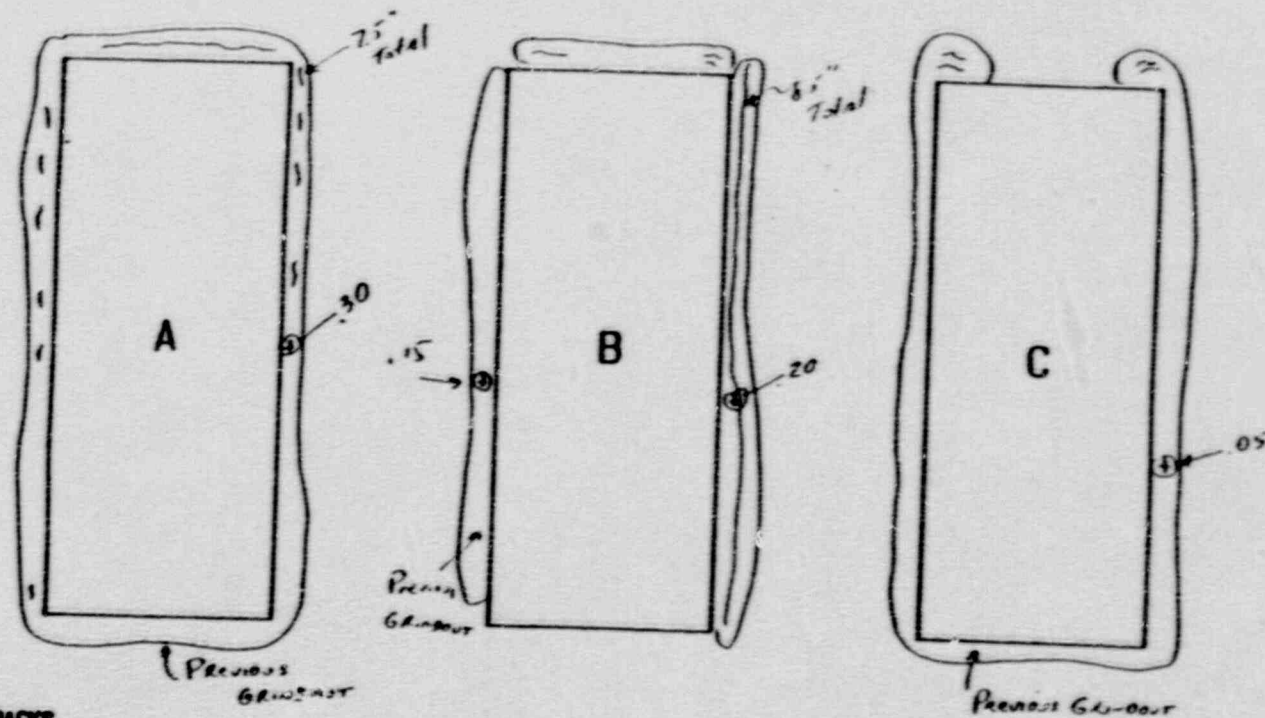


# INDIAN POINT 2 STEAM GENERATOR 21 FEED RING SUPPORT BRACKETS



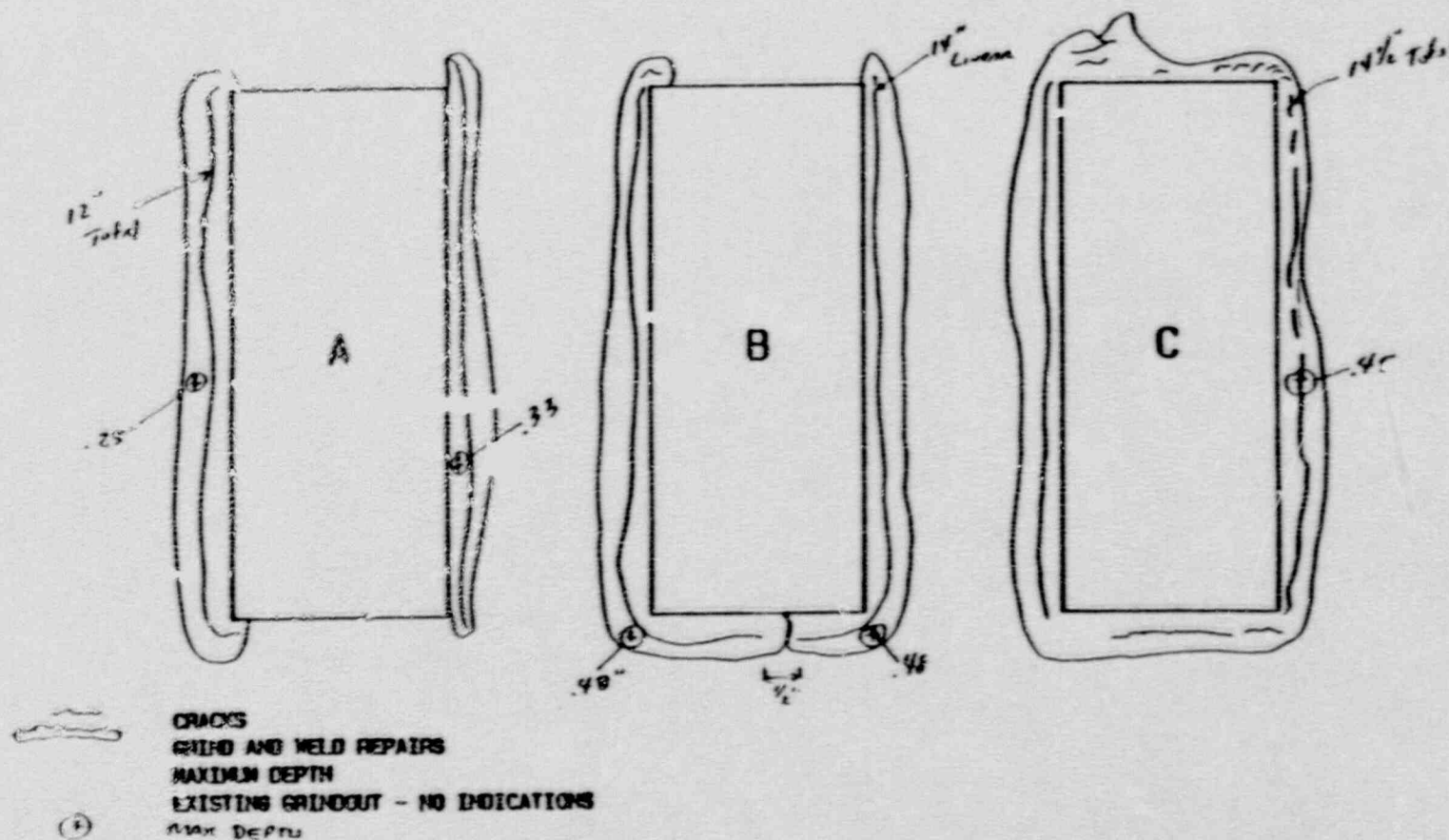
~~~~~ CRACKS  
 ( ) GRIND AND WELD REPAIRS  
 MAXIMUM DEPTH  
 EXISTING GRINDOUT - NO INDICATION  
 (1) MAX DEPTH

# INDIAN POINT 2 STEAM GENERATOR 22 FEED RING SUPPORT BRACKETS



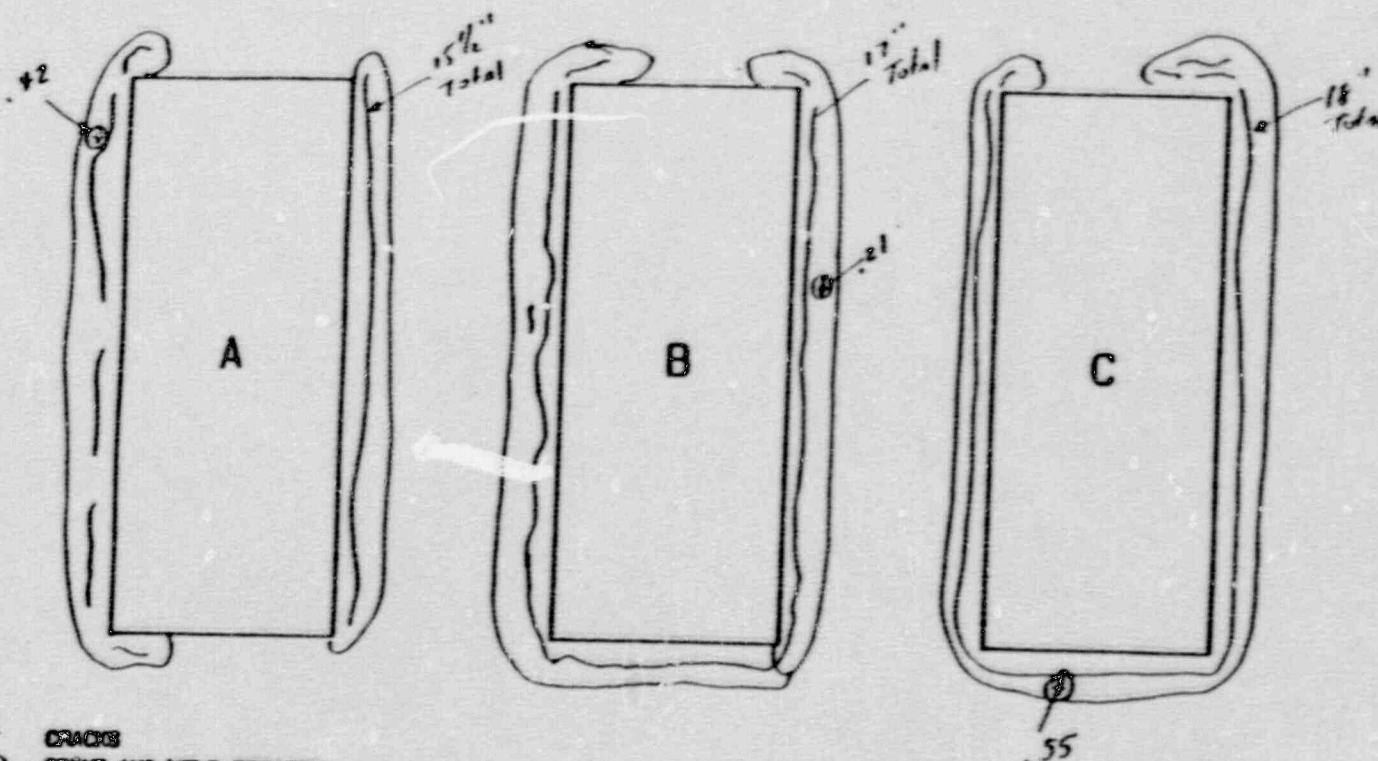
①


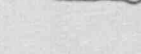
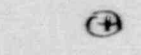


CRACKS  
GRIND AND WELD REPAIRS  
MAXIMUM DEPTH  
EXISTING GRINDOUT - NO INDICATIONS  
MAX DEPTH



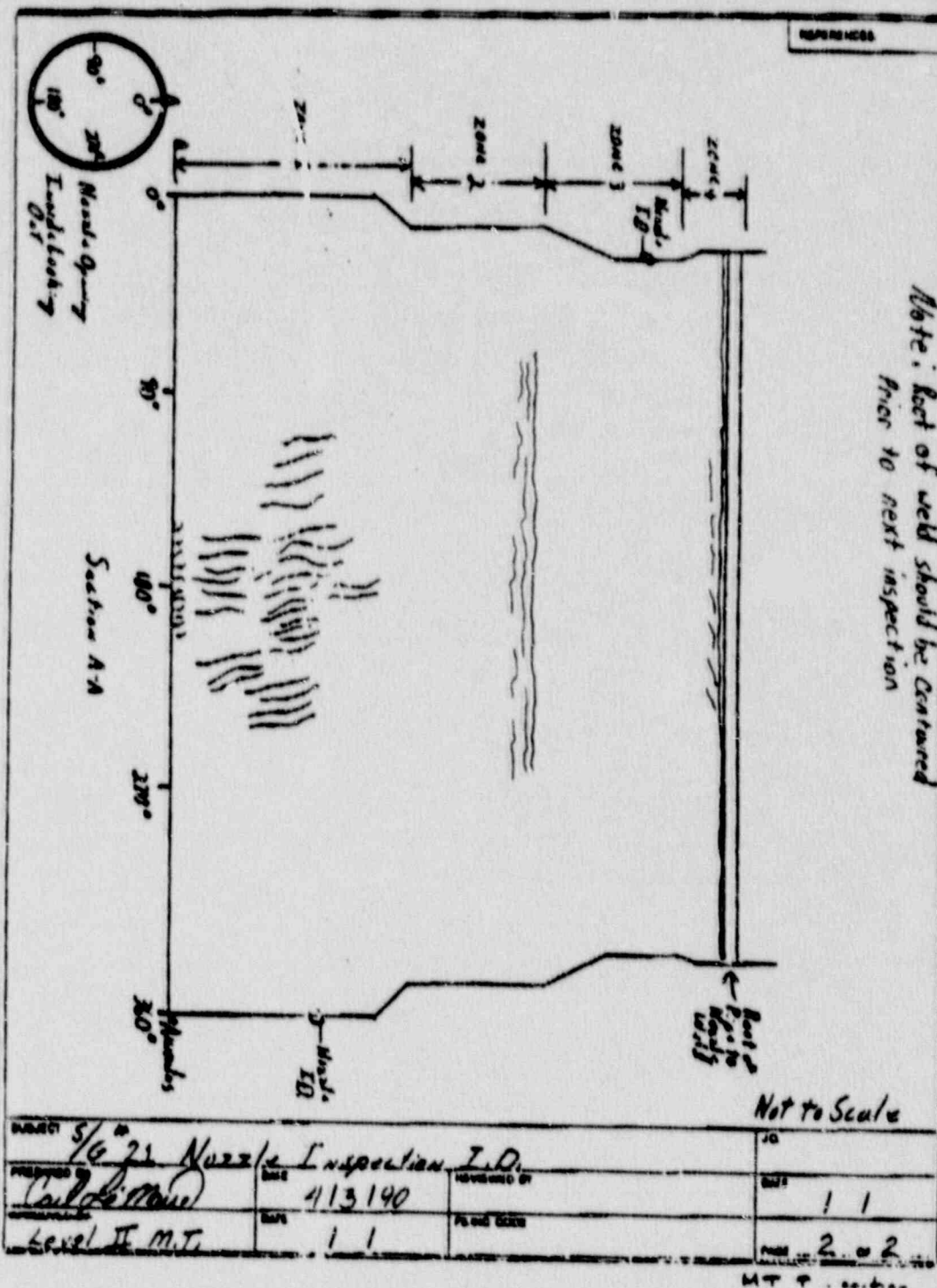


# INDIAN POINT 2 STEAM GENERATOR 24 FEED RING SUPPORT BRACKETS



 CRACKS  
 GRIND AND WELD REPAIRS  
 MAXIMUM DEPTH  
 EXISTING GRINDOUT - NO INDICATIONS  
 MAX DEPTH

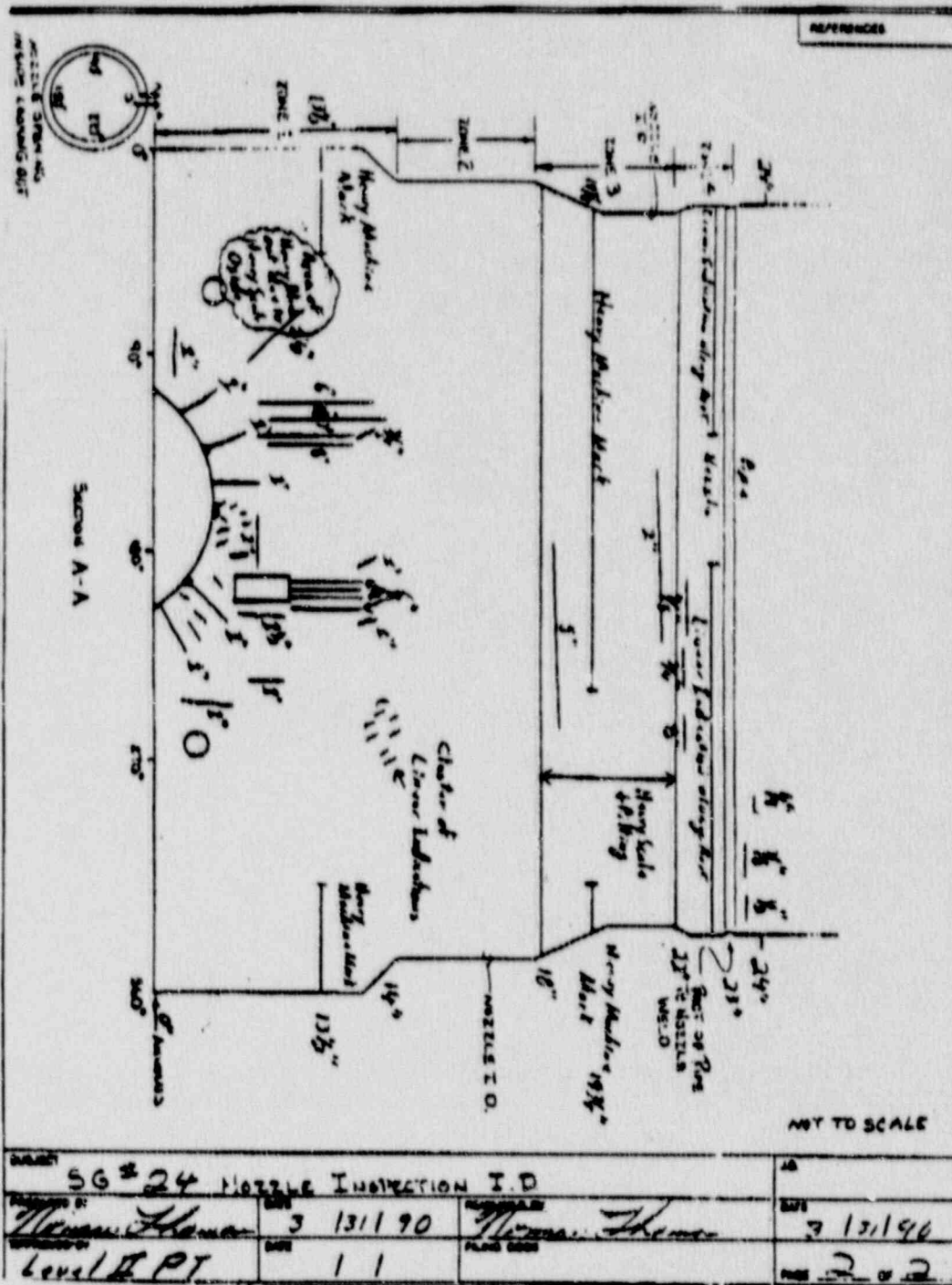
APPENDIX F  
FEEDWATER NOZZLE INSPECTION DATA



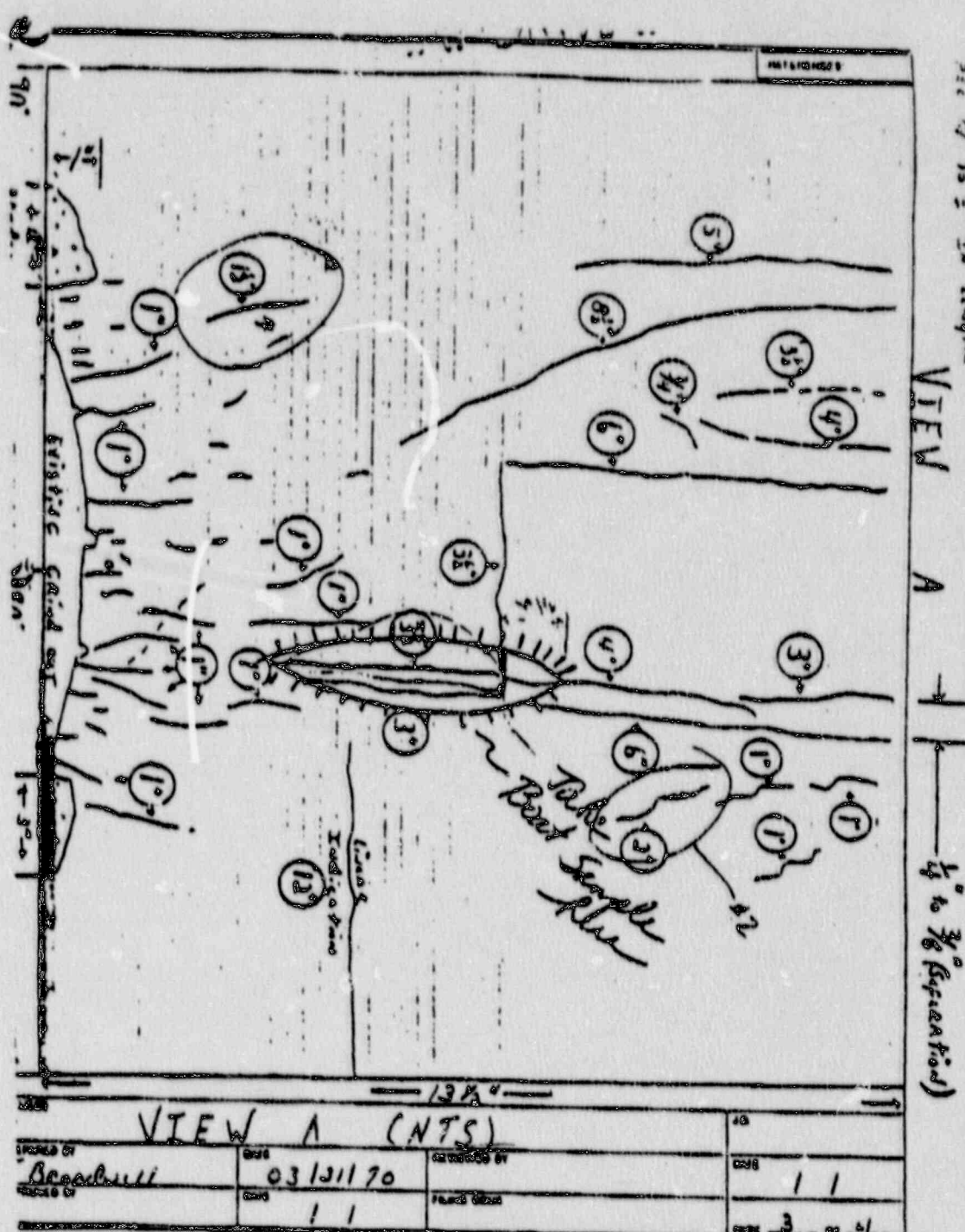




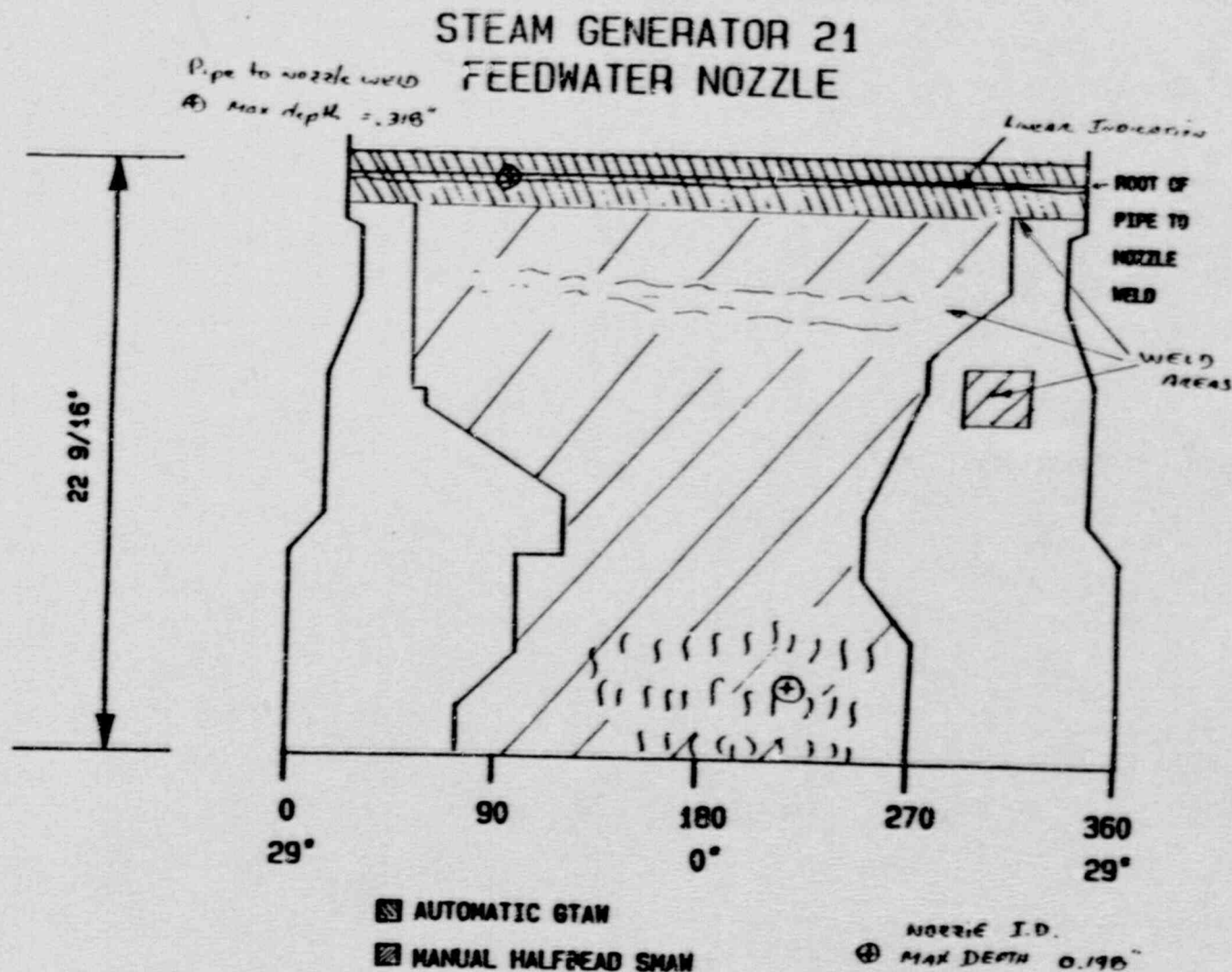








APPENDIX G  
FEEDWATER NOZZLE GRINDING AND REPAIR MAPS

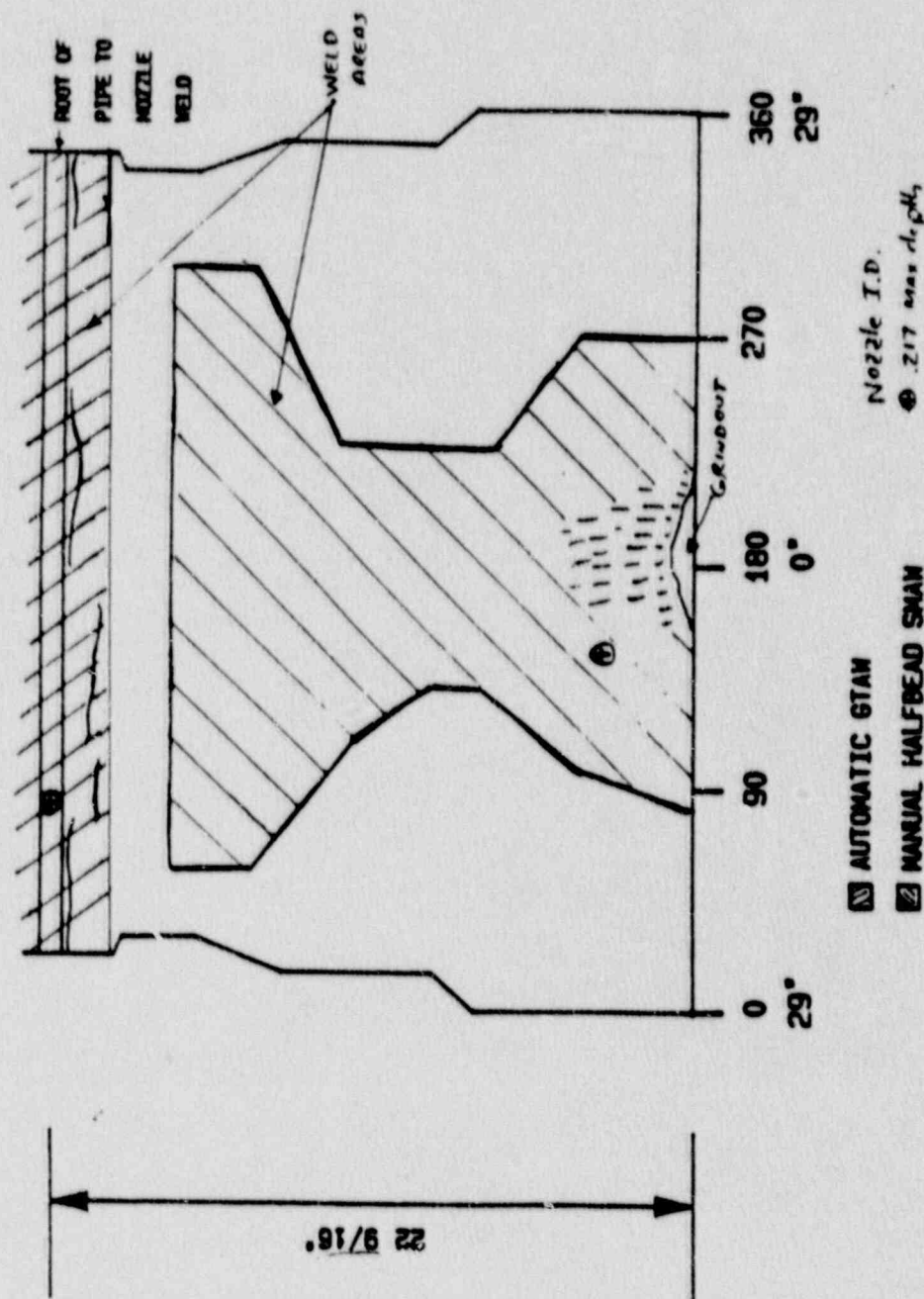






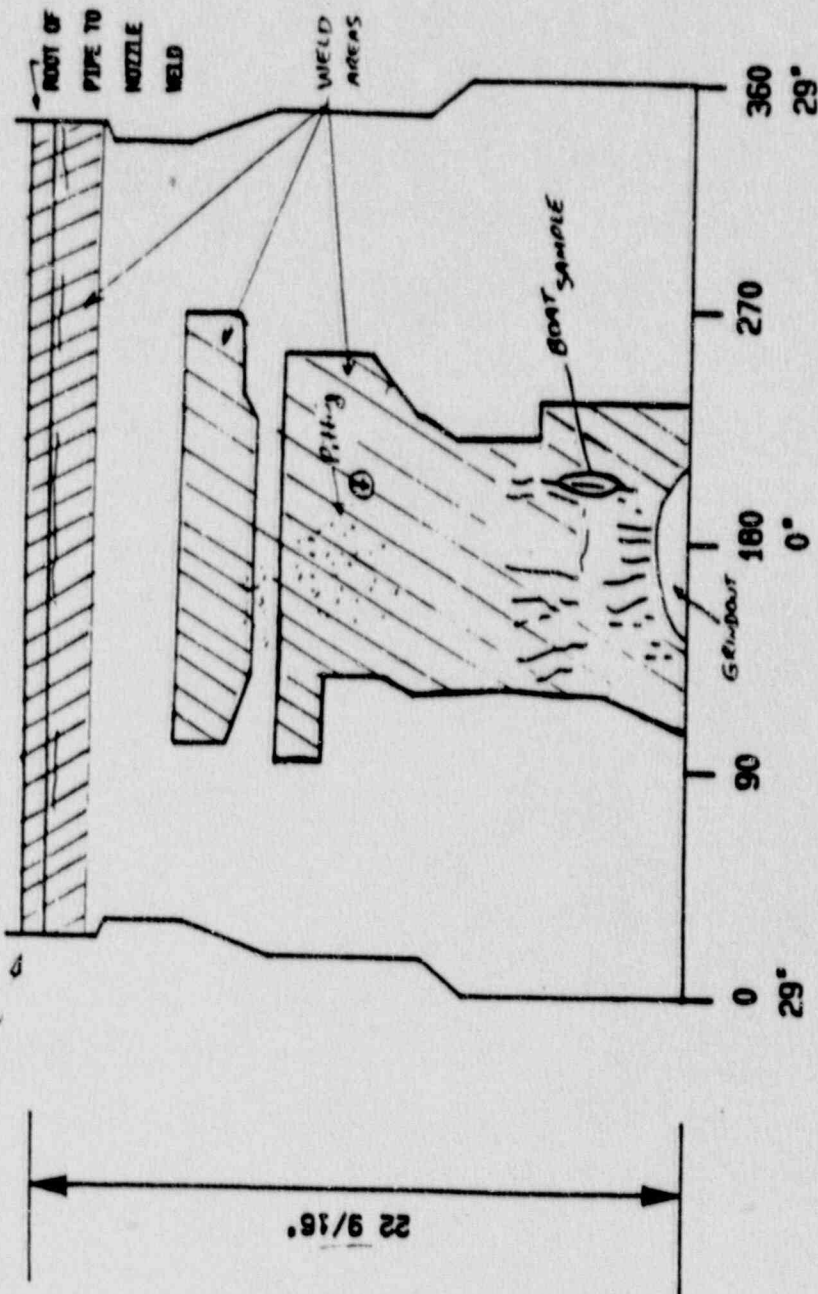
# STEAM GENERATOR 23 FEEDWATER NOZZLE

File to nozzle weld  
(3) 200" max depth



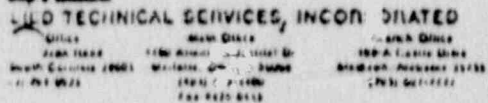
# STEAM GENERATOR 24 FEEDWATER NOZZLE

pipe to nozzle weld  
-270 max depth



- AUTOMATIC GTAW
- MANUAL HALFBEAD SHAW
- NOZZLE I.D.
- ④ .346" max depth

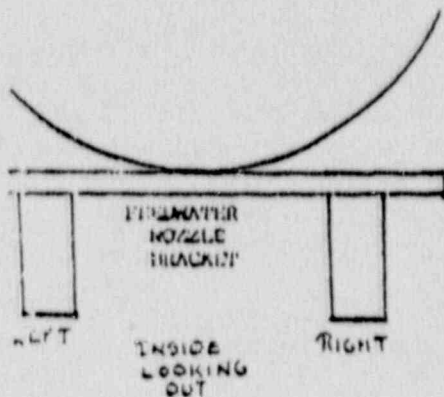




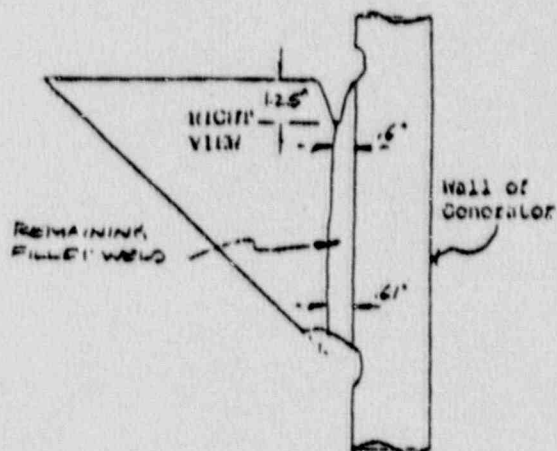
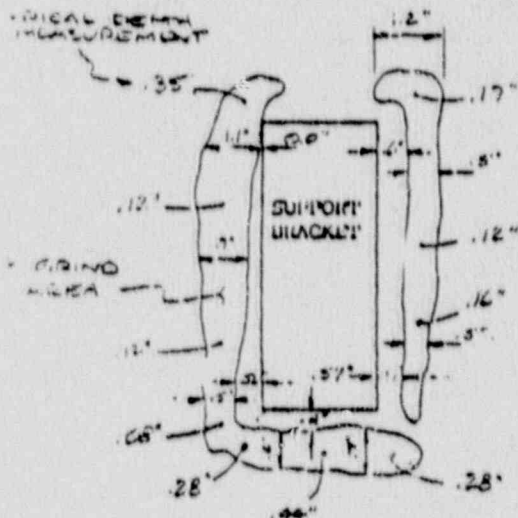
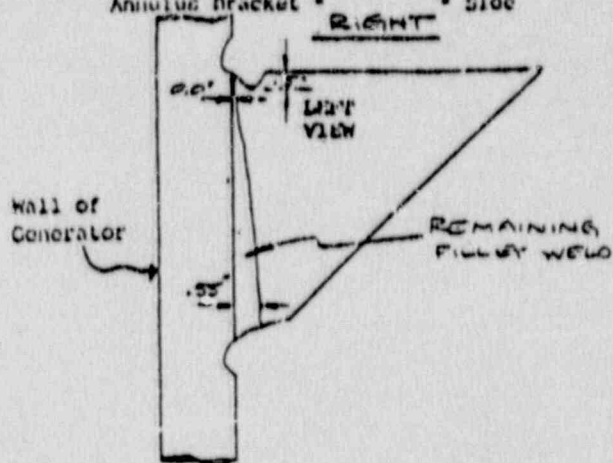
Date, 3-22-90  
 Gen Edison Indian Point Unit #2  
 Holding Services, Inc. Job #60012

STEAM CONDENSATOR # 2-1

Dimension and location of Excavated  
Areas on the Feedwater Nozzle  
Annulus Bracket \* \* Side



NOTE: EXCAVATED AREAS HAVE NOT BEEN CONTOUNDED OR PREPARED FOR WELDING

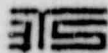


NOTE: Before Contours

Inspection Performed By:

Level: II vfr

Level 4.5 VIT



JTS TECHNICAL SERVICES, INCORPORATED

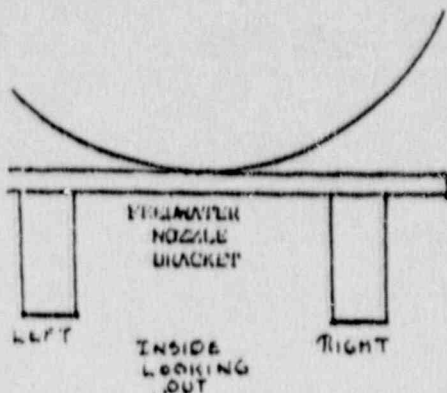
Office: 1100 Atlantic Industrial Dr. South Carolina 29001 (803) 722-1400  
Main Office: 100-A Castle Blvd. Madison, Alabama 37033 (615) 507-1111  
Branch Office: 100-A Castle Blvd. Madison, Alabama 37033 (615) 507-1111

Page 2 of 5

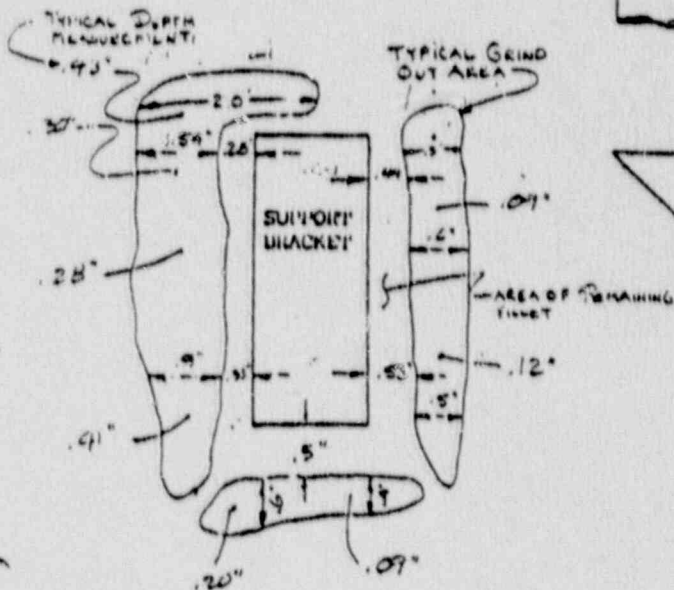
No. PTA06136 IP60012-21-12B

Date 3-22-90

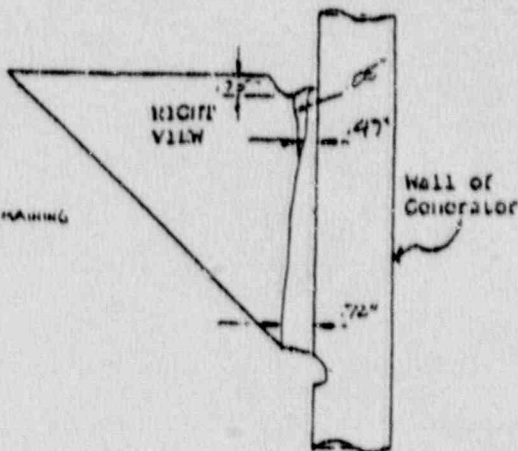
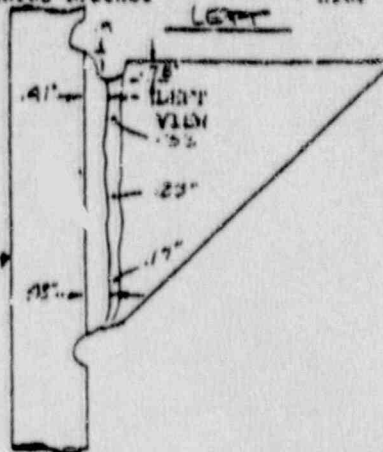
Con Edison Indian Point Unit #2  
Welding Services, Inc. Job #60012



NOTE: EXCAVATED AREAS HAVE NOT BEEN CONTOURED OR PREPARED FOR WELDING

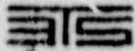


STREAM CONDENSER # 21  
Dimension and location of Excavated Areas on the Feedwater Nozzle Annulus Bracket " LEFT " Side



NOTE: Before Contour

Inspection Performed By: David J. Bond Level II VI  
David J. Bond Level One VI



**EDISON TECHNICAL SERVICES, INCORPORATED**  
 SA Office: 15 Monticello Street, New York, NY 10014  
 MA Office: 1100 Atlantic Industrial Dr., Worcester, MA 01601  
 FL Office: 1800 N. Dixie Ave., Ft. Lauderdale, FL 33305  
 TX Office: 15000 Highway 25138, Houston, TX 77058  
 CA Office: 10000 Wilshire Blvd., Los Angeles, CA 90024

Page 3 of 5

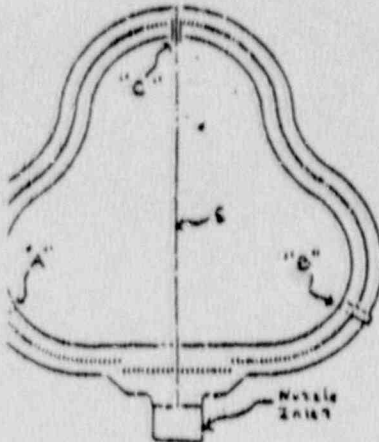
Ref. PIA 06126 IP 60012-21-120

Date 3-22-90

CON Edison Indian Point Unit #2  
 Holding Services, Inc. Job #G0012

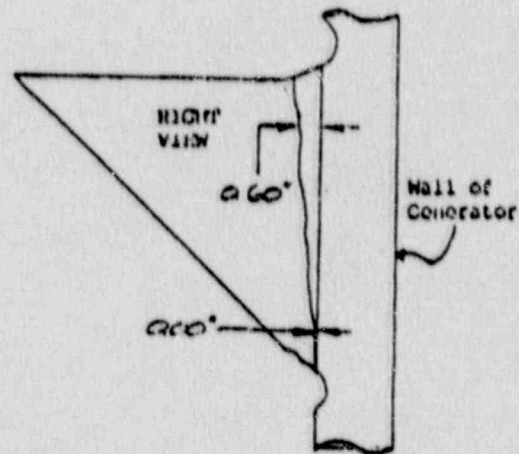
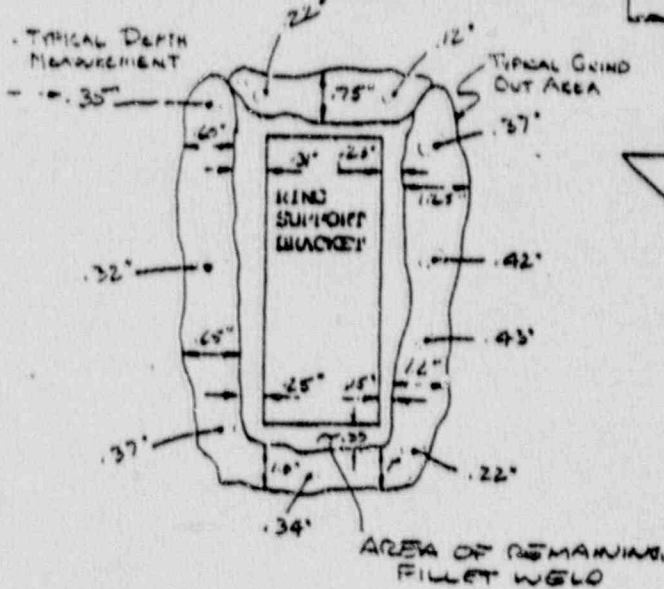
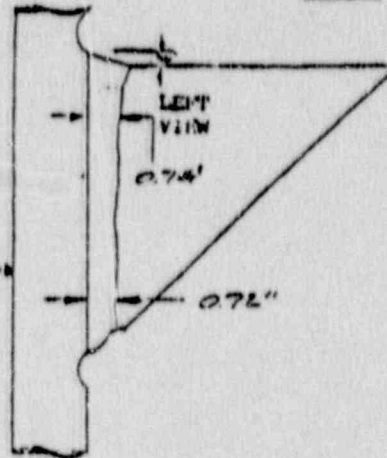
**STEAM GENERATOR # 21**

Dimension and Location of Excavated Areas on the Feedwater Ring Support Attachment Bracket "A"



NOTE: CAVITIES NOT  
 OUTPOURED OR PREPARED  
 FOR WELDING.

Wall of Generator



Note Before Contain

Inspection Performed By: John J. Miller for Period of Cont. Level II VT  
John J. Miller Level III VT





# STEEL TECHNICAL SERVICES, INCORPORATED

A. Office: 1000 N. Central Ave., Suite 100, Oklahoma City, Oklahoma 73102  
 B. Office: 1000 N. Central Ave., Suite 100, Oklahoma City, Oklahoma 73102  
 C. Office: 1000 N. Central Ave., Suite 100, Oklahoma City, Oklahoma 73102

Page 4 of 5

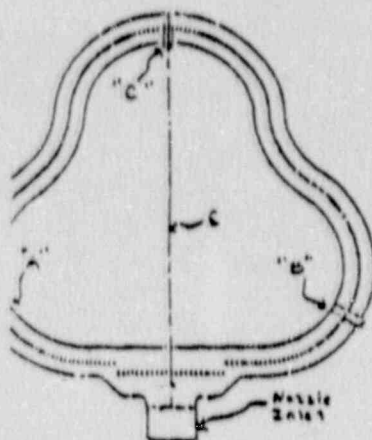
Ref. PFA 06120 J.P. 00012-21-12.0

Date 3-22-90

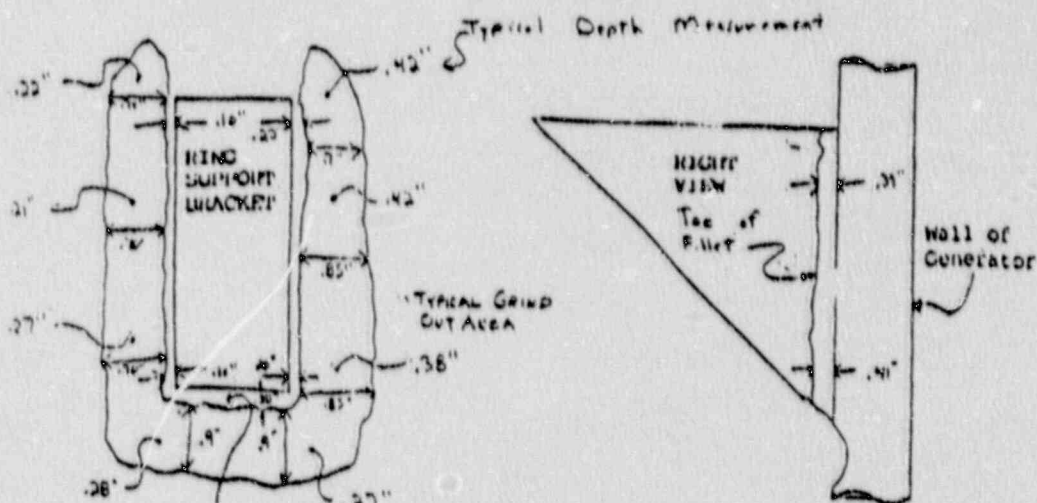
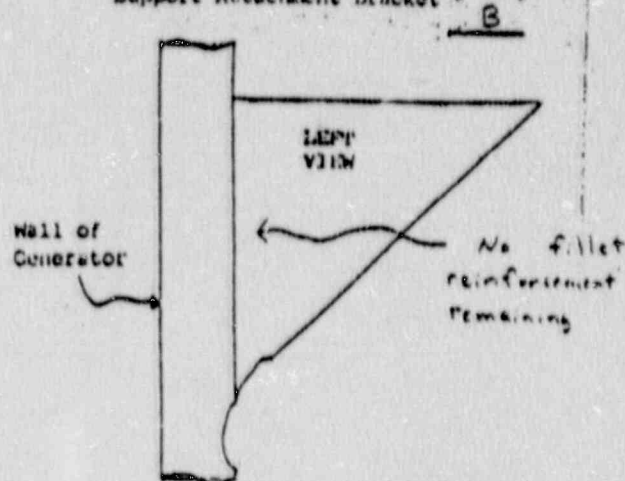
Con Edison Indian Point Unit #2  
Welding Services, Inc. Job #00012

STEAM GENERATOR # 21

Dimension and Location of Excavated Area on the Feedwater Ring Support Attachment Bracket



Areas of excavation have been contoured for welding to a 2:1 slope.



Area of remaining fillet

Note Before Contour

Inspection Performed By: John J. P. [Signature] Level VT  
[Signature] Level GTG

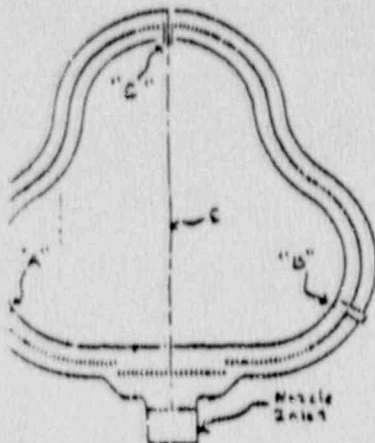


Ref. PIA 06126 IP60012-21-128  
Date 3-22-90

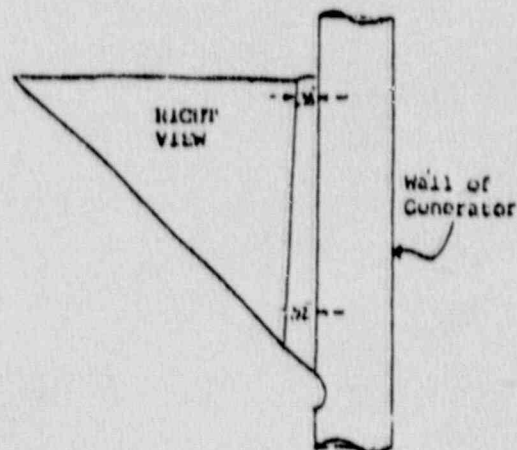
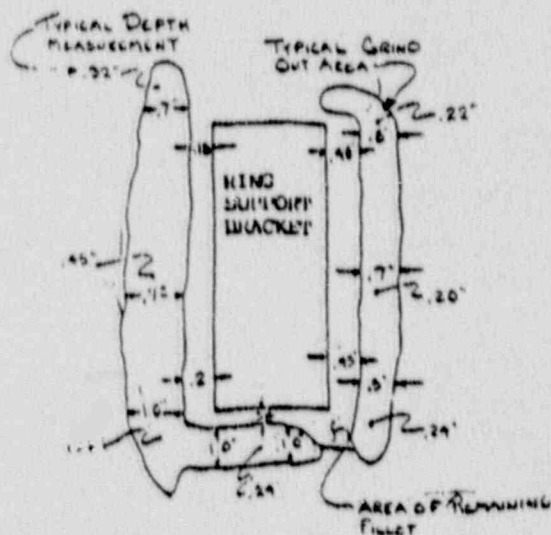
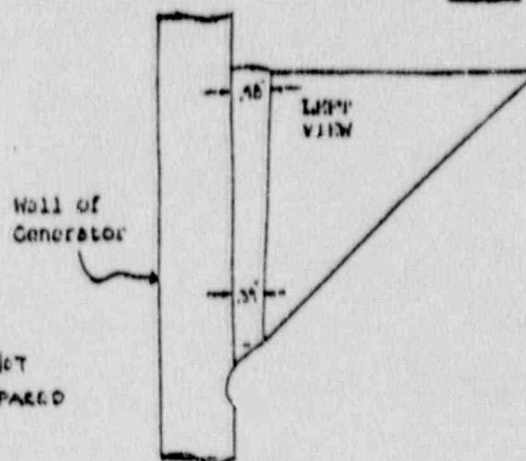
Can Edison Indian Point Unit #2  
Welding Services, Inc. Job #00012

STEAM GENERATOR # 21

Dimension and Location of Excavated Areas on the Feedwater Riser Support Attachment Bracket " " "

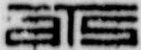


NOTE: EXCAVATED AREAS HAVE NOT BEEN CONTOURED OR PREPARED FOR WELDING.



Note Below Contain

Inspection Performed by John J. Miller for David Cook Level II VI  
Continued above Level II VI



APPLIED TECHNICAL SERVICES, INCORPORATED

Service Office: 1100 N. 10th St., Suite 100, Fargo, ND 58102  
Main Office: 1100 N. 10th St., Suite 100, Fargo, ND 58102  
Branch Office: 1100 N. 10th St., Suite 100, Fargo, ND 58102

Page 552 of 552

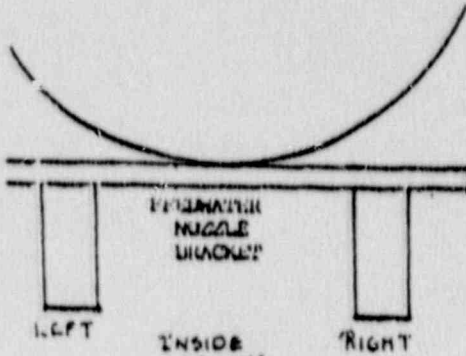
Ref: 172-06176 1P-60012-24-97

Date: 3-24-90

Con Edison Indian Point Unit #2  
Welding Services, Inc. Job #60012

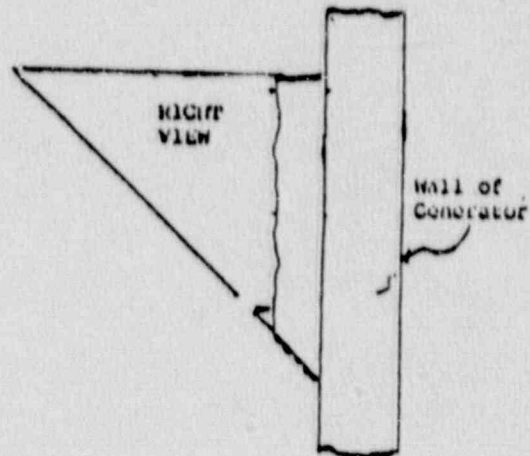
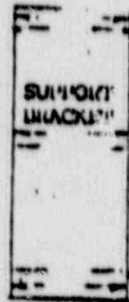
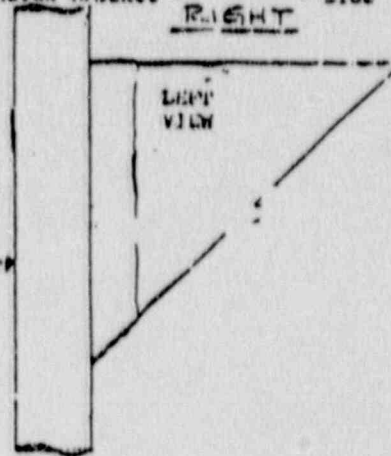
### SITING GENERATOR # 22

Dimension and location of Excavated Areas on the Feedwater Nozzle Minimum Bracket "RIGHT" Side



NOTE: CAVITIES NOT OUTLINED BY PREVIOUS WORK.

Wall of Generator

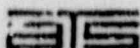


No INDICATIONS

Client  
Approved

Inspection Performed By: \_\_\_\_\_ Level: VR





APPLIED TECHNICAL SERVICES, INCORPORATED

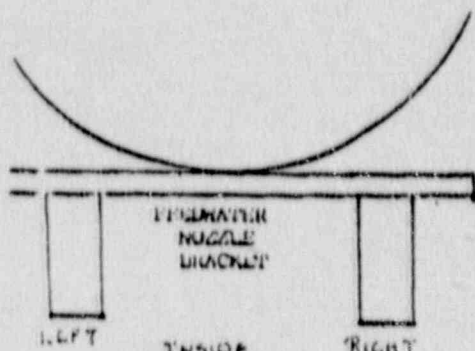
South Office: 1100 Avenue C, Suite 100, San Francisco, CA 94103  
 West Office: 1100 Avenue C, Suite 100, San Francisco, CA 94103  
 East Office: 1100 Avenue C, Suite 100, San Francisco, CA 94103

Page 32 of 32  
 Ref. Mr. G. L. 12/12/70 IP-10012-2-2-70  
 Date 3-27-70

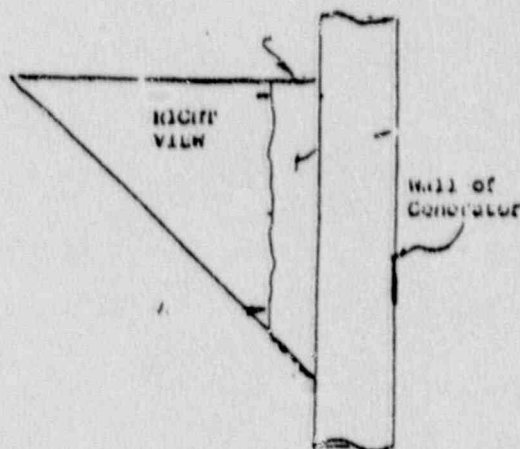
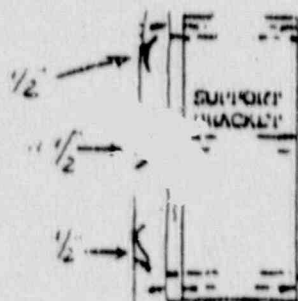
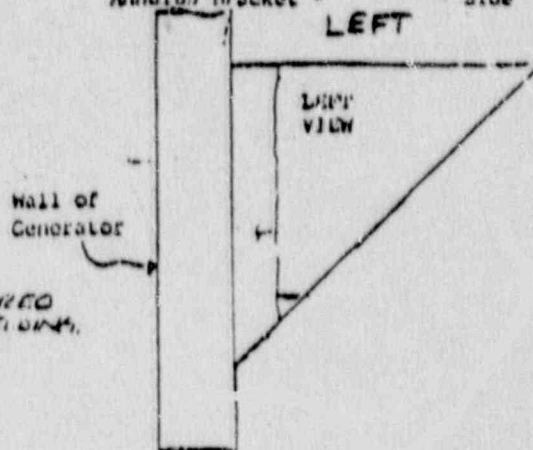
Con Edison Indian Point Unit #2  
 Welding Services, Inc. Job #00012

# SITING CONSTRUCTION # 22

Dimension and location of Excavated  
 Areas on the Feedwater Nozzle  
 Annular Bracket " Side



NOTE: CAVITIES NOT DIMENSIONED  
 EX. DIMENSIONED FOR SECTION.



Client

Inspection Performed By:

Level -- VP

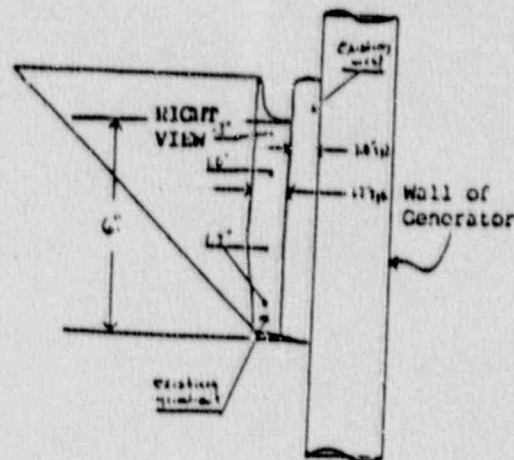
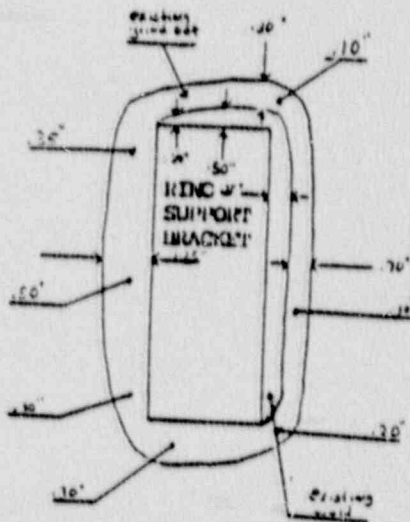
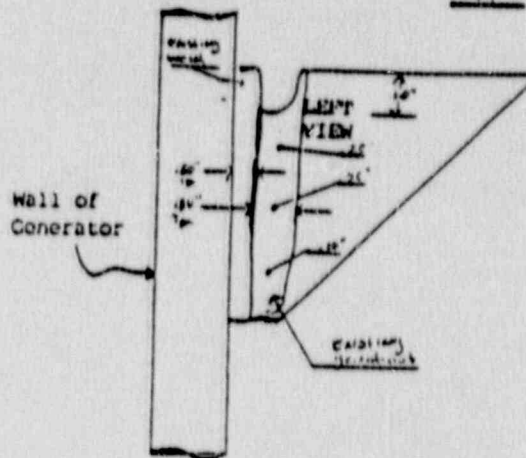
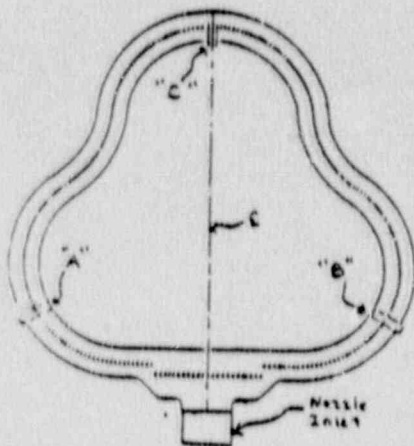
Ref. PIA 06126

Date 4-19-90

Con Edison Indian Point Unit #2  
 Welding Services, Inc. Job #G0012

**STEAM GENERATOR # 22**

Dimension and Location of Excavated  
 Areas on the Feedwater Ring  
 Support Attachment Bracket "A"



Client Approval: \_\_\_\_\_ Inspection Performed By: K.P. Jones Level II VT  
 Level \_\_\_\_\_ VT



**APPLIED TECHNICAL SERVICES, INCORPORATED**

MEMPHIS OFFICE: 1115 GERMANTOWN ROAD, MEMPHIS, TENNESSEE 38103, (901) 725-9511  
 MIAMI OFFICE: 1100 CANAL DRIVE, MIAMI, FLORIDA 33136, (305) 422-1000  
 SEATTLE OFFICE: 100 N. LOMB ST., SEATTLE, WASHINGTON 98101, (206) 447-1111

Page 2 of 3

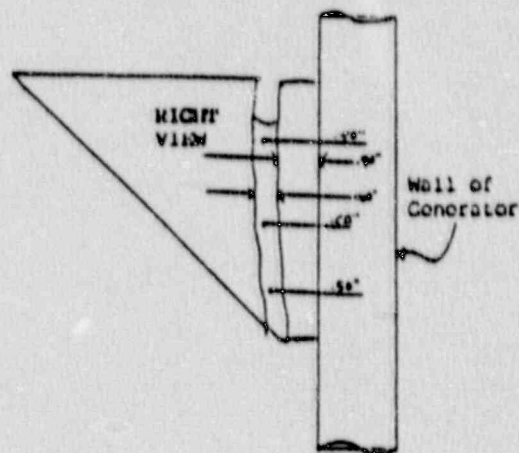
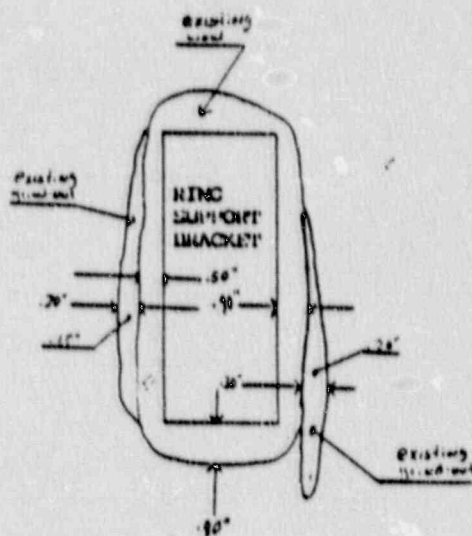
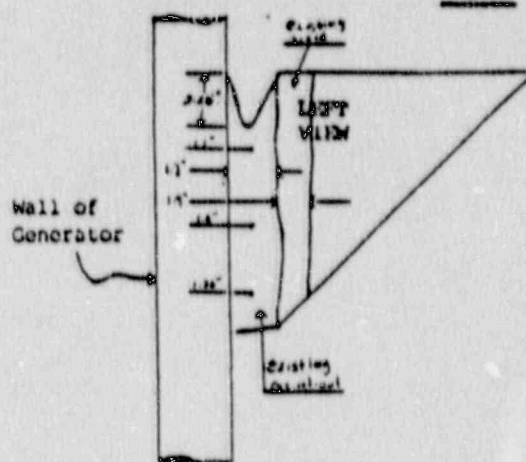
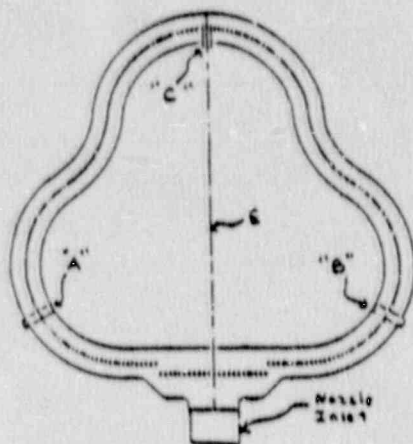
Ref. PIA 06126

Date 4-17-70

Con Edison Indian Point Unit #2  
Welding Services, Inc. Job #G0012

**STEAM GENERATOR # 22**

Dimension and Location of Excavated Areas on the Feedwater Ring Support Attachment Bracket "B"



Client  
Approval

Inspection Performed By: Kip Jones

Level II VT  
Level VT



**ATC**  
**APPLIED TECHNICAL SERVICES, INCORPORATED**  
 1715 W. 10th Street, Suite 100, Oklahoma City, Oklahoma 73106  
 (405) 241-1111  
 1101 Atlantic Industrial Dr., Oklahoma City, Oklahoma 73106  
 (405) 241-1111  
 100-A Canal Drive, Oklahoma City, Oklahoma 73106  
 (405) 241-1111

Page 3 of 3

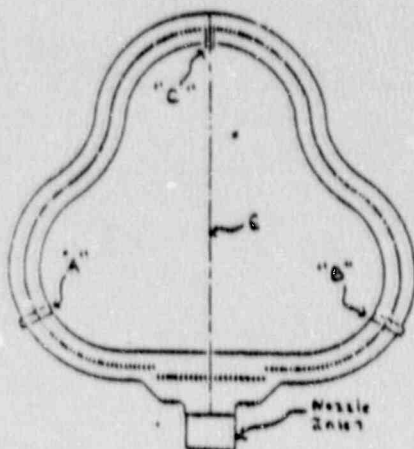
Ref. MIA 06126

Date 4-19-90

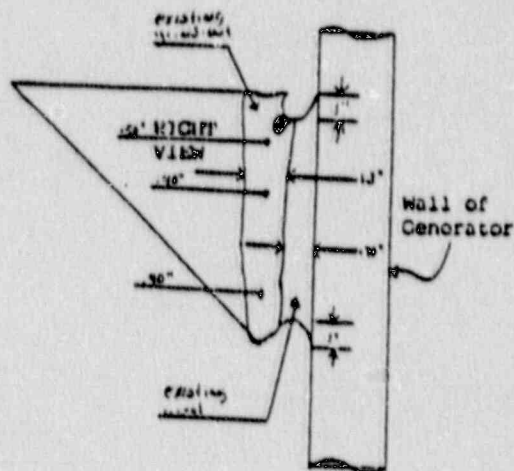
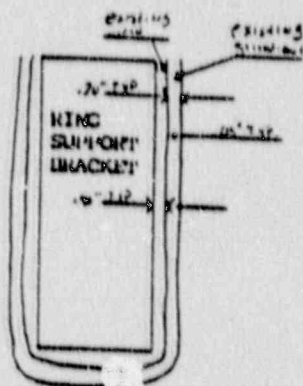
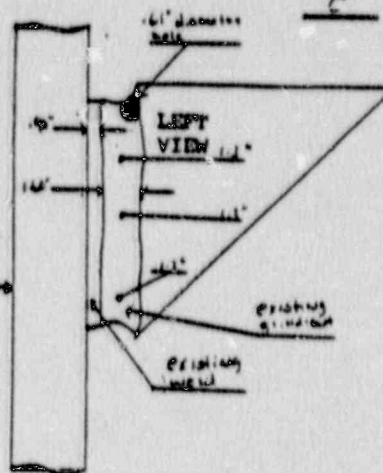
Con Edison Indian Point Unit #2  
 Welding Services, Inc. Job #00012

STEAM GENERATOR # 22

Dimension and Location of Excavated  
 Areas on the Feedwater Ring  
 Support Attachment Bracket "



Wall of  
 Generator

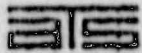


Client  
 approval \_\_\_\_\_

Inspection Performed By K.P. Jones

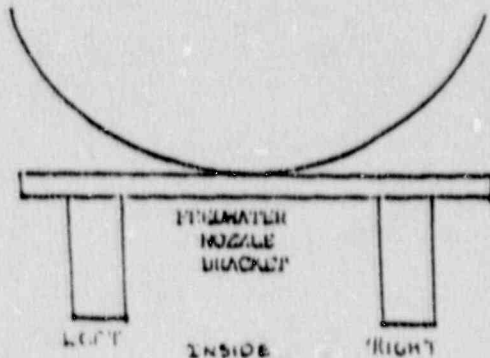
Level II VT

Level \_\_\_\_\_ VI



APPLIED TECHNICAL SERVICES, INCORPORATED

Branch Office: 1210 S. W. 10th Ave., Miami, FL 33135  
 Branch Office: 1100 Atlantic Blvd., Miami, FL 33135  
 Branch Office: 1000 N. E. 10th Ave., Miami, FL 33135



NOTE: CAVITIES NOT CONFOURED OR PREPARED FOR WELDING.



(SEE ATTACHED FOR GENERATOR WALL GRIND OUTS.)

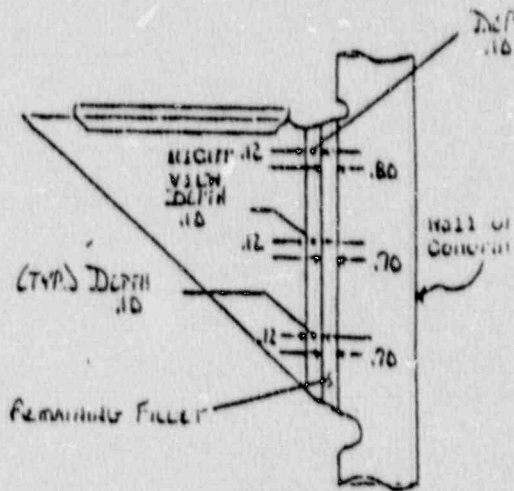
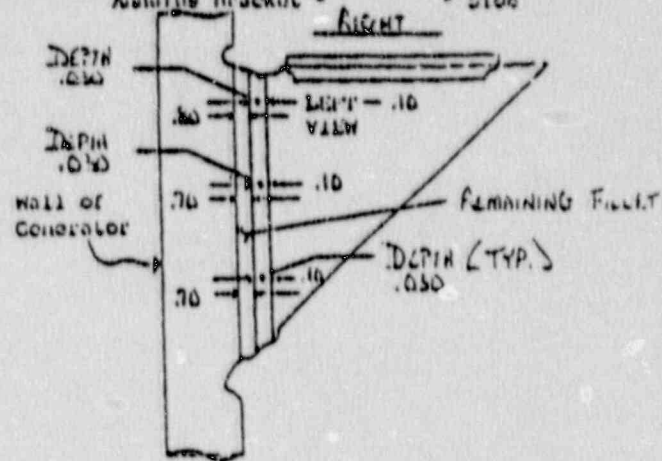
Net. PTA 00136 JP 00012-21-107

Date 2-23-90

CON EDISON Indian Point Unit #2  
 Welding Services, Inc. Job #00012

STEAM GENERATOR # 23

Dimension and location of Excavated Areas on the Feedwater Nozzle Assembly Bracket - Side

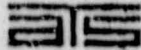


Client Approval \_\_\_\_\_

Inspection Performed By: [Signature]

Level JP

Level \_\_\_\_\_



APPLIED TECHNICAL SERVICES, INCORPORATED

San Diego Office  
1218 San Diego Ave.  
San Diego, California 92101  
(619) 591-0511

San Diego Office  
1100 Alameda Blvd.  
San Diego, California 92101  
(619) 591-0511

San Diego Office  
100 A Cedar St.  
San Diego, California 92101  
(619) 591-0511

Page 2 of 2

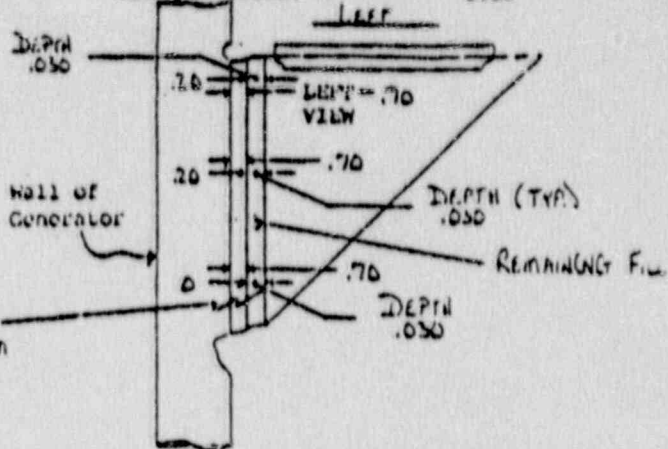
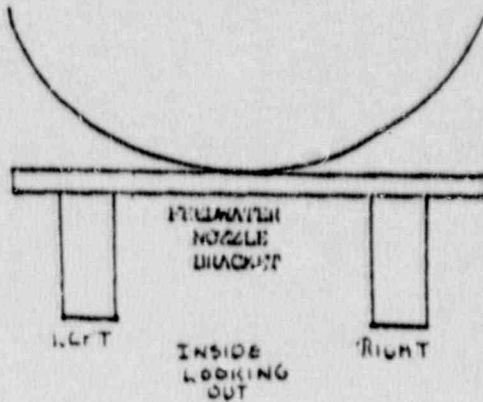
Ref. PTA 06126 IP-00012-23-107

Date 7-23-90

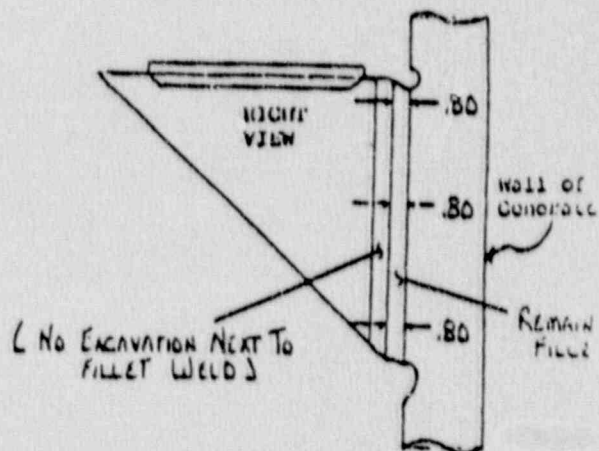
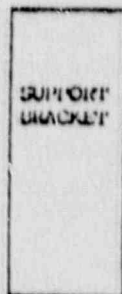
Con Edison Indian Point Unit #2  
Welding Services, Inc. Job #00012

STEAM GENERATOR # 23

Dimension and location of excavated  
area on the Feedwater Nozzle  
Annulus Necked "Side"



NOTE: CAVITIES NOT CONTOURED  
OR TREATED FOR WELDING.



(SEE ATTACHED FOR GENERATOR  
WALL GRIND OUT.)

Client  
Approval

Inspection Performed By:

*Jim G. Hilde*

Level II V

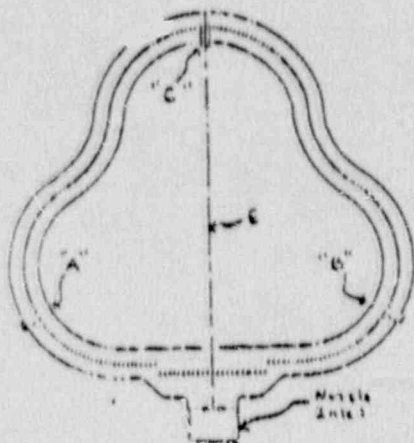
Level    V



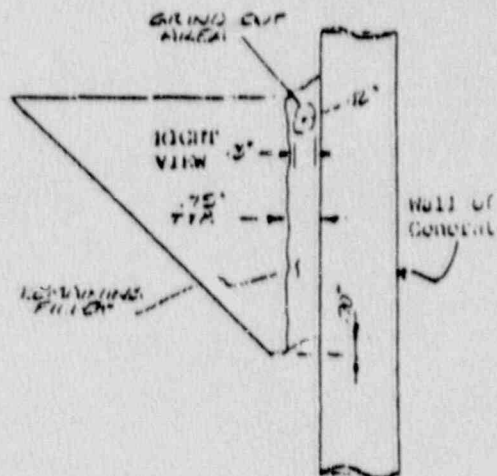
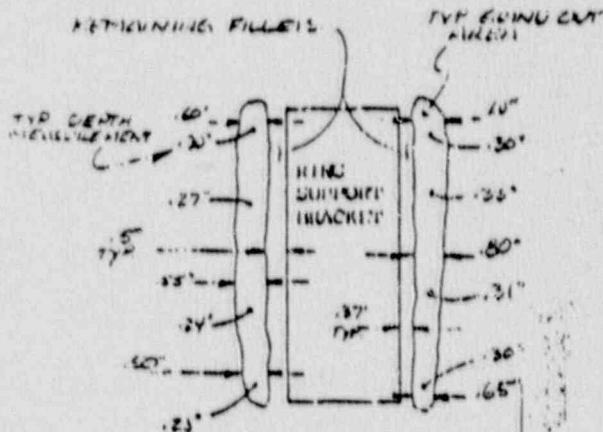
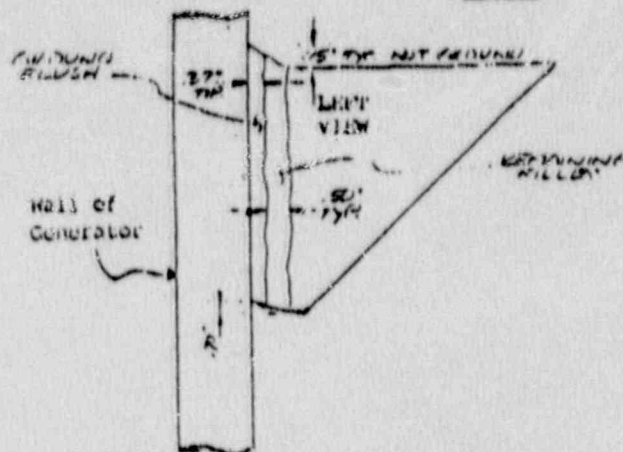
On Order: Indian Point Unit #2  
 Welding Services, Inc. Job #00012

**STEAM GENERATOR # 23**

Dimension and Location of Excavated Area on the Feedwater Ring Support Attachment Bracket "A"



NOTE: CAVITIES NOT CONTIGUOUS  
 USE MILLER 1/2" FILLER WELDING



Chief  
 Approval

Inspection Performed By

*John S. Smith*  
*John S. Smith*  
 Level II  
 License 113

APPLIED TECHNICAL SERVICES, INCORPORATED

| French Office          | French Office          | French Office          |
|------------------------|------------------------|------------------------|
| 1111 (Nagasaki) Street | 1111 (Nagasaki) Street | 1111 (Nagasaki) Street |
| 1111 (Nagasaki) Street | 1111 (Nagasaki) Street | 1111 (Nagasaki) Street |
| 1111 (Nagasaki) Street | 1111 (Nagasaki) Street | 1111 (Nagasaki) Street |

Page 1 of 1

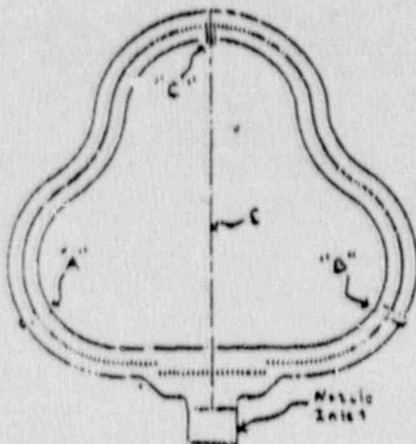
Ref. FIA C-26 IP 66012-23-105

Date 3-22-90

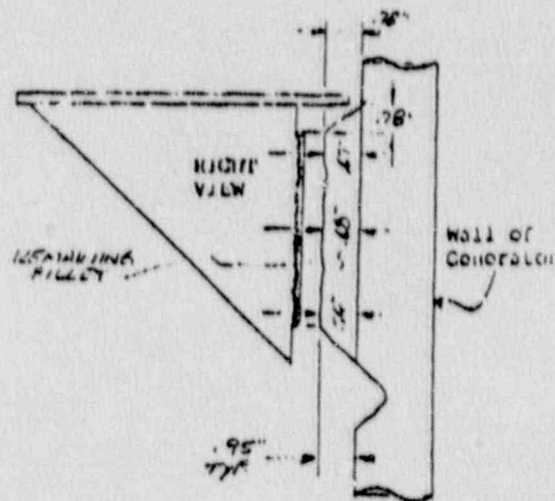
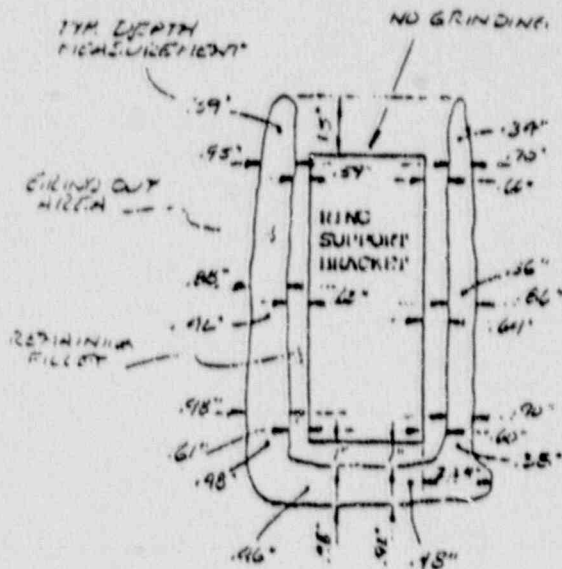
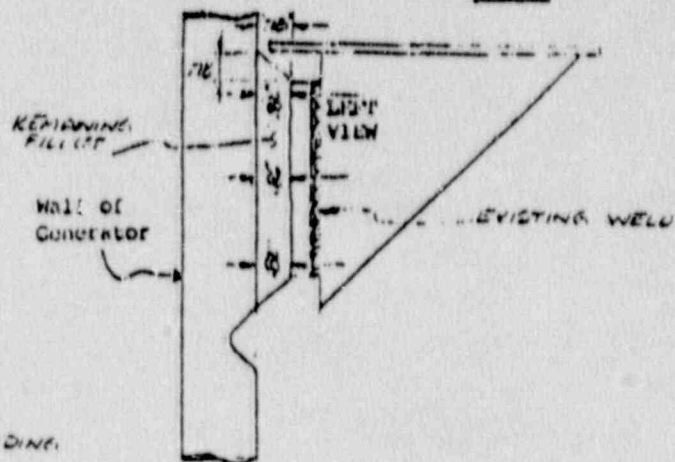
Can Edison Indian Point Unit #2  
Helding Services, Inc. Job #60012

SITAM CONFIDENTIAL • 23

Dimension and Location of Excavated Areas on the Feedwater Ring Support Attachment Bracket " " "



NOTE: CAVITIES NOT CONTAINED  
OR PREPARED FOR WELDING



### Control

Inspection Performed By: John J. [Signature] Level: VT  
Level: VT

APPLIED TECHNICAL SERVICES, INCORPORATED

| Branch Office                                                      | Branch Office                                                                               | Branch Office                                                         |
|--------------------------------------------------------------------|---------------------------------------------------------------------------------------------|-----------------------------------------------------------------------|
| 1278 Broadway Street<br>Brooklyn, New York 10002<br>(212) 791-9121 | 1100 Atlantic Boulevard N.<br>Norfolk, Virginia 23502<br>(804) 721-1000<br>Fax 804-721-1111 | 100 N. W. 11th Street<br>Miami Beach, Florida 33139<br>(305) 641-1111 |

FILE 157A 06126

Page 1 of 1

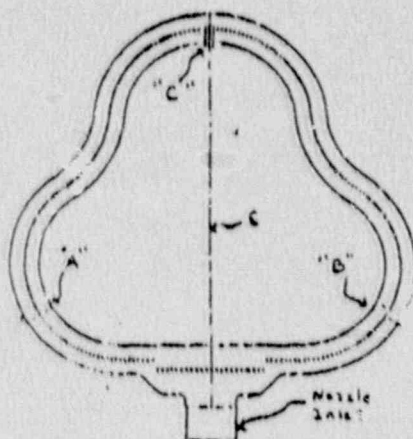
IP-CC-25-108

File 3-22-70

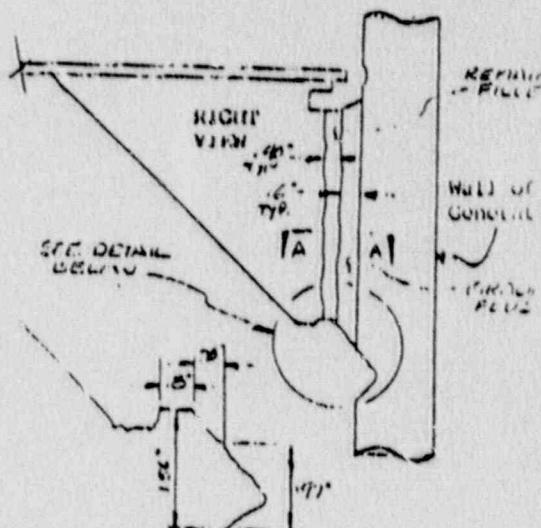
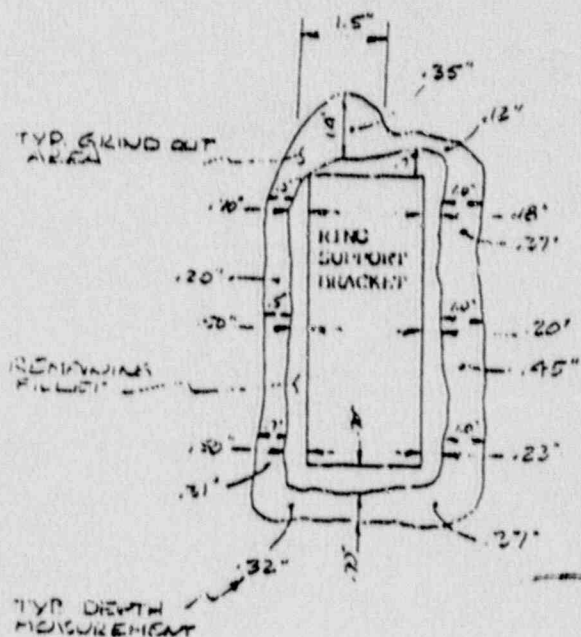
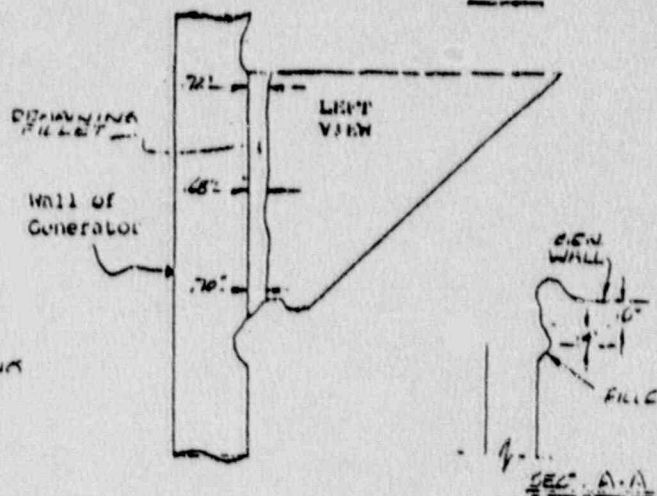
Con Edison Indian Point Unit #2  
Welding Services, Inc. JOB #00012

STEAM CONDENSATE 23

Dimension and Location of Excavated  
Areas on the Feedwater Ring  
Support Attachment Bracket " " "



NOTE CAVITIES NOT CONToured  
OR PREPARED FOR WELDING



Consent  
Acquiescence

Inspection Performed By:

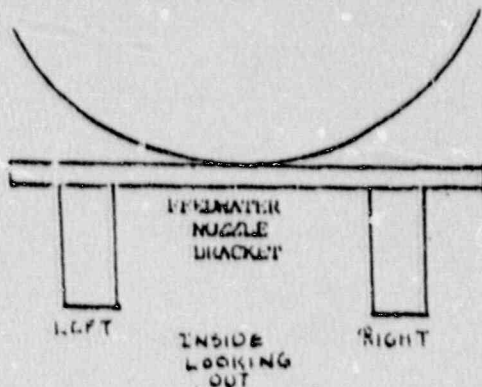
[illegible]



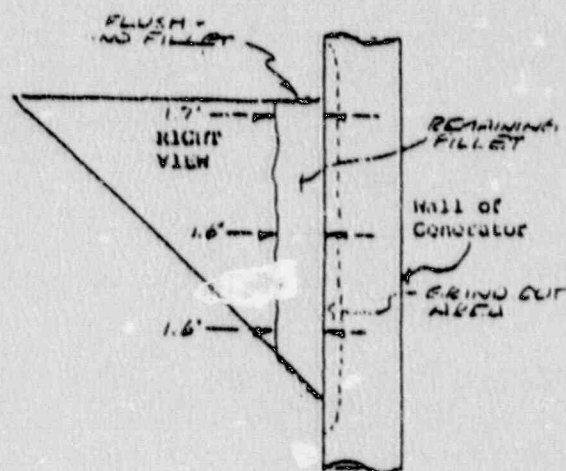
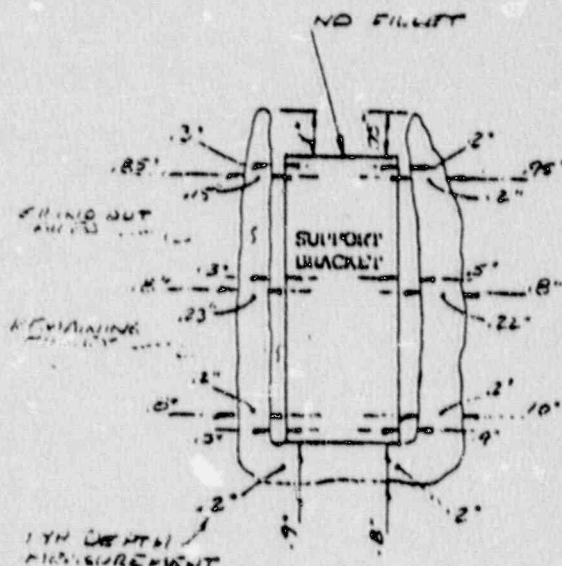
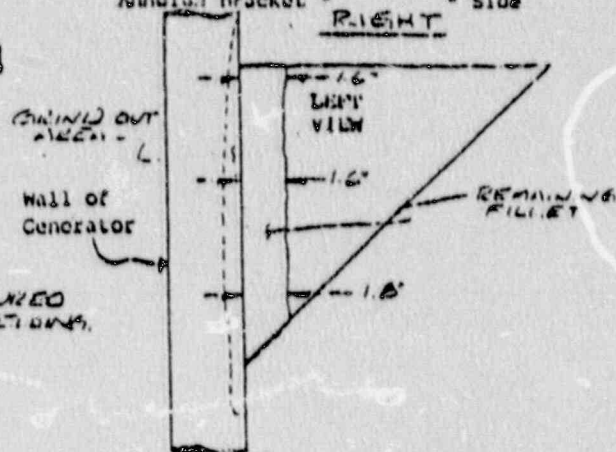


SITAM CONFIDENTIAL 24

Dimension and location of Excavated  
Areas on the Feedwater Nozzle  
Annular Bracket " " Side



NOTE: CAVITIES NOT STOUTURED  
BY MECHANIZED OR WELDING.



Inspection Performed By: William N. Lewis Level VP  
3/24/92 Level VP



APPLIED TECHNICAL SERVICES, INCORPORATED

Branch Office: 1125 N. 1st St., Suite 100, Milwaukee, WI 53233  
 Main Office: 1125 N. 1st St., Suite 100, Milwaukee, WI 53233  
 Branch Office: 1125 N. 1st St., Suite 100, Milwaukee, WI 53233

Page 1 of 2

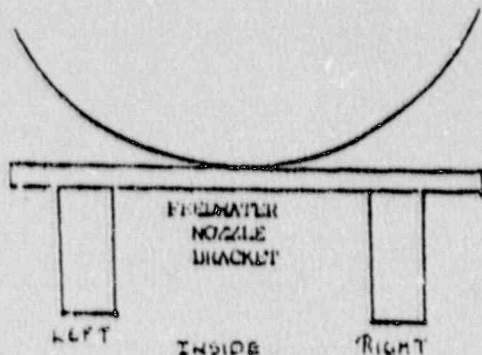
Ref. PTA 17-1760 TP-10002-24-97

Date 3-24-90

CON Edison Indian Point Unit #2  
 Welding Services, Inc. Job #00012

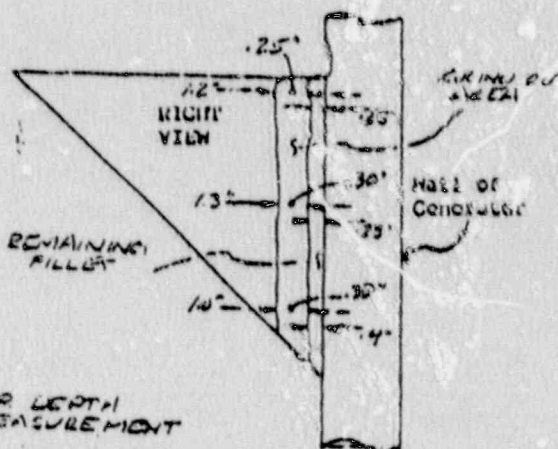
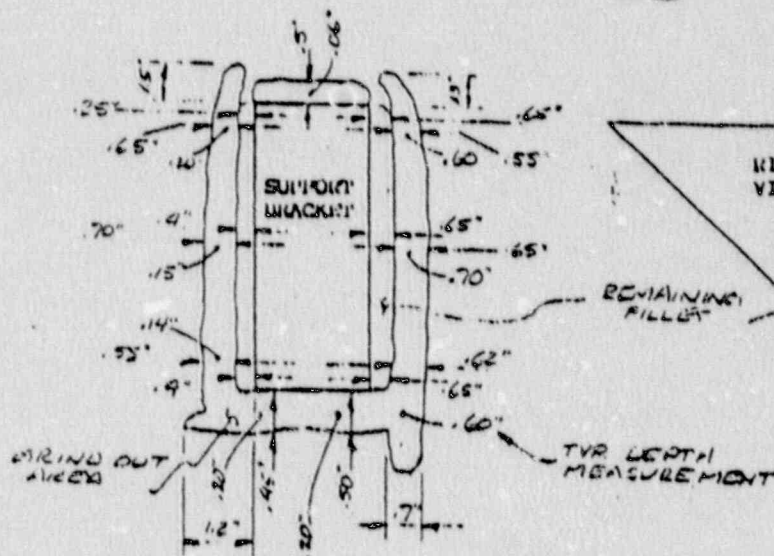
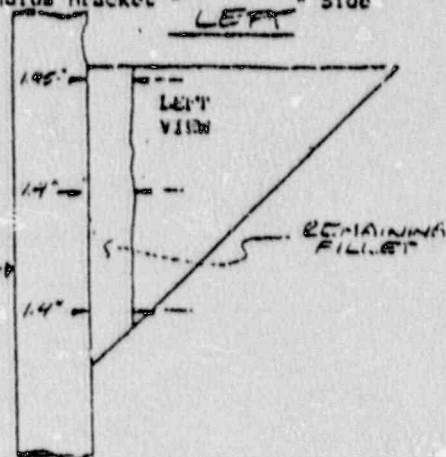
SKETCH CONTINUATION # 24

Dimension and location of Excavated Areas on the Feedwater Nozzle Annulus Bracket "LEFT" Side



NOTE: CAVITIES NOT CONTIGUOUS OR REPAIRED FOR WELDING

Wall of Generator



Client Approval \_\_\_\_\_

Inspection Performed By: \_\_\_\_\_

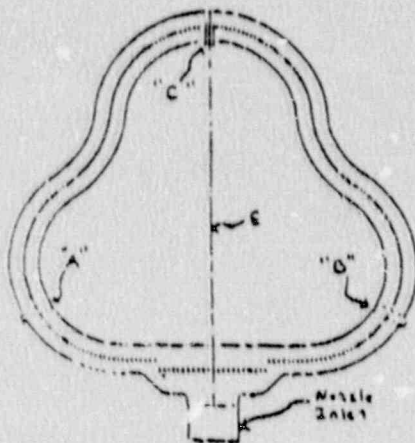
Level VT  
 Level OUT VT

**ATE**  
**APPLIED TECHNICAL SERVICES, INCORPORATED**  
 10000 100th Ave. N. #100  
 Minneapolis, MN 55428  
 (612) 835-1111  
 11000 100th Ave. N. #100  
 Minneapolis, MN 55428  
 (612) 835-1111  
 10000 100th Ave. N. #100  
 Minneapolis, MN 55428  
 (612) 835-1111

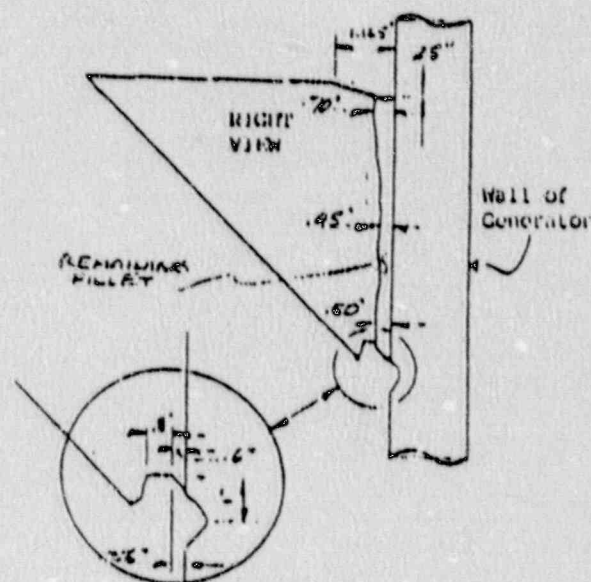
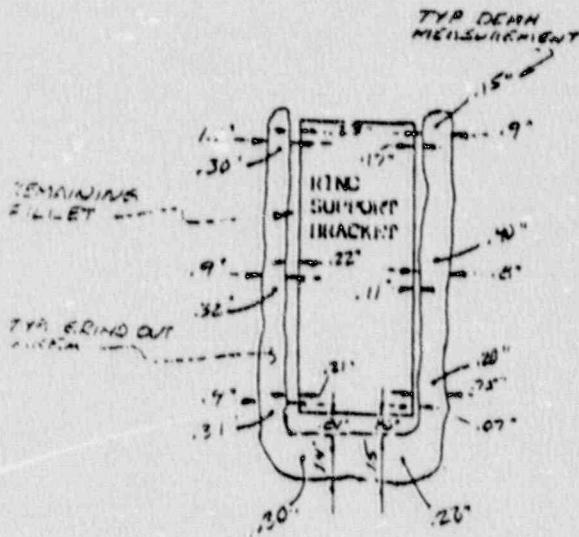
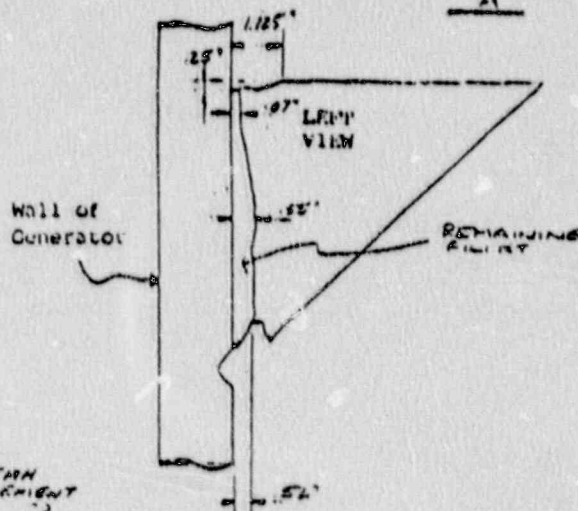
Page 1 of 3  
 Ref. TPA 00126  
 Date 3-23-90  
TP-C0012-24-95  
 Can Edison Indian Point Unit #2  
 Welding Services, Inc. Job #00012

SITAM CORRECTION B 24

Dimension and Location of Excavated Areas on the Feedwater Ring Support Attachment Bracket "A"



NOTE: CAVITIES NOT CONTOURED OR PREPARED FOR WELDING.



Inspection Performed By James J. [Signature] Level II VT  
[Signature] Level III VT

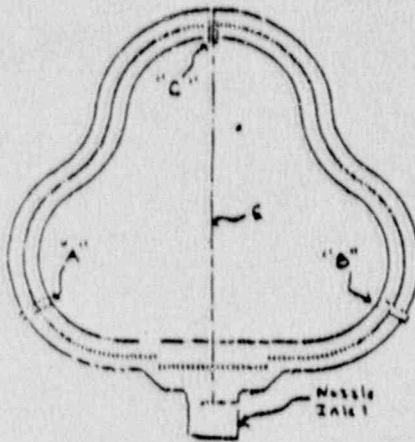


**ATS**  
**APPLIED TECHNICAL SERVICES, INCORPORATED**  
 Branch Office: 1100 Atlantic Industrial Dr., Mechanicsville, Virginia 23103  
 Branch Office: 1000 A. Lewis Drive, Mechanicsville, Virginia 23103  
 Branch Office: 1000 A. Lewis Drive, Mechanicsville, Virginia 23103

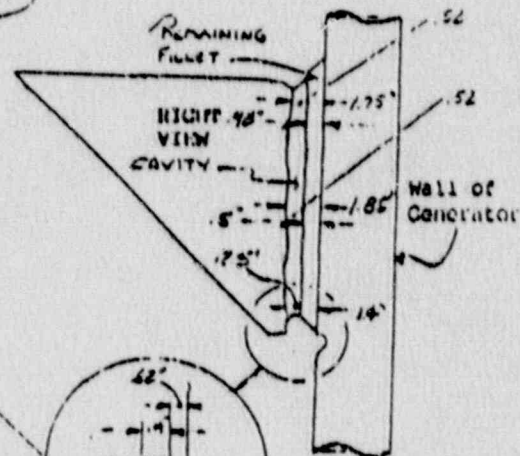
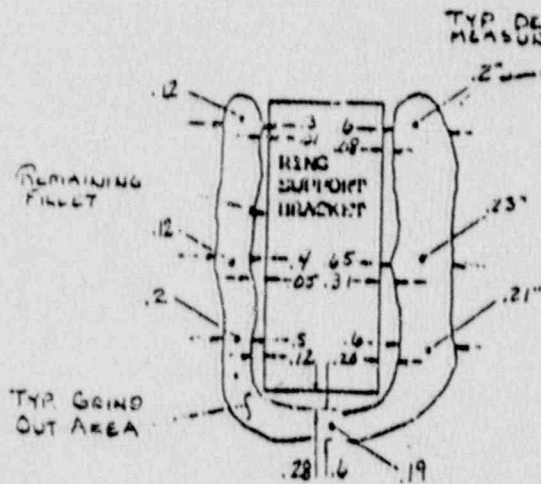
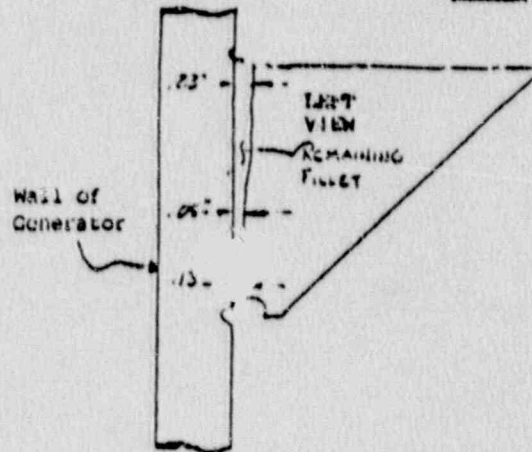
Page 3 of 3  
 No. MA 06176 LP 60012-24-95  
 Date 3-23-90  
 Con Edison Indian Point Unit #2  
 Welding Services, Inc. Job #00012

SITAM CRACKER # 24

Dimension and Location of Excavated Areas on the Pedestal Ring Support Attachment Bracket "B"



NOTE: CAVITIES NOT CONTOURED OR PREPARED FOR WELDING.



Consent

Inspection Performed by David Cochran Level II VT  
David Cochran Level VT



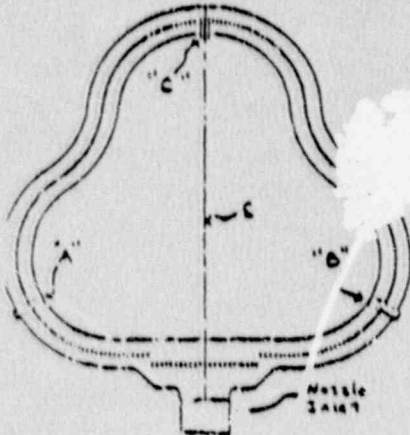
**APPLIED TECHNICAL SERVICES, INCORPORATED**  
 South Office: 1200 Charleston Road, Charlotte, North Carolina 28203, (704) 361-0121  
 Main Office: 1100 Atlantic Industrial Dr., Charlotte, North Carolina 28203, (704) 361-1000  
 Branch Office: 100 N. Centre Street, Winston-Salem, North Carolina 27101, (704) 361-1111

Page 3 of 3  
 No. WPA 06126 IP 60018-34-95  
 Date 3-23-97

Con Edison Indian Point Unit #2  
 Welding Services, Inc. Job #G0012

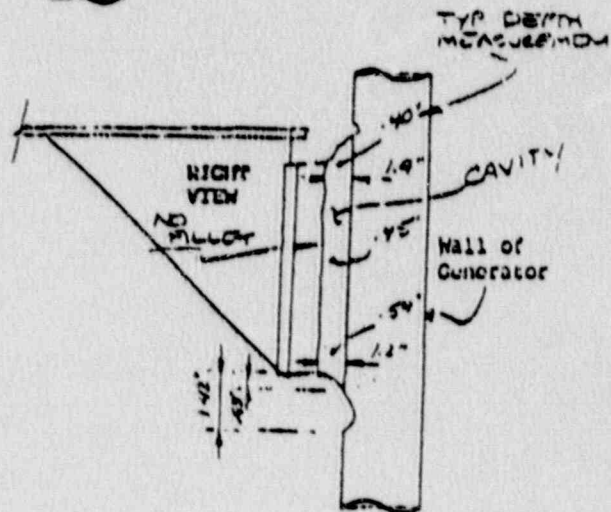
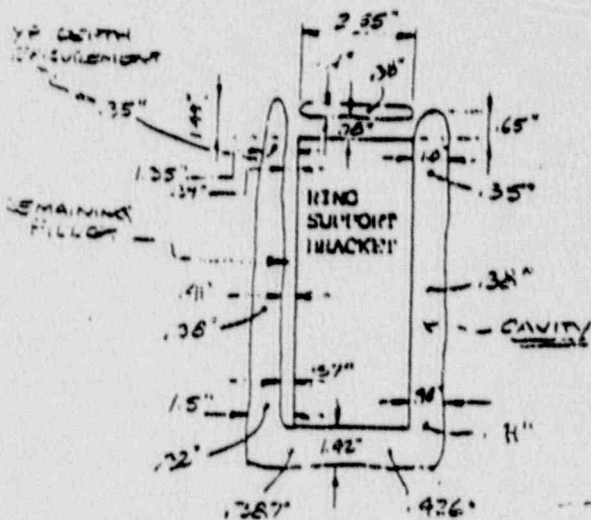
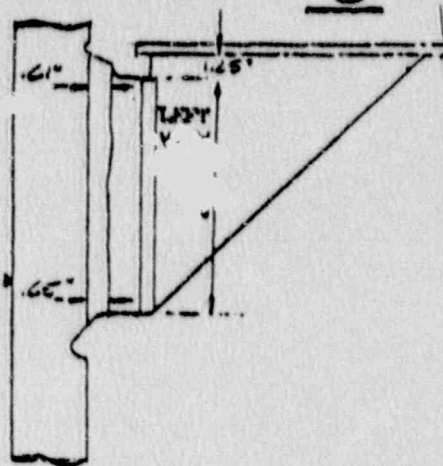
**SIPRAH GENERATOR # 24**

Dimension and Location of Excavated Areas on the Feedwater Ring Support Attachment Bracket "C"



NOTE: CAVITIES NOT CAPTURED OR PREPARED FOR WELDING.

Wall of Generator



Client

Inspection Performed By:

*James H. Smith*

Level VT

Level 31E VT

